Describing size and shape changes in the human mandible from 9 to 15 years - comparison of elliptical Fourier function and Procrustes methods

UNIVERSITY
of
GLASGOW

Valerie J. Easton

A Dissertation Submitted to the

University of Glasgow

for the degree of

Doctor of Philosophy

Department of Statistics

September 2000

BRITISH LIBRARY

IMAGING SERVICES NORTH

Boston Spa, Wetherby
West Yorkshire, LS23 7BQ
www.bl.uk

CONTAINS X-RAY

Acknowledgements

This thesis has taken *slightly* longer than I had anticipated. There are many people who have helped me along the way. Thank you very, very much.

To John McColl my supervisor. Your help, commitment and enthusiasm has been a constant source of inspiration and encouraged me at all times.

To my family. My Mum and Dad for giving me chances. Alex and Tara (and Emily plus one other), and Linda and Andy for their companionship and ability to keep me smiling. You have encouraged me along the way and only occasionally nagged!

To my friends. For all the good times we have had. You have helped (and hindered!) me from Glasgow to Edinburgh to Glasgow to Edinburgh and now to Dublin - my final resting place, I doubt it!

Above all to Matt. For putting up with me all this time, and for helping me get over those (occasional!) moments of crisis. You have been very, very patient. Look out for much more attention, and a lot more gin!

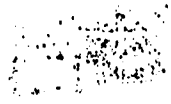

Abstract

In the past, there have been many attempts to capture the size and shape information inherent in complex irregular objects by numerical representation. There is much to be gained in a biological sense by numerical description of complex forms, like the cranio-facial complex, in the field of dentistry. This thesis aims to review, utilise and build on past research methods in an attempt to describe the size and shape changes of a sample of human mandibles from the age of 9 through to 15 years. Specifically, two methods are considered and contrasted, the elliptical Fourier function and Procrustes analysis (including Bookstein co-ordinates).

In chapter 1 the background and motivation for such an investigation is introduced, describing the need for a mathematical description of complex irregular forms with an emphasis on the importance of such models in dentistry with particular reference to the way in which the human mandible grows over time. The methodological and clinical issues of the problem are outlined, including a summary of up to date methods that have been used to capture size and shape information of a growing complex morphological form and an overview of the way in which the mandible grows. Both the so-called

landmark dependent and landmark independent (boundary outline) methods are summarised. Whilst all the methods considered are not without constraint in describing the size and shape of complex forms, all have been seen in the past to be beneficial in some way in that they all model 'form' in one way or another at the very least.

Chapter 2 then considers in more depth, what is fast becoming a much-promoted method of describing irregular forms, the elliptical Fourier function (EFF). The use of conventional Fourier methods, as well as the newer EFF method in describing size and shape changes is reviewed. A suite of programs that have been specially written to apply the EFF method in the description of complex irregular forms is introduced and an overview of the specific routines available in the package is given.

The data sample available for investigation, which consists of a series of lateral head cephalograms (x-rays) from the BC Leighton Growth Study, is described in Chapter 3. The way in which a subset is selected following certain inclusion and exclusion criteria from the available x-rays is outlined. The way in which the mandibular data is then prepared for subsequent use in the EFF suite of programs, as well as with the method of Procrustes (and Bookstein co-ordinates) is also described in some detail.

In Chapter 4, an error study is undertaken to investigate the reproducibility of the tracings of the sample of mandibular outlines prepared in the previous chapter. Both

within- and between-rater studies are looked at. The EFF method is then applied to the sample of tracings collected by one observer to explore any changes in size and shape that may occur as the mandible grows, concentrating on ages 9, 11, 13 and 15 years. As well as producing some very informative plots of the observed and predicted mandibular outlines, and centroid to boundary outline distances, the usefulness of the harmonic information available from the EFF procedure for numerically describing size and shape changes of a complex irregular form is investigated. Whether or not there are differences between males and females in the data sample, in terms of the size and / or shape of the mandible is also explored.

Finally, the method of Procrustes analysis (and Bookstein co-ordinates) is described in more depth in Chapter 5. This particular method is also applied to the same sample of mandibular outlines in order to investigate its usefulness in describing size and shape changes of the human mandible from age 9 to 15 years. Shape variability within samples is also explored by way of principal components analysis. In addition, the method of thin plate splines (TPS) is applied in order to examine shape change between males and females.

Similar observations were made about mandibular growth in the sample investigated using both the EFF and Procrustes (along with Bookstein co-ordinates) procedures. Overall, the mandible was observed to be 'growing' between ages 9 and 15 i.e. changing

in both size and shape over a period of time. There was no difference in terms of the size and shape of the bone between males and females in the sample, for each age. Further, using Procrustes analysis (and Bookstein co-ordinates) there did not appear to be any association between the size and shape of the mandibular outlines in either the male or female samples, for all ages. In addition, investigating shape variability using Procrustes methods by way of principal components analysis, resulted in broadly similar patterns for males and females, as well as combined samples, and different age groups.

It is concluded in Chapter 6 that the methods of elliptical Fourier function and Procrustes (and Bookstein co-ordinates) both provide a very useful framework in which to describe the size and shape of complex irregular forms like the mandible. Although both methods have their advantages and disadvantages, Procrustes (including the very useful method using Bookstein co-ordinates) is preferred for statistical purposes.

Table of Contents

List of Figures

List of Tables

Chapter 1

Introduction

1.1 Background and Motivation

1.1.1 The Mathematical Description of Complex Irregular Forms

What is 'shape'? Let us consider a standard dictionary definition of the word shape (Combined Dictionary and Thesaurus 1995).

Shape: the outline or form of anything; form; outline; silhouette; profile; lines; contours

From this definition, how do we actually 'describe' shape? What is meant by outline; by form; by silhouette? In particular, how do we describe shape in numerical terms rather than words?

Shape is a familiar concept. It is a word we use in everyday language, without thought, or quantification. The shape or overall appearance of an object can be described in many ways, as in the above definition. Such descriptions are usually

qualitative in nature, often in terms of another, more familiar shape - the world is round, for example. We all know what round means, and can easily visualise 'round', but how do we quantify 'round'? The human visual system uses shape as an important feature to recognise and order things in the world that surrounds us. We are all capable of recognising shape and associating shape, and it is probably because of such ease in recognition and association that we have not developed a rich vocabulary for describing shape, let alone ways of quantifying the shape of something or indeed differences between shapes. How then do we capture this very subjective boundary information of any 'shape' or 'form' in mathematical terms? And why would it be useful to do so?

The analysis of shape has a long, well established place in history and is by no means exhaustive in nature. Applications are diverse and span many branches of the arts and sciences, including the rapid identification of aircraft in engineering (Kuhl and Giardina 1982) and the classification of species of mosquitoes by the shape of their wings in biology (Rohlf and Archie 1984).

1.1.2 The Importance of Size and Shape in Dentistry

Observations and studies on shape and changes in shape (as well as size and changes in size) of the mandible have their own place in the history of shape analysis. The way in which the mandible grows i.e. changes in size and shape over time, is of great importance in many branches of dentistry, particularly orthodontic dentistry. Mandibular bone growth is a complex process, a summary of which is given in section

1.3, and it is the job of the orthodontist to ensure that this growth is as 'normal' as possible. During normal growth and development of the face, compensatory changes in the path of eruption of the teeth occur which tend to even out positional changes between the jaws. If such compensation is insufficient or does not occur at all, defective occlusion (the way the teeth 'meet' when you bite down together) and irregular spacing of the teeth will result. It is the job of an orthodontist to monitor and predict such problems. If a baseline of data on 'normal' growth changes of the mandible during a child's development could be identified, the orthodontist would be able to tailor any treatment plan required for individual patients. In fact, if such a baseline of information concerning the normal longitudinal growth and development patterns of the craniofacial region could be provided, earlier diagnosis of developing malocclusion might be possible and therefore intercepted thus minimising, or hopefully eliminating the need for any corrective therapy. The mechanics of size and shape analysis would allow monitoring of any improvement attributed to treatment given, to be compared to such a baseline of data on 'normal' growth changes. For example, consider an 8-year-old child who attends a dental surgery and happens to need orthodontic treatment. The orthodontist would be able to utilise a baseline of data to help decide what a 'normal' mandible should look like at the age of 8. The child could then be treated accordingly, using some functional appliance to encourage or inhibit bone growth so that, at the end of the treatment period, that child's mandible would be as normal as possible in terms of the size and shape of the bone. If however, that same child had gone for regular exploratory examinations, the orthodontist might have noticed some problem developing, using the baseline of normal growth changes of the mandible, and intercepted sooner using some non-surgical technique, hopefully avoiding the need for corrective therapy at a later date. It would be of interest therefore

to assess the differences in size and shape between a 'normal' mandible and what looks like a 'non-normal' mandible that would of course require quantification of the size and shape of the mandible.

An orthodontist (or indeed anthropologist) might also be interested in the change over time of the size and shape of the bone. They might also wish to examine / assess whether there are any size and shape differences between males and females, or differences between different ethnic groups. Again such comparisons would require quantification of the size and shape of the mandible, or indeed size and shape changes over time.

Further, diagnosis and treatment-planning objectives from a parental point of view is often aimed at producing a pleasing dental and facial appearance. Seldom is a child brought to a dental surgery by an anxious parent due to lack of functional efficiency in the dentition. A dentist and / or orthodontist on the other hand, will almost certainly have other aspects on their agenda. In addition to the aesthetic look of a face, they must be concerned with the quality of the individual teeth, and the functional efficiency and stability of the masticatory apparatus (chewing, biting, grinding, talking, laughing etc), which is not static during childhood. The dentition and occlusion are undergoing constant change during the process of normal bone remodelling and development and any dentist and / or orthodontist must be familiar with the constantly changing picture. They must also be aware of the influence of ethnic factors as well as characteristics inherited from each parent, and whether the child is male or female. Armed with this knowledge, the dentist and / or orthodontist should be able to recognise abnormalities during the early stages of a child's

development and advise upon any treatment that might be necessary. All such observations and considerations require quantification of size and shape for accurate description.

The initialisation of such quantification began almost certainly with the discovery of X-rays by Roentgen in 1895. Before this, researchers had to rely on post-mortem analysis and observation of patients with craniofacial defects. In fact, a great deal was already known about the size and proportions of the head before x-rays became available. Hippocrates (460 – 357 B.C.) was a pioneer in describing the variety of skull forms, and Leonardo da Vinci (1452 - 1519) applied specific head measurements to assist in his study of the human form. In addition, many scientific researchers have studied the human skull in great detail, and the changing dimensions and proportions of the face that occurred during growth came to be appreciated. However, although these early observations and studies were as thorough as they could be, they suffered from two fairly obvious deficiencies. First, the aid of calipers in measuring structures like the human head was crude and second, no accurate longitudinal studies were possible due to such a crude measuring system. These shortcomings were overcome to a certain extent with the invention of x-rays where precise measurements of the bony structures of the head could be made without interference from the soft tissue structures. Also, serial head films could be taken of the same person allowing observation of a child's growth and development over time, utilising certain techniques of superimposition of serial head films. In short, skull radiographs could now be used to isolate, observe and compare craniofacial bone development. Indeed, since the roentgenographic cephalometric technique became popular, the term cephalometrics has become synonymous with head films and the determination of

angles and distances between radiographic landmarks (as opposed to the meaning of cephalometrics in its classic sense defined as simply 'measurement of the head'). Further, the invention of the cephalostat simultaneously by Broadbent in the USA and Hofrath in Germany in 1931 allowed more meaningful and precise comparisons between individuals and within individuals over time. The cephalostat (or head holder) illustrated in Figure 1.1 below, is a standardised system of cephalometric radiography and most radiographic head films are still taken according to these standards.

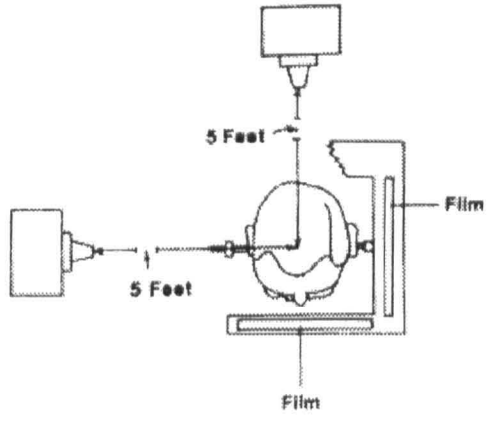

Figure 1.1 The Cephalostat.

The cephalostat ensures that the head is restrained in a precise manner. Films are taken using the cephalostat with the Frankfort plane horizontal, the teeth in occlusion, the adjustable ear rods positioned in the external auditory meati (holds the head stable antero-posteriorly and prevents lateral rotations). The source of the x-ray is set 5 feet from the middle of the cephalostat, and the central ray is designed to pass through the ear rods. Updated versions are obviously used today which are less obtrusive and less expensive than the original, but the method remains the same in that the positioning of the head and the distance between the head holder and the x-ray unit remain the same.

The orientation of the patients' head is then, standardised and consistent, which allows valid comparisons among individuals, and consistency in longitudinal studies.

Subsequent research into facial growth and the results of orthodontic treatment have had a major impact on orthodontic theory and practice. References include Broadbent 1937, Bjork 1955, Harris 1962, Bjork and Skieller 1972, Enlow 1975, Bjork and Skieller 1983, McNamara 1985, McNamara et al 1985. Longitudinal growth studies in particular have provided population norms for the purposes of comparison and insight into normal and abnormal growth trends.

The past few decades have seen further advances in orthodontic treatment, coupled of course with those in orthodontic appliances, capable of considerable precision in correcting irregularities of the teeth by manipulating bone growth. The demand for more accurate information about the way in which complex morphological forms, like the mandible, change in size and shape over a period of time has therefore increased. This could be considered particularly important to individuals and orthodontists alike since the size and shape of the mandible ultimately determines the size and shape, and thus aesthetic look, of the lower part of our faces.

1.1.3 How do we capture 'form'?

In order to assess and compare differences in size and shape for different forms then, we would like to be able to capture all the visual information readily seen, on the size and shape of a complex form like the mandible, in mathematical terms. Visualising and describing regular, geometric objects like circles, squares etc is fairly easy and well established where it is just as easy visualising irregular forms like the mandible. It is not so easy however, to describe complex irregular forms mathematically. While growth has been simply defined as a change in dimensions over time (Huxley's allometry equation 1924 and 1932), this is clearly an oversimplification when complex shape changes occur, in other words, the measurement of shape is further complicated by the process of growth. It is possible however to partition the overall growth of a form into separate components of size and shape. It is widely reported that Form = size + shape (Needham 1950, Penrose 1954, Sprent 1972, Healy and Tanner 1981) but it is still not at all clear what linear measurements show the correct size increases during growth and which available measurements can adequately and efficiently describe shape changes. Size can be defined as a quantity that depends upon dimensional space. In a one-dimensional world, differences in size can be viewed as a difference in vector length. In two dimensions, linear measurements in combinations (such as ratios) have proved to be inadequate (Dodson 1978 and related citations) and area becomes one definition of size, and in three dimensions, volume would be an appropriate measure of size. Shape, on the other hand, is a difficult quantity to define. It is thought to be the 'residual', or what is left over after controlling for size, that which remains invariant under scaling, translation, rotation and reflection (Lele 1991).

Consequently, the development of quantitative procedures which accurately describe growth patterns of complex irregular forms, like those encountered in morphological studies of biological organisms, has prompted a great deal of research effort over the last century.

1.2 Review of Existing Methods for Describing Complex Irregular forms

One of the first workers to attempt to deal with morphological size and shape changes was D'Arcy Thompson. His classic work on Cartesian transformation grids, On Growth and Form, was first published in 1917 and reissued in 1942 (Figure 1.2).

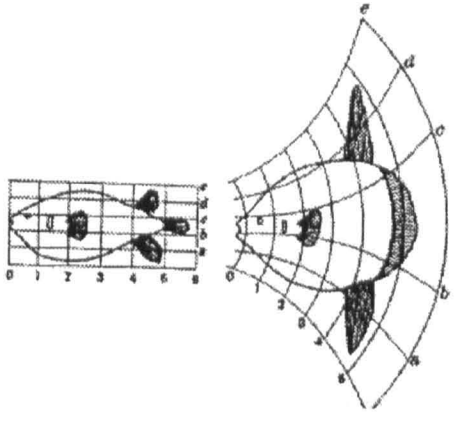

Figure 1.2 D'Arcy Thompson's Cartesian transformation Grid.

By using these so called Cartesian transformation grids, he illustrated that the external configuration of organisms could often be transformed, one onto another. Instead of

comparing the actual corresponding points on two configurations using a fixed co-ordinate system, he transformed the co-ordinate system for the second configuration so that corresponding points in the two co-ordinate systems had identical co-ordinates. The transformations to do this were however, often mathematically very complicated and so this method was often used for descriptive purposes only.

This method has however been the impetus to newer approaches however, such as Biorthogonal Grids and Finite Element Methods introduced in sections 1.2.2 and 1.2.3, in attempts to quantify size and shape changes of growing irregular forms.

According to Goldstein 1979, the first to quantify size and shape changes in a general way was Huxley 1924 and 1932 by the introduction of the study of allometry. Allometry is simply the study of the relationships between size and shape, differences in shape associated with size, in particular the manner in which shape depends on size. Huxley attempted to quantify size and shape changes using what became known as the simple allometry formula, where two size variables x and y satisfy, at least approximately, a relationship of the form $y = \alpha x^{\beta}$ or $\log y = \beta \log x + \log \alpha$. This formula was used to describe the relationship between the growth of part of an organism, to that of the organism as a whole. Mosimann 1975a, b and 1988, became a well-known name in the study of allometry. Reeve and Huxley 1945 discuss the pros and cons of using the simple allometry formula to describe size and shape changes of complex forms as well as discussing deviations from it. A general overview of some of the work done in this field which involved the fitting of linear or non-linear regression equations between size and / or shape measures is given by Sprent 1972, as well as an outline of some other alternative approaches to studies of size and shape.

Allometric descriptions of growth of this kind are fundamentally different to the boundary-outline and landmark-based methods that are introduced later. Richards and Kavanagh 1945 attempt to combine the simple allometry formula with D'arcy Thompson's Cartesian transformation grids, with some success in the description of size and shape changes of growing complex forms, although not without limitation.

The literature relating to such 'traditional' techniques then is sizeable. There has also been much written about some of the more current analytical methods which are used to describe irregular biological forms. These more recent methods can be considered as being split into two broad categories (Read and Lestrel 1986, Chen et al 2000). Some may be described as homologous point methods (where each point on the form relates to exactly the same point, usually anatomical position, on any other similar form). Others are described as boundary outline methods (where the whole outline of the form is characterised by a set of closely related points), which can be further divided into techniques and applied to data sets, some of which are discussed in Lestrel 1989a and 1997a, b.

Homologous point approaches include Conventional Metrical Analysis (CMA); Biorthogonal Grids (BOG); Finite Element Method (FEM); Euclidean Distance Matrix Analysis (EDMA); Thin Plate Splines (TPS) and Procrustes Analysis (PA). Under the boundary outline methods umbrella we have Medial Axis Analysis (MAA); Resistant-fit Theta Rho Analysis; Eigenshape Analysis and the Elliptical Fourier Function (EFF) method. Each of these techniques will now be briefly described and discussed in turn.

1.2.1 Conventional Metrical Analysis (CMA)

Conventional metrical analysis is a method which was developed in the main for measuring regular geometric objects, not objects of the type typically encountered in craniofacial morphology studies and other branches of biology and the like. It is considered to be a homologous point representation and consists of distances, angles and ratios from or between such points, rather than the actual points themselves. To consider these measures however, is thought to be inferior to using the actual co-ordinate points of any outline or boundary of a form, because the geometry of that form is essentially being ignored. Ratios of distances can often be calculated from the actual co-ordinate points for example, where the converse is not generally true. The possibility that size and shape are confounded cannot be excluded when using CMA as a method for describing form, as well as the problem of angular measurement of shape since the shape inside an angle could indeed be any shape. This is not to suggest that it is useless, far from it, since it clearly depends on the questions asked. It is a good overall descriptor of size and shape and problems arise only when the quantification of complex shape changes is of central importance. In spite of its shortcomings then, CMA has been, and still is, widely used in a biological setting (Corruccini 1973, Krieborg et al 1981, Roberts et al 1983, Strauss and Bookstein 1982). Specifically, there are many applications of CMA in dentistry (Mills 1970, Bibby 1979, Kerr 1979, O'Reilly and Yanniello 1988). Figure 1.3 illustrates the angles that are typically calculated in cephalometric analysis, in the Glasgow Dental Hospital and School. The form used to collect such information is given in the Appendix.

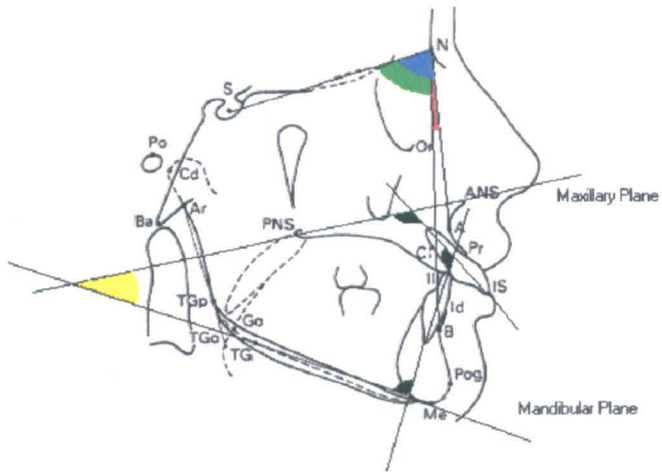

Figure 1.3 **Illustration of conventional cephalometric analysis in dentistry.**

The most common x-ray of the head, specific to craniofacial description, which includes the mandible, is the lateral skull radiograph (cephalogram). An example is given in the Appendix. A typical head film reduces the three-dimensional head to a two-dimensional representation of the head. In order to compare cephalometric radiographs, the outline of the relevant structure has to be traced and the traced outlines can then be superimposed on one another. Meaningful comparisons are made by superimposition on a precise registration point, which should be as free as possible from the influences of growth (usually Sella Turcica when considering the craniofacial complex). Further location is required in order to orientate the tracing around the registration point, and the line Sella-Nasion is frequently used for this. Principal landmarks and planes are identified and drawn on the tracings so that appropriate distances and angles can be measured, some of which are illustrated in Figure 1.3. Linear distances and angles that are typically calculated in cephalometric analysis, specific to craniofacial description are given in the Appendix (adapted from 'A Textbook of Orthodontics' edited by Houston et al 1992).

Commonly known as 'multivariate morphometrics' in biology (see Reyment et al 1984 for a review) and in the context of conventional cephalometrics, the linear distances between points measure size, whilst angles, being independent of size, are used as 'shape' measures. Ratios of these measures are also calculated and typically submitted to a multivariate statistical analysis (Rao 1948). Problems with these measures in this context are instantly seen since, when dealing with two- or three-dimensional morphological forms such as the mandible, how can a single linear distance measure the 'size' of such forms? Are such measurements comparable over a range of forms? Surely a single linear distance just serves as an overall size measure, where area would have to be taken into consideration in order to standardise for size across all forms. Also, the 'shape' measure of angles is surely not measuring shape in a true sense at all, since the shape within an angle could be anything. In addition, much effort has gone in to standardise even this simple linear, ratio and angular measurements in order to make meaningful comparisons between forms. The biometric technique for measuring the human mandible was first described in a paper entitled 'A First Study of the Tibetan Skull' by Morant in Biometrika in 1923. Many problems existed in several observers' measurements taken of the same series of specimens however, since it was difficult to specify the extent of defect that made it necessary to exclude a particular measurement, as well as differences in personal equations used in identifying particular measurements. These problems are highlighted in the early literature where, although measurements of several thousand mandibles taken for anthropological purposes have been published, they are actually of little value in a quantitative sense. This is primarily due to the fact that the technique of measurement differs, or is modified, and therefore is not standardised 'across the

board'. Also, many of the data obtained by following the techniques that have been most widely utilised cannot be compared accurately in cases where direct comparison should be possible (as discussed by Morant 1930). Techniques that capture 'form' in a quantitative manner that can be directly compared over a series of forms would then be very useful.

Such problems and issues with CMA have been discussed in a general biological context by many authors including Medewar 1950, Zuckerman 1950, Corruccini 1973, Lestrel 1974, and Bookstein 1978. Colourful debate on the theoretical and practical use of CMA for the description of complex forms can be found in papers by Blackith and Reyment 1971, Atchley et al 1976 and 1978, Corruccini 1977, Albrecht 1978, Hills 1978, and Dodson 1978.

As way of a summary, it is thought that the deficiencies of conventional cephalometrics stem from

1. a limited number of isolated landmark points are usually employed (where there is unavoidable bias in the choice of these landmark points)
2. an incomplete mapping between the measurement set and the actual morphology
3. a derived multivariate space – it would be easier to interpret pictures in original space rather than some derived multivariate space
4. the fact that the interpretation of linear combinations of lengths, angles and ratios is difficult
5. the use of a measurement system intended for regular geometric objects and not for irregular morphological forms of the type encountered in craniofacial biology.

Such limitations found researchers seeking alternative methods for the size and shape description of complex forms.

1.2.2 Biorthogonal Grids (BOG)

Developed by Bookstein (1978, 1982, 1983 and elsewhere), biorthogonal grids is another method used in an attempt to quantify size and shape changes of growing irregular morphologies. This method shares a common element with conventional cephalometrics in that it is also considered to be a homologous point representation, again dependent on anatomical landmarks, chosen at the observer's discretion. It is related to the finite element method (FEM) of size and shape description (see section 1.2.3), where the method of BOG represents the simplest form of FEM. Although both methods are dependent on homologous points or landmarks, which have to be identifiable across the forms that are to be compared, they deal with many of the shortcomings of conventional metrical analysis, the major advantage being that they are both invariant with respect to the co-ordinate system.

In BOG, any three homologous points can form a reference triangle (Bookstein 1977, 1978). A concentric circle can then be drawn touching all three sides of the triangle. With growth or treatment, changes in the position of the homologous points that characterise the form under scrutiny means that a new triangle is formed. If the relative position of the circle's contact points is maintained, the deformation of the reference triangle into the second would transform the circle into an ellipse. Thus, the circle would be effectively stretched along one axis and the direction of this distortion

may be calculated. The longest and shortest diameters of the ellipse are known as its principal axes and these lengths can be measured. The greater the discrepancy between them, the larger the difference in shape. Bookstein suggested that this change in shape be expressed as a ratio, the larger axis measurement divided by the smaller i.e. major axis divided by minor axis measurement. Changes in size were described as the product of these two lengths. BOG is then measuring size and shape *change* between two time points of the same form, rather than the size and shape of the form at time points one and two separately.

Examples of such applications of BOG to describe size and shape changes of complex forms can be found in Bookstein 1977 and 1980.

1.2.3 Finite Element Method (FEM)

The FEM has been borrowed from engineering where it is a well-established procedure for measuring the effect of stresses or loadings on engineering materials (Bathe and Wilson 1976). It has been adapted to the task of characterising shape changes and like conventional metrical analysis and biorthogonal grids, the finite element method of quantifying size and shape changes of complex biological forms is limited to homologous points. It is very similar in mathematical terms, to the method of BOG. It too is invariant with respect to the co-ordinate system, it is registration free since it provides information about the 'stretching' of elements rather than the movement of landmarks relative to the co-ordinates system. The FEM can also be extended to describe three-dimensional data.

Hexahedrons or cubes in the context of FEM replace the triangles in BOG. Each cube element is composed of eight homologous points in the x, y, z Cartesian plane. Using an initial form as a base, each element in the structure is pair wise compared, and the shape change is computed as a deformation. As in BOG, these cube elements are independent of one another with the exception of where the surfaces are joined. These elements are 'non-homogeneous' in the sense that they represent spatially varying tensor fields in contrast to BOG in which the principal dilations are based on a constant tensor field. For each element, it is possible to estimate a 'form difference' tensor that is equal to a 'shape difference' tensor, plus a 'size difference' tensor. Shape changes are then found by subtraction, and by averaging these shape changes at all nodes and over the whole form, summary estimates can be obtained.

Examples of applications of FEM to describe size and shape changes of complex forms can be found in Cheverud et al 1983 and Cheverud and Richtsmeier 1986.

FEM can be seen to have at least two advantages over BOG. First, it can be extended to three dimensions and second, the cube elements are 'non-homogeneous' with varying tensor fields. Like BOG though, it deals with *changes in size and shape* rather than the actual numerical description of size and shape.

1.2.4 Euclidean Distance Matrix Analysis (EDMA)

Euclidean distance matrix analysis (EDMA) was largely developed for applications in biology. It is also a landmark-dependent method that is applicable to two- and three-dimensional structures (Lele 1991 and Lele and Richtsmeier 1991). It was developed to avoid some the problems inherent in the superimposition of landmark-based outlines. This method, as with CMA, FEM and BOG, is a co-ordinate free method.

A series of equivalent landmarks is identified on each 'form' to be compared. The distances between these landmarks are determined, and for each morphology under consideration a matrix of these interlandmark distances is produced (a form matrix), Lele and Richtsmeier 1991. The geometric relations of all landmarks are preserved in the form matrix, since it contains all interlandmark distances. Form difference matrices (containing the ratios of corresponding distances between complex forms under consideration) are then calculated between pairs of single complex forms, or between the average form matrices for different populations of complex forms. The magnitudes of the ratios in the form distance matrix can be used to assess differences between complex forms and it is also possible to identify what areas of the morphology exhibit the largest shape differences. Landmarks whose locations vary between forms can also be identified.

Examples of applications of EDMA can be found in Richtsmeier and Lele 1990 and Lele and Richtsmeier 1992, and in a craniofacial biology context in Singh et al 1998.

1.2.5 Thin Plate Splines (TPS)

A comparatively new so-called homologous point technique is thin plate splines (TPS). Using the theory of surface spline interpolations (Bookstein 1991), the development of TPS represents a continuation of Bookstein's work on deformations which started with BOG (Bookstein 1978, 1982, 1983 and elsewhere), which represented an approach to put D'Arcy Thompson's (1917, 1942) Cartesian transformation grids on a more solid mathematical footing. The method of BOG did not provide for a sophisticated graphical display of the point-to-point deformations sought by Bookstein (Reyment 1991), whereas TPS goes a long way in doing so.

TPS is a technique for visualising form change as a deformation. It uses an interpolation function representing a mapping that models the 'biological homology' of pairs of points. The interpolant can be thought of as a smooth (well-behaved) function that is fitted to a data point set (in two dimensions these are the spline functions such as the Bezier curves). The TPS function may be visualised as an infinitely thin metal plate placed over a set of landmarks. This surface allows visualisation of the pairwise displacement of landmarks as a deformation. Computing the 'bending energy' carries this out. If this plate is 'flat' then it has zero bending energy. If bending energy is involved, it acts to 'wrinkle' the plate in some fashion. The larger the deformation, the greater the bending energy and the more 'buckled' the thin plate becomes. These TPS deformations can also be expressed as a sum of what are referred to as 'principal warps'. These are eigenvectors of the bending energy which correspond to the orthogonal displacements of the landmarks (above and below) from the thin plate.

Further explanation of TPS method as a size and shape descriptor of complex forms can be found in Reyment 1991 and Bookstein 1991.

An example of the application of TPS in a craniofacial biology context can be found in Singh et al 1998, and also applied to the mandibular data in this thesis in Chapter 5.

1.2.6 Procrustes Analysis (PA)

Procrustes analysis (PA) can be thought of as another homologous point technique that provides us with the tools to describe size and shape information of any complex form in mathematical terminology, as well as allowing comparison between forms.

The basic idea is a very simple one. Consider two forms or configurations of homologous landmark points of two complex outlines i.e. a pre-assigned correspondence between the points of the two configurations. Procrustes analysis allows comparison of two such forms by matching the two forms with similarity transformations of translation, rotation / reflection and scale change to be as close as possible according to Euclidean distance using least squares techniques. Since 'shape' is defined to be that which remains after differences in location, orientation and scale have been removed from forms we have such an optimal matching method in Procrustes analysis.

The method of Procrustes analysis using orthogonal (rotation / reflection) matrices was developed initially for applications in psychology and early papers on the topic

appeared in Psychometrika. The technique can also be traced back to Mosier 1939, where it was originally developed for use in factor analysis, but has been developed over the years by many researchers including Gower 1971 and 1975, Goodall and Bose 1987, Mardia and Dryden 1989b, Rohlf and Slice 1990, Goodall 1991. It has attracted much attention in more recent years in the application of describing size and shape of growing forms by Dryden and Mardia 1992, Ziezold 1994, Shepstone et al 1999. Further, it has been utilised in the context of craniofacial biology by Singh et al 1999 as well as in a discriminatory context by Glasby et al 1995.

Procrustes analysis is considered and described further in Chapter 5 where the method is also utilised in an attempt to describe the size and shape changes of a growing mandible.

In summary then, Procrustes analysis, as well as EDMA and the three deformation methods: BOG, FEM and TPS can all be considered as novel contributions to morphometrics. They represent sophisticated mathematical methods for eliciting new information present in biological forms as well as dealing with the shortcomings inherent in CMA. These methods also share one aspect with CMA, in that each depends on homologous points.

The next few sections describe methods that utilise the boundary outline or curve information of any form in an attempt to describe how that form may be growing, and therefore changing in size and shape.

1.2.7 Medial Axis Analysis (MAA)

Medial axis analysis or MAA is considered to be one such boundary outline method. It is based on the symmetric axis of an outline form passing down a precisely defined middle of an extended structure (Blum 1973 and Lavelle 1985). The medial axis of a curve is simply the collection of all the points that are 'in the middle'. In this way, all centres of circles that touch the curve at two distinct points. The medial width of the form at a middle point is the radius of its circle. That is, a curve can be constructed by connecting the centres of circles that touch the boundary of the form at two distinct points. This curve, plus an expression of its distance from the boundary (based on the radii of the circles), is sufficient to completely describe the shape of the structure. These medial axes provide 'stick' figures for complex biological forms, which serve as a means for registering slow changes in curvature, relative position of parts of objects etc (for organs assembled out of poorly delimited parts). An alternative way of looking at this is by way of what is called the 'grassfire model' (Blum 1973). The shape of an object is characterised as an area of dry grass which, if set fire to simultaneously all around its edge will burn towards the interior. If an even rate of burning is assumed, the line of points at which the fire meets itself make up the points defining the medial axis, and the time taken to reach these points is the medial width function. This axis and function describe the form then, and allow for complete reconstruction of the object.

An application of this technique (there are very few) can be found in Webber and Blum 1979.

1.2.8 Resistant-fit Theta Rho Analysis

The resistant-fit Theta Rho analysis has not received much attention (Siegel and Benson 1982 and Benson et al 1982). It is in fact, a combination of what is known as Theta Rho analysis with a more 'robust' statistical method. The method is useful for morphologies where it is known that the variability of substructures is not randomly distributed across the form. The advantage of this method is that it is relatively stable against departures from the assumptions of analysis, such as independent, identically and normally-distributed errors. It is also protected against the potentially strong influences of atypical or incorrect data values, which is achieved by using medians of ranked changes in proportion instead of least squares to compute the transformation factors of scale, rotation and translation (Benson et al 1982). For instance, two shapes can rarely be superimposed perfectly; different fitting criteria will generally yield different results. By allowing regions with large deformations to have a large impact on the fit, methods such as the least squares methods can potentially minimise true shape differences and thereby obscure them. A resistant technique, however, limits the influence of large deformations and the resulting fit is close in similar regions and not so close in relatively deformed regions. In this way, resistant techniques can help to identify similarities and differences in form more effectively than least squares methods. Siegel and Benson 1982 have demonstrated the superiority of resistant fitting technique over the least squares fit technique.

Applications of resistant-fit Theta Rho analysis are few but can be found in the same papers as above and citations relating to them.

1.2.9 Eigenshape Analysis

Eigenshape analysis represents another approach for numerically describing the boundary outline of a complex form, and thereby the shape of biological organisms. This technique was developed using data (comparatively smooth microfossil outlines) derived from palaeontology. It is based on the presumption that the use of eigenshape analysis facilitates the reduction of the morphological shape space to a comparatively few dimensions (Lohmann 1983 and Schweitzer et al 1986). Eigenshape analysis is misleading in one sense. It actually represents the sequential use of two techniques rather than representing a single development. It represents the initial application of Zahn and Roskies' 1972 Fourier-based algorithm, the results of which are then subsequently subjected to a factor analytical method. Lohmann and Schweitzer 1990 proposed three measures for describing planar outlines within the context of Eigenshape analysis. These were form, size and angularity. Form referred to two aspects of the outline: scaling (size) and amplitude (variance). Form was computed using the standardised (for size and variance) formulation of Zahn and Roskies' Fourier formulation. Size was defined in two ways; as the perimeter of the outline of the form and by the bounded area of the form. Angularity was measured by the magnitude of the amplitudes of the angular part of Zahn and Roskies' algorithm but, before these amplitudes were standardised to unit variance.

Zahn and Roskies' formulation has the advantage that it is always a single-valued function and does not require a vector centre such as the centroid. Lohmann 1983 correctly indicated that if the centroid was not used, incorrect computed amplitudes

were the result. This had been noted earlier by Parnell and Lestrel 1977 and Full and Ehrlich 1982. However, the use of n equal-divisions as advocated by Lohmann 1983, negates the possibility of maintaining homology. As Full and Ehrlich 1986 have argued, there is very little possibility that homology between outlines can be consistently maintained with eigenshape analysis. Finally, a comparison of a number of Fourier methods (Rohlf and Archie 1984) suggested that Zahn and Roskies' algorithm was the least satisfactory (Rohlf 1986). Thus, morphologies with complex irregularities such as the mandible cannot easily be handled with either conventional Fourier methods or Eigenshape analysis.

Applications relating to this particular boundary outline technique can be found in the above references and related citations.

1.2.10 Elliptical Fourier Function (EFF)

The Elliptical Fourier Function (EFF) method is one of the more recent so-called boundary outline methods which has been proposed in the quest to quantify size and shape changes of growing irregular forms. Like many of the other methods outlined, it too was developed to circumvent some of the problems inherent in conventional cephalometrics.

The development of the EFF procedure in engineering is attributed to an algorithm devised by Kuhl and Giardina 1982 as a method to scan rapidly and identify incoming aircraft. The methodology was utilised and further developed in the morphometric field by Drs

Lestrel and Read, School of Dentistry, University of California, Los Angeles, to try and overcome some of the difficulties that occur with conventional cephalometrics for studying size and shape.

According to Lestrel 1980, 1987, 1989a and b, 1997a and b and elsewhere, the use of elliptical Fourier functions represents one method that goes some way towards extracting a much greater percentage of the biological information present in complex irregular forms, information that is readily visualised and yet has remained difficult to describe in numerical terms. Its ability to control for, or standardise, the size of any complex form whilst maintaining its shape is thought to be one particularly useful characteristic of the EFF.

Numerous papers have appeared since Kuhl and Giardina published their algorithm. Applications with a biological thrust are diverse. Ferrario et al 1994 have investigated the shape of the human corpus-callosum from magnetic resonance scanning using the EFF technique. In a zoological context, Rohlf and Archie 1984 have investigated the shape of mosquito wings and Ferson et al 1985 have looked at the outlines of mussel shells. Examples in cytology can be found in Diaz et al 1989, 1990, Nafe et al 1992 and in botany in Kincaid and Schneider 1983, White and Prentice 1988. Lestrel and Kerr 1993, Lowe et al 1994 and more recently Chen et al 2000 have described the application of this technique in dentistry.

In Chapters 2, 3 and 4 of this thesis the elliptical Fourier function method is described in more detail and utilised in an attempt to analyse and describe any size and shape changes which might be taking place during mandibular growth for a data sample

between the ages of 9 and 15 years. We discuss the usefulness of the EFF in such a task in contrast to the method of Procrustes in Chapter 6.

1.3 Mandibular Growth

In order to get a feel for what we are trying to describe in mathematical terms, this section attempts to summarise and describe bone growth in general, as well as specific mandibular growth. Such a summary will follow four headings according to Thilander 1995. There is a wealth of literature on the subject of mandibular growth, considered as part of the more general area of craniofacial growth. The book 'A Synopsis of Craniofacial Growth' has been an invaluable introductory source in this area, which is referred to throughout this section.

Bone growth is a highly complex process, it is basically the same for all of us, but varies enormously between individuals. Bone is the fundamental supporting tissue of our bodies. The way in which our bones grow is of great importance to all of us since the size and shape of each one of us is influenced and ultimately determined by bone growth. How is such an important tissue formed then? And how does it grow, and how quickly? And what influences, helps or hinders bone growth?

1.3.1 Growth Mechanism - How bone is formed

The composition of bone matrix and the percentage of calcium hydroxyapatite impregnation relative to the organic constituents is consistent throughout the bones of an individual. The difference between and within bones occurs at morphologic and histologic levels. Most bones, whether in limbs, or the head, have at least one surface of dense bone called compact, or cortical bone and interior to this compact layer, cancellous or spongy bone is usually found. This is illustrated in Figure 1.4. A network of cells (osteoblasts) on the surface of this bone marrow, called the endosteum, helps to regulate the exchange of solutes between body and bone fluids. The outer covering of bone is the periosteum, which gives the bone structure. It is a sheath composed of an outer layer of fibrous connective tissue and an inner layer of surface cells (osteoblasts) next to the bone.

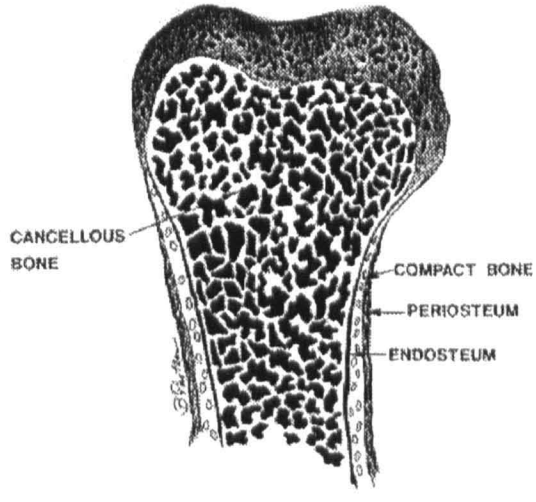

Figure 1.4 **Illustration of the make-up of bone.**

There are three classes of bone cells: osteoblasts, osteocytes and osteoclasts. These three types of cells each have a different function in the formation of bone. In short, some are responsible for the synthesis of bone, and initiation of calcification; some are responsible for maintaining bone tissue equilibrium; and some are important for the resorptive aspects of bone remodelling.

The deposition and calcification of bone tissue can occur in two ways i.e. there are two types of bone growth - indirect or direct; endochondral and intramembraneous ossification.

In endochondral formation, bone is derived from a cartilage precursor, where space has already been gained by the cartilage, which acts as a kind of scaffold on which bone is deposited. In this process, cartilage is first formed by cells called chondroblasts, undergoes mineralisation, and then is invaded by bone resorbing cells which reduce the matrix to a framework. Next, the osteoblasts, which have differentiated from the invading vasculature tissue, deposit bone matrix around the cartliage model. The second time it occurs in bone, a new architecture of tissue is established and eventually, the remnants of the cartliage matrix are completely lost in the process of growth and remodelling.

In intramembraneous formation, bone is formed directly, from condensation of a particular cell type, mesenchymal cells, within a membraneous structure. Intramembraneous bone formation occurs on the outer surface of the periosteum, the endosteum, on the surfaces of certain structures (trabeculae) of cancellous bone, and in

the case of a few bones in the skull, at the edges in specialised structures called sutures.

The mandible is developed from what is the known as the first branchial arch. Cartilage acts as a scaffold for endochondral bone formation and mesenchymal cell condensation initially starts just lateral to this cartilage and proceeds entirely as intramembraneous bone formation.

1.3.2 Growth Pattern - Changes in the size and shape of the bone

Bone grows by surface apposition, both by periosteum and endosteum, and alters its shape by bone remodelling.

The mandible can be thought of as being split up into different areas as illustrated in Figure 1.5 and can be considered to grow in three directions: height, length and width, with concurrent remodelling of all areas of the bone taking place. Landmark points are noted only (see section 3.3.1).

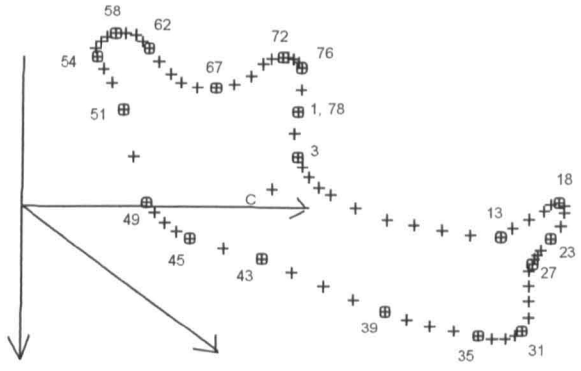

Figure 1.5 Directions of mandibular growth.

where,

Points 1-7: Anterior border of the ramus

Points 7-13: Alveolus

Points 13-23: Lower incisor

Points 23-31: Anterior border of the mandible

Points 35-45: Lower border of the mandible

Points 45-49: Angle of the mandible

Points 49-54: Posterior border of the ramus

Points 54-62: Condyle

Points 62-67: Mandibular notch

Points 72-78: Coronoid process

According to investigations by Enlow and Harris 1964 amongst others, remodelling of the mandible (similar to other craniofacial structures) follows three basic principles:

area relocation (drift versus displacement), surfaces facing the directions of growth (surface apposition and resorption), and what is known as the V principle.

1.3.2.1 Area relocation

The deposition process in bone remodelling can be referred to as 'drift'; and a 'push' contribution referred to as 'displacement'. Most bone growth in the head is a combination of these to processes. Specific to mandibular growth, the chin point (Gnathion) moves away from sella turcica by a combination of deposition of new bone on the chin by the osteoblasts (drift) and growth of the condyle, pushing the chin forward (displacement). Of the total increase in overall length of the mandible, this anterior apposition of bone on the chin is minimal however. In fact, most of the lengthening process of the mandible occurs on the ramus and at the condyle. The leading edge of the ramus is resorbed, balanced by deposition on the posterior surface (else the ramus would narrow), synchronised with cartilage replacement activity in the condyle. Since the condyle articulates against an immovable wall (the glenoid fossa), its posterior growth is 'pushed' and the mandible is displaced anteriorly. This is referred to as posterior growth – anterior displacement (backward growth – forward movement).

1.3.2.2 Surfaces facing the directions of growth

The idea of backward growth – forward movement assumes that the surfaces of new bone formation always face the direction of growth and for consistency, the surface of bone away from the direction of growth must then undergo resorption. Therefore, a

bone increases its width by adding bone matrix to the surface facing the direction of growth and subtracts bone matrix from the surface away from the direction of growth. The two processes are not necessarily always equal however, sometimes apposition (to the surface facing the direction of growth) will exceed resorption (from the surface away from the direction of growth) and vice versa. Patterns of bone apposition and resorption contributing to the overall growth of the mandible occur in many areas of the bone.

1.3.2.3 The V principle

Whilst considering surface apposition and resorption it is sometimes the case that the direction of bone growth and the 'growing' surface are not readily apparent. It is thought that many surfaces are better expressed as V's, rather than flat surfaces. The inside of the V represents the surface of new bone deposition, where new bone tissue is formed. It also then, following on from our 'flat surface' argument of bone apposition and resorption, represents the surface facing the direction of growth. In contrast, the outside of the V now represents the surface of bone resorption. As previously mentioned, patterns of bone apposition and resorption contributing to the overall growth of the mandible occur in many areas of the bone. These patterns mainly follow the V principle. The coronoid process represents an area of the mandible that can be visualised as following the V principle, as can remodelling of the condyles.

In summary, each of the areas of the mandible undergoes growth and bone remodelling to give overall change by way of a combination of the above three principles. The overall increase in height of the body of the mandible is primarily by

formation of alveolar bone, though some bone is also deposited along the lower body of the mandible. The overall increase in mandibular length is by bone deposition on the posterior surface of the ramus, and compensating resorption on its anterior surface, deposition on the posterior coronoid, and resorption on the anterior surface of the condyle. The overall increase in the width is by deposition of bone on the outer surface and resorption on the inner surface. At the same time, the mandible is displaced from its spatial position in the craniofacial complex by bone deposition at the articulating surfaces with other bones. Further, it is translated in space by the movements of other bones when they are growing themselves. There is also significant individual variation.

1.3.3 Growth Rate - The speed at which bone is formed

It is widely known that the rate of growth is different in different parts of the body, is different for males and females, and varies between individuals, and so, the rate at which different parts of the body, males and females and individuals reach adult size / maturity will also vary. This obviously applies to the growth of the mandible.

Many studies have attempted to find reliable indicators of periods of rapid facial change due to a suggestion by Burstone 1963 and Bjork and Skieller 1972. They suggested that the timing and hence the effectiveness of treatment can be affected by rates of growth and levels of circulating hormones which are related in turn to levels of maturity. It would therefore be advantageous for the orthodontist to carry out any treatment during the so-called 'growth spurt'. It comes as no surprise then to find that

the orthodontist would be interested in the timing of the growth spurt and the rate of growth of various parts of the craniofacial complex.

It is generally agreed that the timing, duration and magnitude of the pubertal growth spurt in the mandible vary from individual to individual. According to Farkas 1992 this so-called growth spurt has been determined to be around ages 10-13 for females, and 12-15 for males. Other studies, Lewis and Roche 1972 and 1974 and Lewis et al 1982 have showed that the first pubertal spurt in the cranial base tends to occur about 1.6 years earlier in girls than in boys, with similar differences in the timing of mandibular spurts.

1.3.4 The Regulation Mechanism - A mechanism to initiate and direct

The Regulation Mechanism is a mechanism that initiates and directs the above three factors; growth mechanism, growth pattern and growth rate.

There are many factors that affect and regulate the overall growth of individuals. Those that affect the growth of the mandible have been studied extensively by many researchers, including genetic and environmental factors, growth of other structures within the craniofacial complex, hormone levels and diet. References can be found in Dudas and Sassouni 1973, Mills 1983, Kiliaridis 1995, Meikle 1973, Bevis et al 1977, Vogl et al 1993, Tuomenin et al 1993, Bozzini et al 1989.

In most investigations of the growing mandible; how it changes in size and shape, what might influence mandibular growth, the rate at which it grows etc, conventional cephalometric methodology has been called upon to 'measure' change, which has no doubt provided us with useful information and observation over the years. A way of sensibly quantifying the size and shape of the growing mandible would be an obvious step forward however.

1.4 Aims and Outline

The main aims of this thesis are then

1. to utilise the elliptical Fourier function method in an attempt to characterise and describe the size and shape of a growing complex morphological form, the mandible, for a sample of subjects during puberty

and thus

2. to illustrate and summarise the longitudinal size and shape changes present in this sample of 'normal' mandibles

so that further work might

3. provide visual and numerical norms against which the growth in children's' mandibles might be measured.

We also want to be able

4. to use the information (predicted points, harmonics, amplitudes etc) from the elliptical Fourier function (EFF) method to statistically analyse size and shape changes in this sample of 'normal' mandibles.

Further, we want

5. to investigate the usefulness of EFF methodology in its role as a size and shape descriptor, with another method, namely Procrustes analysis (PA).

To this end, Chapter 2 describes the EFF method in more detail and gives a general overview of the specific routines of the EFF software used in this thesis. Chapter 3 describes the data sample, including the preparation of such a sample for use in the program and Chapter 4 explores any changes in size and shape that may occur as the mandible grows, concentrating on ages 9, 11, 13 and 15 years using this program. Whether or not differences exist between males and females in this data sample as regards mandibular growth is also investigated in Chapter 4 as is the usefulness of the harmonic information available from the EFF procedure for numerically describing size and shape changes of a complex irregular form. In addition, the validity and reproducibility of the data sample is also explored at this time. Chapter 5 turns to another method, Procrustes analysis. This method is applied to the same data sample and its usefulness as a size and shape descriptor is investigated and contrasted to EFF methodology.

1.5 Conclusion

This introductory chapter has established the background and motivation for such a study, from a dental point of view, as well as on a mathematical standpoint. Several methods that have been, and are currently used by various researchers in the mathematical description of size and shape of complex morphological forms have been described. However, all of the methods discussed are not without limitations in their use for describing the size and shape of a growing complex form and no one individual method is truly accurate and 'best'. This thesis aims to utilise one of those methods, the elliptical Fourier function (EFF), in describing a sample of 'normal' mandibles between the ages of 9 and 15 and contrasts this particular methodology in its quest to another, that of Procrustes analysis.

Chapter 2

Elliptical Fourier Function as a curve fitting tool

2.1 Introduction

This chapter gives a general introduction to the development of elliptical Fourier functions in the light of conventional Fourier analysis. A general overview of the actual elliptical Fourier function software that is used later in this thesis in an attempt to describe the size and shape changes of the human mandible for a data sample of mandibular outlines from age 9 to 15 years is then given. The hardware requirements for this particular EFF program are also outlined.

2.2 Review of Fourier function methodology

The main application of Fourier analysis in physics and mathematics is the study of complex waveforms, a procedure more commonly known as 'curve fitting'. Although this type of approach as a curve fitting tool has attracted criticism (Bookstein et al 1982, with replies from

Ehrlich et al 1983 and Read and Lestrel 1986), the applicability of Fourier series as a biometric curve fitting function is well established as a descriptive method of boundary outlines. Applications are diverse and plentiful using conventional Fourier analysis, as well as the newer elliptical Fourier function approach.

The development of elliptical Fourier functions can perhaps be better understood in the light of conventional Fourier analysis (Lestrel 1989a).

2.2.1 Conventional Fourier function

Before the development of the elliptical Fourier function (EFF), use was made of the conventional Fourier series as a curve-fitting tool to boundary outlines. This has been, and continues to be widely applied (Lu 1965, Ehrlich and Weinberg 1970, Kaesler and Waters 1972, Anstey and Delmet 1973, Full and Ehrlich 1982, Lestrel 1974, Lestrel and Brown 1976, Lestrel and Roche 1976, Gero and Mazzullo 1984, Johnson et al 1985, O'Higgins and Williams 1987).

Fourier analysis results in the decomposition of a periodic function into a series of sinusoidal waves of differing frequencies, composed of phases and amplitudes which, when summed, can reproduce an original form. The conventional Fourier series contains both sine and cosine terms and is often written in the familiar finite form

$$y = f(t) = A_0 + \sum_{n=1}^{k} a_n \cos(nt) + \sum_{n=1}^{k} b_n \sin(nt).$$

The a_n are the cosine components and the b_n are the sine components which describe the amplitude of cosine and sine waves (harmonics) at a particular frequency, given by n, and k is the maximum degree or harmonic number of the calculated series. The period is defined over a 2π interval. Often referred to as a single Fourier series, this is a convergent series that will provide a fit to any known piecewise-smooth function and as more terms (harmonics) are added, the function converges onto the measured boundary outline, allowing for a close and accurate representation of the measured form. The contribution that each term in the series makes toward the approximation of the function $y = f(t)$ can be separately assessed. The interval over which the data points are sampled and the height of the waveform, or amplitude, provide a flexible system that will fit many forms. The series is periodic, or 'circular', in the sense that it repeats over a set interval. That is, the last data point is followed by the first data point and the process is then repeated.

This definite form of the Fourier series can be represented in polar co-ordinate form by

$$y = f(\theta) = A_0 + \sum_{n=1}^{k} a_n \cos(n\theta) + \sum_{n=1}^{k} b_n \sin(n\theta)$$

where the period is defined over a 2π interval and θ is in radians. As above, k is the maximum degree or harmonic number of the calculated series and it is a convergent series that will provide a fit to any known piecewise-smooth single-valued function, converging on to the measured boundary outline as more terms are added, allowing a close and accurate representation of the measured form. The a_n and b_n are the Fourier coefficients for the k harmonics and the fit is improved as more terms are added in the series. It could be presumed then that terms should be added to the series expansion until a perfect fit is obtained. However,

the maximum number of terms taken in the series is subject to something called Nyquist frequency constraints. Viewed in a biological context this means that given n points on the outline of a form, the maximum number of harmonics attainable, k, is equal to (n-1)/2 if the number of points is odd, or n/2 if the number is even. The improvement in fit as the series is expanded with the addition of terms can be assessed by the computation of residuals between the observed data points and the expected values derived from the series expansion. As with the finite form, the separate contributions that each Fourier component makes to the form can be plotted. The first harmonic describes the contribution of an offset circle, the second describes a figure of eight (a two leafed rose), and the third, a three-leafed rose, and so on. In other words, any irregular single-valued form can be decomposed into a set of simpler components, or harmonics, which when summed, will re-create the outline. Also, the larger the magnitude of the amplitude associated with the harmonic number, the greater the contribution of that particular harmonic to the total form. The constant or A_0 term is defined as the mean of all observations, which is a circle in polar co-ordinates, defined as

$$A_0 = k^{-1}\sum_{i=0}^{k-1} r_i$$

where r_i are the observations or radii (distances from a predetermined origin, the centroid here) and k is the total number of measurements. The a_n and b_n coefficients are found by least squares estimation procedures, again subject to the Nyquist frequency

$$a_n = \frac{2}{k}\sum_{i=0}^{k-1} r_i \cos n\theta,\ n = 0,1,2,\ldots\ldots\frac{k-1}{2}$$

$$b_n = \frac{2}{k}\sum_{i=0}^{k-1} r_i \sin n\theta,\ n = 1,2,\ldots\ldots\frac{k-1}{2}$$

where the r_i are the observed measurements over the 2π interval.

Once the Fourier coefficients have been calculated, the amplitude, power and phase angle values associated with each harmonic number can be computed.

Besides the requirement of a function which accurately fits the sampled data points on the boundary of an outline, there are two other critical considerations that need to be resolved before complex biological shapes can be meaningfully compared. Since the shape of a particular form is generally thought to be what is left behind when the effects of location and rotation, as well as scale are removed, normalisation procedures are required to ensure that 'like with like' is being compared. Such normalisation procedures in the context of comparing the shape of objects have been referred to as positional-orientation and size-standardisation.

1. Positional-orientation (translation and / or rotation)

Positional-orientation consists of the orientation of the outline of any form in space (which has an effect on the initial phase angle of the first harmonic). In polar co-ordinates, we require that the centre from which the vectors are measured is common to all forms because the harmonic amplitudes are dependent on this centre. If the origin is changed, the amplitude values also change. A neutral centre such as the centroid (which is invariant with rotation) should be used. The translation of any object to the centroid is computed via a recursive process to ensure that equal angular intervals are preserved and new vectors computed to the observed points on the boundary, ensuring then that the shape as measured by the original vectors is faithfully maintained.

2. Size-standardisation

The size of an object has to be 'normalised' since the presence of substantial differences in size of any two or more forms may overwhelm any differences in shape. Three scaling factors have been suggested as normalisation approaches based on

a) the A_0 term - the use of a scaling factor based on the constant A_0 can be defined in polar co-ordinates as the mean of the vectors from the centroid to the outline of the form. It can be readily used as a scaling factor and the remainder of the coefficients are adjusted by multiplication of the factor, $\frac{\text{constant}}{A_0}$. Although rapidly computed, this has the drawback that if forms being compared differ considerably in shape, this scaling factor becomes inaccurate.

b) arc length or perimeter of the outline – using the perimeter as a scaling factor has a serious drawback if used directly since significant differences can arise. For example, consider one form which is smooth, and one which has multiple curves. The second will produce an unduly large perimeter in contrast to the smooth outline.

c) the actual area under the boundary outline of each form – an algorithm for the calculation of the area within the boundary outline, in polar form, based on integration by parts, can be found in Lestrel 1980. This scaling factor is more computationally involved.

Details of preferred normalisation procedures within the scope of this thesis whilst using the suite of EFF programs are discussed later.

In spite of its success as a shape descriptor, conventional Fourier analysis is thought to have some limitations, restricting the type of forms that can be successfully characterised. In practical terms, limitations with conventional Fourier descriptors include

1. equal divisions between points (equal angular divisions ones if dealing with polar co-ordinates) to avoid complications of a weighted analysis that is mathematically cumbersome
2. the use of a centre and a starting point on the boundary in polar co-ordinates, resulting in a dependency on the co-ordinate system, i.e. if the co-ordinates of the centre are changed and / or the starting point co-ordinates then the harmonics change in value – the method is not co-ordinate free
3. the presence of complex forms requiring multi-valued functions for a satisfactory fit (arises when outlines curve back on themselves)
4. integration is required for the evaluation of the Fourier coefficients

These restrictions tend to limit the use of conventional Fourier analysis to comparatively simple classes of two-dimensional forms.

2.2.2 Elliptical Fourier Function (EFF)

The development of the EFF procedure is attributed to an algorithm devised by Kuhl and Giardina 1982 as a method to scan rapidly and identify incoming aircraft. In more recent times, is thought to be a significant step forward in the quest for a method that efficiently captures boundary outline information of complex biological forms. The transition to EFF

methodology effectively removes the limitations of the conventional Fourier series, thereby allowing for an analysis of a much larger class of two-dimensional forms (Rohlf and Archie 1984, Ferson et al 1985).

The elliptical Fourier function (EFF) represents a parametric formulation in the sense that the x- and y-directions are separately set up as functions of a third variable t. The requirement of equal divisions along the outline is now relaxed and multi-valued functions are no longer a problem. Further, the parametric EFF coefficients can now be generated using an algebraic approach, instead of the integral solutions required in the conventional series, which makes computation simpler and faster.

The EFF is then, derived as a parametric formulation from conventional Fourier analysis, composed of sine and cosine terms in Cartesian coordinates, set up as a pair of equations for x and y, as functions of a third variable t. These parametric functions are defined in x(t) as

$$x(t) = A_0 + \sum_{n=1}^{k} a_n \cos(nt) + \sum_{n=1}^{k} b_n \sin(nt)$$

and in y(t) as

$$y(t) = C_0 + \sum_{n=1}^{k} c_n \cos(nt) + \sum_{n=1}^{k} d_n \sin(nt)$$

where n equals the harmonic number, k is the maximum number of harmonics and the interval is over 2π as before. Kuhl and Giardina 1982 have derived estimates for the elliptical Fourier coefficients (a_n, b_n, c_n, d_n) that do not require integrals. These Fourier coefficients for the x-projection are

$$a_n = \frac{1}{n^2\pi}\sum_{p=1}^{q}\frac{\Delta x_p}{\Delta t_p}\left[\cos(nt_p) - \cos(nt_{p-1})\right]$$

and

$$b_n = \frac{1}{n^2\pi}\sum_{p=1}^{q}\frac{\Delta x_p}{\Delta t_p}\left[\sin(nt_p) - \sin(nt_{p-1})\right]$$

where q is the total number of points along the outline of the form, n is the harmonic number (to a maximum of k), t_p is the distance between point p and point p+1 along the outline, and x_p and y_p are the respective projections of the segment p to p+1. Similarly, the Fourier coefficients for the y-projection are

$$c_n = \frac{1}{n^2\pi}\sum_{p=1}^{q}\frac{\Delta y_p}{\Delta t_p}\left[\cos(nt_p) - \cos(nt_{p-1})\right]$$

and

$$d_n = \frac{1}{n^2\pi}\sum_{p=1}^{q}\frac{\Delta y_p}{\Delta t_p}\left[\sin(nt_p) - \sin(nt_{p-1})\right].$$

Besides the four coefficients a_n, b_n, c_n, d_n that need to be evaluated, the two constants, A_0 and C_0 also need to be estimated. These are computed from

$$A_0 = \frac{1}{2\pi}\sum_{p=1}^{q}\frac{\Delta x_p}{2\Delta t_p}\left[t_p^2 - t_{p-1}^2\right] + \alpha_p\left[t_p - t_{p-1}\right]$$

and

$$C_0 = \frac{1}{2\pi}\sum_{p=1}^{q}\frac{\Delta y_p}{2\Delta t_p}\left[t_p^2 - t_{p-1}^2\right] + \beta_p\left[t_p - t_{p-1}\right]$$

where the α_p and the β_p terms are derived from

$$\alpha_p = \sum_{j=1}^{p-1}\Delta x_j - \left[\frac{\Delta x_p}{\Delta t_p}\sum_{j=1}^{p-1}\Delta t_j\right]$$

and

$$\beta_p = \sum_{j=1}^{p-1} \Delta x_j - \left[\frac{\Delta x_p}{\Delta t_p} \sum_{j=1}^{p-1} \Delta t_j \right].$$

Kuhl and Giardina's paper give details of all the above formulations.

Once the expected x and y co-ordinates have been separately computed using the above equations, they can be rejoined (for identical values of t) and the expected shape recreated.

Each harmonic in the series is described by four coefficients then (a_n, b_n, c_n, d_n), as well as the two constants A_0 and C_0. If the separate harmonics are plotted, they produce ellipses and the four coefficients account for the size, angulation and displacement of the starting point of the ellipse. The harmonic ellipse's angle of rotation and starting point, in turn, depend on the angle of rotation and starting point of the outline of an object (Kuhl and Giardina 1982). An approximation of the original outline can then be obtained by summing, in an identical fashion to the conventional Fourier function, the contributions of all harmonic ellipses included in the series. Again, the maximum number of harmonics used in describing complex forms using the EFF method are subject to Nyquist frequency restrictions and therefore cannot exceed half the number of points located on the outline of the form.

Once the EFF's have been generated, there is again the question of the goodness of fit to the observed form. Since the EFF represents a convergent series it is simply a matter of summing enough terms in the series (harmonics) to ensure a satisfactory fit (subject to Nyquist frequency restrictions). As with conventional Fourier analysis, computing the residual or

difference between the observed data points and their expected or predicted values derived from the EFF can test the goodness of fit.

Also, as with conventional Fourier analysis, objects must be normalised for size and orientation before meaningful comparisons can be made. Details of the preferred normalisation procedures within the scope of this thesis whilst using the suite of EFF programs are discussed later.

Finally, another of the early criticisms of conventional Fourier analysis, the fact that homology of points across forms was lost has been dealt with the use of elliptical Fourier functions. Homology is now maintained by a specific computational procedure in the EFF program used in this thesis. The first homologous predicted point is computed to be at the same location on the Fourier approximating (interpolating) function as the first digitised point is on the digitised form (observed data file). The second and subsequent homologous predicted points are computed so that they have the same arc length from the first computed point as their counterpart (pseudo-) landmarks do from the first digitised point on the original, digitised curve. This maps the pseudo-landmark points from the digitised curve onto the EFF (Wolfe 1997). This is equivalent to shifting the observed co-ordinates of the polygonal representation of the form, onto the EFF curve (Lestrel and Huggare 1997). This shift is quite small since it is incumbent upon the investigator to keep the residual, the difference between the observed points and the predicted points derived from the EFF, as small as practically possible. Mean values based on all points should not rise above 0.10-0.20 mm, i.e. these values need to be well below the errors

arising from locating the points, tracing the cephalograms and digitising. The EFF software maintains the homology of the points, and hence, maintains the homology of the entire form. These points are termed pseudo-homologous, after the suggestions of Sneath and Sokal 1973. The application of this technique to cephalometry has been described in some detail by Lestrel (1997b) and Lestrel and Kerr (1993).

In this thesis the elliptical Fourier function method described above is utilized in an attempt to describe the size and shape changes of a sample of growing human mandibles between the ages of 9 and 15 years. The exact methodology used in describing complex forms of the craniofacial complex, like the mandible, is explained in a number of papers by Lestrel, including Lestrel 1989a and b.

Using a dedicated suite of programs developed by Professor Lestrel and colleagues, attention is now drawn to the specific description of the growing mandible in order to discuss issues in using elliptical Fourier function methodology on a real set of data.

2.3 Overview of EFF Software

2.3.1 Summary

The purpose of this software is to provide an approach aimed at the numerical description of complex irregular forms, particularly shape as distinct from size so as to facilitate comparisons between forms. It is a suite of routines that aid in fitting elliptical Fourier functions (EFF) to boundary outline data of complex irregular forms, like the mandible. A summary of the routines available in the EFF software is shown in Figure 2.1 and discussed below.

The EFF approach begins with the original outline of the object one wishes to describe, known as a specimen, which is characterised by a set of closely located points. It is useful to note that a specimen could be a tracing of the actual object itself or an x-ray of the actual object or a tracing of an x-ray of the object i.e. some representation of the real object. Once the specimen has been prepared the initial step is to digitise the points which characterise the outline to be entered as (x,y) co-ordinates to the elliptical Fourier function program. A digitised data file is created, known as the observed form, which is simply a digitised representation of the specimen.

After digitisation, the next step is to compute the EFF and predicted points. These elliptical Fourier functions provide a very close fit to the original data points i.e. a close

predicted fit to the observed (digitised) form. The observed form generated in the digitising process is fitted with points computed from the elliptical Fourier function, known as a computed or a predicted form. The goodness of fit of this predicted outline can be tested by the calculation of residuals (the difference between the original (digitised) data points and the expected (predicted) values from the elliptical Fourier function). If this residual is acceptable, then the original (digitised) data can be theoretically thrown away and replaced by the elliptical Fourier function that now serves as an analogue of the original form. The predicted form only 'lives' as a computerised representation of the real object then (the specimen), which is the tracing of the mandible from the lateral skull radiograph in this thesis. It is important to emphasise that the predicted form must be a close representation or analogue of the specimen for accurate results. The resulting (x,y) co-ordinate points of this close representation can be compared between forms to investigate where there might be differences.

The area and centroid values of each predicted form are also computed at this time for use in further analyses. The area of a form is needed to perform size-standardisation; the centroid, to compute distances from centroid to boundary and for superimposition of forms for visual comparison.

As discussed previously, elliptical Fourier functions (as well as the conventional Fourier series) are dependent on spatial relationships within a Cartesian co-ordinate system. In the context of the EFF suite of programs, this dependency must be taken into consideration if

forms are to be meaningfully compared. The same two possibilities have to be considered i.e. positional-orientation and size-standardisation.

Kuhl and Giardina 1982 suggest the use of the form itself to generate an internal positional-orientation for comparison by rotating the form until the major axis of the first harmonic ellipse is parallel to an axis. By orienting the first ellipse in this manner, the higher-order ellipses are also oriented, which results in the actual form being oriented. This same procedure has been utilised by Professor Lestrel in the elliptical Fourier function software, where the form is rotated until the major axis of the first harmonic ellipse is parallel to the x-axis. Oriented files of this nature were not however considered in this thesis (this part of the program did not actually operate accurately at the time of analysis). In the context of this thesis, 'no positional orientation' implies that we have defined the orientation of each individual form on predefined biological criteria to standardise for orientation, discussed in section 2.3.3.

In order to standardise each form for size, Kuhl and Giardina 1982 recommend scaling the length of the semi-major axis of the first harmonic ellipse so that it is equal to 1 and adjust the remaining coefficients accordingly. This is however only an approximation. Another way of standardising for size is available, which is the one used in this thesis, is outlined in section 2.3.3.

In this suite of programs, files that contain data that have had size information effectively minimised, leaving only shape information behind can be created. These are referred to as

area-standardised or size-standardised files. If such files are created, they are treated as if they are original digitised data files, even though, strictly speaking, they are not. Additionally, files can be created which have been positionally-oriented with respect to the co-ordinate system, known as oriented files (and these files can also be area-standardised).

Once the elliptical Fourier function has been computed, the predicted form (and size-standardised predicted form) can be described using the harmonic coefficients from the EFF and the predicted data points themselves. In addition, a number of other files can be created and other measures computed, and used to explore the fitted forms. These include computation of harmonic amplitudes, power and phase angles of the functions, as well as ellipse parameters, distance functions and descriptive statistics of the predicted EFF. However, although the suite of programmes is able to produce all this information, we will see in Chapter 4 that only a limited amount is utilised in the description of a complex form such as the mandible.

The raw data can also be viewed by plotting the observed form as traced and digitised from the original specimen, as well as being able to plot the predicted outlines computed from the EFF and other related information.

Additionally, much of the computed data can be exported for future use in spreadsheets statistics programs or plotted with graphics software.

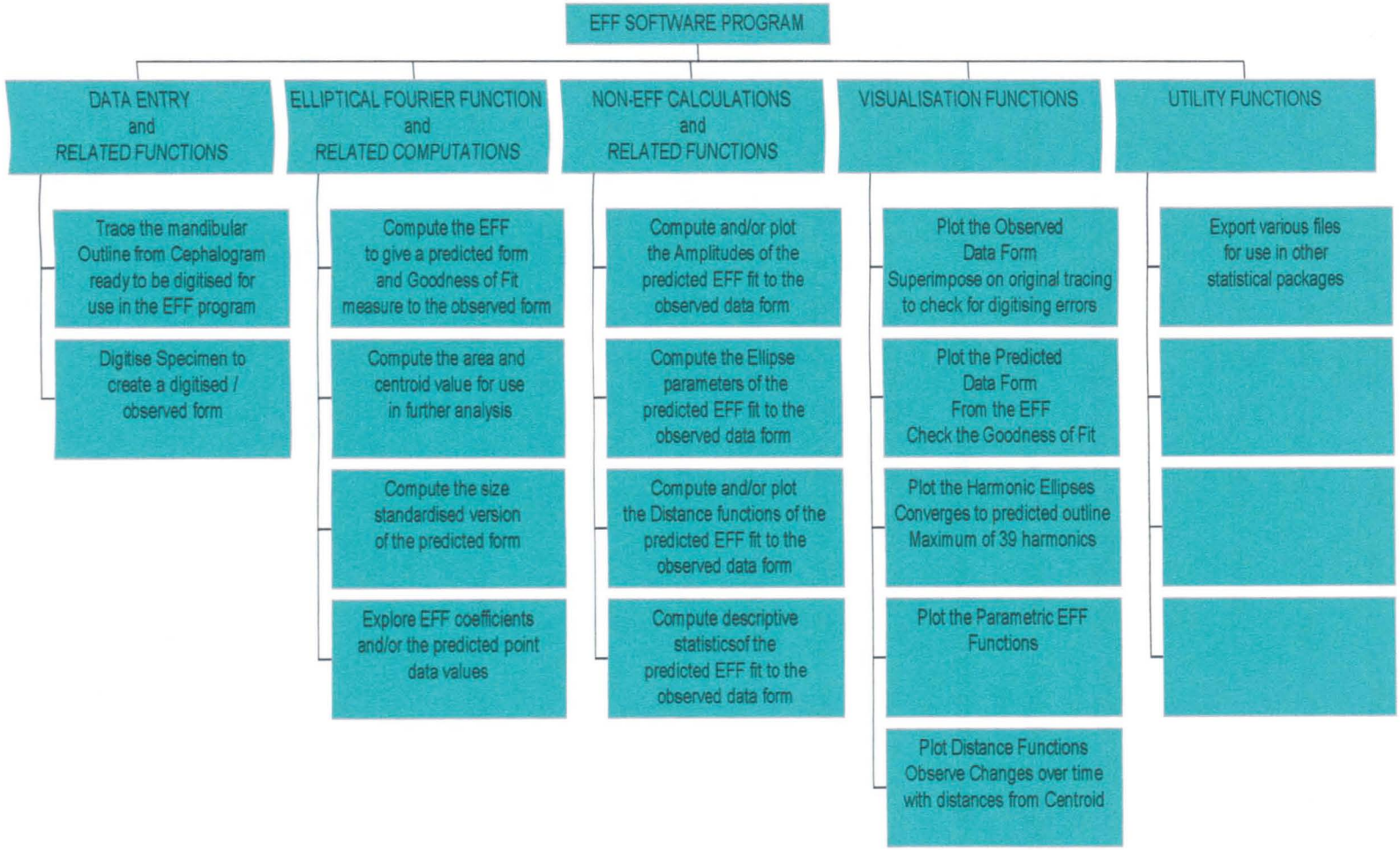

Figure 2.1 **Summary of available routines in the EFF software.**

2.3.2 Observed (digitised) Data Points

The elliptical Fourier function (EFF) approach begins then with a set of closely located points which characterise the outline of any complex morphological form. In the case of our real set of data described in the next chapter and analysed using this software in Chapter 4, this is a tracing of a mandible from a lateral skull radiograph, made up of 78 points. These points, ideally if not always in reality, should be homologous i.e. a 1:1 mapping between different specimens for direct comparison. If the outline contains sharp curves then the more points may be required, particularly at sharp corners in a form like the lower incisor or the condylar / mandibular notch areas of the mandible. Once the tracing has been prepared the initial step is to digitise each point located on the tracing of the original specimen (the tracing of the mandible from a lateral skull radiograph here) to be entered as (x,y) co-ordinates to the elliptical Fourier function program and plotted. The plotted outline at this stage is our observed (digitised) outline. A quick superimposition of each observed form on each original tracing of the radiograph checks for any digitising errors. Digitising then, results in the observed (digitised) analogue of the original specimen, the tracing of the mandible in this case.

2.3.3 Normalisation Procedures

As mentioned previously, before meaningful comparisons can be made in terms of the shape of objects, the forms have to be normalised for size and orientation. Within the context of this thesis and the way the EFF suite of programs were applied, size and

shape changes and shape changes only between objects were investigated and the way in which objects were 'normalised' were dealt with as follows:

1. Size and shape changes: The original, unaltered digitised data was oriented according to predefined criteria. The original tracings were orientated in exactly the same position to be digitised according to predefined biological criteria using the maxillary plane as an aid to comparable registration of each observed form (a line drawn from Anterior Nasal Spine to Posterior Nasal Spine (ANS - PNS)).
2. Shape changes only: The original, unaltered digitised data was oriented according to predefined criteria and standardised for size. In order to size-standardise a form, the size of the form is computed and then standardised. Size is defined to be area in this system and is computed as a line integral using Stokes' and Green's Theorems. Because of the mathematics involved i.e. the line integral, this is done from the predicted points file of the original specimen (the predicted points file of the observed, digitised data) instead of the actual observed data. This insures that the area is computed accurately, provided a sufficient number of harmonics have been taken. The size-normalised digitised point file is computed using the area bounded by the polygon from this predicted points file and then each size normalised file is 'blown-up' to fill a 10000 square unit area. Further, since it has been computed from the predicted points file, it will contain the same number of points. The resulting size-standardised file is considered to be an observed (digitised) size-standardised file because it is created in a fashion identical to the digitised file based on the original data. The resulting figures have had size effectively minimised and shape information retained. A series of forms can then be compared on the basis of shape only and size will not unduly affect the comparisons. The various measures used to work out these size-standardised forms

are available from the program if required, i.e. the bounded area of the observed form, the area correction factor (10000/area), the square root of the area correction factor, and the x- and y-centroid values.

It is necessary to generate appropriate size-standardised 'digitised', observed data files before size-standardised elliptical Fourier function curve fits can be obtained, either as size-standardised harmonics or predicted points. Orientation is dealt with automatically at the digitisation stage as per above. The suite of programs available can then be followed in an identical manner for the original, observed (digitised) data, as well as the size-standardised, observed (digitised) data.

2.3.4 Computation of Elliptical Fourier Functions (EFF)

Once the observed (digitised) data points have been submitted to the EFF program (and a size-standardised version computed also), the next step is to compute the Fourier descriptors (elliptical Fourier functions) for each specimen i.e. each mandible, from the parametric formulation of the conventional Fourier function where the parametric equations are defined in x(t) and y(t) (as before in section 2.2.2) as

$$x(t) = A_0 + \sum_{n=1}^{k} a_n \cos(nt) + \sum_{n=1}^{k} b_n \sin(nt)$$

$$y(t) = C_0 + \sum_{n=1}^{k} c_n \cos(nt) + \sum_{n=1}^{k} d_n \sin(nt)$$

Computations in the elliptical Fourier function program produce, in particular, two kinds of data files

1. the calculated or predicted data points file from the elliptical Fourier function (which fit either the original (digitised) form, or the size-standardised form).

and

2. elliptical Fourier function harmonic coefficients file (again, for the original (digitised) form, or the size-standardised form)

These will now be dealt with in turn.

2.3.4.1 Predicted Data Points

Two different sets of predicted points can be computed

1. a set of evenly spaced points about the figures boundary as for conventional Fourier analysis
2. a set of homologous points – as discussed previously, the distances between the points can now vary unlike with the conventional Fourier series. Predicted data points of this type are used in this thesis.

Homologous points can be thought of as a way to force a set of computed points derived from the elliptical Fourier function solution to closely maintain their spatial relationship with the original set of digitised points, or observed form. Enough homologous points are required on the outline of the form together with sufficient intermediate points inserted, so that a smooth plot can be produced. The location of each homologous point on the elliptical Fourier function curve is computed by taking it to be the same distance from the beginning of the curve as the observed (digitised) point is from the beginning of the digitised curve. Therefore, the points will have

equal arc lengths on their respective curves. The homologous points therefore mirror the observed data and thus will have the same point number on each set of observed (digitised) figures and their corresponding computed figures for a given set of specimens (tracings of x-rays of mandibles here). This is necessary for performing distance and statistics computations and comparing specimens. When homologous points are being computed, the number of predicted points computed is determined by the equation

Number of predicted points = (Number of digitised points)
+ (Number of intermediate points)
* (Number of digitised points)

The same number of intervals between points on the boundary of a specimen must therefore be specified for all forms that are to be compared. This does not matter in the context of this thesis however since the mandibular outline is characterised by 78 points which does not require additional intermediate points to give a smooth representation of the specimen.

Using the parametric equations above to compute a predicted outline for the mandible, whilst preserving homology, the elliptical Fourier functions are able to provide a very close fit to the original data points (see Chapter 4). The closer the spacing of the observed points, the more accurate the representation. In technical terms, the observed form is treated as a polygon where the closely located adjacent points on the periphery have been connected with straight-line segments. Any two dimensional outline can be approximated with a polygon by connecting the observed data points with straight lines.

2.3.4.2 Harmonics (computation of elliptical Fourier coefficients)

As well as the predicted points files (area standardised or not), harmonic coefficient files can also be created from the elliptical Fourier function.

As previously mentioned, the number of harmonics used in describing any complex forms with the elliptical Fourier function method are subject to Nyquist frequency restrictions and cannot exceed half the number of points located on the outline. The numerical description of the mandible using this pair of equations, consists of 158 separate terms; 39 harmonics (since the mandibular outline is characterised with 78 points) multiplied by the 4 harmonic coefficients (a_n, b_n, c_n and d_n), plus the 2 constants A_0 and C_0.

These elliptical Fourier functions represents a convergent series solution being fitted to the polygon (the observed (digitised) mandibular outlines) and as more terms (harmonics), are taken in the series, the closer this convergence and the better the predicted curve fit.

The first few harmonics measure the global aspects of the bone, while the higher harmonics are responsible for the more localised sculpturing of the outline. When dealing with a specific mandibular outline (as with others in the sample) as seen in Chapter 4, it would seem that the elliptical Fourier function could be truncated at 15 / 20 harmonics, which still ensures a satisfactory fit to the bone. If the EFF is truncated at 20 harmonics, the form would still be accurately captured, and a matrix of 80 separate terms, 4 coefficients for each harmonic and 2 constants for each function (equation) would be required.

2.3.4.3 Computation of Residuals

Once the Elliptical Fourier Function has been computed, for the desired number of harmonics, the goodness of fit of the predicted mandibular outline can be tested by the calculation of residuals. The mean residual error is defined to be the mean Euclidean distance between a set of computed points on the curve and their corresponding digitised or observed points. That is, the goodness of fit of the predicted form computed from the elliptical Fourier function to the original, observed form i.e. the difference between the original (digitised) data points and the expected (predicted) values computed from the elliptical Fourier function. If this residual is found to be small enough (< 0.5mm for anatomical work is acceptable) then the observed (digitised) data could be, theoretically thrown away and replaced by the elliptical Fourier function which now serves as an analogue of the original form, which was traced and digitised from the original x-ray of the mandible.

2.3.5 Amplitude and Related Computations

Once the EFF coefficients have been computed, they can be used to calculate amplitudes, power and phase angles. These are useful as abstract measures of shape change from the elliptical Fourier function fit of the observed form.

2.3.5.1 Amplitudes

The elliptical Fourier function coefficients can be used to compute amplitude estimates where the value for the nth harmonic is

$$a_n = \sqrt{(\alpha_n^2 + \beta_n^2)}$$

where the α's are the coefficients preceding the cosine terms and the β's are the coefficients preceding the sine terms.

The amplitude, or height of the wave, is then, the square root of the sum of the squared coefficients preceding the cosine and sine terms for each harmonic. These are separately computed for the x- and y-axes. The larger the amplitude the more that term plays a major part in the shape of the form.

2.3.5.2 Power spectrum (raw power or variance)

The raw power or variance of the nth harmonic is defined to be

$$S_n^2 = (\alpha_n^2 + \beta_n^2) / 2 = (\text{amplitude}_n^2) / 2$$

where the contribution that each harmonic makes to the variance (%) i.e. the percentage variation explained by the nth harmonic is defined as

$$\%Explained = \frac{S_n^2}{S_T^2} = \frac{power\ for\ the\ nth\ harmonic}{power\ for\ all\ harmonics}$$

2.3.5.3 Phase angles

The phase angle of the nth harmonic is

$$\Phi_n = \tan^{-1}(\frac{\beta_n}{\alpha_n})$$

Amplitudes, power spectra and phase angles can all be plotted as an aid to assessing shape changes of complex forms. Plots of amplitude versus harmonic number are considered further in Chapter 4.

2.3.6 Ellipse Parameters

A set of parameter values associated with the elliptical Fourier function ellipses can also be computed. There are two options within the suite of programs:

1. only parameter values associated with the 1st ellipse are calculated
2. a set of parameter values associated with the 1st and subsequently higher ellipses are computed

where

a. the angle that the ellipse makes with the x-axis (always measured in an anti-clockwise direction)
b. the lengths of the major and minor axes of the ellipse
c. their ratios
d. the area of the ellipse
e. the natural log of the ellipse area

f. the base 10 log of the ellipse area

g. a specialised estimate of the area of the ellipse derived from Diaz et al 1990 can also be calculated.

These estimates can be viewed and compared between (harmonic) ellipses and specimens. The differences in the 1st ellipses between specimens could also perhaps be statistically evaluated.

2.3.7 Distance Computations

Where amplitudes, power and phase are useful abstract measures of shape change, the calculation and plotting of distances provide a more direct visual assessment of shape change. Three types of distances can be computed in the context of the EFF suite of programs.

2.3.7.1 Distance from the centroid

The distances from the centroid of the form to each predicted point on the boundary outline can be calculated. These distances can be exported, plotted and compared between specimens at different ages and between sexes. Plots of the centroid to outline distances are considered in Chapter 4.

Since it is necessary to compute a reasonably large number of closely spaced points on the specimen outline for accuracy between observed and predicted form from the

elliptical Fourier function, a large set of distances from the centroid to the outline are also generated, 78 in the case of the mandible used in this thesis. The points characterising the boundary outline by their very nature however, will be highly correlated and therefore the computed distances from the centroid will have high correlations between them. Modified distance measures called Section Mean Distances are calculated in order to try and compensate for this, where the entire form can be considered as one section, and divided up into a chosen number of sections and a mean distance computed for each section, rather than computing every distance from centroid to outline. These distances can be plotted in a similar manner to the distances from the centroid. Alternatively, we can also choose to concentrate only on the 19 anatomical landmarks on the boundary outline of the mandible.

2.3.7.2 Distance from a vertical base line to the soft and hard tissue profile

These distances are calculated from a vertical base line to the soft and hard tissue profile as depicted on either a photograph or radiograph. This is a special case used in dental research, and not considered further in this thesis.

2.3.7.3 A pseudo-distance measure

This so-called pseudo-distance measure is composed of differences in distances computed as differences between predicted forms using one form as a base and the other as a target. The purpose here is to generate summary measures of the percentage contributions of the separate components of size and shape. This was not considered further in this thesis.

2.3.8 Some statistical measures

The EFF suite of programs also allows for the calculation of

1. means
2. standard deviations (s.d)
3. standard error of the mean (sem)

for

a. observed points
b. predicted points
c. harmonic coefficients
d. amplitude, power and phase angles
e. distances; centroid to boundary, plus x and y components and also section mean distances.

2.3.9 Exporting Data

The resulting data from the EFF suite of programs can be exported for use in other packages.

Exporting the data results in a file containing certain records that are the actual data (often separated by commas that may have to be stripped out) as well as any header lines. This is useful in that the data can be manipulated further in more powerful plotting and statistical packages.

2.3.10 Plotting the Data

The plotting modules within the EFF suite of programs are useful for a variety of purposes. Certain files can be plotted and visualised on screen, or printed directly, or exported for manipulation in other plotting and statistical packages. These include:

1. the original digitised data which can be superimposed on the actual observed data i.e. tracing of the lateral skull radiograph of the mandible to detect for presence of digitising errors
2. the computed elliptical Fourier function, i.e. the predicted points form upon which the observed (digitised) form can be overlaid to see how well the EFF fit the observed data
3. the convergence of the EFF series as more harmonics are added to the function
4. the separate ellipses for each harmonic to see the effect (in terms of magnitude and direction) they have on the form
5. the individual as well as mean curves of the predicted outlines from the computed elliptical Fourier functions
6. the x(t) and y(t) functions - usually with predicted data - plots how the Fourier wave form looks along the x- and y-axis before being parametrically joined to for the fitted object since these are predicted points computed from the final summation of all the ellipses
7. distances for comparisons between different ages of the same specimen etc

2.4 Hardware Requirements

The EFF suite of programs outlined above is designed to process series of x,y (or x,y,z) co-ordinate points. It supports the Housten Instruments HIPAD and the Summagraphics SUMMASKETCH III digitisers, and those fully compatible with them. For plotting, it supports HEWLETT-PACKARD HP7470 (two pen) or HP7475A (six pen) plotters, or LASERJET III printer or other true PCL5 language compatible printers. The program requires 1.6 megabytes of free hard disk space and will run on an IBM PC or compatible running PC with MS DOS 3.1 or later.

2.5 Conclusion

Conventional Fourier analysis, as well as elliptical Fourier function methodology has been introduced in this chapter where the benefit of using EFF as a curve fitting tool has been outlined. Related features between the two methods have also been addressed such as Nyquist frequency limitations and normalisation issues.

An overview of what the EFF suite of programs can produce has been described and the practical issues of implementation have been discussed with a more detailed exploration of each individual component. Some of the more useful components of the program are utilised and illustrated in Chapter 4 in an attempt to describe size and shape changes in the human mandible for a sample of subjects between 9 and 15 years. In the past, these form alterations have generally not been partitioned into size and

shape changes when it would seem apparent that the existence of large size increases can confound the recognition of changes in shape. By standardising for size, shape differences become clearly evident and the EFF method facilitates the analysis of these separate components of a complex form.

Chapter 3

The Data Sample

3.1 Overview and Introduction

There have been numerous studies involving the growth of the craniofacial complex in humans and many animal studies. Much has been gained from these studies, providing a wealth of knowledge on the way in which bones grow, at what rate they grow, and what influences growth. The use of more traditional methods and measures like cephalometric analysis in such studies has contributed to this knowledge but there remains a gap in the mathematical quantification of changes in a growing complex form, like the mandible. Also, few of the investigations have dealt directly with size and shape description of a growing mandible and many past studies were not longitudinal in nature, were based on small sample sizes and were limited to comparatively few measurements. It is one of the aims of this thesis to add to and / or corroborate current knowledge in the literature, specific to human mandibular size and shape description, for a particular sample of data. In this chapter, the way in which such a sample of data was selected and prepared for subsequent description using numerical methods is described.

3.2 *A Sample for Analysis*

3.2.1 Origin of data sample

A longitudinal sample of archive lateral skull cephalograms (x-rays) from the B.C. Leighton Growth Study that was started in the early 1950's at Kings College School of Medicine and Dentistry, London, were made available for analysis. Professor Leighton collected an impressive amount of data in this growth study, where his study sample initially comprised of 550 British white Caucasians, of both sexes, born at the King's College Hospital Maternity Department, London. Such data included study models, clinical recordings of skeletal class, incisor class, height and weight measurements as well as lateral skull head films and a wealth of other associated data on familial problems of dentition, sucking habits, swallowing behaviour etc. By 1971 the sample had reduced to approximately 90, from which the sample used in this thesis was extracted. A duplicate set of study models and lateral skull cephalograms compiled by Professor Leighton, was obtained by The Royal College of Physicians and Surgeons of Glasgow, through the TC White bequest fund, and stored in the Glasgow Dental Hospital and School.

The sample utilised in this thesis consisted of the lateral skull cephalograms (an example of which is included in the Appendix) of 84 subjects each x-rayed annually on their birthday, as far as possible, from around the age of 2 years, through to the age

of 20 years. An illustration of a picture typically used in dental literature as a representation of such a x-ray is given in Figure 3.1 (a) and (b).

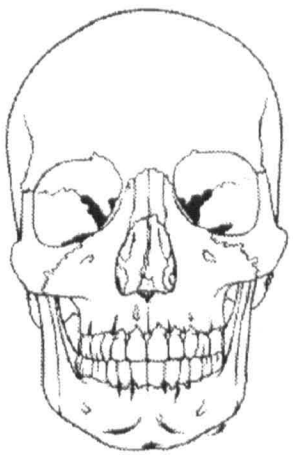

Figure 3.1a **A typical illustration of the location of the mandible. Antero-posterior view.**

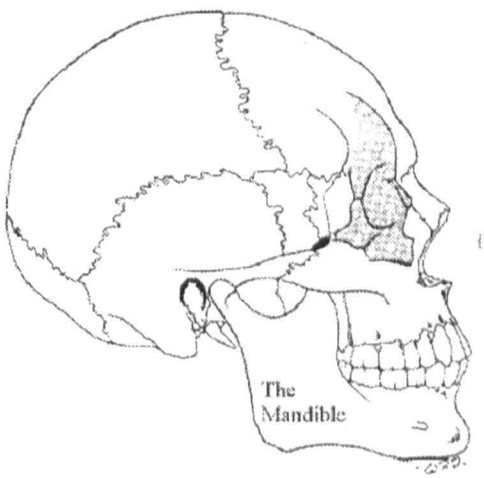

Figure 3.1b **A typical illustration of the location of the mandible. Lateral view.**

3.2.2 Description of the age & sex distribution of x-rays in the sample

Of the initial 84 subjects available for analysis, as illustrated in Tables 3.1 and 3.2, 47 subjects were male and 37 were female. It can be seen that not all x-ray films were available at each age for each subject. Further, of the films that were available, some were of such poor quality they had to be discounted and considered unavailable (labelled as IRad = inadequate radiographs in the tables). Some of the subjects had also undergone orthodontic treatment (labelled as OPat = orthodontic patient in the tables). Of the males, 9 subjects had received some sort of orthodontic treatment during the study period, 7 did not have adequate radiographs, and 3 subjects had both undergone orthodontic treatment as well as not having adequate radiographs. This resulted in 37 potential males for analysis, on the basis that the films were considered adequate enough for tracing. Similarly for the females, 11 had undergone orthodontic treatment, 4 did not have adequate radiographs, and 3 subjects had both undergone orthodontic treatment as well as not having adequate radiographs which resulted in 30 females who could potentially be included in any analyses, again on the basis that the films were considered adequate enough for tracing.

From this set of 37 males and 30 females, a further sub-sample was identified for analysis.

Leighton ID	Age																				Notes
2			4		6	7	8	9	10	11	12	13		15		17	18		20	21	Irad
18			4	5	6	7	8	9	10		12	13	14	15	16	17	18	19	20		OK
37			4		6		8	9		11	12		14	15	16	17	18	19	20		OK
79				5		7	8	9	10		12	13	14	15	16	17	18				OK
87			4	5	6	7			10	11	12	13	14		16	17	18		20		Opat
111			4	5	6	7	8	9	10	11	12	13	14	15	16	17	18	19			OK*
116				5	6	7	8	9	10	11		13		15	16	17	18	19			OK*
128			4	5	6	7	8	9	10	11	12	13	14	15	16	17	18	19	20		OK*
141		3		5	6	7		9	10		12	13	14	15	16	17					OK
145			4	5	6	7	8	9	10		12	13	14	15	16	17	18				OK
154		3		5	6	7	8	9	10	11	12	13		15		17		19	20	21	OK*
156										11	12	13	14	15	16	17	18	19			OPat, IRad
175			4		6	7	8	9	10	11	12	13	14	15	16	17	18	19		21	Opat
178				5	6	7	8	9		11	12			15	16				20	21	OK
222			4	5		7	8	9	10	11	12	13		15	16	17					Opat
241			4	5		7	8				12			15	16		18	19	20		Irad
253		3		5	6	7	8	9	10	11			14	15	16	17	18	19		21	OK
266		3		5	6	7	8		10	11	12	13	14	15	16	17	18				OK
271		3		5			8	9			12		14	15		17					OPat, IRad
275		3		5	6	7	8	9	10	11		13	14	15	16	17	18	19			Opat
281		3		5	6	7	8			11	12	13	14	15	16	17	18	19		21	Opat
301		3		5	6	7	8	9	10	11	12	13	14	15	16	17	18	19			Opat
319				5	6	7		9	10	11	12	13	14		16	17	18	19			OK
327					6	7	8	9			12	13	14	15	16	17					Opat
342		3			6	7	8	9	10	11	12	13	14	15	16	17	18	19	20	21	Irad
343				5	6	7	8	9	10	11	12	13		5	16	17	18				Irad
398			4	5	6	7	8	9	10	11	12		14	15	16	17	18	19			OK
419			4			7	8		10	11		13		15	16	17	18				OK
454			4	5	6	7	8	9	10	11	12	13	14	15							OK*
456				5	6	7	8	9	10	11		13	14	15	16	17	18	19			OK*
468				5	6	7	8		10	11		13	14	15		17	18	19	20		OK*
469		3	4	5	6	7	8	9	10	11	12	13	14	15	16	17					OK*
490		3	4	5		7	8	9	10	11	12			15	16	17			20		Opat
495		3			6		8	9	10	11	12	13	14	15	16		18				OK*
507		3	4	5	6	7	8	9	10	11	12	13	14	15	16	17	18		20		OK*
521			4	5	6	7		9	10	11		13	14	15	16	17	18				OPat, IRad
543						7	8	9	10	11	12		14	15	16	17	18	19	20		OK
564					6	7	8	9	10		12	13	14	15	16	17	18	19			OK
566	2	3	4	5	6	7		9	10		12	13	14	15	16	17		19			OK
586		3	4	5		7		9	10	11	12	13	14	15	16	17	18				OK*
594	2	3	4		6	7	8	9			12		14	15	16					21	Opat
599		3	4	5	6	7	8	9	10		12	13	14			17					Irad
600						7	8	9	10		12	13	14	15	16		18	19			Irad
601			4		6	7	8			11	12		14	15	16						Irad
612		3	4	5	6	7			10	11	12	13	14	15		17					OK
632		3	4	5				9	10	11	12	13		15		17	18	19			OK*
645	2		4	5	6		8	9	10	11	12	13	14	15		17					OK*

Table 3.1 Males in the sample of 84 subjects : Which films are available?

Leighton ID	Age																				Notes
31				5	6	7	8	9	10	11	12	13	14	15	16	17	18	19	20		OK*
35				5	6	7	8	9	10	11	12	13	14	15		17		19			Opat
38			4	5	6	7	8	9	10	11	12	13	14	15	16	17	18	19	20		Opat
54				5	6	7	8	9	10	11	12	13	14	15	16	17		19	20		OK*
66			4	5	6		8	9	10	11	12	13	14	15	16	17	18	19	20		OK*
67				5			8	9	10	11	12	13			16	17	18	19		21	OK
118		3	4	5	6	7	8	9	10			13	14	15	16	17	18	19		21	OK
120				5	6	7	8	9	10	11	12	13	14	15	16						OK*
122			4	5	6	7	8	9	10	11		13	14	15	16	17	18	19		21	OK*
124		3			6	7	8	9	10	11	12	13	14	15	16	17	18	19	20	21	Opat
126			4	5	6	7		9	10	11	12	13	14		16	17	18				Opat
132			4	5	6	7	8	9	10		12	13	14	15	16	17	18	19			OK
161			4	5	6	7	8			11		13	14	15	16	17	18	19		21	OK
177		3			6	7	8	9	10	11	12	13	14	15	16	17	18	19	20	21	Opat
197					6	7	8	9	10	11	12	13	14	15	16	17	18		20	21	OK*
199			4		6	7	8	9	10	11	13		14	15	16			19			Opat
249			4									13	14	15	16	17	18	19		21	Irad
264			4	5	6	7	8	9	10	11	12	13	14	15		17					OK*
320		3		5	6	7	8	9	10	11	12	13	14	15	16	17	18	19		21	Opat
325		3		5	6	7		9		11	12	13	14	15	16	17	18	19	20	21	Opat
336						7	8	9		11		13	14	15	16	17	18	19			OK*
352		3		5	6	7	8	9		11			14		16	17	18	19			Irad
359		3		5	6	7	8	9	10		12	13									Irad
404				5	6	7	8		10	11		13	14	15	16	17	18	19			OK
411			4	5	6	7	8	9	10	11	12		14	15	16						OPat, IRad
418		3		5	6	7	8	9	10	11		13	14	15	16		18	19			OK*
445		3	4	5	6	7	8		10	11	12	13	14		16	17	18				Irad
451		3	4	5	6	7	8	9	10	11		13	14	15	16	17	18	19			OK*
470			4	5	6	7	8	9	10			13	14	15	16	17	18				OK
471		3	4	5	6	7	8	9	10	11	12	13	14	15	16	17	18				OPat, IRad
473		3	4	5	6	7			10	11	12	13	14	15		17	18		20		Opat
477		3		5	6	7		9		11		13		15	16		18				OPat, IRad
494		3	4	5	6			9	10	11			14	15	16	17	18		20		OK
501		3			6			9				13	14	15	16	17			20		OK
503		3		5	6	7	8	9	10	11	12	13	14	15		17			20		OPat
510		2			6	7	8	9	10	11	12	13	14	15	16	17	18				OK*
565	2	3	4	5	6	7	8	9	10	11	12	13	14	15	16	17					Opat

Table 3.2 **Females in the sample of 84 subjects : Which films are available?**

3.2.3 Choosing a sub-sample of x-rays for analysis

The selection criteria for the sub-sample were:

1. cephalograms taken at ages 9, 11, 13 and 15 were selected from the 'super sample' where exactly 3 out of these 4 x-ray films for these ages were present and of good enough quality to be traced.

These age bands were so selected in order that any changes that might be taking place during puberty might be observed. In addition to my study, a co-worker in the Glasgow Dental Hospital and School, Dr Simon Chen, collected a parallel set of tracings which included subjects with exactly four tracings from the ages 9, 11, 13 and 15. This resulted in 13 males and 11 females, indicated by an * in Tables 3.1 and 3.2. It is well documented in dental literature and elsewhere, that the mandibles (and other bony structures) are known to grow rapidly during the period of the pubertal growth spurt. This is generally agreed to be between 11 and 15 years of age (Tanner 1962), between 13 and 15 years and between 11 and 13 years for males and females respectively. It is sensible then to assume that any changes in size and shape during the growth of a bone like the mandible, would tend to be more pronounced around these ages.

2. Exclusion criteria were also identified (for both my study and that of my co-worker) and were as follows:

a) patients who had undergone any orthodontic treatment were excluded

b) films showing more than 5-6 degrees of rotation at the mandibular border were also rejected.

This was to ensure as 'normal' a sample as possible as regards bone growth.

In addition,

c) patients whose radiographs were considered inadequate were excluded, as above.

For my study then, a total of 23 subjects from the original 84, 15 males and 8 females satisfied the above inclusion and exclusion criteria as shown in Tables 3.3 and 3.4.

It can be seen then, that from these 15 males and 8 females there are 12 males and 6 females age 9; 9 males and 4 females age 11; 10 males and 7 females age 13 and 14 males and 7 females age 15. Due to these resulting small sample sizes, for each age, it is simply not possible to pick out the repeated measures aspect of the data. This means that analyses are concentrated on differences over the range of ages for all subjects at each age (and sex), regardless of which films are available for any individual, at each age.

Leighton ID	Age																				
18				4	5	6	7	8	9	10			12	13	14	15	16	17	18	19	20	
37				4		6		8	9		11	12		14	15	16	17	18	19	20		
79					5		7	8	9	10			12	13	14	15	16	17	18			
141			3		5	6	7		9	10			12	13	14	15	16	17				
145				4	5	6	7	8	9	10			12	13	14	15	16	17	18			
178					5	6	7	8	9		11	12				15	16				20	21
253			3		5	6	7	8	9	10	11				14	15	16	17	18	19		21
266			3		5	6	7	8		10	11	12	13	14	15	16	17	18				
398				4	5	6	7	8	9	10	11	12		14	15	16	17	18	19			
419				4			7	8		10	11		13		15	16	17	18				
543							7	8	9	10	11	12		14	15	16	17	18	19	20		
564						6	7	8	9	10		12	13	14	15	16	17	18	19			
566	2	3	4	5	6	7			9	10		12	13	14	15	16	17		19			
612		3	4	5	6	7				10	11	12	13	14	15		17					

Table 3.3 Males for analysis.

Leighton ID	Age																				
67				5			8	9	10	11	12	13			16	17	18	19		21	
118	3	4	5	6	7	8	9	10				13	14	15	16	17	18	19		21	
132		4	5	6	7	8	9	10		12	13	14	15	16	17	18	19				
161		4	5	6	7	8			11		13	14	15	16	17	18	19		21		
404			5	6	7	8		10	11		13	14	15	16	17	18	19				
470		4	5	6	7	8	9	10			13	14	15	16	17	18					
494	3	4	5	6			9	10	11			14	15	16	17	18		20			
501	3			6			9				13	14	15	16	17			20			

Table 3.4 Females for analysis.

3.3 Data Preparation

Before the data sample consisting of a series of lateral cephalograms for the 23 subjects can be described in a quantitative manner using elliptical Fourier function methodology, it must be prepared for utilization in the EFF suite of programs outlined in Chapter 2.

3.3.1 Tracing of the Cephalograms

A tracing protocol designed by Lestrel (found in Lestrel and Kerr 1992 and elsewhere) was used to prepare the cephalograms for analysis.

First of all, the outline of the mandible was traced from the x-ray film (like the one given in the Appendix) for each of the 23 subjects for each of the available ages 9, 11, 13 and 15. The mandibular outline was carefully traced onto 0.003 inch, non-stretched, single-sided, matte acetate using a Staedtler pencil, HB 0.3mm nib. Where bilateral images appeared on the x-ray, a template method was used to trace the average position of the two images. Each series of x-rays i.e. x-rays at different ages for the same subject, were traced at the same sitting and each x-ray was placed on the same light table at the bottom left hand corner, in the same position, as far as possible.

To help visualise the building-up of the 'tracing to representation of the bone' procedure, an example of a representation of this basic tracing of the bone is illustrated in Figure 3.2.

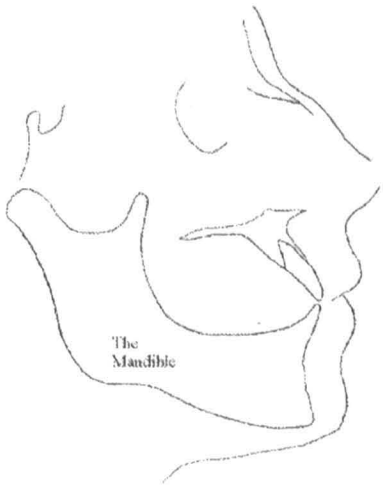

Figure 3.2 Basic tracing of the outline of the mandible.

This traced outline had then to be characterised by a set of 78 closely located points using a radiograph Rotring pen with a 0.18mm nib. These 78 points consisted of 19 anatomical landmarks and 59 associated points.

Before these points were located on the mandibular outline, five reference planes were located and drawn on the traced image using the same Staedtler pencil, to act as an aid in locating some of the anatomical landmarks on the mandibular outline.

The planes were:

1. Sella to Nasion

This line can be taken to represent the anterior cranial base. The landmarks for Sella and Nasion are relatively easily to locate reliably.

2. The Maxillary Plane

Anterior Nasal Spine to Posterior Nasal Spine (ANS - PNS)

3. The Mandibular Plane

Gonion – Menton. All the points on the body of the mandible are relative to the mandibular plane.

4. The Condylar Plane

A tangent to the posterior aspect of the condyle and the angle of the mandible (not Condylion – Orbitale). All the points on the condyle and coronoid process are relative to the condylar plane.

and

5. The Frankfort Horizontal

Orbitale – Porion, where Porion is defined as the top of ear rod for easy location purposes on the head film.

Location of these planes is illustrated in Figure 3.3.

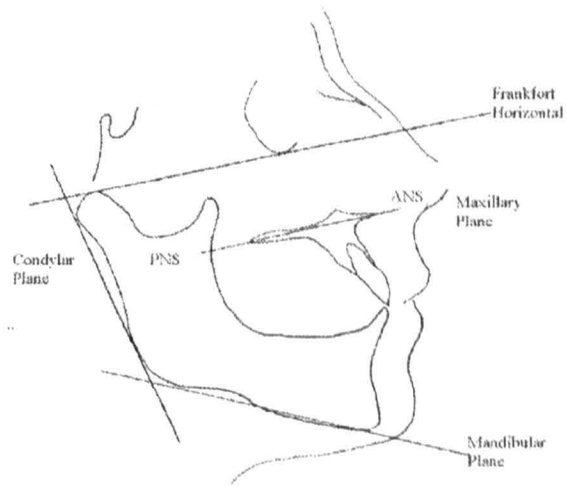

Figure 3.3 Picture of tracing with required planes located.

The anatomical landmarks had then to be located and drawn onto the tracing of the mandibular outline. An anatomical landmark is a point assigned by an expert that corresponds between organisms in some biologically meaningful way e.g. the tip of the nose, the corners or the mouth etc. Anatomical landmarks designate parts of an organism that correspond in terms of biological derivation and these parts are called homologous (Dryden and Mardia 1998).

The anatomical landmarks were located on the mandibular outline using Lestrel's guidelines once again as follows, and illustrated in Figure 3.4.

Point 1 (and point 78, PNS)

the point of intersection of the ANS-PNS plane with the outline of the anterior ascending ramus

Point 3

the most posterior aspect of the anterior ascending ramus with respect to the condylar plane

Point 13

the point of intersection of the border of the alveolar bone and the posterior lower central incisal margin

Point 18

the tip of the lower central incisor

Point 23

the point of intersection between the anterior lower central incisal margin and the alveolar bone

Point 27 (Point B)

the most posterior point on the anterior aspect of the body of the mandible with respect to the mandibular plane

Point 31 (Pogonion)

the most anterior point on the anterior mandibular body with respect to a perpendicular drawn from the mandibular plane

Point 35 (Menton / Cephalometric Gnathion)

The most inferior point on the symphysis of the mandible

Point 39

the most inferior point on the anterior mandibular body with respect to the mandibular plane

Point 43

the most superior point of the lower border of the mandible with respect to the mandibular plane

Point 45 (Gonion)

the most inferior point of the posterior mandibular body with respect to the mandibular plane

Point 49

the most posterior point on the lower aspect of the posterior ascending ramus with respect to the condylar plane

Point 51

the most anterior point on the posterior aspect of the ascending ramus with respect to the condylar plane

Point 54 (+ point 49 = condylar plane)

the most posterior point on the mandibular condyle with respect to the condylar plane

Point 58

the most superior point of the condyle with respect to the condylar neck

Point 62

the point of intersection on the anterior surface of the condyle drawn by a perpendicular from point 54 (tangent point that marks the change in curvature between the condyle head and the mandibular notch)

Point 67

the most inferior point of the mandibular notch with respect to a perpendicular drawn from the condylar plane

Point 72

the tip of the coronoid process

Point 76

the most anterior point of the coronoid process with respect to a parallel from the condylar plane

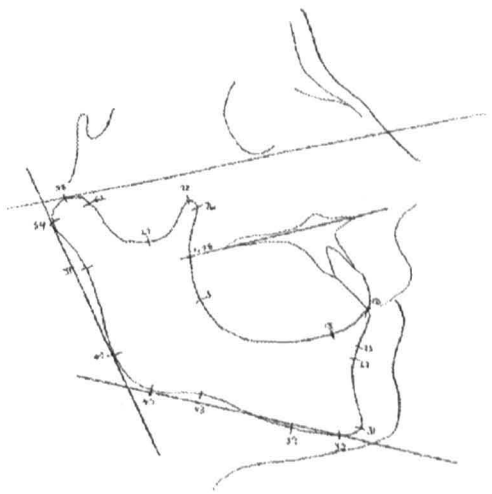

Figure 3.4 Picture of tracing with planes and anatomical points located.

Finally, the remaining 57 points that characterise the mandibular outline, completing the full 78 point system, were located as bisections or trisections between these 19 anatomical landmarks as shown in Table 3.5, and illustrated in Figure 3.5.

Point	Bisection / Trisection	Point	Bisection / Trisection	Point	Bisection / Trisection
2	1 and 3	25	23 and 27	48	47 and 49
9	3 and 13	24	23 and 25	50	49 and 51
7	3 and 9	26	25 and 27	52	51 and 54
5	3 and 7	29	27 and 31	53	52 and 54
4	3 and 5	28	27 and 29	55, 56, 57	equal bisects between 54 and 58
6	5 and 7	30	29 and 31	59, 60, 61	equal bisects between 58 and 62
8	7 and 9	33	31 and 35	64	62 and 67
11	9 and 13	32	31 and 33	63	62 and 64
10	9 and 11	34	33 and 35	65, 66	trisection 64 and 67
12	11 and 13	37	35 and 39	69	67 and 72
15	13 and 18	36	35 and 37	68	67 and 69
14	13 and 15	38	37 and 39	70	69 and 72
16	15 and 18	41	39 and 43	71	70 and 72
17	16 and 18	40	39 and 41	74	72 and 76
21	18 and 23	42	41 and 43	73	72 and 74
20	18 and 21	44	43 and 45	75	74 and 76
19	18 and 20	47	45 and 49	77	76 and 78
22	21 and 23	46	45 and 47		

Table 3.5 Bisections and trisections of the anatomical landmarks which characterise the mandibular outline.

These points can be referred to as pseudo-landmarks (Dryden and Mardia 1998). A mathematical landmark is a point located on an object according to some mathematical or geometrical property of the figure, at a point of high curvature for example, or at an

extreme point. Pseudo-landmarks are simply constructed points on an object, located either around the outline or in between anatomical or mathematical landmarks.

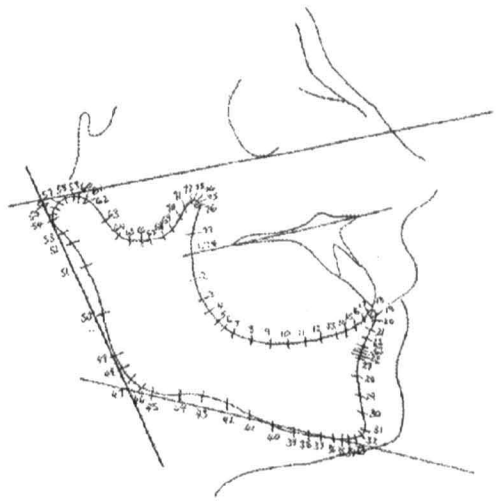

Figure 3.5 Picture of tracing with planes and all 78 points.

The mandibular outline can be thought of as being divided into nine areas in terms of this 78-point characterisation as in Table 3.6 (and already outlined in Section 1.3.2).

Points	Description
1-7	Anterior border of the ramus
7-13	Alveolus
13-23	Lower incisor
23-31	Anterior border of the mandible
35-45	Lower border of the mandible
45-49	Angle of the mandible
49-54	Posterior border of the ramus
54-62	Condyle
62-67	Mandibular notch
72-78	Coronoid process

Table 3.6 Areas of the mandibular outline.

Further, it can be seen from this final tracing where all 78 points have been located, that where the outline contains sharp curves i.e. areas of high curvature, the more points are required. This is obvious from the incisal region and the coronoid process. In such regions of abrupt change / high curvature, the points were spaced closer together to obtain a good fit with the elliptical Fourier function. The reverse applies in areas of low curvature, for example, the lower border of the mandible.

3.3.2 Digitisation of specimens for use in EFF program

Each mandible tracing, characterised by the 78 points, was placed on a Houston Instruements HIPAD digitising pad using the Maxillary plane, ANS-PNS as an orientation aid. PNS (Point 1) was superimposed on the origin (0,0) of the digitiser co-ordinate system, identified by a set of cross-hairs extending vertically and horizontally to the borders of the digitising pad, where the plane ANS-PNS extends along the horizontal axis of the digitiser. This ensured that each tracing was placed on the digitising pad in exactly the same position. Each located point on the mandibular outline was then digitised, in a clockwise fashion, proceeding from Point 1, and subsequently recorded as (x,y) co-ordinate pairs for utilisation in the elliptical Fourier function program. An example of one of the original tracings ready for digitising is given in the Appendix.

As a first check on the sample of digitised data, plots of the observed (digitised) data points were superimposed on the original tracings of the cephalograms to check for any discrepancies in the digitising process. The tracings for each of the 23 subjects, at

each available age from 9, 11, 13 and 15 were found to have been digitised satisfactorily.

3.3.3 Any problems with tracing / digitising procedures

It is worth noting that although each of the 23 subjects, at each available age from 9, 11, 13 and 15 were found to have been digitised satisfactorily. This was not without careful instruction and attention to detail at every stage in the 'building up' of the mandibular outline, from the initial tracing of the x-rays, through to the digitisation of the located points for subsequent use in the EFF suite of programs. I was given training in tracing the x-rays to ensure a satisfactory representation of the mandible was captured from the original x-ray, where it was occasionally extremely difficult to trace the actual outline. In addition, an experienced orthodontist checked each of my tracings. This process was repeated at the landmark identification stage, where it could be extremely difficult to locate some of the anatomical landmarks, especially to the untrained eye. Training was also given to establish a correct digitisation technique. An assessment of the validity and reproducibility of the within-observer tracings and identification of landmark points was also undertaken. Results of this study are given in Chapter 4.

3.4 Conclusion

In this chapter, the origin of the data sample utilized in this thesis has been described. The way in which data from this sample was initially assessed and prepared for use in the elliptical Fourier function suite of programs (and subsequent use with Procrustes methods also) has also been described in some detail, as well as any problems tackled along the way.

The final sample for analysis then, consisted of 23 non-orthodontic patients, 15 males and 8 females, where 3 out of the 4 x-ray films for ages 9, 11, 13, 15 were available and of good enough quality to trace the mandibular outline.

From the tracing procedure outlined, a representation of the mandibular outline for each of the 23 patients in the sample, at each available age from 9, 11, 13 and 15 was built up in an identical manner, as a set of 78 closely located points, ready for digitisation, and subsequent utilisation in the elliptical Fourier function program.

It should be emphasized at this point that this data collection task was not trivial! A considerable amount of time and attention to detail was dedicated to the collection of this data.

The next two chapters attempt to describe the size and shape of the mandible in numerical terms, paying particular attention to mandibular growth which might be occurring around the pubertal growth period for this data sample of 23 subjects. Chapter 4 utilises the

elliptical Fourier function method described in Chapter 2 and the method of Procrustes analysis is then introduced and used in Chapter 5.

Chapter 4

Evaluation Of the Data Sample Using the Elliptical Fourier Function

4.1 Introduction

In Chapter 2 elliptical Fourier function methodology was introduced and the capabilities of the suite of programs to be used in this chapter outlined. Chapter 3 described the origin of the data sample we wish to make observations on, how this data sample was selected and how it was prepared for subsequent use in the elliptical Fourier function suite of programs. We now wish to investigate whether or not the elliptical Fourier function (EFF) method is a useful tool for locating and depicting the pattern of bone growth and whether or not it is useful in illustrating the pattern of active growth that a bone undergoes over time. To this end, we shall describe the selected data sample of 23 subjects in more depth using the EFF suite of programs to try to pinpoint where and when the size and shape changes of the growing mandible are actually taking place. Whether or not there are any differences as regards size and shape of the bone at various ages between the males and females in this group will also be investigated. An assessment of within observer (intra-rater) error, and between observer (inter-rater) error in the tracing of the specimens is also made.

4.2 *Preliminary Descriptive Plots with the EFF*

There are many plots available to us within the EFF suite of programs as outlined in Chapter 2. Some are more useful than others in the description of the size and shape of a complex irregular form, like the mandible. This section covers specific examples for specific subjects within the data sample between 9 and 15 years of age. We reintroduce some of the descriptive plots outlined in Chapter 2 and further explain some of the aspects of the EFF program that can be used to describe the size and shape of the mandible over a range of ages.

4.2.1 Observed (digitised) data and Predicted Form

We begin the path of description by plotting the observed (digitised) form for each of the 23 subjects in the data sample, at each available age of 9, 11, 13 and 15. The original tracings are superimposed (by hand) on these observed outlines to check for any errors that may have occurred in the digitising process. Each of the three tracings, for all 23 subjects in our sample (69 tracings in total then) was found to have been digitised satisfactorily. The observed form can also be size-standardised as described in Chapter 2, in order to isolate only the shape component of the form. The observed forms (and area-standardised equivalents) are then compared with the predicted outlines computed using the EFF from these original observed (digitised) data points. For illustration purposes, each of the 3 available tracings from ages 9, 11, 13 and 15 for one particular subject in our data sample are shown, not standardised for size at this stage. Figures 4.1 (a), (b) and (c) show the (un-standardised) observed and predicted outlines superimposed for the available ages 9, 13

and 15 respectively. The observed and predicted outlines are superimposed on the centroid. The (x,y) centroid value is subtracted from each of the (x,y) co-ordinate pairs for each of the points which characterise the mandibular outline, so these outlines are all centred at the point (0,0) in this co-ordinate system.

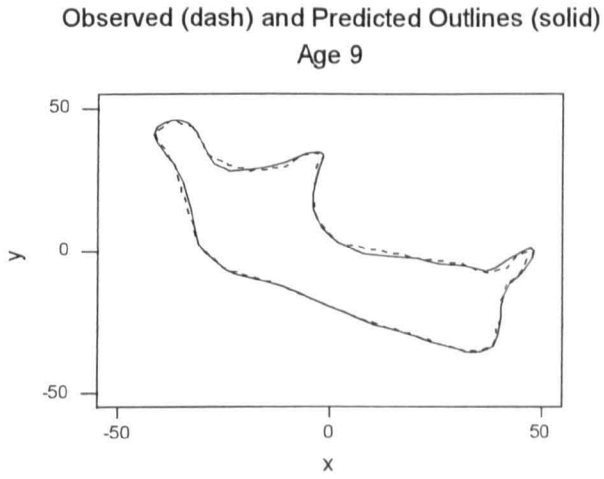

Figure 4.1a **Observed and predicted outlines superimposed for a particular subject. Age 9.**

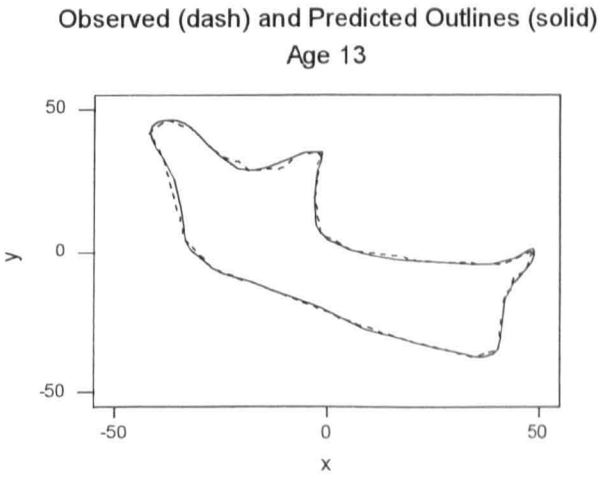

Figure 4.1b **Observed and predicted outlines superimposed for a particular subject. Age 13.**

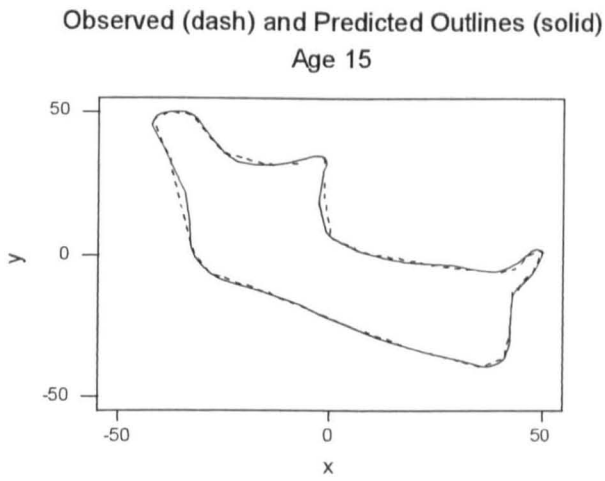

Figure 4.1c Observed and predicted outlines superimposed for a particular subject. Age 15.

For each of the three available ages for this particular subject in the data sample it can be seen that the predicted outline computed by the EFF is in fact a very close representation of the original digitised data. This was the case for all tracings, at all ages in our data sample. Further, it was found that the size-standardised predicted outlines computed by the EFF were also very close representations of the size-standardised observed forms.

4.2.2 Residual and Harmonic Analysis

As described before, once the EFF has been computed for a particular form, the goodness of fit between the predicted and observed forms can be tested by the calculation of residuals. The mean residual error is defined to be the root mean square Euclidean distance between a set of computed points on the curve and their corresponding digitised or observed points. That is, the distance between the original, observed data points and the expected or predicted values derived from the EFF fit, averaged over all 78 points. The value of this residual serves as an indicator of the

closeness of the fit of the computed EFF to the observed data points. The smaller the residual the better the fit. In fact, we illustrate in Figure 4.2 that the elliptical Fourier function represents a convergent series where the value of the residual decreases as more terms, harmonics, are taken in the series. It is found that residual values in tenths of a mm are generally obtainable with 20-40 harmonics. For anatomical work, like that in this thesis, residuals should be approximately 0.2-0.3mm, and should definitely be no more than 0.5mm. Points at sharp corners of the form are likely to have the largest residuals e.g. the tip of the mandible. If the residuals are acceptable, the original data could be theoretically thrown away and replaced by the computed EFF (the predicted outline) which now serves as an analogue for the original form. In the illustration of this stepwise procedure in Figure 4.2, the observed data points are shown as dots, and the predicted outlines as solid lines where predicted outlines are calculated from the Fourier function using 1, 2, 5, 10, 15 and 20 harmonics.

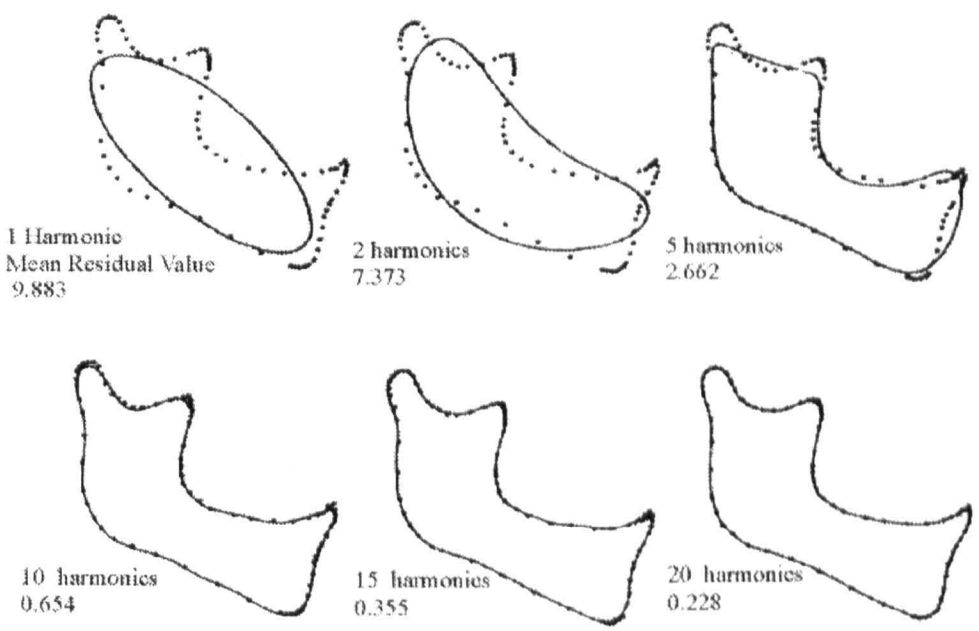

Figure 4.2 **Stepwise curve fitting procedure of the Elliptical Fourier Function.**

It can be seen from this figure that the first harmonic represents an ellipse, and by the time the function is fitted with 20 harmonics, the predicted outline is extremely close to the observed outline, with an acceptable, overall mean residual value of 0.228 mm.

Similar observations were made for all computed outlines to the observed points in the data sample. Tables 4.1 (a) and (b) show the mean residual values for the whole data sample for males and females respectively, where the predicted outlines are calculated from the Fourier function using 1, 5, 10, 15, 20, 30 and 39 harmonics.

As an example, the mean residual corresponding to the predicted outline for the subject used in Figures 4.1 (a) to (c) (actually Female 2 in Table 4.1b) for the first harmonic was 9.122mm at age 9 (9.768mm and 10.213mm for ages 13 and 15 respectively). With 5 harmonics included in the EFF, the mean residual fit decreased to 2.629mm (2.501mm and 2.623mm). Using 10 harmonics, the mean residual fit was 0.754mm (0.695mm and 0.769mm), with 15 harmonics, 0.383mm (0.361mm and 0.379mm), with 20 harmonics this fit becomes even closer, dropping to 0.233mm (0.249mm and 0.243mm) and with 30 harmonics the mean residual values were to 0.141mm (0.137mm and 0.156mm). With the maximum number of harmonics included in the EFF, namely 39 harmonics, the over all predicted fit is extremely close to the actual observed form with a mean residual of 0.102mm for age 9 (0.102mm and 0.109mm for ages 13 and 15 respectively). Similar patterns can be seen for the other subjects, at their available ages from 9, 11, 13 and 15, as outlined in Tables 4.1 (a) and (b), for male and female subjects respectively.

Male Subjects: Age 9, 11, 13 or 15		Number of Harmonics / Mean Residual Value						
		1	5	10	15	20	30	39
1	Age 9	9.728	2.654	0.859	0.338	0.192	0.135	0.095
	Age 13	9.815	2.868	0.917	0.358	0.219	0.147	0.119
	Age 15	10.500	2.966	0.770	0.391	0.247	0.146	0.108
2	Age 9	9.202	2.507	0.696	0.292	0.221	0.135	0.099
	Age 11	10.473	2.551	0.886	0.343	0.220	0.137	0.104
	Age 15	10.549	2.865	0.777	0.411	0.222	0.160	0.107
3	Age 9	9.210	2.555	0.824	0.323	0.188	0.119	0.094
	Age 13	10.710	2.966	0.942	0.406	0.250	0.165	0.113
	Age 15	11.057	2.998	0.859	0.452	0.266	0.152	0.110
4	Age 9	9.684	2.495	0.685	0.316	0.224	0.142	0.093
	Age 13	10.656	2.773	0.639	0.339	0.220	0.156	0.119
	Age 15	12.382	3.077	0.836	0.387	0.210	0.146	0.109
5	Age 9	10.497	2.662	0.677	0.429	0.253	0.149	0.102
	Age 13	11.798	3.227	0.749	0.457	0.269	0.147	0.112
	Age 15	12.484	3.239	0.814	0.459	0.279	0.161	0.122
6	Age 9	9.946	2.439	0.859	0.320	0.216	0.121	0.100
	Age 11	10.283	2.409	0.823	0.342	0.242	0.136	0.098
	Age 15	11.843	2.842	1.037	0.362	0.240	0.151	0.115
7	Age 9	9.883	2.662	0.654	0.355	0.228	0.152	0.099
	Age 11	10.967	2.860	0.753	0.402	0.244	0.150	0.110
	Age 15	12.612	2.990	0.865	0.508	0.268	0.158	0.125
8	Age 11	11.119	2.778	0.980	0.356	0.243	0.140	0.108
	Age 13	11.350	2.892	0.957	0.358	0.227	0.149	0.106
	Age 15	11.961	2.728	0.853	0.379	0.231	0.151	0.123
9	Age 9	10.228	2.693	0.821	0.317	0.203	0.143	0.105
	Age 11	11.168	2.858	0.810	0.383	0.232	0.147	0.101
	Age 13	11.740	3.014	0.852	0.365	0.231	0.127	0.108
10	Age 9	10.815	2.572	0.662	0.399	0.186	0.128	0.098
	Age 11	10.926	2.990	0.706	0.465	0.221	0.129	0.104
	Age 15	11.284	2.985	0.788	0.522	0.258	0.136	0.106
11	Age 11	10.412	2.888	0.757	0.372	0.239	0.142	0.104
	Age 13	11.934	3.025	0.867	0.453	0.217	0.143	0.105
	Age 15	12.088	3.135	0.904	0.514	0.241	0.139	0.108
12	Age 9	8.583	2.326	0.596	0.317	0.192	0.122	0.097
	Age 11	10.538	2.642	0.719	0.389	0.226	0.141	0.101
	Age 15	11.679	2.937	0.773	0.481	0.255	0.138	0.104
13	Age 9	9.971	2.571	0.617	0.412	0.220	0.114	0.087
	Age 13	10.479	2.654	0.658	0.434	0.254	0.134	0.099
	Age 15	10.724	2.803	0.667	0.463	0.205	0.124	0.087
14	Age 9	9.485	2.315	0.692	0.329	0.193	0.115	0.078
	Age 13	10.490	2.591	0.650	0.445	0.242	0.122	0.093
	Age 15	10.451	2.701	0.641	0.460	0.244	0.145	0.101
15	Age 11	10.088	2.436	0.617	0.406	0.199	0.132	0.096
	Age 13	10.214	2.748	0.786	0.364	0.247	0.133	0.106
	Age 15	10.815	2.828	0.729	0.508	0.261	0.145	0.114

Table 4.1a Mean residual values for 1, 5, 10, 15, 20, 30 and 39 harmonics. Males.

Female Subjects: Age 9, 11, 13 or 15		Number of Harmonics / Mean Residual Value						
		1	5	10	15	20	30	39
1	Age 9	8.154	2.220	0.582	0.308	0.199	0.116	0.096
	Age 11	9.270	2.524	0.758	0.324	0.200	0.143	0.098
	Age 13	10.129	2.593	0.753	0.392	0.207	0.131	0.100
2	Age 9	9.122	2.629	0.754	0.383	0.233	0.141	0.102
	Age 13	9.768	2.501	0.695	0.361	0.249	0.137	0.102
	Age 15	10.213	2.623	0.769	0.379	0.243	0.156	0.109
3	Age 9	8.608	2.087	0.552	0.341	0.174	0.110	0.092
	Age 13	9.248	2.577	0.692	0.424	0.215	0.146	0.121
	Age 15	10.568	2.851	0.830	0.432	0.254	0.151	0.123
4	Age 11	9.641	2.325	0.700	0.271	0.197	0.128	0.096
	Age 13	9.928	2.316	0.634	0.330	0.176	0.115	0.091
	Age 15	10.743	2.390	0.736	0.336	0.223	0.141	0.107
5	Age 11	9.648	2.620	0.700	0.353	0.218	0.127	0.089
	Age 13	10.721	2.629	0.825	0.359	0.219	0.146	0.103
	Age 15	11.272	2.724	0.860	0.411	0.236	0.137	0.096
6	Age 9	11.273	2.962	1.014	0.420	0.262	0.153	0.117
	Age 13	12.343	2.950	0.880	0.483	0.307	0.203	0.137
	Age 15	12.767	2.924	0.970	0.469	0.265	0.164	0.125
7	Age 9	9.300	2.303	0.556	0.330	0.194	0.107	0.085
	Age 11	10.121	2.555	0.673	0.350	0.193	0.113	0.082
	Age 15	10.767	2.564	0.647	0.428	0.228	0.123	0.088
8	Age 9	10.581	2.444	0.677	0.351	0.187	0.123	0.093
	Age 13	11.979	2.657	0.868	0.452	0.226	0.129	0.087
	Age 15	11.456	2.749	0.880	0.446	0.254	0.158	0.120

Table 4.1b Mean residual values for 1, 5, 10, 15, 20, 30 and 39 harmonics. Females.

Similarly, the size-standardised predicted outlines were also found to be close analogues of the size-standardised observed forms for each of the 23 subjects in the data sample, at each of the available ages from 9, 11, 13 and 15.

The question is where should we stop? 5, 10, 15, 20 harmonics? Certainly, a function with 5 harmonics is too soon but it might be sensible to stop at around 20 harmonics since the overall residual value is very small by then, and the dimensionality of the data function describing the form would be significantly reduced. However, we proceeded in this thesis by including all 39 harmonics in the elliptical Fourier function to ensure the best predicted fit possible.

In addition, the residual sum of squares was calculated for each subject in the data sample, for each available age, and plotted against the number of harmonics taken in the series. This results in a useful graphical illustration of how the residual decreases as the number of harmonics increases.

The residuals for each of the 78 co-ordinate points that characterise the mandibular outlines in the sample are calculated as

$$\text{residual}_n = \sqrt{(x_n\text{-diff})^2 + (y_n\text{-diff})^2}$$

where,

$(x_n\text{-diff})$ is the difference in the x co-ordinates between the observed and predicted outlines for each n = 1,....,78 points

and similarly,

(y_n-diff) is the difference in the y co-ordinates between the observed and predicted outlines for each n = 1,…,78 points.

The residual sum of squares is then computed as

$$RSS = (residual_1)^2 + (residual_2)^2 + \ldots\ldots\ldots\ldots + (residual_{78})^2$$

Examples of such plots are given in Figures 4.3 and 4.4 (a) for each of the males and females aged 9 in the sample, with plots on a log scale being more informative after the first harmonic, as shown in Figures 4.3 and 4.4 (b).

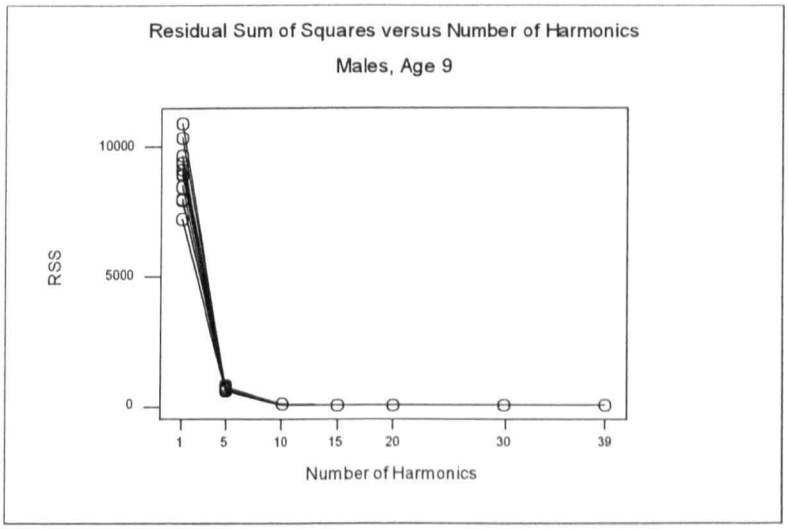

Figure 4.3a **Residual Sum of Squares against Number of Harmonics. Males. Age 9.**

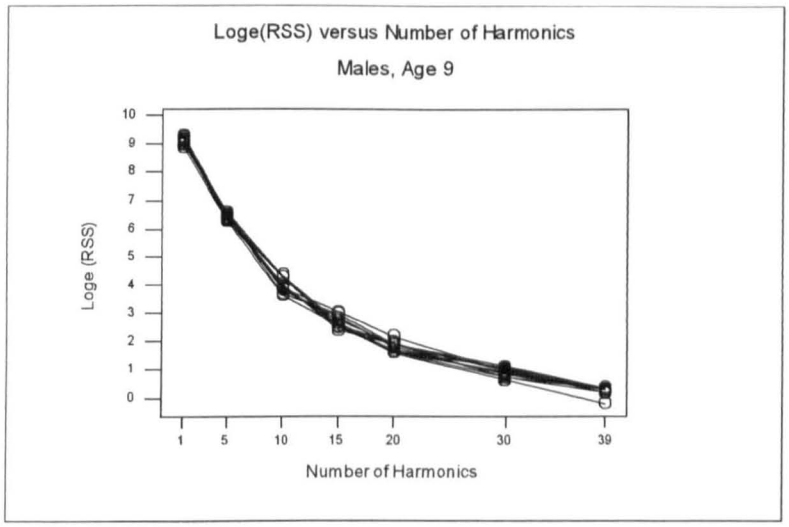

Figure 4.3b **Log Residual Sum of Squares against Number of Harmonics. Males. Age 9.**

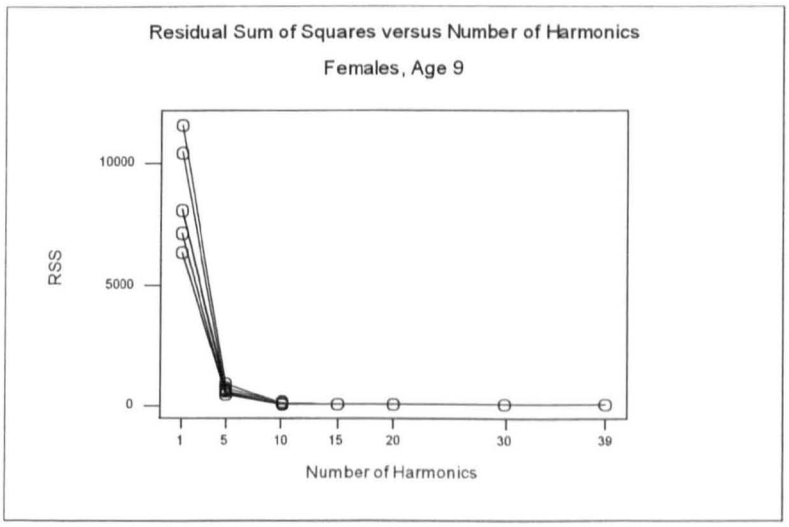

Figure 4.4a **Residual Sum of Squares against Number of Harmonics. Females. Age 9.**

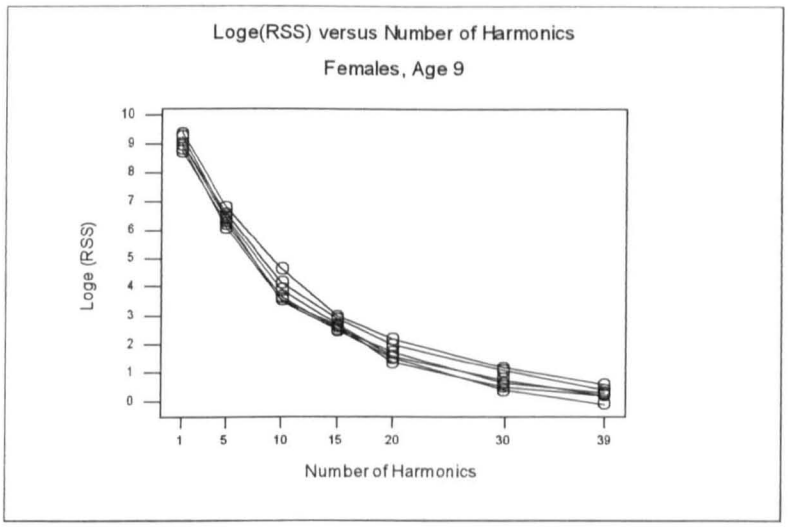

Figure 4.4b Log Residual Sum of Squares against Number of Harmonics. Females. Age 9.

It is very clear from these plots that the overall residual sum of squares does indeed reduce as more harmonics are taken in the function, quite drastically from the first harmonic, and more subtly as more and more harmonics are added, essentially the more localised sculpturing of the form.

Similar patterns were seen for available males and females at ages 11, 13 and 15.

It can be seen then, that the harmonic information produced by the EFF method is of some use in preliminary description, and is tied up with the analysis of residuals as illustrated above. What else can be done with the harmonics?

The amplitude spectrum computed from the data can be investigated by plotting the harmonic amplitude values versus harmonic number for individual subjects in the sample of mandibular data for each age, or for the male and female samples etc. The

amplitude spectrum is thought to be a useful depiction of the importance of each harmonic in determining the size and shape (or shape only when using size-standardised data) of the outline of an object. The larger the amplitude, the more that term is thought to play a major part in the size and / or shape of the form. Interpretation of such plots however, is not easy and does not seem to add anything to the overall description of the size and shape of the form.

Figures 4.5 and 4.6 represent amplitude versus harmonic number plots of the three different ages, 9, 13 and 15 for a particular specimen in the mandibular data sample. All figures are on a log scale to depict patterns in the higher harmonics. Figures 4.6 (a) and (b) are size-standardised representations. The amplitude plots of the x co-ordinate data are shown in Figures 4.5 and 4.6 (a) while the amplitude plots of the y co-ordinate data are depicted in Figures 4.5 and 4.6 (b).

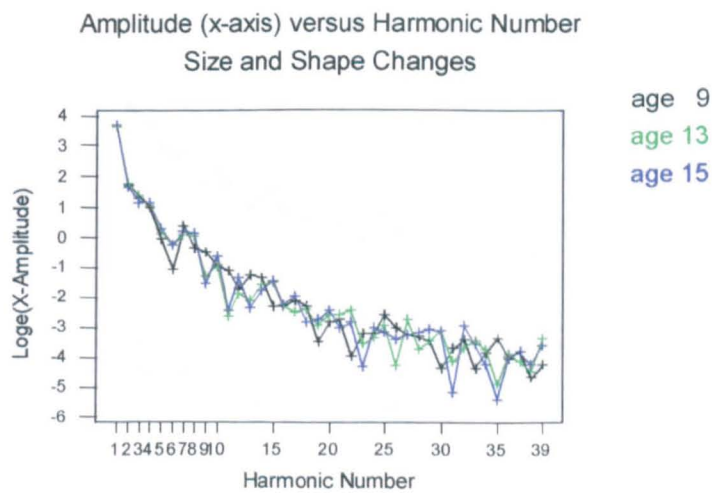

Figure 4.5a Amplitude (x-axis) versus Harmonic Number Plot. Size and shape changes. Age 9, 13 and 15.

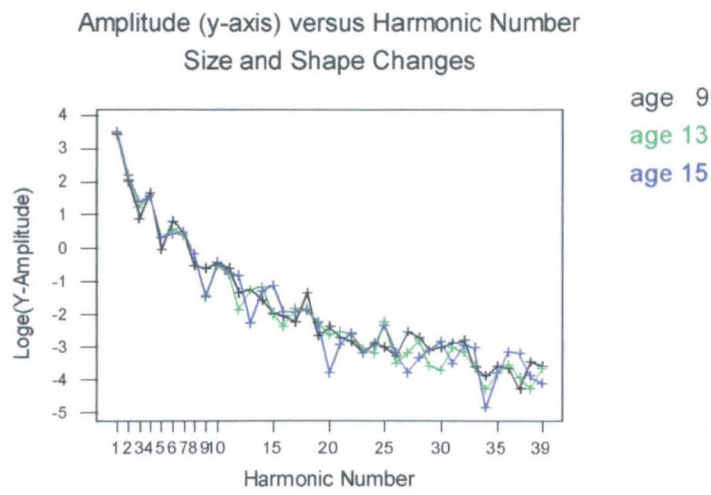

Figure 4.5b **Amplitude (y-axis) versus Harmonic Number Plot. Size and shape changes. Age 9, 13 and 15.**

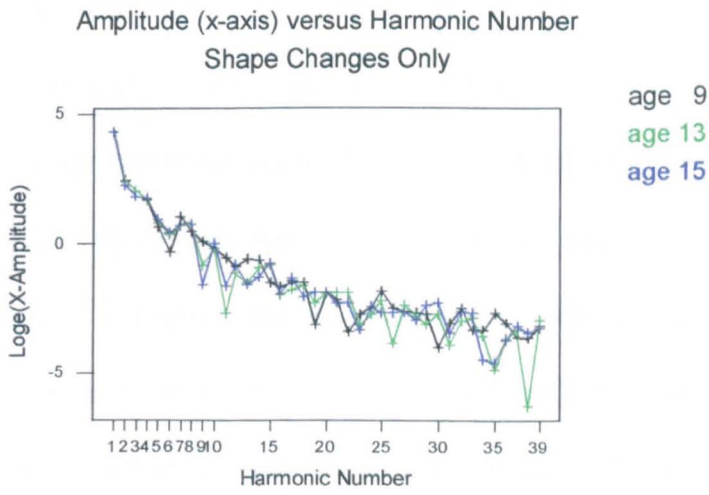

Figure 4.6a **Amplitude (x-axis) versus Harmonic Number Plot. Size-standardised. Age 9, 13 and 15.**

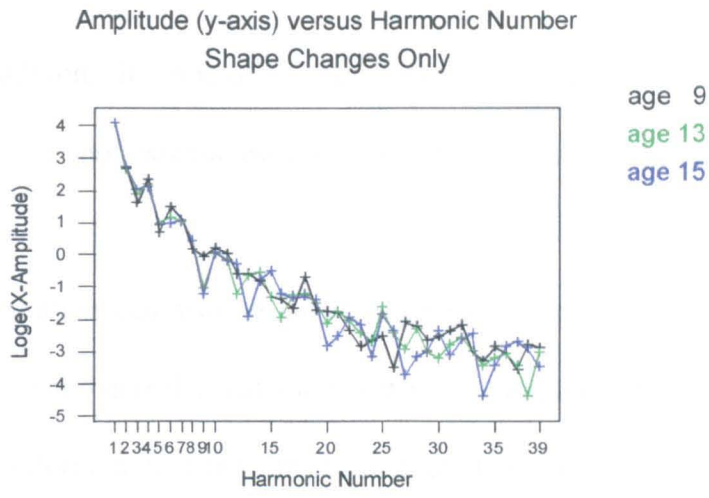

Figure 4.6b Amplitude (y-axis) versus Harmonic Number Plot. Size-standardised. Age 9, 13 and 15.

The figures show the x- and y- amplitude spectra of the 39 harmonics from the Fourier function of the mandibular data at each of the three ages available for that particular subject in the sample. It can be seen that the x- and y- amplitudes for the first few harmonics are all very similar for the range of ages, and are bigger in magnitude than the amplitudes for the higher harmonics. A small amount of variation is observed over the range of ages in the amplitudes for the higher harmonics. What does this say about the data however? Interpretation isn't easy. As defined in Chapter 2, the raw power, or variance that is explained by each harmonic is defined as the square of the amplitude for that harmonic divided by 2. Further, the contribution that each harmonic makes to the variance, i.e. the percentage variation explained by that particular harmonic is defined as the power for that particular harmonic divided by the power for all harmonics. We might conclude that much of the variation in the data is being captured in the first few harmonics and so we might discard of some of the higher harmonics. The danger on relying on this too heavily is that it encourages the discarding of harmonics (those with small magnitude), at times resulting in a consequent loss in

information. In addition, it should be noted unlike principal components, the successive harmonics do not explain less and less of the variance in the data.

The harmonic information can also be used to recreate the form, although this was fairly labour intensive and is really just another way of computing a predicted outline (from the harmonic information of the already computed outline).

4.3 Error study

In the context of this thesis, it was important that we incorporated an assessment of the validity and reproducibility of the tracings and identification of the landmark points, both within my own set of tracings and between my tracings and those of a co-worker (as outlined in Section 3.2.3). Obviously, this investigation was best placed before any further analysis was carried out on the data sample. Also, if the between observer variability was not too large, the subjects of the two parallel studies could perhaps be combined and any further analysis carried out on a bigger sample.

According to Houston 1983, errors which occur in cephalometric analysis can be split into 2 broad categories: validity and reproducibility, which in turn can be split into a further two categories, systematic error and random error.

1. Validity / Accuracy

In the absence of measurement error, validity, or accuracy, is the extent to which the value obtained represents the object of interest, the extent to which the tracing of the mandible actually represents the radiographic image of the mandible in this case. Validity, both of what is measured and the method of measurement, has to be considered.

Therefore, as well as the extent to which the tracing of the bone represents the x-ray film, the extent to which the x-ray of the mandible represents the actual bone must also be considered. We have to consider whether or not the x-ray image might have been distorted or enlarged which in turn would make any tracing, or series of tracings from different cephalostats invalid. The enlargement of radiographic images may also be different when different cephalostats are used, but can be compensated for by the use of a correction factor. Distortion of images can be treated similarly. This is invariably more difficult to deal with since the extent of rotation of the skull from the normal position of having a lateral head film taken (where the ear-rod axis should be perpendicular to the midsagittal plane of the head) is usually unknown. Unless it is noted at the time x-ray of course, although this is not normal procedure. In view of the validity of this study, the magnification of the radiographs was not important as linear measurements were almost always made only after the observed tracing had been submitted to the elliptical Fourier function program and the outline standardised for area. The quality of the radiographs and the positioning of the patients in the cephalostat were out with the author's control. It is noted however that, as far as possible, all radiographs of subjects in the BC Leighton study were taken following

the same positioning criteria, under identical conditions, which ensured consistency between series of images within individual subjects as well as consistency between subjects.

In terms of landmark identification, many cephalometric landmarks have been defined for convenience of identification and reproducibility, rather than on the grounds of anatomic validity. This is often unavoidable and no better alternative may be available so, rather than rendering such landmarks invalid, they should be used with caution and we should recognise that in certain circumstances they may be misleading, e.g. these points may move after orthodontic treatment. Patients who had undergone orthodontic treatment were excluded from the analysis in this thesis in an attempt to minimise such a limitation.

Unless these problems are appreciated, it is easy to draw at best misleading, and at worst invalid conclusions from a simplistic approach to cephalometric analysis.

2. Reproducibility / Precision

Reproducibility is the closeness of successive measurements of the same object. The 'closeness' of successive measurements on any tracing taken by any measurer might vary according to factors such as the quality of the x-ray films, the conditions under which the tracing was done, and the care, skill and expertise of the measurer. This variation would of course affect the interpretation of results, prompting such an error assessment.

There are two main categories of measurement error, systematic error (bias) or random error.

a. Systematic Error

If a particular measurement is persistently under- or over-recorded, systematic error arises e.g. an observer consistently under- or over-recording one or more of the particular landmark points which characterise the mandibular outline. In the case where two series of x-rays are traced by two observers, and the landmark points therefore located by two different people, who may have different concepts about the identification of one or more landmarks, the risk of bias is again introduced. The two observers might systematically identify landmark points according to their perception and training of where those points should be. This may also be true for the case of a single measurer whose practice of tracing and locating points changes, as they become more experienced over a sustained period of time. Also, although not true in this inter-rater comparison, if measurements from two different studies are compared on the assumption that the magnifications are the same, and they are not, the comparison will again be biased, a systematic difference in the collection of the appropriate data.

b. Random Error

The greatest source of random error is most probably the difficulty in locating a particular landmark point, or the imprecision in defining points. The exact location of any landmark point may vary at random, depending very much on the observers

opinion of where it should be, and also on the quality of the x-ray film, another reason that random error may arise.

Attempts were of course made to minimise the magnitude of both systematic and random errors. In an attempt to minimise random error in the study, training was provided in tracing the lateral cephalograms, as well as training in identifying 'textbook' landmark points, before any tracing was undertaken. Any film of very poor quality (and series of ages for that subject) was excluded from the study also. To minimise systematic error, all tracings were subsequently checked and verified by an expert orthodontist in Glasgow Dental Hospital and School in order to ensure correct location of landmark points and tracing of outline of films, especially those of poor quality. Also, series of tracings for any one patient, at different ages, were carried out at the same sitting, under identical conditions.

In order to assess the reproducibility of tracings and identification of landmark points, two error studies were conducted, an intra-rater agreement study and an inter-rater agreement study.

4.3.1 Intra-rater Agreement

From the original 23 subjects, a randomly selected group of 5 subjects x-ray films were re-traced and re-digitised i.e. 15 films in total. For each of the available films, from ages 9, 11, 13 and 15, plots of the observed points for the 2nd tracing were superimposed on those for the 1st tracing and areas of disagreement identified.

Differences were evident from these plots, but they were usually small and predominantly in areas that many of the landmark points were more difficult to locate. Such discrepancies between the 1st and 2nd tracings for one observer were in the main, isolated to complicated areas such as the anterior border of the ramus (points 1-7), the incisal region (points 13-35), and the condylar region; the condyle, the mandibular notch and the coronoid process (points 54-78). The alveolus (points 7-13), the lower border of the mandible (points 35-45), the angle of the mandible (points 45-49) and the posterior border of the ramus (points 49-54) were invariably in closer agreement between different tracings of the same x-ray film. A typical example illustrating evidence of small discrepancies between the 1st and 2nd tracings is shown for one particular subject, for all available ages in Figures 4.5 (a), (b) and (c).

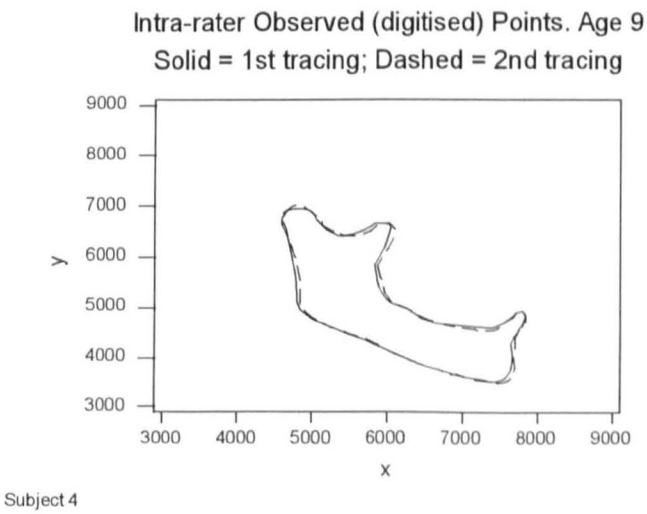

Figure 4.7a **Intra-rater agreement between 1st and 2nd tracings. Age 9.**

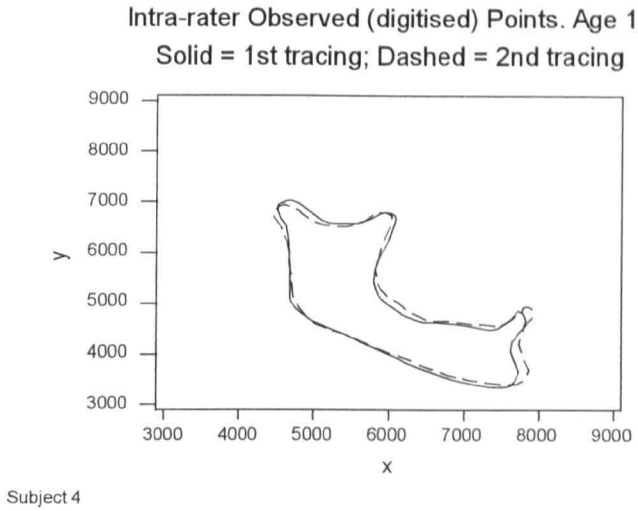

Figure 4.7b **Intra-rater agreement between 1st and 2nd tracings. Age 11.**

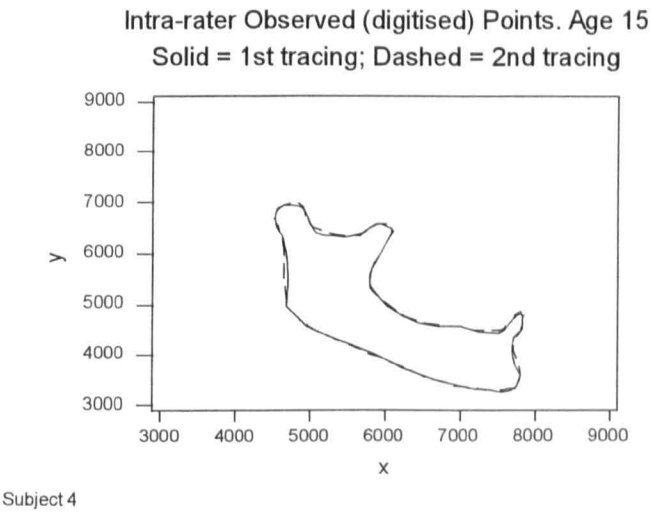

Figure 4.7c **Intra-rater agreement between 1st and 2nd tracings. Age 15.**

From these plots we can see that most of the 'disagreement' seems to be in the anterior incisal region (points 13-35), and perhaps some around the condyle and mandibular notch (points 54-62 and 62-67 respectively) areas. The two tracings do however look like they are in good overall 'agreement', where similar patterns can be seen for all three available age groups.

Similar results were observed for the other four subjects who had been re-traced and re-digitised in this intra-rater sample.

In order to test if these differences between the 1st and 2nd tracings were significant, the predicted fit of each mandible was first of all calculated using the EFF software package (in fact, these predicted outlines had already been calculated for the 1st lot of tracings). For each predicted outline (5 subjects, each with 3 films), linear distances from the centroid to each point on the mandibular outline were calculated for each pair of tracings. The difference between the 1st and 2nd tracings for these centroid-to-outline points were then calculated resulting in 78 calculated differences for each of the 5 subjects, each with 3 films from ages 9, 11, 13 and 15.

Student t-tests were subsequently carried out to see if the *mean* differences (for the 15 mandibular outlines) between the distances from the centroid to each of the 78 points on the mandibular outline of the two tracings, for each subject at each available age, were significantly different from zero. The null hypothesis is then

$$H0: \mu_{difference} = \mu_{1st\ tracing} - \mu_{2nd\ tracing} = 0.$$

Intra-class correlation coefficients for each pair of boundary outline points on the mandibular outline between the 1st and 2nd tracings were also calculated, again for all 15 mandibular outlines. This provides an indication of 'agreement' for each point on the mandibular outline between the 1st and 2nd tracings for the 5 subjects included in the study, at each available age.

Although the tests were carried out for every point on the mandibular outline, particular attention was paid to the 19 anatomical landmarks since the other points are dependent on the accuracy of these landmark points, and there will obviously be some correlation between clusters of points anyway. It should also be noted that a Bonferroni correction is necessary for the purpose of this study. This is because there are so many homologous points being assessed at once, and therefore there are bound to be some significant differences between the points at a conventional individual 5% level by chance alone. This correction reduces the conventional significance level of 0.05 to 0.05/19 = 0.0028 for an approximate overall 5% significance level.

Results are reported for the anatomical landmark points in Table 4.2 (a) and for the intermediate points in Table 4.2 (b), where significant differences exist between tracings for those landmark points marked with an *.

Overall there does not seem to be much disagreement between the 1st and 2nd tracings for the 5 subjects in this study, where each available film was traced by the same observer. The only significant difference ($p<0.0028$), between the 1st and 2nd tracings for anatomical landmarks, lies at point 23. There are also significant discrepancies at nearby, associated intermediate points 21, 22 and 24 (as well as intermediate point 52). The 95% CI for the mean difference does not include zero and is wholly negative. This suggests that the mean distance from the centroid to point 23 on the 1st tracing is less than the corresponding distance for the 2nd tracing for this particular landmark point (and perhaps neighbouring points). In other words the 2nd tracing of the mandibular outline for this set of subjects is further away from the centroid than the 1st tracing in this particular region of the mandible. Such a discrepancy for this particular

landmark point between the two tracings does not seem surprising since this was one of the regions in which landmark points were difficult to identify. The intra-class correlation coefficients between the 1st and 2nd tracings, for each of the anatomical landmarks are satisfactory, where all but two are >0.75, which backs up the suggestion of good agreement. It is perhaps of some concern that the correlation coefficients for landmark points 3 and 39 are as low as 0.516 and 0.358 respectively, but this is probably due to difficult identification of those particular landmark points on one film. Any observations on these points should never the less be interpreted with caution. Further, the magnitude of any disagreements between the tracings for this intra-rater agreement study are probably small, according to our subjective impression of the plots of observed points previously.

It could be argued here that the Bonferroni correction might make the test too conservative. Indeed, if the individual 95% confidence intervals are examined at face value, we find more significant differences between tracings, both in the landmark points and when including the intermediate points. For example, the discrepancy between tracings for point 3 could be nearly 5mm, which would possibly be considered very important clinically, although is not found to be statistically significant at p=0.0028. Some people might prefer then, to look at intra-rater agreement in the context of equivalence, which might reveal more of a difference between tracings.

Point	N	Mean Difference	Standard Deviation	SE Mean	T-Statistic	P-value	95% C.I.	I.C.C
1	15	-0.086	0.861	0.222	-0.38	0.71	(-0.562, 0.391)	0.971
3	15	-2.381	4.098	1.060	-2.25	0.041	(-4.650, -0.110)	0.516
13	15	-0.125	1.140	0.294	-0.42	0.68	(-0.756, 0.506)	0.951
18	15	-0.376	0.781	0.202	-1.86	0.084	(-0.808, 0.057)	0.960
23*	15	-0.451	0.401	0.104	-4.36	0.0007	(-0.674, -0.229)	0.986
27	15	-0.001	0.646	0.167	-0.00	1.0000	(-0.358, 0.357)	0.966
31	15	-0.329	0.441	0.114	-2.89	0.012	(-0.573, -0.085)	0.992
35	15	-0.770	1.129	0.291	-2.64	0.019	(-1.396, -0.145)	0.951
39	15	-1.870	3.984	1.030	-1.82	0.091	(-4.080, 0.340)	0.358
43	15	0.278	0.595	0.154	1.81	0.092	(-0.051, 0.608)	0.962
45	15	0.186	1.171	0.302	0.61	0.55	(-0.463, 0.834)	0.858
49	15	-0.159	0.716	0.185	-0.86	0.40	(-0.556, 0.237)	0.935
51	15	-1.337	1.975	0.510	-2.62	0.02	(-2.431, -0.243)	0.755
54	15	0.282	1.438	0.371	0.76	0.46	(-0.514, 1.079)	0.924
58	15	0.019	1.057	0.273	0.07	0.95	(-0.567, 0.605)	0.958
62	15	0.724	1.804	0.466	1.55	0.14	(-0.275, 1.723)	0.891
67	15	0.046	1.615	0.417	0.11	0.91	(-0.849, 0.940)	0.899
72	15	0.111	1.255	0.324	0.34	0.74	(-0.585, 0.806)	0.952
76	15	0.234	1.846	0.477	0.49	0.63	(-0.789, 1.256)	0.878

Table 4.2a Intra-rater agreement. Landmark points only. Unadjusted data.

Point	N	Mean Difference	Standard Deviation	SE Mean	T-Statistic	P-value	95% C.I.	I.C.C
2	15	-1.092	2.237	0.578	-1.89	0.080	(-2.331, 0.147)	0.775
4	15	-2.166	3.802	0.982	-2.21	0.045	(-4.272, -0.060)	0.518
5	15	-1.625	3.307	0.854	-1.90	0.078	(-3.456, 0.207)	0.552
6	15	-0.816	2.638	0.681	-1.20	0.25	(-2.277, 0.646)	0.599
7	15	-0.014	1.788	0.462	-0.03	0.98	(-1.004, 0.977)	0.655
8	15	0.414	2.677	0.691	0.60	0.56	(-1.069, 1.896)	0.507
9	15	0.157	2.609	0.674	0.23	0.82	(-1.288, 1.602)	0.592
10	15	0.002	1.838	0.474	0.00	1.00	(-1.016, 1.020)	0.779
11	15	0.072	1.435	0.370	0.19	0.85	(-0.723, 0.866)	0.876
12	15	0.002	1.137	0.294	0.01	0.99	(-0.628, 0.632)	0.939
14	15	-0.085	0.826	0.213	-0.40	0.70	(-0.756, 0.506)	0.971
15	15	-0.175	0.674	0.174	-1.01	0.33	(-0.542, 0.373)	0.978
16	15	-0.223	0.705	0.182	-1.22	0.24	(-0.614, 0.168)	0.971
17	15	-0.464	0.776	0.200	-2.31	0.036	(-0.894, -0.034)	0.964
19	15	-0.397	0.781	0.202	-1.97	0.069	(-0.830, 0.035)	0.960
20	15	-0.382	0.614	0.158	-2.41	0.030	(-0.722, -0.043)	0.974
21*	15	-0.398	0.424	0.109	-3.64	0.0027	(-0.633, -0.164)	0.987
22*	15	-0.510	0.449	0.116	-4.40	0.0006	(-0.759, -0.261)	0.983

ctd...

Point	N	Mean Difference	Standard Deviation	SE Mean	T-Statistic	P-value	95% C.I.	I.C.C
24*	15	-0.430	0.365	0.094	-4.56	0.0004	(-0.632, -0.228)	0.989
25	15	-0.312	0.412	0.106	-2.93	0.011	(-0.540, -0.084)	0.986
26	15	-0.187	0.526	0.136	-1.38	0.19	(-0.479, 0.104)	0.978
28	15	0.515	0.970	0.251	2.06	0.059	(-0.022, 1.053)	0.923
29	15	0.159	0.880	0.227	0.70	0.50	(-0.329, 0.646)	0.944
30	15	-0.212	0.606	0.157	-1.36	0.20	(-0.548, 0.124)	0.982
32	15	-0.251	0.450	0.116	-2.16	0.049	(-0.500, -0.002)	0.992
33	15	-0.228	0.641	0.165	-1.38	0.19	(-0.583, 0.127)	0.983
34	15	-0.410	0.943	0.243	-1.68	0.11	(-0.932, 0.112)	0.965
36	15	-1.090	1.206	0.311	-3.50	0.0035	(-1.759, -0.422)	0.938
37	15	-1.467	2.260	0.584	-2.51	0.025	(-2.719, -0.215)	0.793
38	15	-1.701	3.425	0.884	-1.92	0.075	(-3.599, 0.196)	0.559
40	15	-1.453	2.482	0.641	-2.27	0.040	(-2.827, -0.078)	0.624
41	15	-0.780	1.602	0.414	-1.89	0.080	(-1.668, 0.108)	0.795
42	15	-0.147	0.742	0.191	-0.77	0.46	(-0.557, 0.264)	0.945
44	15	0.408	1.086	0.280	1.45	0.17	(-0.051, 0.608)	0.863
46	15	0.119	1.260	0.325	0.37	0.72	(-0.579, 0.817)	0.845
47	15	-0.029	0.807	0.208	-0.14	0.89	(-0.476, 0.418)	0.925
48	15	-0.117	0.684	0.177	-0.66	0.52	(-0.496, 0.262)	0.942
50	15	-0.744	1.372	0.354	-2.10	0.054	(-1.504, 0.016)	0.769
52*	15	-0.765	0.956	0.247	-3.10	0.0079	(-1.295, -0.235)	0.949
53	15	-0.076	1.105	0.285	-0.27	0.79	(-0.689, 0.536)	0.944
55	15	0.342	1.129	0.292	1.17	0.26	(-0.283, 0.968)	0.953
56	15	0.182	0.943	0.243	0.75	0.47	(-0.340, 0.704)	0.968
57	15	0.068	0.912	0.235	0.29	0.78	(-0.437, 0.573)	0.970
59	15	0.089	1.290	0.333	0.27	0.79	(-0.625, 0.803)	0.940
60	15	0.268	1.455	0.376	0.71	0.49	(-0.538, 1.074)	0.925
61	15	0.569	1.625	0.420	1.36	0.20	(-0.331, 1.469)	0.911
63	15	1.097	1.483	0.383	2.86	0.012	(0.275, 1.918)	0.892
64	15	1.245	1.394	0.360	3.46	0.0038	(0.473, 2.017)	0.878
65	15	0.761	1.483	0.383	1.99	0.067	(-0.061, 1.583)	0.876
66	15	0.462	1.424	0.368	1.26	0.23	(-0.326, 1.251)	0.909
68	15	-0.174	1.539	0.397	-0.44	0.67	(-1.027, 0.679)	0.915
69	15	-0.267	1.375	0.355	-0.75	0.46	(-1.029, 0.494)	0.938
70	15	-0.360	1.166	0.301	-1.20	0.25	(-1.006, 0.286)	0.961
71	15	-0.127	1.155	0.298	-0.43	0.68	(-0.767, 0.512)	0.960
73	15	0.196	1.324	0.342	0.57	0.58	(-0.538, 0.929)	0.944
74	15	0.322	1.526	0.394	0.82	0.43	(-0.524, 1.167)	0.925
75	15	0.294	1.765	0.456	0.64	0.53	(-0.684, 1.271)	0.893
77	15	0.187	1.202	0.310	0.60	0.56	(-0.479, 0.852)	0.903

Table 4.2b Intra-rater agreement. Intermediate Points. Unadjusted data.

4.3.2 Inter-rater Agreement

In order to investigate agreement *between* observers, a set of tracings which had been collected in an identical manner by Dr Simon Chen, a co-worker in Glasgow Dental Hospital and School, who had been conducting a parallel study to my own were utilised. This parallel study selected different cases from the same historical collection of cephalograms, where x-ray films had to be available for all 4 age groups, 9, 11, 13 and 15 years, but following the same exclusion criteria of orthodontic patients and 'untraceable' films (as outlined in Section 3.2.3). This study resulted in a series of 24 subjects, 13 males and 11 females, each with 4 x-ray films corresponding to ages 9, 11, 13 and 15.

In a similar manner to the intra-rater study, a randomly selected group of 5 subjects x-ray films, for each age, were re-traced and re-digitised from this set of 24 subjects i.e. 20 films in total.

The main aim in carrying out this particular error study was to see if the two sets of tracings (23 subjects in my study, 24 in Dr Chen's) could be combined so that any further analyses could be carried out on a bigger sample.

Plots of observed points for each subject were obtained for each age, 9, 11, 13 and 15, from each observer. The tracings by Observer 2 were superimposed on those by Observer 1, as in the intra-rater study, and areas of 'disagreement' identified.

Differences between the tracings were obvious from these plots, more pronounced in places than the differences seen in the intra-rater study, and occurring in almost all areas around the mandibular outline. In some cases, it was difficult to believe that the same mandible had been traced, whilst in others the tracings between observers were extremely close, albeit usually confined to the 'easier' areas such as the lower border of the mandible. A typical example is shown for one particular subject in Figures 4.8 (a) to (d). It can be seen that there is indeed 'more' overall disagreement between the two tracings, for each age, than that seen in the intra-rater study, and such disagreement is not now confined to certain 'difficult' areas of the bone, but rather occurs around the whole outline.

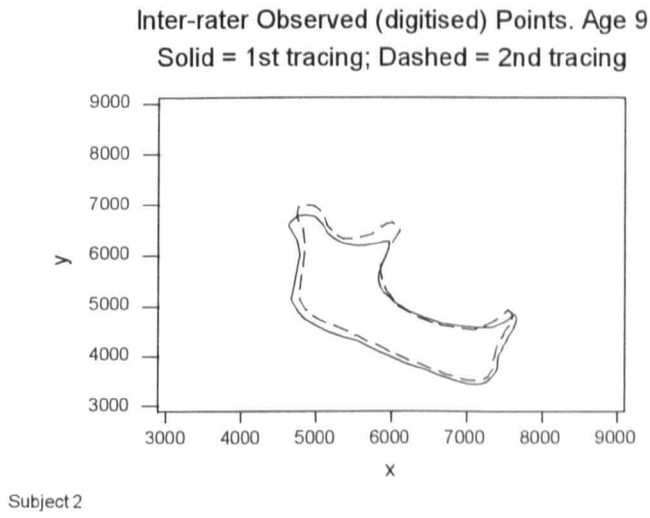

Figure 4.8a **Inter-rater agreement between 1st and 2nd tracings. Age 9.**

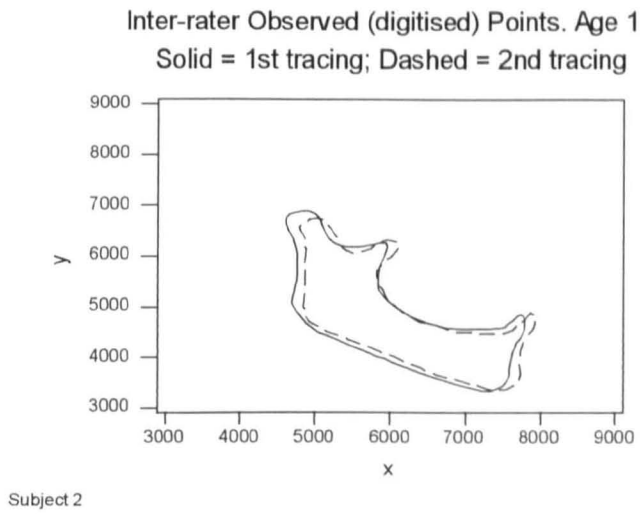

Figure 4.8b **Inter-rater agreement between 1st and 2nd tracings. Age 11.**

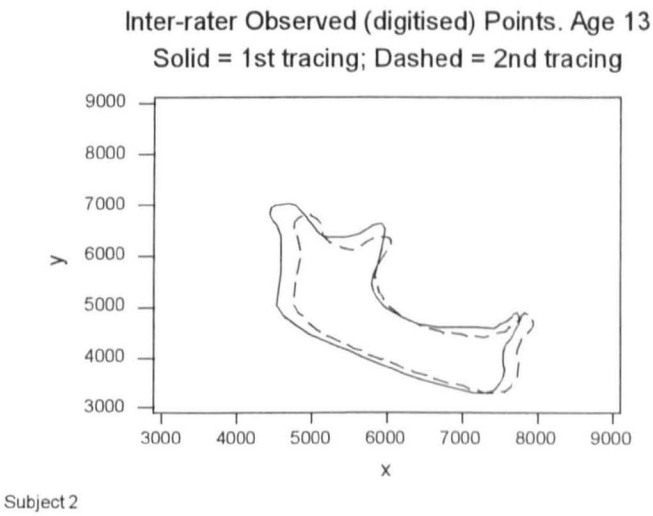

Figure 4.8c **Inter-rater agreement between 1st and 2nd tracings. Age 13.**

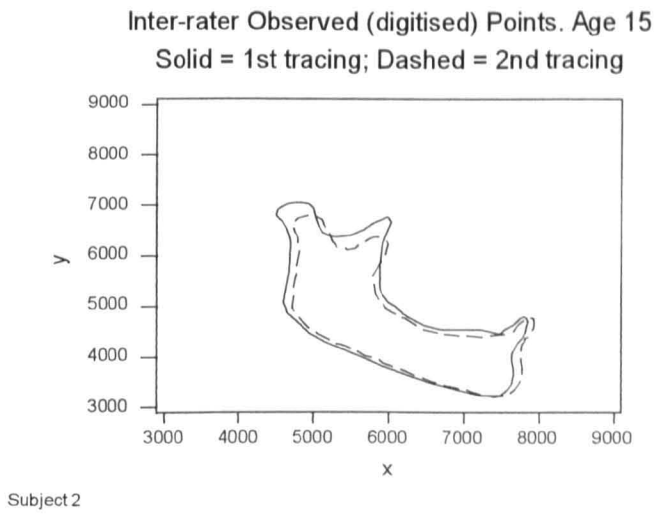

Figure 4.8d Inter-rater agreement between 1st and 2nd tracings. Age 15.

As before, the predicted fit of each mandible was first of all calculated using the EFF software package. For each predicted outline (5 subjects, each with 4 films), linear distances from the centroid to each point on the mandibular outline were calculated for each pair of tracings. The difference between the 1st and 2nd tracings by Observers 1 and 2 respectively, for these centroid-to-outline points were then calculated resulting in 78 calculated differences for each of the 5 subjects, each with 4 films from ages 9, 11, 13 and 15.

The same formal t-test analysis was conducted as for the intra-rater study, in order to see if the *mean* differences (for the 20 mandibular outlines) between the distances from the centroid to each of the 78 points on the mandibular outline of the two tracings, for each subject at each available age, were significantly different from zero. That is, testing the null hypothesis, as before, of

$$H0: \mu_{\text{difference}} = \mu_{\text{1st tracing}} - \mu_{\text{2nd tracing}} = 0.$$

Further, intra-class correlation coefficients for each pair of boundary outline points on the mandibular outline between the 1st and 2nd tracings by Observers 1 and 2 (myself and Dr Chen respectively) were again calculated. Results are shown, for anatomical landmark points and intermediate points respectively, in Tables 4.3 (a) and (b).

Overall, 9 of the 19 landmark points (and a significant proportion (25) of the other 59 intermediate points) are significantly different between the tracings of observer 1 and observer 2 (tracings 1 and 2 respectively). It is of interest that points around the condylar region (points 51-76) are not significantly different. There is however evidence of quite large discrepancies between observers in all other areas around the mandibular outline, as well as some poor intra-class correlation coefficients indicative of poor agreement between observers.

These results suggest that the two data sets of 23 and 24 subjects respectively are too different to be combined.

As with the intra-rater study, it might be considered that the test is too conservative. In fact if the individual 95% confidence intervals are examined at face value, we find many more significant differences between tracings between observers, both in the landmark points and when including the intermediate points. However, it is clear that tracings from different observers should not be combined.

Point	N	Mean Difference	Standard Deviation	SE Mean	T-Statistic	P-value	95% C.I.	I.C.C
1*	20	-1.698	1.675	0.375	-4.53	0.0002	(-2.482, -0.914)	0.884
3*	20	-3.633	3.297	0.737	-4.93	0.0001	(-5.176, -2.089)	0.521
13*	20	2.856	1.695	0.379	7.53	<0.0001	(2.062, 3.644)	0.816
18*	20	1.254	1.393	0.311	4.03	0.0007	(0.602, 1.906)	0.955
23*	20	1.383	1.643	0.367	3.76	0.0013	(0.614, 2.153)	0.845
27*	20	1.556	1.389	0.311	5.01	0.0001	(0.906, 2.206)	0.868
31	20	-0.257	1.583	0.354	-0.73	0.48	(-0.998, 0.483)	0.869
35*	20	2.534	1.56	0.349	7.27	<0.0001	(1.803, 3.264)	0.870
39	20	1.037	3.115	0.696	1.49	0.15	(-0.421, 2.495)	0.696
43*	20	0.967	0.909	0.203	4.76	0.0001	(0.541, 1.392)	0.907
45	20	-0.579	1.759	0.393	-1.47	0.16	(-1.403, 0.244)	0.759
49*	20	0.838	1.022	0.228	3.67	0.0016	(0.359, 1.316)	0.899
51	20	-0.679	3.320	0.742	-0.91	0.37	(-2.233, 0.876)	0.640
54	20	0.639	2.261	0.506	1.26	0.22	(-0.419, 1.698)	0.807
58	20	0.952	2.051	0.459	2.07	0.052	(-0.009, 1.912)	0.828
62	20	-0.401	2.666	0.596	-0.67	0.51	(-1.649, 0.848)	0.731
67	20	-0.468	1.525	0.341	-1.37	0.19	(-1.183, 0.246)	0.896
72	20	-0.845	2.828	0.632	-1.34	0.20	(-2.169, 0.479)	0.697
76	20	-0.091	3.003	0.671	-0.14	0.89	(-1.497, 1.315)	0.723

Table 4.3a Inter-rater agreement. Landmark Points only. Unadjusted data.

Point	N	Mean Difference	Standard Deviation	SE Mean	T-Statistic	P-value	95% C.I.	I.C.C
2*	20	-2.612	2.059	0.460	-5.67	<0.0001	(-3.576, -1.648)	0.753
4*	20	-3.349	3.071	0.687	-4.88	0.0001	(-4.786, -1.911)	0.507
5*	20	-2.727	2.777	0.621	-4.39	0.0003	(-4.027, -1.427)	0.410
6	20	-1.261	2.561	0.573	-2.20	0.040	(-2.460, -0.062)	0.005
7	20	1.094	2.364	0.529	2.07	0.052	(-0.013, 2.200)	-0.329
8*	20	3.752	1.849	0.413	9.08	<0.0001	(2.887, 4.617)	0.662
9*	20	3.726	1.588	0.355	10.49	<0.0001	(2.983, 4.469)	0.752
10*	20	3.779	1.625	0.363	10.40	<0.0001	(3.019, 4.540)	0.717
11*	20	3.560	1.798	0.402	8.85	<0.0001	(2.718, 4.402)	0.695
12*	20	3.242	1.904	0.426	7.61	<0.0001	(2.350, 4.133)	0.714
14*	20	2.638	1.310	0.293	9.01	<0.0001	(2.025, 3.252)	0.904
15*	20	2.104	1.038	0.232	9.06	<0.0001	(1.618, 2.590)	0.956
16*	20	1.965	1.220	0.273	7.20	<0.0001	(1.394, 2.536)	0.967
17*	20	1.697	1.243	0.278	6.10	<0.0001	(1.115, 2.279)	0.964
19*	20	1.133	1.297	0.290	3.91	0.0009	(0.526, 1.741)	0.959
20*	20	1.053	1.138	0.254	4.14	0.0006	(0.520, 1.585)	0.967
21*	20	1.121	1.333	0.298	3.76	0.0013	(0.497, 1.745)	0.951
22*	20	1.197	1.430	0.320	3.74	0.0014	(0.528, 1.867)	0.920

ctd...

Point	N	Mean Difference	Standard Deviation	SE Mean	T-Statistic	P-value	95% C.I.	I.C.C
24*	20	1.050	1.229	0.275	3.82	0.0012	(0.475, 1.626)	0.874
25*	20	0.878	1.012	0.226	3.88	0.0010	(0.404, 1.352)	0.898
26*	20	1.066	1.089	0.244	4.38	0.0003	(0.556, 1.576)	0.895
28*	20	2.040	1.718	0.384	5.31	<0.0001	(1.236, 2.844)	0.828
29	20	1.003	1.803	0.403	2.49	0.022	(0.159, 1.847)	0.806
30	20	-0.079	1.779	0.398	-0.20	0.84	(-0.912, 0.754)	0.822
32	20	0.734	1.471	0.329	2.23	0.038	(0.045, 1.422)	0.894
33*	20	1.889	1.477	0.330	5.72	<0.0001	(1.197, 2.580)	0.890
34*	20	2.674	1.340	0.300	8.93	<0.0001	(2.047, 3.302)	0.904
36*	20	2.128	1.865	0.417	5.10	0.0001	(1.255, 3.001)	0.794
37*	20	1.816	2.258	0.505	3.60	0.0019	(0.759, 5.873)	0.741
38	20	1.494	2.802	0.626	2.38	0.028	(0.182, 2.805)	0.693
40	20	1.171	2.305	0.515	2.27	0.035	(0.092, 2.250)	0.680
41	20	1.262	2.016	0.451	2.80	0.011	(0.319, 2.206)	0.594
42*	20	1.226	1.533	0.343	3.58	0.0020	(0.508, 1.943)	0.754
44	20	0.148	1.444	0.323	0.46	0.65	(-0.527, 0.824)	0.777
46	20	-0.285	1.814	0.406	-0.70	0.49	(-1.135, 0.564)	0.709
47	20	0.029	1.418	0.317	0.09	0.93	(-0.634, 0.693)	0.773
48	20	0.498	0.941	0.210	2.36	0.029	(0.57, 0.938)	0.906
50	20	0.104	1.330	0.298	0.35	0.73	(-0.518, 0.727)	0.853
52	20	-0.192	2.486	0.556	-0.35	0.73	(-1.356, 0.971)	0.699
53	20	0.154	2.249	0.503	0.31	0.76	(-0.899, 1.207)	0.747
55	20	0.923	2.224	0.497	1.86	0.079	(-0.118, 1.964)	0.806
56	20	0.998	1.965	0.439	2.27	0.035	(0.078, 1.918)	0.846
57	20	0.991	1.954	0.437	2.27	0.035	(0.076, 1.905)	0.847
59	20	0.814	2.225	0.498	1.64	0.12	(-0.228, 1.856)	0.799
60	20	0.219	2.389	0.534	0.41	0.69	(-0.899, 1.338)	0.778
61	20	-0.157	2.492	0.557	-0.28	0.78	(-1.323, 1.010)	0.752
63	20	-0.435	2.415	0.540	-0.81	0.43	(-1.566, 0.695)	0.806
64	20	-0.328	2.061	0.461	-0.71	0.49	(-1.293, 0.637)	0.863
65	20	-0.389	1.782	0.398	-0.98	0.34	(-1.223, 0.445)	0.893
66	20	-0.447	1.645	0.368	-1.22	0.24	(-1.217, 0.322)	0.897
68	20	-0.936	1.474	0.329	-2.84	0.010	(-1.626, -0.246)	0.897
69	20	-0.991	1.661	0.371	-2.67	0.015	(-1.768, -0.213)	0.867
70	20	-1.502	2.292	0.513	-2.93	0.0086	(-2.575, -0.429)	0.779
71	20	-1.231	2.636	0.589	-2.09	0.050	(-2.465, 0.003)	0.727
73	20	-0.601	2.952	0.660	-0.91	0.37	(-1.983, 0.781)	0.677
74	20	-0.574	2.989	0.668	-0.86	0.40	(-1.973, 0.826)	0.686
75	20	-0.483	3.016	0.674	-0.72	0.48	(-1.895, 0.929)	0.700
77	20	-0.707	1.310	0.293	-2.41	0.026	(-1.320, -0.094)	0.919

Table 4.3b Inter-rater agreement. Intermediate Points. Unadjusted data.

4.3.3 Adjusting for the Centroid

It was noted that the position of the centroid for the predicted fit calculated by the elliptical Fourier function, between the 1st and 2nd tracings (or for observer 1 and observer 2) had changed due to even the slightest alteration of the boundary outline. In other words, the centroid is not a fixed point between tracings, and therefore the centroid for the 2nd tracing would have different (x,y) co-ordinates than that of the 1st tracing. Consequently, the linear distances from the centroid to each point on the mandibular outline will be different for tracings of the same mandible taken at different time points, even if the difference in centroid values is small. Thus, when direct comparison was made for the linear distances from the centroid to the boundary outline between the two tracings, the magnitude of error might be exaggerated. For example, the distance from the centroid to the boundary outline between the 1st and 2nd tracings, for point 23, in the above unadjusted intra-rater study, was found to be significantly different. This indeed might reflect a true difference between tracings, or might be exaggerated due to the fact that the centroid to boundary outline distances for the two tracings will be different since the positions of the centroids will be different to begin with. To circumvent this problem subjectively, superimposition was done by hand on the centroid of the predicted outlines for the 1st and 2nd tracings. This was equivalent to the superimposition of the observed (digitised) plots where the centroid of the two tracings could be superimposed accurately, resulting in similar pictures of discrepancy for the predicted outlines i.e. minor errors seen between the 1st and 2nd tracings for the one observer, and an overall pattern of 'disagreement' between observers.

More formally, it was decided that an adjustment should be made utilising the centroid position of the 1st tracing to calculate the linear distances from the centroid to the boundary outline of the two tracings and the analysis redone. This adjustment was carried out in the following way.

The centroid values of the 1st and 2nd tracings (or tracings from observer 1 and observer 2) were checked and compared to establish that they were indeed different. The (x,y) co-ordinates of the 2nd tracing were converted using the (x,y) co-ordinates of the centroid of the 1st tracing in order to get adjusted distances for the 2nd tracing, with

$$\text{adjusted distance} = \sqrt{(x_i - x_c)^2 + (y_i - y_c)^2} \qquad \text{for } i = 1,\ldots\ldots,78$$

The linear distances for the 1st tracing remained the same.

This adjustment procedure ensured an identical, fixed starting point for the calculation of the linear distances from the centroid to each point on the mandibular outline for both the 1st and 2nd tracings (or tracings for observer 1 and observer 2).

The same formal analysis was carried out on this new 'adjusted for centroid' data. The results for both the intra- and inter-rater agreement studies were very similar to the previous analysis using the unadjusted linear distances. The results are summarised in Tables 4.4 (a) and (b) and 4.5 (a) and (b) for landmark and intermediate points and intra- and inter-rater studies respectively.

Point	N	Mean Difference	Standard Deviation	SE Mean	T-Statistic	P-value	95% C.I.	I.C.C
1	15	-0.0171	0.2740	0.0708	-0.24	0.81	(-0.169, 0.135)	0.998
3	15	-2.2746	3.9289	1.0144	-2.24	0.042	(-4.450, -0.100)	0.565
13	15	-0.7525	1.5801	0.4080	-1.84	0.086	(-1.628, 0.123)	0.905
18	15	-1.0439	1.7074	0.4408	-2.37	0.033	(-1.990, -0.098)	0.805
23	15	-1.1035	1.6408	0.4237	-2.60	0.021	(-2.012, -0.195)	0.792
27	15	-0.6369	1.8123	0.4679	-1.36	0.19	(-1.641, 0.367)	0.762
31	15	-0.8526	1.5997	0.4130	-2.06	0.058	(-1.739, 0.033)	0.897
35	15	-1.2414	2.0001	0.5164	-2.40	0.031	(-2.349, -0.133)	0.853
39	15	-2.1724	4.7781	1.2337	-1.76	0.10	(-4.820, 0.470)	0.137
43	15	0.5206	0.7096	0.1832	2.84	0.013	(0.127, 0.914)	0.961
45	15	0.7599	1.5470	0.3994	1.90	0.078	(-0.097, 1.617)	0.828
49	15	0.4613	1.5318	0.3955	1.17	0.26	(-0.387, 1.310)	0.847
51	15	-0.8449	1.9757	0.5101	-1.66	0.12	(-1.939, 0.250)	0.797
54	15	0.7445	2.0904	0.5397	1.38	0.19	(-0.413, 1.902)	0.868
58	15	0.4178	1.4720	0.3801	1.10	0.29	(-0.398, 1.233)	0.930
62	15	1.0911	2.2729	0.5869	1.86	0.084	(-0.168, 2.350)	0.844
67	15	0.3100	1.4874	0.3841	0.81	0.43	(-0.514, 1.134)	0.931
72	15	0.1526	1.2654	0.3267	0.48	0.64	(-0.545, 0.857)	0.959
76	15	0.2441	1.6593	0.4284	0.57	0.58	(-0.675, 1.163)	0.910

Table 4.4a Intra-rater agreement. Landmark points only. Adjusted for centroid data.

Point	N	Mean Difference	Standard Deviation	SE Mean	T-Statistic	P-value	95% C.I.	I.C.C
2	15	-1.0005	1.9708	0.5089	-1.97	0.069	(-2.092, 0.091)	0.830
4	15	-2.0724	3.6143	0.9332	-2.22	0.043	(-4.074, 0.070)	0.576
5	15	-1.6067	3.1042	0.8015	-2.00	0.065	(-3.326, 0.113)	0.611
6	15	-1.0790	2.3955	0.6185	-1.74	0.10	(-2.406, 0.248)	0.671
7	15	-0.7052	2.0866	0.5387	-1.31	0.21	(-1.861, 0.451)	0.500
8	15	-0.1895	3.2545	0.8403	-0.23	0.82	(-1.992, 1.613)	0.474
9	15	-0.4521	3.0565	0.7892	-0.57	0.58	(-2.145, 1.241)	0.575
10	15	-0.6116	2.3170	0.5983	-1.02	0.32	(-1.895, 0.672)	0.728
11	15	-0.5401	1.9317	0.4988	-1.08	0.30	(-1.610, 0.530)	0.805
12	15	-0.6173	1.5390	0.3974	-1.55	0.14	(-1.470, 0.235)	0.896
14	15	-0.7283	1.5607	0.4030	-1.81	0.092	(-1.593, 0.136)	0.897
15	15	-0.8364	1.4640	0.3780	-2.21	0.044	(-1.647, -0.025)	0.895
16	15	-0.8923	1.5184	0.3920	-2.28	0.039	(-1.733, -0.051)	0.864
17	15	-1.1346	1.6254	0.4197	-2.70	0.017	(-2.035, -0.234)	0.836
19	15	-1.0625	1.7668	0.4562	-2.33	0.035	(-2.041, -0.084)	0.785
20	15	-1.0450	1.6621	0.4291	-2.44	0.029	(-1.966, -0.124)	0.799
21	15	-1.0576	1.5715	0.4058	-2.61	0.021	(-1.928, -0.187)	0.819
22	15	-1.662	1.5433	0.3985	-2.93	0.011	(-2.021, -0.311)	0.818

ctd...

Point	N	Mean Difference	Standard Deviation	SE Mean	T-Statistic	P-value	95% C.I.	I.C.C
24	15	-1.0785	1.6577	0.4280	-2.52	0.025	(-1.997, -0.160)	0.794
25	15	-0.9563	1.6935	0.4373	-2.19	0.046	(-1.894, -0.018)	0.789
26	15	-0.8282	1.7645	0.4556	-1.82	0.091	(-1.806, 0.149)	0.774
28	15	-0.0979	2.0135	0.5199	-0.19	0.85	(-1.213, 1.017)	0.714
29	15	-0.4251	1.9002	0.4906	-0.87	0.40	(-1.478, 0.627)	0.771
30	15	-0.7660	1.8805	0.4856	-1.58	0.14	(-1.808, 0.276)	0.837
32	15	-0.7628	1.6390	0.4232	-1.80	0.093	(-1.671, 0.145)	0.895
33	15	-0.7240	1.7664	0.4561	-1.59	0.13	(-1.702, 0.254)	0.880
34	15	-0.8917	1.9395	0.5008	-1.78	0.097	(-1.966, 0.183)	0.857
36	15	-1.5284	2.3042	0.5950	-2.57	0.022	(-2.805, -0.252)	0.785
37	15	-1.8675	3.2474	0.8385	-2.23	0.043	(-3.666, -0.069)	0.578
38	15	-2.0541	4.3023	1.1109	-1.85	0.086	(-4.44, 0.33)	0.326
40	15	-1.6917	3.2357	0.8354	-2.02	0.062	(-3.484, 0.101)	0.372
41	15	-0.9234	2.2284	0.5754	-1.60	0.13	(-2.158, 0.311)	0.590
42	15	-0.1260	1.1477	0.2963	-0.43	0.68	(-0.762, 0.510)	0.864
44	15	0.8693	1.2148	0.3137	2.77	0.015	(0.196, 1.542)	0.879
46	15	0.7233	1.7313	0.4470	1.62	0.13	(-0.236, 1.682)	0.789
47	15	0.5914	1.5517	0.4007	1.48	0.16	(-0.268, 1.451)	0.839
48	15	0.5074	1.5433	0.3985	1.27	0.22	(-0.347, 1.362)	0.830
50	15	-0.1642	1.5516	0.4006	-0.41	0.69	(-1.024, 0.695)	0.850
52	15	-0.2921	1.3325	0.3441	-0.85	0.41	(-1.939, 0.250)	0.935
53	15	0.3917	1.7767	0.4588	0.85	0.41	(-0.592, 1.376)	0.889
55	15	0.7928	1.8531	0.4785	1.66	0.12	(-0.234, 1.819)	0.896
56	15	0.6175	1.6606	0.4288	1.44	0.17	(-0.302, 1.537)	0.918
57	15	0.4854	1.5014	0.3877	1.25	0.23	(-0.346, 1.317)	0.930
59	15	0.4704	1.5619	0.4033	1.17	0.26	(-0.395, 1.336)	0.922
60	15	0.6376	1.8447	0.4763	1.34	0.20	(-0.384, 1.659)	0.893
61	15	0.9346	2.0258	0.5231	1.79	0.096	(-0.188, 2.057)	0.872
63	15	1.4599	1.7818	0.4600	3.17	0.0068	(0.473, 2.447)	0.854
64*	15	1.5936	1.6439	0.4245	3.75	0.0021	(0.683, 2.504)	0.857
65	15	1.0910	1.6465	0.4251	2.57	0.022	(0.179, 2.003)	0.873
66	15	0.7610	1.4306	0.3694	2.06	0.058	(-0.031, 1.553)	0.924
68	15	0.0403	1.4216	0.3670	0.11	0.91	(-0.747, 0.828)	0.940
69	15	-0.1084	1.4626	0.3777	-0.29	0.78	(-0.919, 0.702)	0.939
70	15	-0.2576	1.3381	0.3455	-0.75	0.47	(-0.999, 0.484)	0.955
71	15	-0.0558	1.2078	0.3119	-0.18	0.86	(-0.725, 0.613)	0.963
73	15	0.2275	1.2689	0.3276	0.69	0.50	(-0.475, 0.930)	0.957
74	15	0.3437	1.3876	0.3583	0.96	0.35	(-0.425, 1.112)	0.945
75	15	0.3085	1.5787	0.4076	0.76	0.46	(-0.566, 1.183)	0.923
77	15	0.2133	0.8453	0.2183	0.98	0.34	(-0.255, 0.682)	0.960

Table 4.4b Intra-rater agreement. Intermediate points. Adjusted for centroid data.

Point	N	Mean Difference	Standard Deviation	SE Mean	T-Statistic	P-value	95% C.I.	I.C.C
1*	20	-1.829	0.1683	0.0376	-4.86	0.0001	(-0.262, -0.104)	0.999
3	20	-1.9211	2.9629	0.6625	-2.90	0.0092	(-3.308, -0.534)	0.577
13	20	0.3701	3.0019	0.6712	0.55	0.59	(-1.035, 1.775)	0.683
18	20	-1.0026	2.2041	0.4929	-2.03	0.056	(-2.034, 0.029)	0.862
23	20	-1.0963	2.0342	0.4549	-2.41	0.026	(-2.049, -0.144)	0.765
27	20	-0.9888	1.7328	0.3875	-2.55	0.019	(-1.800, -0.178)	0.812
31*	20	-2.8813	1.6703	0.3735	-7.71	0.0000	(-3.663, -2.099)	0.896
35	20	-0.0262	2.0612	0.4609	-0.06	0.96	(-0.991, 0.939)	0.849
39	20	-1.1957	3.3844	0.7568	-1.58	0.13	(-2.780, 0.389)	0.724
43	20	0.5538	1.2976	0.2902	1.91	0.072	(-0.054, 1.161)	0.823
45	20	0.5680	1.9434	0.4346	1.31	0.21	(-0.342, 1.478)	0.697
49*	20	3.0429	1.8467	0.4129	7.37	0.0000	(2.178, 3.907)	0.677
51	20	1.8990	3.4516	0.7718	2.46	0.024	(0.283, 3.515)	0.623
54*	20	3.1070	3.2396	0.7244	4.29	0.0004	(1.590, 4.624)	0.598
58*	20	3.3152	3.3857	0.7571	4.38	0.0003	(1.730, 4.900)	0.562
62	20	1.9094	3.5689	0.7980	2.39	0.027	(0.239, 3.580)	0.518
67	20	1.6748	2.7053	0.6049	2.77	0.012	(0.408, 2.941)	0.666
72	20	0.5691	4.0842	0.9132	0.62	0.54	(-1.343, 2.481)	0.387
76	20	1.1993	4.1294	0.9234	1.30	0.21	(-0.734, 3.132)	0.425

Table 4.5a Inter-rater agreement. Landmark points only. Adjusted for centroid data.

Point	N	Mean Difference	Standard Deviation	SE Mean	T-Statistic	P-value	95% C.I.	I.C.C
2	20	-0.9727	1.4077	0.3148	-3.09	0.0060	(-1.632, -0.314)	0.861
4	20	-1.6413	2.8127	0.6289	-2.61	0.017	(-2.958, -0.325)	0.566
5	20	-1.1649	2.4895	0.5567	-2.09	0.050	(-2.330, 0.001)	0.505
6	20	-0.2591	1.9785	0.4424	-0.59	0.56	(-1.185, 0.667)	0.385
7	20	0.6694	1.7985	0.4022	1.66	0.11	(-0.173, 1.511)	0.323
8*	20	1.2851	1.3364	0.2988	4.30	0.0004	(0.660, 1.911)	0.859
9	20	1.1413	1.8733	0.4189	2.72	0.013	(0.264, 2.018)	0.787
10	20	1.1922	2.2843	0.5108	2.33	0.031	(0.123, 2.262)	0.671
11	20	0.9892	2.6975	0.6032	1.64	0.12	(-0.274, 2.252)	0.599
12	20	0.6962	3.0082	0.6726	1.04	0.31	(-0.712, 2.104)	0.593
14	20	0.2012	2.6699	0.5973	0.34	0.74	(-1.049, 1.451)	0.753
15	20	-0.2679	2.3558	0.5268	-0.51	0.62	(-1.371, 0.835)	0.805
16	20	-0.3464	2.2902	0.5121	-0.68	0.51	(-1.419, 0.726)	0.831
17	20	-0.5734	2.2401	0.5009	-1.14	0.27	(-1.622, 0.475)	0.849
19	20	-1.1382	2.1345	0.4773	-2.38	0.028	(-2.137, -0.139)	0.868
20	20	-1.2498	1.9999	0.4472	-2.79	0.012	(-2.186, -0.314)	0.876
21	20	-1.2556	1.9508	0.4362	-2.88	0.0096	(-2.169, -0.342)	0.853
22	20	-1.2355	1.9910	0.4452	-2.78	0.012	(-2.167, -0.303)	0.819

ctd...

Point	N	Mean Difference	Standard Deviation	SE Mean	T-Statistic	P-value	95% C.I.	I.C.C
24*	20	-1.4461	1.8846	0.4214	-3.43	0.0028	(-2.328, -0.564)	0.781
25*	20	-1.6333	1.8237	0.4078	-4.01	0.0008	(-2.487, -0.780)	0.792
26*	20	-1.4607	1.7741	0.3967	-3.68	0.0016	(-2.291, -0.630)	0.801
28	20	-0.5622	1.7934	0.4010	-1.40	0.18	(-1.402, 0.277)	0.813
29*	20	-1.6294	1.8863	0.4218	-3.86	0.0010	(-2.512, -0.746)	0.827
30*	20	-2.7165	1.8415	0.4118	-6.60	0.0000	(-3.579, -1.854)	0.859
32*	20	-1.8761	1.7406	0.3892	-4.82	0.0001	(-2.691, -1.061)	0.886
33	20	-0.7019	1.8815	0.4207	-1.67	0.11	(-1.583, 0.179)	0.866
34	20	0.1010	1.9190	0.4291	0.24	0.82	(-0.797, 0.999)	0.860
36	20	-0.3887	2.2846	0.5109	-0.76	0.46	(-1.458, 0.681)	0.816
37	20	-0.6347	2.6679	0.5966	-1.06	0.30	(-1.884, 0.614)	0.766
38	20	-0.8661	3.1571	0.7060	-1.23	0.23	(-2.344, 0.612)	0.718
40	20	-0.8633	2.5199	0.5635	-1.53	0.14	(-2.043, 0.316)	0.765
41	20	-0.4498	2.3077	0.5160	-0.87	0.39	(-1.530, 0.631)	0.702
42	20	0.0563	1.8666	0.4174	0.13	0.89	(-0.817, 0.930)	0.722
44	20	0.6048	1.2999	0.2907	2.08	0.051	(-0.004, 1.213)	0.807
46	20	1.2097	2.2382	0.5005	2.42	0.026	(0.162, 2.257)	0.555
47*	20	1.8196	2.0652	0.4618	3.94	0.0009	(0.853, 2.786)	0.571
48*	20	2.5225	1.8535	0.4144	6.09	0.0000	(1.655, 3.390)	0.667
50*	20	2.6828	1.7775	0.3975	6.75	0.0000	(1.851, 3.515)	0.791
52	20	2.3242	3.0740	0.6874	3.38	0.0031	(0.885, 3.763)	0.561
53*	20	2.6448	3.0110	0.6733	3.93	0.0009	(1.235, 4.054)	0.558
55*	20	3.3735	3.3319	0.7450	4.53	0.0002	(1.814, 4.933)	0.571
56*	20	3.4233	3.1998	0.7155	4.78	0.0001	(1.925, 4.921)	0.604
57*	20	3.3900	3.2853	0.7346	4.61	0.0002	(1.852, 4.928)	0.591
59*	20	3.1482	3.4448	0.7703	4.09	0.0006	(1.536, 4.761)	0.544
60	20	2.5333	3.5376	0.7910	3.20	0.0047	(0.877, 4.189)	0.536
61	20	2.1501	3.5433	0.7923	2.71	0.014	(0.491, 3.809)	0.517
63	20	1.8835	3.2505	0.7268	2.59	0.018	(0.362, 3.405)	0.607
64	20	1.9810	3.0608	0.6844	2.89	0.0093	(0.548, 3.414)	0.643
65	20	1.8949	2.8449	0.6361	2.98	0.0077	(0.563, 3.227)	0.668
66	20	1.7830	2.7891	0.6237	2.86	0.010	(0.477, 3.089)	0.669
68	20	1.0554	2.5794	0.5768	1.83	0.083	(-0.152, 2.263)	0.684
69	20	0.8127	2.7870	0.6232	1.30	0.21	(-0.492, 2.117)	0.622
70	20	0.1189	3.4943	0.7813	0.15	0.88	(-1.517, 1.755)	0.496
71	20	0.2958	3.8917	0.8702	0.34	0.74	(-1.526, 2.118)	0.419
73	20	0.7628	4.1794	0.9345	0.82	0.42	(-1.194, 2.719)	0.367
74	20	0.7533	4.1682	0.9320	0.81	0.43	(-1.198, 2.705)	0.385
75	20	0.8182	4.1952	0.9381	0.87	0.39	(-1.146, 2.782)	0.399
77	20	0.6706	2.1520	0.4812	1.39	0.18	(-0.337, 1.678)	0.764

Table 4.5b Inter-rater agreement. Intermediate points. Adjusted for centroid data.

Very little disagreement was evident for tracings taken by the same observer. In fact, not one anatomical landmark was found to be significantly different between tracings by the same observer (and only a single intermediate point, that being point 64 which is a point within a difficult area). In contrast, 5 anatomical landmarks were found to be significantly different between observers, and 15 further intermediate points. These points (1, 31, 49, 54 and 58 and 8, 24, 29, 30, 32, 47, 48, 50, 53, 55, 56, 57 and 59 respectively) do not seem to be confined to any one area, but rather are around the whole of the mandibular outline.

4.3.4 Adjusting for Point 18

The same adjustment procedure was repeated using what can be considered as a 'fixed' landmark point, point 18 (the tip of the central incisor), instead of fixing on the centroid. This point was chosen since it was believed to be one of the more easily identified, and 'fixed' landmark points. As before, results are summarised in Tables 4.6 (a) and (b) and 4.7 (a) and (b) for landmark and intermediate points and intra- and inter-rater studies respectively.

Point	N	Mean Difference	Standard Deviation	SE Mean	T-Statistic	P-value	95% C.I.	I.C.C
1	15	0.300	1.106	0.286	1.05	0.31	(-0.313, 0.913)	0.964
3	15	-0.493	2.335	0.603	-0.82	0.43	(-1.786, 0.801)	0.829
13	15	0.379	1.386	0.358	1.06	0.31	(-0.389, 1.146)	0.829
18*	15	-1.992	1.323	0.342	-5.83	0.0000	(-2.724, -1.259)	0.017
23	15	1.067	1.435	0.371	2.88	0.012	(0.271, 1.862)	0.561
27*	15	1.942	1.641	0.424	4.58	0.0004	(1.033, 2.851)	0.649
31	15	0.032	1.001	0.258	0.12	0.90	(-0.523, 0.586)	0.913
35	15	0.275	0.996	0.257	1.07	0.30	(-0.276, 0.827)	0.925
39	15	1.824	2.592	0.669	2.72	0.016	(0.388, 3.260)	0.760
43	15	1.283	2.790	0.720	1.78	0.097	(-0.263, 2.828)	0.855
45	15	0.905	2.008	0.519	1.75	0.10	(-0.207, 2.017)	0.924
49	15	0.558	1.489	0.384	1.45	0.17	(-0.266, 1.383)	0.955
51	15	-0.203	1.731	0.447	-0.45	0.66	(-1.162, 0.756)	0.940
54	15	0.761	1.922	0.496	1.53	0.15	(-0.303, 1.826)	0.957
58	15	0.507	1.822	0.470	1.08	0.30	(-0.502, 1.516)	0.956
62	15	1.177	2.180	0.563	2.09	0.055	(-0.031, 2.385)	0.940
67	15	1.434	1.844	0.476	3.01	0.0093	(0.412, 2.456)	0.904
72	15	0.815	1.681	0.434	1.88	0.082	(-0.116, 1.746)	0.954
76	15	0.788	1.737	0.448	1.76	0.10	(-0.174, 1.750)	0.925

Table 4.6a **Intra-rater agreement. Landmark points only. Adjusted for point 18.**

Point	N	Mean Difference	Standard Deviation	SE Mean	T-Statistic	P-value	95% C.I.	I.C.C
2	15	-0.083	1.604	0.414	-0.20	0.84	(-0.972, 0.805)	0.920
4	15	-0.439	2.405	0.621	-0.71	0.49	(-1.771, 0.893)	0.810
5	15	-0.362	2.575	0.665	-0.54	0.59	(-1.789, 1.064)	0.765
6	15	-0.063	3.013	0.778	-0.08	0.94	(-1.731, 1.606)	0.680
7	15	0.157	3.257	0.841	0.19	0.85	(-1.647, 1.962)	0.630
8	15	0.425	3.109	0.803	0.53	0.60	(-1.297, 2.147)	0.603
9	15	0.540	2.866	0.740	0.73	0.48	(-1.048, 2.128)	0.533
10	15	0.570	2.294	0.592	0.96	0.35	(-0.701, 1.841)	0.578
11	15	0.307	2.071	0.535	0.58	0.57	(-0.839, 1.454)	0.613
12	15	0.266	1.527	0.394	0.67	0.51	(-0.580, 1.112)	0.789
14	15	0.360	1.116	0.288	1.25	0.23	(-0.258, 0.978)	0.793
15	15	0.513	1.255	0.324	1.58	0.14	(-0.182, 1.208)	0.509
16	15	0.344	1.435	0.370	0.93	0.37	(-0.450, 1.139)	-0.111
17	15	-0.374	0.987	0.255	-1.47	0.16	(-0.921, 0.173)	-0.189
19*	15	-1.467	1.476	0.381	-3.85	0.0018	(-2.284, -0.649)	-0.232
20	15	-0.762	1.420	0.367	-2.08	0.057	(-1.548, 0.025)	-0.152
21	15	0.028	1.299	0.335	0.08	0.93	(-0.691, 0.748)	0.217
22	15	0.649	1.403	0.362	1.79	0.095	(-0.128, 1.427)	0.389

ctd...

Point	N	Mean Difference	Standard Deviation	SE Mean	T-Statistic	P-value	95% C.I.	I.C.C
24*	15	1.396	1.319	0.341	4.10	0.0011	(0.665, 2.127)	0.663
25*	15	1.584	1.364	0.352	4.50	0.0005	(0.829, 2.340)	0.664
26*	15	1.796	1.524	0.393	4.56	0.0004	(0.952, 2.640)	0.640
28*	15	1.656	1.295	0.334	4.95	0.0002	(0.938, 2.374)	0.733
29*	15	1.085	0.731	0.189	5.75	0.0001	(0.680, 1.489)	0.914
30	15	0.332	0.726	0.187	1.77	0.098	(-0.070, 0.734)	0.926
32	15	0.176	1.055	0.272	0.65	0.53	(-0.408, 0.761)	0.908
33	15	0.303	0.939	0.242	1.25	0.23	(-0.217, 0.823)	0.930
34	15	0.330	0.941	0.243	1.36	0.20	(-0.192, 0.851)	0.932
36	15	0.544	1.136	0.293	1.86	0.085	(-0.085, 1.174)	0.912
37	15	0.747	1.341	0.346	2.16	0.049	(0.005, 1.490)	0.900
38	15	1.176	1.657	0.428	2.75	0.016	(0.259, 2.094)	0.873
40	15	1.918	2.495	0.644	2.98	0.010	(0.536, 3.300)	0.811
41	15	1.671	2.331	0.602	2.78	0.015	(0.380, 2.962)	0.856
42	15	1.521	2.388	0.617	2.47	0.027	(0.198, 2.844)	0.871
44	15	1.137	1.920	0.496	2.29	0.038	(0.073, 2.201)	0.925
46	15	0.795	2.009	0.519	1.53	0.15	(-0.318, 1.908)	0.921
47	15	0.634	1.622	0.419	1.51	0.15	(-0.264, 1.533)	0.948
48	15	0.556	1.523	0.393	1.41	0.18	(-0.288, 1.399)	0.952
50	15	0.119	1.521	0.393	0.30	0.77	(-0.724, 0.961)	0.951
52	15	0.018	1.433	0.370	0.05	0.96	(-0.776, 0.812)	0.971
53	15	0.530	1.761	0.455	1.17	0.26	(-0.446, 1.505)	0.960
55	15	0.771	1.871	0.483	1.60	0.13	(-0.265, 1.808)	0.958
56	15	0.631	1.827	0.472	1.34	0.20	(-0.381, 1.642)	0.959
57	15	0.549	1.773	0.458	1.20	0.25	(-0.434, 1.531)	0.960
59	15	0.594	1.901	0.491	1.21	0.25	(-0.459, 1.646)	0.954
60	15	0.797	2.094	0.541	1.47	0.16	(-0.363, 1.957)	0.945
61	15	1.079	2.139	0.552	1.95	0.071	(-0.105, 2.264)	0.941
63	15	1.657	1.853	0.479	3.46	0.0038	(0.630, 2.684)	0.940
64*	15	2.122	1.955	0.505	4.20	0.0009	(1.039, 3.205)	0.911
65	15	1.886	2.102	0.543	3.47	0.0037	(0.721, 3.050)	0.887
66	15	1.800	1.942	0.502	3.59	0.0030	(0.724, 2.876)	0.896
68	15	1.049	1.822	0.470	2.23	0.043	(0.040, 2.058)	0.911
69	15	0.802	1.664	0.430	1.87	0.083	(-0.120, 1.723)	0.934
70	15	0.700	1.657	0.428	1.63	0.12	(-0.218, 1.618)	0.951
71	15	0.757	1.744	0.450	1.68	0.11	(-0.209, 1.723)	0.951
73	15	0.810	1.633	0.422	1.92	0.075	(-0.094, 1.715)	0.951
74	15	0.916	1.670	0.431	2.12	0.052	(-0.009, 1.841)	0.942
75	15	0.848	1.723	0.445	1.91	0.077	(-0.106, 1.803)	0.932
77	15	0.599	1.422	0.367	1.63	0.12	(-0.188, 1.387)	0.939

Table 4.6b Intra-rater agreement. Intermediate Points. Adjusted for point 18.

Point	N	Mean Difference	Standard Deviation	SE Mean	T-Statistic	P-value	95% C.I.	I.C.C
1	20	-0.1499	0.3049	0.0682	-2.20	0.041	(-0.293, -0.007)	0.998
3*	20	-1.3732	1.3749	0.3074	-4.47	0.0003	(-2.017, -0.730)	0.980
13	20	-2.1844	3.2181	0.7196	-3.04	0.0068	(-3.691, -0.678)	0.323
18*	20	-2.1449	1.3307	0.2976	-7.21	0.0000	(-2.768, -1.522)	-0.215
23	20	-0.1567	2.2050	0.4931	-0.32	0.75	(-1.189, 0.876)	0.519
27*	20	3.8189	2.3083	0.5162	7.40	0.0000	(2.738, 4.899)	0.886
31	20	-3.8873	2.0467	0.4576	-8.49	0.0000	(-4.845, -2.929)	0.833
35*	20	0.3262	0.6005	0.1343	2.43	0.025	(0.045, 0.607)	0.985
39	20	1.6906	2.2298	0.4986	3.39	0.0031	(0.647, 2.734)	0.905
43	20	0.8040	3.9736	0.8885	0.90	0.38	(-1.056, 2.664)	0.814
45	20	0.3536	2.9695	0.6640	0.53	0.60	(-1.036, 1.744)	0.892
49*	20	3.1383	1.9898	0.4449	7.05	0.0000	(2.207, 4.070)	0.943
51*	20	2.2674	2.4998	0.5590	4.06	0.0007	(1.097, 3.438)	0.897
54*	20	3.4451	2.8150	0.6295	5.47	0.0000	(2.127, 4.763)	0.893
58*	20	3.1508	3.2000	0.7155	4.40	0.0003	(1.653, 4.649)	0.858
62	20	1.6178	3.2856	0.7347	2.20	0.040	(0.080, 3.156)	0.850
67	20	1.8533	3.0096	0.6730	2.75	0.013	(0.444, 3.262)	0.855
72	20	0.7792	3.0042	0.6718	1.16	0.26	(-0.627, 2.186)	0.843
76	20	1.5412	2.5666	0.5739	2.69	0.015	(0.340, 2.743)	0.877

Table 4.7a Inter-rater agreement. Landmark points only. Adjusted for point 18.

Point	N	Mean Difference	Standard Deviation	SE Mean	T-Statistic	P-value	95% C.I.	I.C.C
2*	20	-0.8412	0.7601	0.1700	-4.95	0.0001	(-1.197)-0.485	0.922
4*	20	-1.3992	1.3346	0.2984	-4.69	0.0002	(-2.024, -0.774)	0.981
5*	20	-1.5789	1.4159	0.3166	-4.99	0.0001	(-2.242, -0.916)	0.977
6*	20	-1.6203	1.4775	0.3304	-4.90	0.0001	(-2.312, -0.929)	0.974
7*	20	-1.5185	1.4509	0.3244	-4.68	0.0002	(-2.198, -0.839)	0.971
8*	20	-1.4150	1.2861	0.2876	-4.92	0.0001	(-2.017, -0.813)	0.970
9	20	1.2493	1.8493	0.4135	-3.02	0.0070	(-2.115, -0.384)	0.916
10	20	-1.5259	2.3140	0.5174	-2.95	0.0082	(-2.609, -0.443)	0.853
11	20	-1.6625	2.7185	0.6079	-2.73	0.013	(-2.935, -0.390)	0.762
12	20	-1.9139	2.9649	0.6630	-2.89	0.0094	(-3.302, -0.526)	0.638
14	20	-1.8051	2.5375	0.5674	-3.18	0.0049	(-2.993, -0.617)	0.347
15	20	-0.9386	1.8077	0.4042	-2.32	0.031	(-1.785, -0.092)	0.385
16*	20	-1.0056	1.2874	0.2879	-3.49	0.0024	(-1.608, -0.403)	0.294
17*	20	-1.3771	0.9412	0.2105	-6.54	0.0000	(-1.818, -0.936)	-0.039
19*	20	-1.5008	1.5453	0.3455	-4.34	0.0003	(-2.224, -0.777)	-0.077
20	20	-0.7266	1.6355	0.3657	-1.99	0.062	(-1.492, 0.039)	-0.199
21	20	-0.4382	1.5374	0.3438	-1.27	0.22	(-1.158, 0.281)	-0.059
22	20	-0.2910	1.7368	0.3884	-0.75	0.46	(-1.104, 0.522)	0.297

ctd...

Point	N	Mean Difference	Standard Deviation	SE Mean	T-Statistic	P-value	95% C.I.	I.C.C
24	20	0.9457	1.7021	0.3806	2.48	0.022	(0.149, 1.742)	0.769
25*	20	2.0293	1.5859	0.3546	5.72	0.0000	(1.287, 2.772)	0.834
26*	20	3.0363	1.8452	0.4126	7.36	0.0000	(2.173, 3.900)	0.868
28*	20	2.2012	2.0087	0.4492	4.90	0.0001	(1.261, 3.142)	0.909
29	20	-0.1021	1.8278	0.4087	-0.25	0.81	(-0.958, 0.754)	0.901
30*	20	-2.1130	1.8283	0.4088	-5.17	0.0001	(-2.969, -1.257)	0.865
32*	20	-2.9666	1.6193	0.3621	-8.19	0.0000	(-3.725, -2.209)	0.891
33*	20	-1.7849	1.0987	0.2457	-7.27	0.0000	(-2.299, -1.271)	0.948
34	20	-0.4856	0.6872	0.1537	-3.16	0.0052	(-0.807, -0.164)	0.980
36*	20	0.6964	0.8758	0.1958	3.56	0.0021	(0.286, 1.106)	0.972
37*	20	1.0311	1.2243	0.2738	3.77	0.0013	(0.458, 1.604)	0.955
38	20	1.2429	1.6465	0.3682	3.38	0.0032	(0.472, 2.014)	0.933
40*	20	1.8205	2.0057	0.4485	4.06	0.0007	(0.882, 2.759)	0.930
41	20	1.5760	2.1575	0.4824	3.27	0.0041	(0.566, 2.586)	0.928
42	20	1.1635	2.9030	0.6491	1.79	0.089	(-0.195, 2.523)	0.886
44	20	0.5261	3.1361	0.7012	0.75	0.46	(-0.942, 1.994)	0.878
46	20	1.3302	2.7956	0.6251	2.13	0.047	(0.021, 2.639)	0.896
47*	20	2.0277	2.4077	0.5384	3.77	0.0013	(0.901, 3.155)	0.919
48*	20	2.7447	2.0880	0.4669	5.88	0.0000	(1.767, 3.722)	0.940
50*	20	2.5185	1.6678	0.3729	6.75	0.0000	(1.738, 3.299)	0.955
52*	20	2.7075	2.4954	0.5580	4.85	0.0001	(1.539, 3.876)	0.902
53*	20	3.0460	2.5527	0.5708	5.34	0.0000	(1.851, 4.241)	0.901
55*	20	3.6075	2.9024	0.6490	5.56	0.0000	(2.249, 4.966)	0.885
56*	20	3.5840	2.9367	0.6567	5.46	0.0000	(2.209, 4.959)	0.884
57*	20	3.3069	3.0985	0.6928	4.77	0.0001	(1.856, 4.757)	0.871
59*	20	2.7653	3.2683	0.7308	3.78	0.0013	(1.235, 4.295)	0.851
60	20	2.0052	3.3858	0.7571	2.65	0.016	(0.420, 3.590)	0.843
61	20	1.6899	3.3504	0.7492	2.26	0.036	(0.122, 3.258)	0.842
63	20	1.7623	2.9975	0.6703	2.63	0.017	(0.359, 3.166)	0.885
64	20	1.9171	3.0780	0.6883	2.79	0.012	(0.476, 3.358)	0.877
65	20	1.8169	3.0312	0.6778	2.68	0.015	(0.398, 3.236)	0.873
66	20	1.7656	3.0466	0.6812	2.59	0.018	(0.339, 3.192)	0.865
68	20	1.0590	2.5785	0.5766	1.84	0.082	(-0.148, 2.266)	0.888
69	20	0.7016	2.3246	0.5198	1.35	0.19	(-0.387, 1.790)	0.903
70	20	0.3126	2.6377	0.5898	0.53	0.60	(-0.922, 1.547)	0.876
71	20	0.3354	2.8814	0.6443	0.52	0.61	(-1.013, 1.684)	0.854
73	20	1.1270	2.9824	0.6669	1.69	0.11	(-0.269, 2.523)	0.840
74	20	1.1871	2.8368	0.6343	1.87	0.077	(-0.141, 2.515)	0.852
75	20	1.2953	2.7546	0.6160	2.10	0.049	(0.006, 2.585)	0.859
77	20	0.8446	1.3361	0.2988	2.83	0.011	(0.219, 1.470)	0.965

Table 4.7b Inter-rater agreement. Intermediate points. Adjusted for point 18.

Again we see a similar pattern emerging. It would seem that there is evidence of little disagreement between tracings taken by the same observer, where only 2 of the anatomical landmarks were significantly different between tracings, with a further 7 if intermediate points were considered also. Further, this disagreement seems to be confined to one difficult area on the mandibular outline, the anterior incisal region (with significant differences for landmark points 18 and 27 and associated intermediate points 19, 24, 25, 26, 28, 29 and exception 64 which is of course within a difficult region itself). There is again evidence of much more disagreement between observers, with significant differences for 7 anatomical landmarks and a further 27 intermediate points, around the whole mandibular outline (points 3, 8, 18, 27, 31, 49, 51, 54, 58 and points 2, 4, 5, 6, 7, 8, 16, 17, 19, 25, 26, 28, 30, 32, 33, 36, 37, 40, 47, 48, 50, 52, 53, 55, 56, 57 and 59 respectively).

4.3.5 Summary

Number of points which are significantly different (1st Tracing – 2nd Tracing)	*Intra-rater*		*Inter-rater*	
	Anatomical landmarks only	**Including intermediate points**	**Anatomical landmarks only**	**Including intermediate points**
Unadjusted	1	5	9	34
Centroid Adjusted	0	1	5	20
Point 18 Adjusted	2	9	7	34

Table 4.8 Summary table of intra- and inter-rater studies.

It would seem reasonable to conclude from the above summary table that tracings taken by the same person on the two occasions are in close, overall 'agreement'. The same cannot be said however about those films traced by two different people, where there were many more significant differences between both anatomical landmark points and intermediate points. This reflects our initial impression from the plots of observed points between the 1st and 2nd tracings or tracings between observer 1 and observer 2. Furthermore, the significant differences between the 1st and 2nd tracings for those tracings done by the same person, were concentrated in a few main areas, mainly areas of high curvature, including the condylar and anterior incisal areas, as we first suspected. In contrast, differences between observers seemed to occur in all regions of the mandibular outline.

Our overall results suggest that observations on particular points where a significant difference was found for the *same* observer should not cause too much concern, but should however be interpreted with caution. Overall, tracings between *different* observers should not be combined.

4.4 Description of the whole data sample between 9 and 15 Years

From the error studies we concluded that it would not be possible to combine the two samples of patients (inter-rater study). The reproducibility of films done by the same person however was satisfactory (intra-rater) and our attention is now drawn back to

the original sample of the 23 patients collected by one observer for further investigation.

In order to get a feel for any changes as regards bone growth, which might be taking place between the ages of 9 to 15 years, a few simple descriptive plots were produced of the sample of 23 subjects, as well as for the 15 males and 8 females separately. Each age group, for the whole data sample and for male and female data samples was considered in turn. There were 12, 9, 10 and 14 males and 6, 4, 7 and 7 females aged 9, 11, 13 and 15 respectively in this data sample. Average predicted outlines were calculated and drawn for each age group, for both sexes. Average size-standardised predicted outlines were also considered in order to investigate shape changes only.

Linear distances from the centroid of these mean predicted outlines to each of the 78 points on the mandibular outlines were also calculated and plotted for each age (as well as the individual x- and y- component distances).

Superimposition of these mean predicted forms and distances from the centroid, for each of the four ages illustrated where there might be differences between the ages.

4.4.1 Changes in Size and Shape between 9 and 15 years

In order to investigate overall size and shape changes in the whole data sample, the predicted data points from the EFF were plotted, averaged for each age group, to produce a mean predicted mandibular outline for each of the ages 9, 11, 13 and 15.

These outlines were superimposed on the centroid in order to pinpoint any overall 'growth' changes between ages 9 to 15. The (x,y) centroid value is subtracted from each of the (x,y) co-ordinate pairs for each of the points which characterise the mandibular outline, so these outlines are all centred at the point (0,0) in this co-ordinate system. Linear distances from the centroid of these mean predicted outlines to each of the 78 points on the mandibular outlines were also calculated and plotted for each age in an attempt to monitor any overall growth changes of the mandible. Resulting plots are shown in Figures 4.9 (a) and (b).

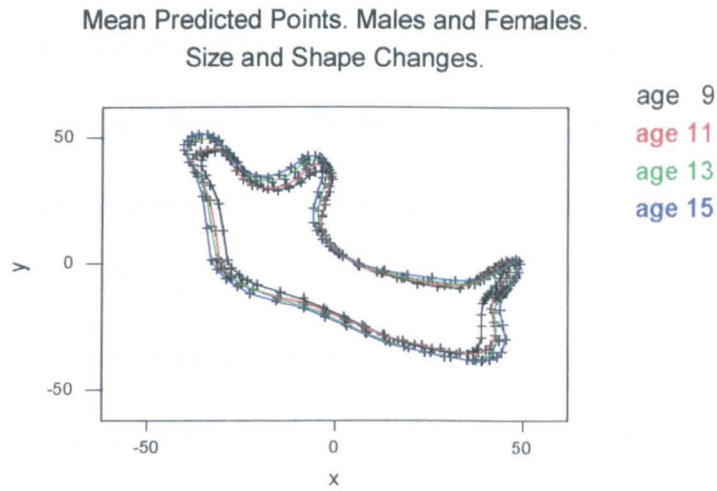

Figure 4.9a **Mean predicted outlines. 23 subjects. Age 9, 11, 13 and 15.**

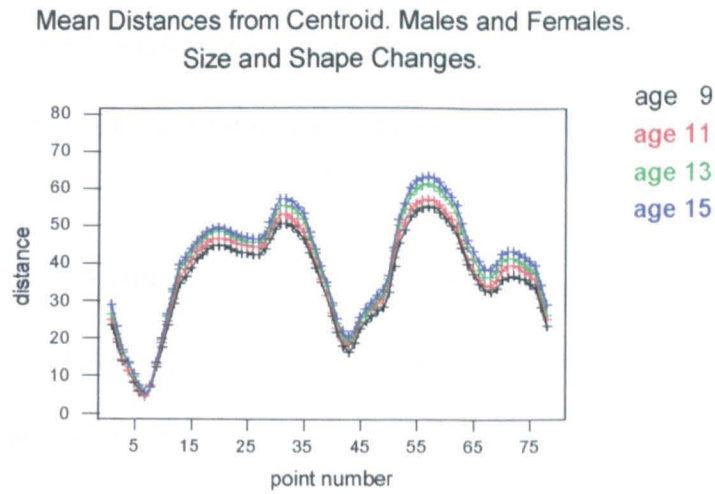

Figure 4.9b **Distances from the centroid. 23 subjects. Age 9, 11, 13 and 15.**

For all 23 patients then, an overall pattern of growth of the mandibular outline is observed. This 'overall' difference in the size and shape of the bone does seem to be small over the range of ages but is nevertheless more pronounced in the both the anterior and posterior regions of the bone as well as around the condyle, mandibular notch and coronoid process. There appears to be a slight forwards, as well as backwards shift of the whole bone over the range of ages, contributing to an overall lengthening of the bone from age 9 through to 15. The bone also seems to be increasing in height, with a slight downwards shift evident in the lower border of the mandible, and an increase in condylar height, as well as a shallowing of the mandibular notch area and an increase in the height of the coronoid process. Overall, the main growth changes are evident on the lower incisal region (points 13-23), the anterior and posterior borders (points 23-35 and points 49-54 respectively) and the whole 'top' area of the bone which includes the condyle, the mandibular notch and the coronoid process (points 54 through to 78). These patterns can also be clearly seen from the distance from the centroid plot where the distances are larger for age 15 compared to 13 compared to 11 compared to age 9 in these areas of apparent 'growth'. The x- and y- component distances from the centroid can also be plotted but they do not say anything more about the pattern of growth and so are not included here.

With the exception of the latter part of the coronoid process (points 72-78) and the anterior border of the ramus (points 1-7), the pattern of overall growth might be compared to throwing a stone in a pool where the centroid represents where the stone lands and the ages 9, 11, 13 and 15 represent a ripple effect where the bone is 'growing' in length, width and height from age 9 through to age 15.

Differences between males and females cannot be discerned from these plots however. In order to make comparisons within the sexes, separate mean plots of predicted points and also of the distances from the centroid were produced, shown in Figures 4.10 and 4.11 (a) and (b) for males and females respectively.

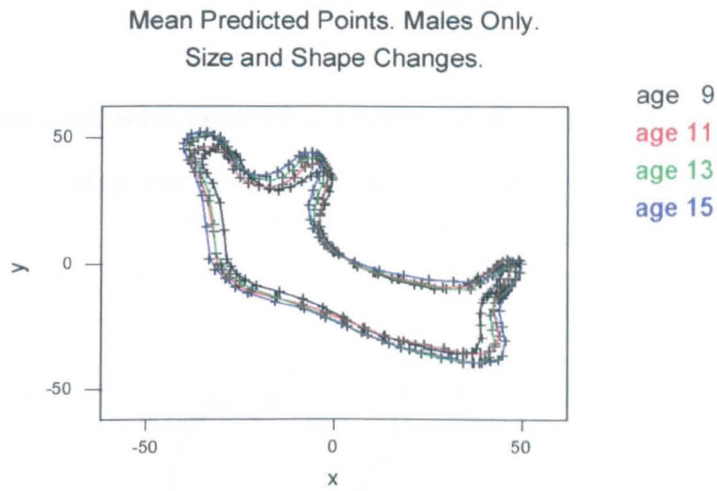

Figure 4.10a **Mean predicted outlines. 15 Male subjects. Age 9, 11, 13 and 15.**

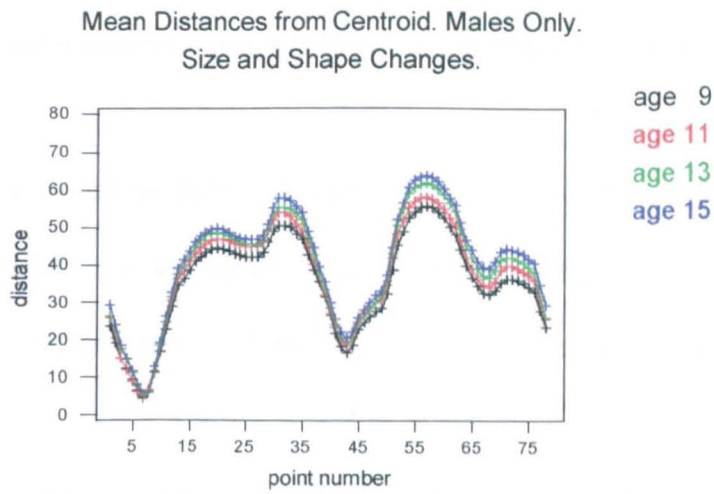

Figure 4.10b **Distances from the centroid. 15 Male subjects. Age 9, 11, 13 and 15.**

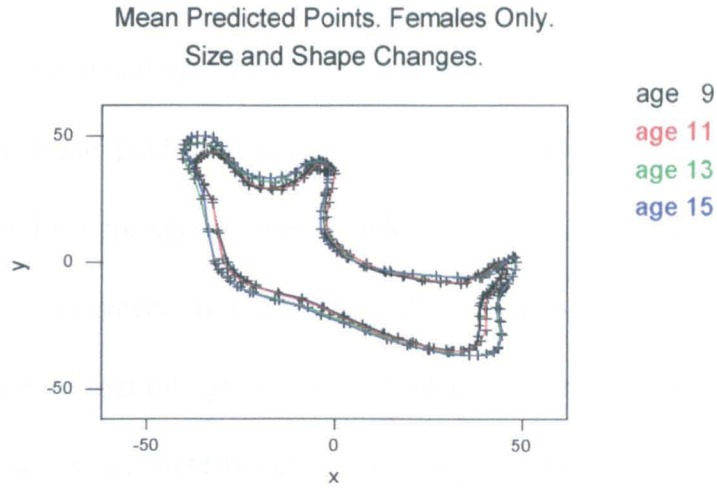

Figure 4.11a **Mean predicted outlines. 8 Female subjects. Age 9, 11, 3 and 15.**

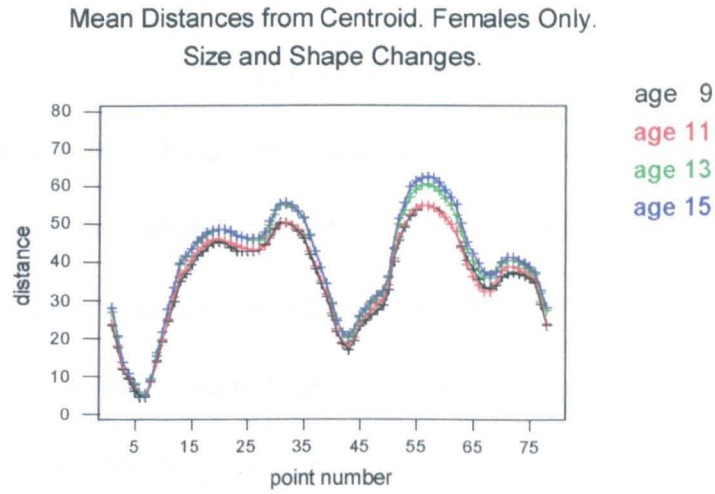

Figure 4.11b **Distances from the centroid. 8 Female subjects. Age 9, 11, 13 and 15.**

Similar trends are observed for both males and females separately, as with the group as a whole, with a similar looking overall change in size and shape, that being an overall increase in length, width and height of the bone from age 9 through to age 15.

The female growth spurt (ages 11-13, approximately) is very clearly illustrated around some of the areas which show evidence of 'growth'. This growth spurt is particularly evident in the anterior region of the mandible (points 23 through to approximately 35)

and in the angle of the mandible, the posterior border of the ramus, as well as the condyle, where the mean predicted outlines for ages 9 and 11 are very close and separate from the outlines for ages 13 and 15, which are also very close. This can also be observed from the distances from the centroid plot for the 8 females in the data sample. It could be said that this growth spurt probably does not extend beyond the age of 13, on average, since there is very little change between the outlines for the ages of 13 and 15.

The male growth spurt (ages 13-15, approximately) is not as obvious from the plots however. The bone seems to change more gradually with age, much like the pattern depicted for both males and females in the data sample. There appears to be yet again an overall pattern of growth around the whole of the bone from age 9 through to age 15, with an increase in overall length, height and width of the bone. The changes do not seem so clear cut over the range of ages as we see in the combined sample and in the females alone however. The predicted outlines for ages 11 and 13 for example, seem to 'cross over' one another in some areas of the mandibular outlines where it would appear that age 11 is 'bigger' than age 13, on average, in these areas. In the anterior region, points 23 to 31 for example. These somewhat inconsistent changes are however extremely small and are not apparent around the whole outline so should not cause too much concern. They are perhaps due to the fact that there are more males in the sample and perhaps there exists more variation within the ages, on average. In fact, these somewhat inconsistent changes are not even evident on the distance from centroid plot since the difference between ages 11 and 13 in the areas concerned is so small.

4.4.2 Changes in Shape between 9 and 15 years

In order to observe any shape changes that maybe occurring during the growth of the mandible, the size component of 'form' must be minimised. This size-standardisation is achieved by scaling every form to be the same area as explained in Chapter 2.

Having standardised for size then, leaving any patterns of change observed being those of shape only we can again obtain plots of the (size-standardised) predicted points for each individual subject in our sample. Means for each age can then be calculated and size-standardised mean plots for both males and females together and also for the sexes separately produced. Similarly, plots of the linear distances from the centroid to the size-standardised mean predicted outlines can also be produced.

Once again these size-standardised predicted outlines were superimposed (centred at (0,0)) in order to pinpoint any shape changes which might be occurring between ages 9 to 15. The distance from the centroid plots were also superimposed for each age in an attempt to capture shape change and / or corroborate the shape changes seen in the predicted outlines.

These descriptive plots for both males and females together i.e. all 23 subjects, are shown in Figures 4.12 (a) and (b).

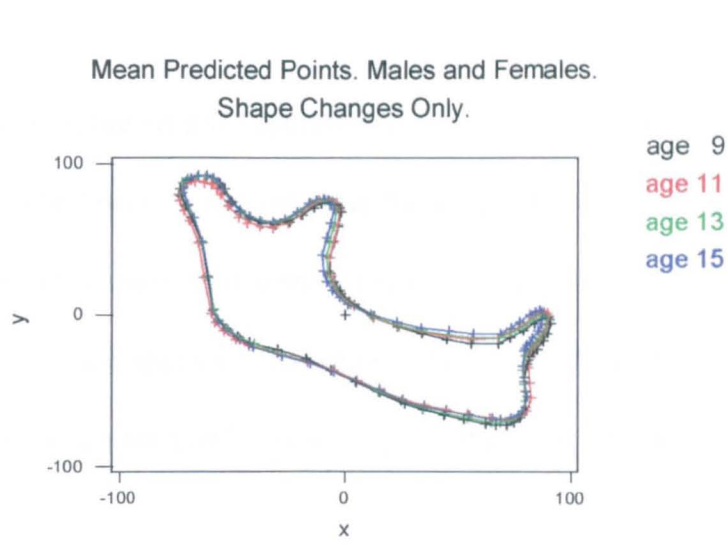

Figure 4.12a **Mean predicted outlines. Size standardised. 23 subjects. Age 9, 11, 13 and 15.**

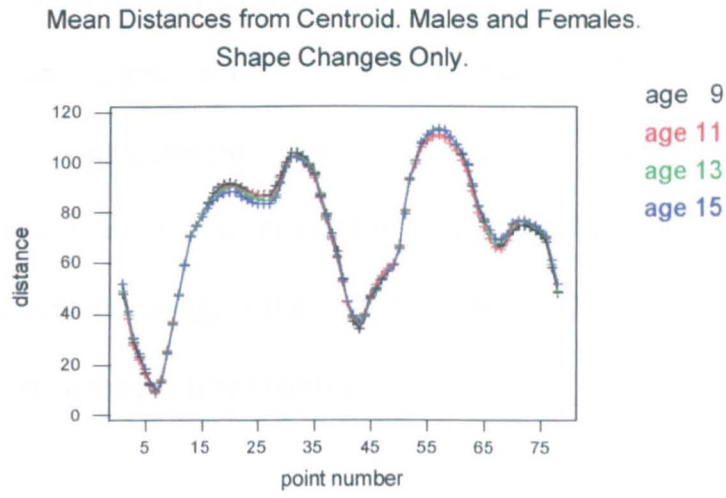

Figure 4.12b **Distances from the centroid. Size standardised. 23 subjects. Age 9, 11, 13 and 15.**

It can be seen then, that the overall changes become harder to discern when dealing with shape alone. For the 23 subjects, 18 aged 9, 13 aged 11, 17 aged 13 and 21 aged 15 it is observed that the main shape changes seem to be occurring in the anterior border of the ramus (points 1-7), the alveolus and the lower incisor (points 7-13 and points 13-23 respectively). There also appears to be a slight shape change in the area of the coronoid process (points 72-78). There appears to be a slight increase in concavity between points 1 and 7, the anterior border of the ramus and a slight

decrease in concavity in the alveolus (points 7-13) over the range of ages, from age 9 through to age 15. The lower incisor becomes more upright over time (points 13-23) and the mandibular notch seems to become more shallow (points 62-67). The coronoid process (points 72-78) also appears to move posteriorly, undoubtedly tied in with the increase in concavity in points 1 to 7. These shape changes are all very small.

The distances from the centroid show this pattern of shape change fairly clearly. These distances are shorter for age 15, then 13, then 11 and 9 between points 13 to 35 approximately, which suggests a posterior shift of the frontal incisor over time, evident from the plot of the predicted outline of the mandible. Also, it can be seen that the linear distances from the centroid from point 67 through to point 75 (approximately) are shorter for age 9 than age 15 capturing the posterior shift in the coronoid process seen in the predicted outline plot.

Redoing this same analysis for the 15 males only (Figures 4.13 (a) and (b)), it can be seen that shape changes are again occurring in the same regions as those for the combined male and female group i.e. the anterior border of the ramus (points 1-7), the alveolus and the lower incisor (points 7-13 and points 13-23 respectively) regions of the bone and in the area of the coronoid process (points 72-78).

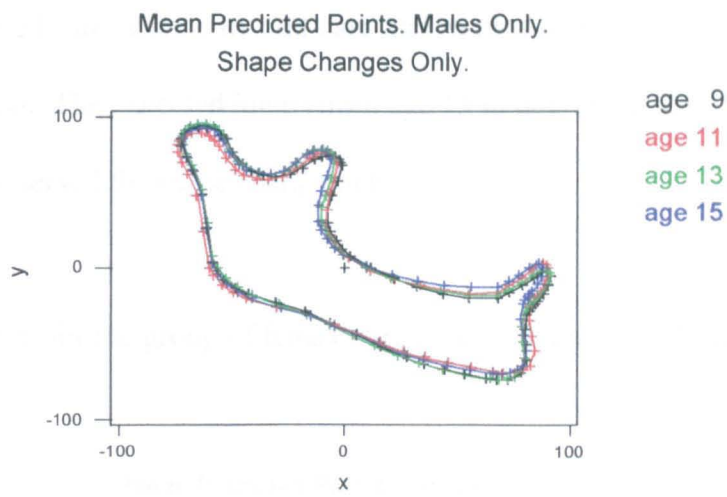

Figure 4.13a **Mean predicted outlines. Size standardised. 15 Males. Age 9, 11, 13 and 15.**

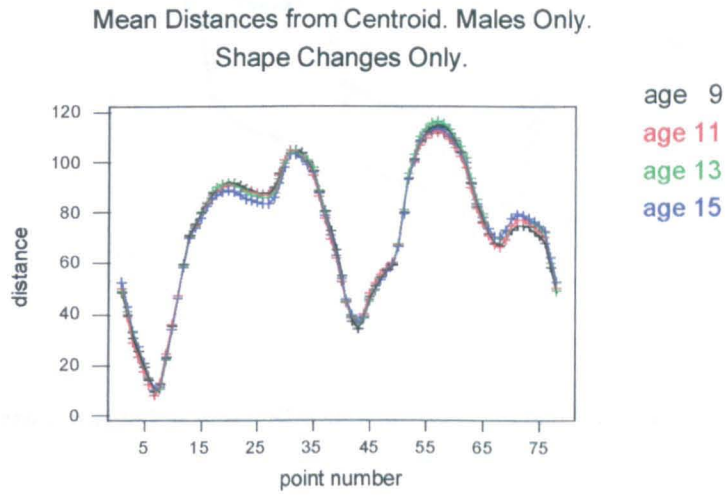

Figure 4.13b **Distances from the centroid. Size standardised. 15 Males. Age 9, 11, 13 and 15.**

The changes for the group of males however, are not as clear-cut as those observed for the group as a whole, in some regions of the bone. This would appear to be due to the outline for age 11. For example, the frontal incisor has indeed moved posteriorly from age 9 to age 15, but it is not so clear what changes are taking place at ages 11 and 13. The outline for age 11 is rather inconsistent. It appears that the frontal incisor for age 11 has moved further back than age 13, which would suggest that any change in shape is going back, then forward, then back again. It could be that one (or more) of the

tracings at this age is an extreme or odd case and in turn will have an influential effect on the overall mean. The expected jump (from age 13 to age 15) at the time of the male growth spurt is observed for shape change only.

Finally, similar plots for the group of females are given in Figures 4.14 (a) and (b).

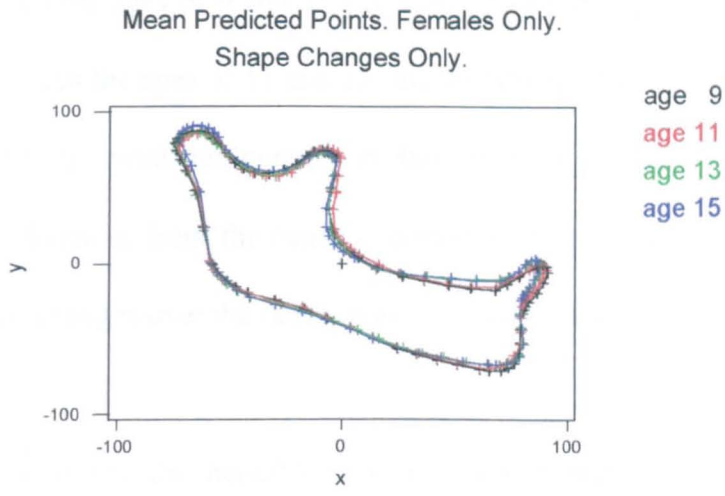

Figure 4.14a **Mean predicted outlines. Size standardised. 8 Females. Age 9, 11, 13 and 15.**

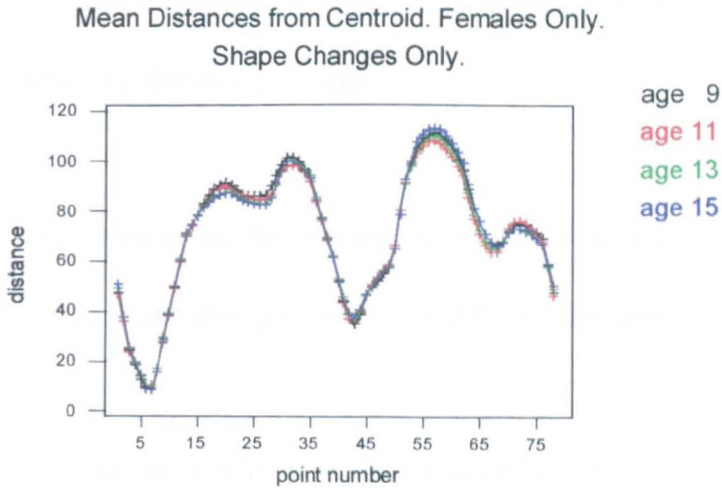

Figure 4.14b **Distances from the centroid. Size standardised. 8 Females. Age 9, 11, 13 and 15.**

From the mean predicted outlines produced for the 8 females in our sample it can be seen once again that the main shape changes are occurring in the same regions of the bone as for the combined sample, as well as just the males. A clear posterior shift of the frontal incisor and a slight increase in concavity between points 1 and 7, the anterior border of the ramus as well as a slight decrease in concavity in the alveolus (points 7-13) between the ages of 9 and 15 years are observed. Further, the expected jump in change between the ages of 11 and 13, the growth spurt for females, is fairly clear from the plot of the predicted outlines in these regions of subtle shape change. The plot of linear distances from the centroid corroborate these observations, again depicting very small changes over the range of ages in certain areas.

Overall then, we can say that the mandible is obviously 'growing' i.e. changing in size and shape, between 9 and 15 years old where males and females tend to be displaying similar patterns of overall growth, although the female growth spurt is more noticeable than the male growth spurt. The bones tend to be, on average, increasing in overall length, height and width over the range of ages.

It should also be stressed once more, that it is important that forms are standardised for the size component so that shape changes can be isolated and observed.

Concentrating on shape change only then, it was observed that these changes were in the main, occurring in the anterior border of the ramus, the alveolus and the lower incisor. There also appeared to be a slight shape change in the area of the coronoid process. A slight increase in concavity in the anterior border of the ramus was observed and a slight decrease in concavity in the alveolus, over the range of ages. The

lower incisor moved posteriorly and became more upright over time. Further, the mandibular notch seemed to shallow and the coronoid process also moved in a posterior direction, undoubtedly tied in with the increase in concavity in the anterior border of the ramus. These shape changes were all very small and broadly similar patterns were found in males and females.

Plots of the linear distances from the centroid to each point on the mean predicted outlines for each age corroborate observations regarding size and shape change (and shape change only) from the mean predicted points plots, for each age. Plots of the x- and y- component distances did not add anything to any observations made and are therefore not illustrated.

4.5 Comparison of Males and Females

Although the main analyses above concentrated on males and females separately, it is of interest to investigate whether or not the 15 males and 8 females in the data sample are in fact different in terms of size and shape or indeed in terms of shape only, at different ages.

To this end, each age group was considered in turn. For age 9, we have 12 males and 6 females; for age 11, 9 males and 4 females; age 13, 10 males and 7 females and age 15, 14 males and 7 females. Average predicted outlines and average size-standardised predicted outlines were calculated and drawn for both sexes at each of the 4 ages. To

illustrate, superimposition of the mean size-standardised predicted forms (on the centroid, as before) are given in Figures 4.15 (a) to (d) in an attempt to pinpoint any difference in shape between males and females.

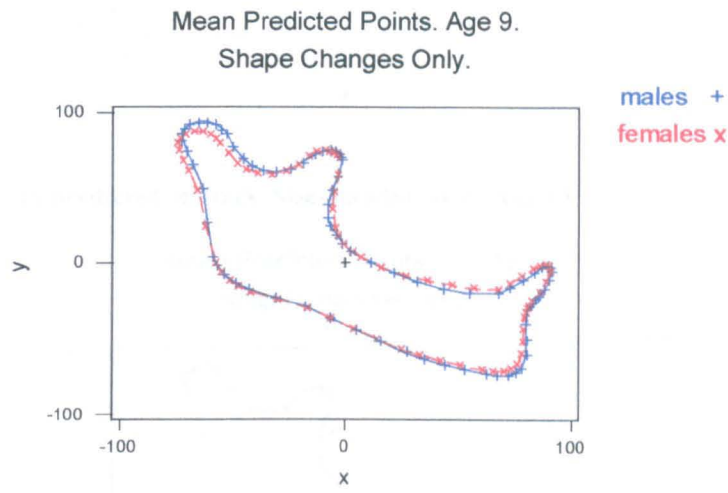

Figure 4.15a **Mean predicted outlines. Size-standardised. Age 9.**

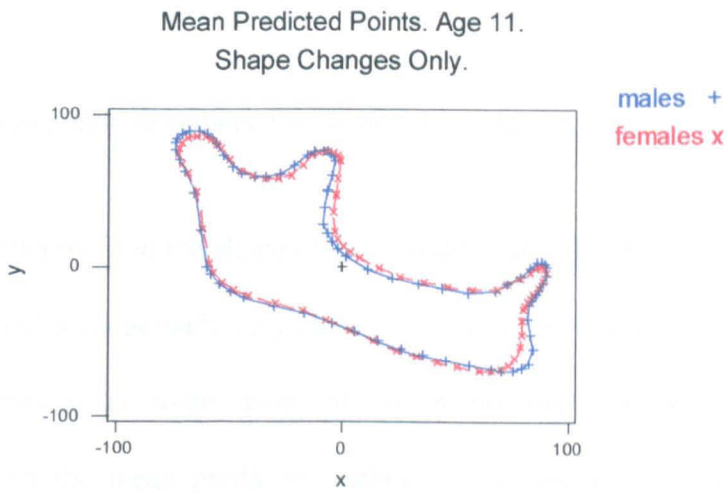

Figure 4.15b **Mean predicted outlines. Size-standardised. Age 11.**

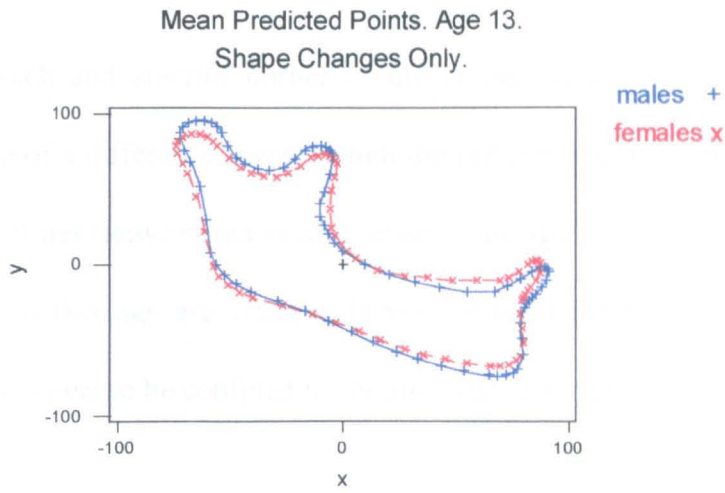

Figure 4.15c Mean predicted outlines. Size-standardised. Age 13.

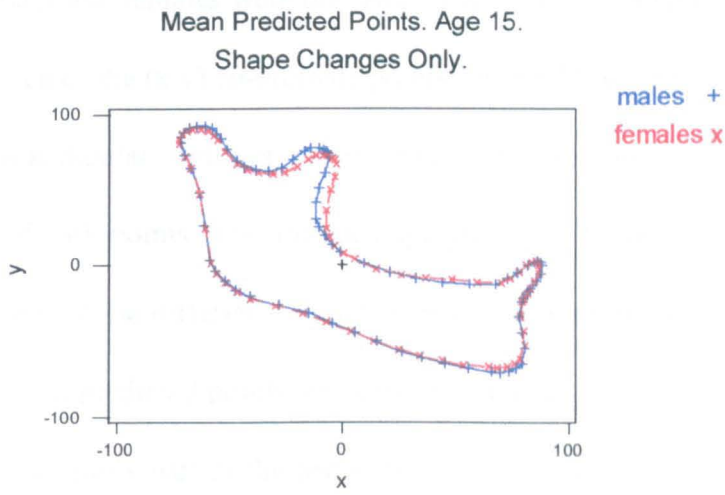

Figure 4.15d Mean predicted outlines. Size-standardised. Age 15.

In terms of any differences in the shape of the mandible at different ages, it would seem that males and females are actually very close to one another. There is some evidence of very slight differences in some areas of the mandibular outline however. Such differences between the mean predicted outlines for males and females seem to be confined to the posterior border of the ramus and the condyle for age 9; mainly in the anterior border of the mandible and perhaps in the condylar, mandibular notch, coronoid process and anterior border of the ramus regions for age 11; and confined to

the mandibular notch and anterior border of the ramus for age 15. Overall, there appears to be more of a difference (even though the outlines still remain close) in the mean predicted outlines between males and females for age 13 however. The mean predicted outlines at this age are slightly different around most of the mandibular outline, and do not appear to be confined to certain areas as for the other ages.

Hotelling's T-Squared test was utilised to formally check the null hypothesis that the mean shapes for males and females were the same in term of their shape, for each age, 9, 11, 13 and 15. Each of the (x,y) co-ordinate points for the 78 predicted points which characterise the mandibular outlines were tested in this analysis. Results are summarised for landmark points only, for each age group, in Table 4.9. For each age then, a null hypothesis of 'no difference in mean shape' between males and females is tested, at each of the 78 predicted points, as (x,y) co-ordinates. The first column in the table, for each age, is simply part of the test statistic of the test, the second column is the observed value of the test statistic, and the third, its corresponding p-value.

It can be seen from the table of results that there is no significant difference between the males and females for ages 9, 11 and 15 for any of the anatomical landmark points (in fact, this was the case for all 78 points). This corroborates the subjective impression from the superimposed size-standardised mean predicted outlines for males and females, at these ages. For age 13 however, there were 14 points which showed evidence of a significant difference in mean shape between the male and female outlines (3 of which were anatomical landmark points as seen in the table). This could be due to an unusual film in this age group, or perhaps that there is in fact more

variability between males and females at this age since it is generally the time that the female growth spurt is ending and the male growth spurt starting.

There is again a case to be made for testing each age using a Bonferroni correction which reduces the conventional significance level of 0.05 to 0.05/19 = 0.0028 for an approximate overall 5% significance level, as we did when testing the linear distances from the centroid in the error studies. In addition, there is of course a power issue in dealing with very small male and female samples here, which makes differences between the samples difficult to detect.

Point	Age 9	TS	p	Age 11	TS	P	Age 13	TS	p	Age 15	TS	p
1	0.069	2.05	0.16	0.061	0.84	0.46	0.047	1.36	0.29	0.022	0.94	0.41
3	0.096	2.88	0.09	0.018	0.25	0.78	0.227	6.55	0.01	0.019	0.79	0.47
13	0.028	0.84	0.45	0.099	1.36	0.30	0.091	2.63	0.11	0.034	1.44	0.26
18	0.019	0.58	0.57	0.022	0.31	0.74	0.164	4.73	0.03	0.047	1.96	0.17
23	0.033	0.99	0.39	0.043	0.60	0.57	0.095	2.74	0.10	0.024	1.01	0.38
27	0.032	0.94	0.41	0.041	0.56	0.59	0.073	2.10	0.16	0.024	1.01	0.39
31	0.041	1.23	0.32	0.238	3.30	0.08	0.062	1.79	0.20	0.063	2.64	0.10
35	0.053	1.59	0.24	0.144	2.00	0.19	0.039	1.11	0.36	0.063	2.67	0.10
39	0.025	0.74	0.49	0.040	0.56	0.59	0.029	0.84	0.45	0.015	0.63	0.54
43	0.016	0.48	0.63	0.066	0.91	0.43	0.045	1.29	0.31	0.032	1.34	0.29
45	0.018	0.53	0.60	0.057	0.79	0.48	0.063	1.83	0.20	0.014	0.59	0.56
49	0.027	0.81	0.46	0.157	2.18	0.16	0.097	2.81	0.09	0.009	0.36	0.70
51	0.032	0.95	0.41	0.042	0.59	0.57	0.076	2.20	0.15	0.014	0.61	0.55
54	0.041	1.21	0.32	0.009	0.12	0.89	0.124	3.57	0.05	0.023	0.97	0.40
58	0.037	1.11	0.35	0.008	0.11	0.90	0.114	3.29	0.07	0.030	1.27	0.30
62	0.041	1.23	0.32	0.011	0.15	0.87	0.103	2.96	0.08	0.029	1.24	0.31
67	0.046	1.39	0.28	0.028	0.39	0.69	0.056	1.62	0.23	0.016	0.68	0.52
72	0.094	2.83	0.09	0.046	0.63	0.55	0.074	2.14	0.15	0.000	0.01	0.99
76	0.088	2.64	0.10	0.038	0.53	0.60	0.061	1.74	0.21	0.000	0.01	0.99

Table 4.9 Hotelling's T^2 Test for 9, 11, 13 and 15 year olds.

In a similar manner, concentrating on differences between males and females in terms of overall size *and* shape changes it was observed that there were indeed differences, again in the main confined to particular regions of the bone, for all ages. These differences were again found to be very small and were not statistically significant.

In summary then, we can say that whilst there appears to be subjective evidence of some difference on average, between males and females at each age, in terms of both overall size and shape, and in terms of the shape of the bone alone, these differences are not statistically significant. Further, they should be interpreted with caution due to the very small sample sizes available at each age.

4.6 Conclusion

In this chapter, using elliptical Fourier function methodology as outlined in Chapter 2, on a longitudinal set of human x-ray data, we have

1. investigated its usefulness in describing the size and shape of a growing form, specific to the study of mandibular form
2. attempted to quantify and localize areas of size and shape changes in the mandible during growth between 9 and 15 years

and

3. identified differences in the size and shape of the mandible between males and females.

We have demonstrated in this Chapter that the EFF method is indeed a useful descriptive tool for observing size and shape changes of growing morphological forms, such as the mandible. The predicted outline, computed by the EFF has been seen to be a very close representation of the observed data. Descriptive plots of these predicted outlines have been produced, as well as plots of centroid-to-outline distances in an attempt to summarise which size and shape changes may be occurring over a range of ages in the sample. It has also been possible to isolate the shape component of the 'form' using the method of area standardisation and investigate only the shape changes that may be occurring over the same range of ages.

However, nothing has been gained from the EFF method in terms of the harmonic information. Overall the set of harmonics does not simplify the description of a complex form, like the mandible. Plots using the harmonic information have been useful for descriptive purposes, but this information has not been used directly in the description of the size and shape of the form. Instead, the predicted outlines have been used for description.

Overall, it was observed that the mandible was 'growing' i.e. changing in size and shape, between 9 and 15 years old where males and females tend, on average, to display similar patterns of overall growth. It was also observed that the female growth spurt was more noticeable than the male growth spurt in this sample of data. The bones tend, on average, to increase in overall length, height and width over the range of ages.

Concentrating on shape change only, it was observed that changes were apparent in a few areas around the mandibular outline. Shape changes were observed in the anterior border of the ramus, the alveolus and the lower incisor. There also appeared to be slight shape changes in the area of the coronoid process. A slight increase in concavity in the anterior border of the ramus was also observed and a slight decrease in concavity in the alveolus, over the range of ages. The lower incisor moved posteriorly and became more upright over time. Further, the mandibular notch became shallower and the coronoid process also moved in a posterior direction. The observed shape changes were all very small however and probably not statistically significant, although this was not tested formally due to the small sample sizes. Broadly similar patterns were again found in males and females in respect of shape change only.

Comparison between average predicted outlines for males and females found no significant difference between the sexes as regards overall size and shape and shape only changes for ages 9, 11, 13 and 15.

In addition, from the error study analyses carried out in this chapter we could conclude that the repeatability of tracings done by the same observer is satisfactory, but those tracings carried out by different observers were not in close enough 'agreement' to allow those two studies to be combined together.

In the next chapter, the method of Procrustes analysis is utilised in an attempt to capture the size and shape information for this same sample of mandibular data.

Chapter 5

Evaluation Of the Data Sample Using Procrustes Methods

5.1 Introduction

It has been established that the shape of any object is invariant under the Euclidean similarity transformations of translation, rotation and scaling. For example, the shape of the human mandible consists of all the geometrical properties of the bone that are unchanged when it is translated, rotated or re-scaled in an arbitrary co-ordinate system. Further, two such mandibles will have the same shape if they can be translated, rotated and re-scaled to each other so that they match each other exactly. In practice, we would be interested in comparing objects, in our case human mandibles over a range of ages for a sample of males and females, which may have different shapes.

Introduced briefly in Chapter 1, the method of Procrustes analysis is a landmark-based approach that can describe the shape of an object, or objects. When utilising the method of Procrustes analysis, objects that are characterised by a set of points (landmarks) are considered, as with the Elliptical Fourier Function method. These objects (the mandibular outlines) are referred to as 'configurations'. A similar method based on what are known as Bookstein shape variables is also considered as a useful

first step in describing the size and shape of a sample of 'configurations', such as the mandibular data.

In this chapter both of these methods are utilised in an attempt to describe the size and / or shape of our sample of mandibular data, for males and females, from age 9 to 15 years.

5.2 Procrustes Analysis

The idea of Procrustes analysis is to work with the complete geometrical object (up to similarity transformations of translation, rotation and scale change) rather than working with derived quantities such as linear distances and ratios as in the conventional metrical approach described in Chapter 1. This follows much the same philosophy as D'Arcy Thompson 1942, as he also worked with complete geometrical pictures of organisms rather than derived quantities, albeit on a less quantitative footing than Procrustes analysis.

According to Dryden and Mardia 1998, methods based on Procrustes superimposition are a major step forward in the field of shape analysis as providing a useful tool for analysing landmark data. Supposing a random sample of objects is available for analysis, they consider the most important aims of shape analysis on that sample to be

1. to obtain a measure of distance between shapes in the sample of objects
2. to estimate an 'average' shape from the sample of objects

and

3. to estimate and explore the structure of shape variability in the sample of objects.

The method of Procrustes analysis provides the tools required to pursue these aims successfully. We now consider each of them in turn.

5.2.1 Distance between shapes and Procrustes matching

Prior to Procrustes matching, objects are described in terms of the (x,y) co-ordinates of a set of anatomical landmarks. Anatomical landmarks (discussed in Chapter 1) are points assigned by an expert that correspond between objects (forms) in some biologically meaningful way. They designate parts of an object that correspond in terms of biological derivation and these parts are called homologous. In order to compare the shapes of two such objects (configurations of homologous points), a measure of distance between the two 'shapes' is required. Before analysis or comparison then, it is necessary to register and superimpose co-ordinates from different forms within the same reference frame in order to measure the distance between them. It should be noted that the particular patterns of between form variation, represented by particular principal components in the scope of this thesis, will be entirely dependent on the way in which the forms have been registered with respect to each other and therefore, the perceived displacement of any particular landmark from one shape to another depends upon this registration. Different registrations will produce different impressions of the shape transformations, and regions close to registration points (if registration is undertaken using such points) will appear to change less than those more distant to the points.

Under the method of Procrustes, a suitable procedure is to match one configuration of landmark points as closely as possible to the other using similarity transformations of location, rotation and scale change. In the context of this thesis, configurations are pre-scaled to unit centroid size in order to standardise for size. The remaining differences between the fitted and observed configurations indicate the magnitude of the difference in shape between the two configurations. The procedure of 'matching' the two configurations is known as the full Procrustes fit (superimposition) of one configuration onto the other, and this so-called superimposition is actually obtained by complex linear regression of one configuration onto the other. The full Procrustes distance between the complex configurations is calculated from a least squares criterion, optimising over the full set of similarity transformation parameters. In other words, Procrustes analysis registers forms by minimising the fit, e.g. the mean square distance between landmarks on each form. The term 'full' is used because the full set of Euclidean similarity transformations is estimated in the matching (translation, rotation and scale). In addition, the term 'Procrustes' is used because the matching operations are identical to those of Procrustes analysis which is a commonly used technique for comparing matrices (up to similarity transformations) in multivariate analysis. Therefore, differences between objects after Procrustes fitting can be expressed in terms of Procrustes distances and this so-called full Procrustes distance between the two matched configurations can be used to assess the closeness of shapes (obviously, the smaller the distance value, the closer the configurations are). It is also used to provide a criterion for estimating mean shape. Further, an overall measure of shape variability can also be obtained by considering the root mean square of the full Procrustes distance from each configuration in the sample to the full Procrustes

estimate of mean shape (the smaller the value, the closer that particular configuration is to the 'average' shape i.e. the smaller the variability).

There are two types of Procrustes analysis:

1. Ordinary Procrustes Analysis – OPA

Used for matching two configurations i.e. when a single object is fitted to one other. The two configurations are matched as closely as possible, up to similarity transformations (translation, rotation and scale). The method of full ordinary Procrustes analysis involves the least squares matching of the two configurations using similarity transformations, where the similarity parameters for location, rotation and scale have to be estimated. This is done by minimising a squared Euclidean distance between the two configurations which involves estimating these three similarity parameters. In fact, location can be removed initially by simply centring the two configurations (the centroids of the two configurations are matched at the origin). The resulting full Procrustes fit provides full Procrustes co-ordinates of one configuration onto the other, and a residual matrix is also obtained. Examination of this residual matrix can sometimes tell us something about the difference in shape between the two configurations e.g. if one residual is particularly large, or if large residuals are confined to a particular region of the object.

2. Generalised Procrustes Analysis - GPA

Used when several objects are fitted using Procrustes superimposition (Gower 1975). The use of GPA is similar to that of OPA but with more than two configurations. GPA can however be considered to match only two objects, an advantage of this being that the matching procedure of GPA is invariant under re-orderings of the objects, whereas OPA is not symmetrical in the ordering of the objects unless the two objects are

exactly the same size. GPA also provides a least squares approach to finding an estimate of the shape of a population mean, with an 'average' shape from a sample of more than two objects, as explained in the next section.

5.2.2 Estimation of Mean Shape

There are many situations in practical data analysis where it would be useful to provide an idea of the average shape of a sample of objects. For example, in the context of the data sample considered in this thesis, an estimate of the average shape of the mandible for a sample of 9 year old females might be useful as a diagnostic tool for an orthodontist wishing to plan a course of treatment for a child of that age and sex. A sample of configurations is considered, from which it is of interest to obtain the population mean configuration. The shape of this population mean can be estimated using what is known as the full Procrustes estimate of mean shape. The method of full GPA involves translating, rotating and re-scaling the configurations in a sample relative to each other so as to minimise a total sum of squares. The estimate of mean shape is obtained by minimising (over the mean shape) the sum of square full Procrustes distances from each individual configuration in the sample to an unknown unit size mean configuration. The full Procrustes estimate of mean shape is actually the eigenvector corresponding to the largest eigenvalue of the complex sum of squares and products matrix, which is unique (up to a rotation) provided that there is a single largest eigenvalue of the complex sum of squares and products matrix. The full Procrustes fits (or co-ordinates) of each individual configuration can also be obtained, providing an alternative estimate of mean shape as the arithmetic mean of these co-

ordinates. This is analogous to the EFF approach in taking the arithmetic mean of the predicted points from the EFF to produce an estimate of average 'form' i.e. size and shape, or average shape if using size-standardised predicted points. Again, Procrustes residuals can be calculated which are useful for investigating shape variability in a sample of configurations.

5.2.3 Shape Variability

Once an average configuration from a sample of objects has been estimated by Procrustes methods (GPA), it might be of interest to follow on by examining the structure of the shape variability in the sample. A suitable method is to investigate the shape variability in a linearised space about the estimated 'average' shape, referred to as a tangent space. Principal component analysis (PCA) of the Procrustes residuals (which are approximate tangent co-ordinates) provide a method for such an investigation.

First of all the Procrustes estimate of mean shape is obtained from the dominant eigenvector of the complex sum of squares and products matrix. The Procrustes estimate of mean shape is centred (at the centroid, on the origin) with unit size and rotated so that the line joining two sensibly chosen landmarks is horizontal. The Procrustes co-ordinates of this estimate of mean shape are easily calculated, as are the Procrustes residuals. To examine the structure of variability in the sample of configurations, the eigenstructure of the sample covariance matrix of these Procrustes residuals is examined. The eigenvectors of the sample covariance matrix are in fact the

principal components of the sample covariance matrix, with corresponding eigenvalues from which the percentage of variability explained by each principal component (eigenvector) can be calculated. Further, for each principal component, the shape of the configuration at ± 3 standard deviations away from the mean shape can be calculated. Certain shifts of the different principal components can be interpreted in an attempt to explain what might be happening to the shape $\pm$ 3 standard deviations, or whatever, from the Procrustes estimate of the mean configuration. There are some very useful plotting techniques available that allow simple visualisation of the effect of each principal component in a data set. These will be demonstrated in section 5.5.3 where the mandibular data is investigated using Procrustes analysis.

It can often be the case that only a few principal components are required to explain a high percentage of the shape variability in a sample of objects, especially if there are strong dependencies between landmark points.

Some principal components correspond to easily interpretable aspects of shape variability in a data set such as length, width, height, bending etc. It can be the case however, that many combined effects are taking place in each principal component that in turn makes interpretation difficult.

It is worthwhile to note that in data sets where the variability between configurations is very small, it can be beneficial to magnify the range of the standard deviations away from the mean shape, say to $\pm$ 6 standard deviations, in order to easily visualise the effect of each principal component.

5.3 Bookstein Co-ordinates

In addition to Procrustes analysis, another helpful way of representing 'shape' data is Bookstein co-ordinates (or Bookstein shape variables as they are sometimes known). The method, attributed to Bookstein 1984, is straightforward and makes a useful first step illustration in the initial stages of any shape analysis. Bookstein co-ordinates provide a suitable choice of co-ordinate system for shape analysis in that each configuration in the sample under consideration will be invariant under translation, rotation and scale change. In this case, the similarity transformations are removed by translating, rotating and re-scaling a configuration so that two sensibly chosen 'baseline' landmarks are sent to a fixed position, (-0.5, 0), (0.5, 0) for the purposes of the analysis used in this thesis. For practical data analysis it is sensible to choose the baseline as landmarks that are 'not too close together'. However, where the baseline is sent is an arbitrary choice. Once these two sensibly chosen 'baseline' landmarks are sent to a chosen baseline then, suitable so-called shape variables are then considered to be the (x,y) co-ordinates of the remaining k-2 points after the similarity transformation operations are completed. Here, k is defined as the total number of landmark points used to characterise the outline and the resulting Bookstein shape variables are defined to be (u_i, v_i) co-ordinate points where $i = 3,\ldots\ldots,k$.

In essence, Bookstein co-ordinates (shape variables) are just registered co-ordinate points, referenced on a baseline after removal of similarity transformations which represent the shape of a particular form. They could perhaps be considered analogous

to the EFF approach, which centres configurations on the centroid and measures their shapes by calculation of centroid-to-boundary outline points.

Also, as with Procrustes analysis, an estimate of the 'average' shape of an object can be obtained as an estimate of the mean shape of the configuration by simply taking the arithmetic mean of the Bookstein co-ordinates. This is referred to as the Bookstein mean shape and is again analogous to the EFF approach where the arithmetic mean of the predicted points from the EFF was considered as an estimate of average 'form' i.e. size and shape, or average shape if using size-standardised predicted points.

The Bookstein co-ordinates for each configuration in a sample of objects can be plotted and superimposed on the chosen baseline to get an idea of within sample variability. The Bookstein mean shape for a particular sample can then be calculated and plotted. Estimates of mean shape for different samples can be superimposed (on the chosen baseline) and compared in order to get a feel for whether or not there are differences between two groups (males and females for example) in terms of their shape. The relationship between size and shape of an object can also be investigated by plotting each of the u_i and the v_i co-ordinates, $i = 3,\ldots,k$, the Bookstein co-ordinates (shape variables) representing the shape of the object, against any appropriate 'size' measure of the same object where the measure of the 'size' of an object used in this part of the analysis is the centroid size of the object. The centroid size of an object is defined to be the square root of the sum of the squared Euclidean distances from each landmark point to the centroid. It is calculated (as any other size measure would be) before any re-scaling of the object is undertaken. Area could of course be used as a 'size' measure as in the EFF approach. A relationship between the

size and shape of an object would be assumed where the scatter plots of such a size measure against any of the shape variables resulted in strong positive (or negative) correlations. Pair wise scatter plots of these so-called shape variables can also be plotted i.e. relationships between each of the u_i's and each of the v_i's, as well as between the u_i's and v_i's, can be investigated. Particular shape variables might be highlighted which show strong positive and strong negative correlations. Such correlations can be difficult to interpret however, since an artefact of this particular co-ordinate system, in registering each object to a given edge, is that correlations may be induced into the Bookstein shape variables, even when the landmarks themselves are uncorrelated.

Examples of these plots illustrate the use of Bookstein co-ordinates in Section 5.5.2.

Standard multivariate analysis on the Bookstein co-ordinates, ignoring the non-Euclidean nature of the Bookstein shape space, using normal models for shape variables for approximate inference, is one approach to shape analysis for a random sample of objects.

This method is sufficient for mean estimation and hypothesis testing, provided that variations in the data are small (between objects). What is meant by 'small' variations is of course a matter for debate. As a rough guide, if the standard deviation at landmarks is less than about one tenth of the length of the baseline, than this approach can be considered reasonable. If the original landmarks have a multivariate normal distribution, then it can be shown that if variations are small i.e. as the variation in a sample of data approaches zero then the shape distribution is also approximately

multivariate Normal. On the other hand, as the variation in a sample of data approaches infinity i.e. is large then the shape distribution tends to a Uniform distribution (Bookstein 1984 and 1986).

The structure of shape variability of the shape variables in a sample of objects is however less straightforward to interpret. As mentioned already, transforming (or registering) each object to a given edge (two sensibly chosen landmarks to (-0.5, 0), (0.5, 0)) induces correlations into the shape variables in general and this can lead to spurious correlations. The method of Bookstein co-ordinates should therefore not be used to investigate the structure of shape variability unless there is good reason to believe that the baseline landmarks are essentially fixed. Another point to note that often happens with using Bookstein co-ordinates, is the fact that the variability in the points away from the origin appears larger than the points nearer the origin. In other words, if the mean location of the landmark points under consideration are far away from the mid-point of the baseline, (0,0) here, then the variability appears larger than that found in points closer to (0,0). These two artefacts of the Bookstein co-ordinate system are to do with the covariance structure in the multivariate Normal distribution between the shape variables.

This is why many researchers prefer to use Procrustes tangent co-ordinates to investigate shape variability in a sample.

Nevertheless, the use of Bookstein co-ordinates does provide a very useful first step analysis of the shape of a sample of objects and should not be ignored completely. We have included such an analysis of the mandibular data in Section 5.5.2.

5.4 *Inference using Procrustes and / or Bookstein co-ordinates*

Obviously the ultimate aim of any study similar to the investigation in this thesis is to say something about the size, shape, or size and shape of an object or differences in a group of objects. Many of the methods used for analysing differences in size and / or shape are based on subjective examination of various plots as outlined here and applied to the mandibular data sample in section 5.5.

5.4.1 Size and shape analysis using Procrustes and / or Bookstein co-ordinates

As discussed previously, it is sometimes of interest to examine whether the size of an object or objects is related to the shape of the object or objects e.g. to investigate concurrent changes in size and shape of the mandible over a period of time. An appropriate measure of size has to be identified (similar to choosing suitable shape co-ordinates as the Bookstein co-ordinates or Procrustes tangent co-ordinates). The relationship between size and shape of objects (previously defined as allometry), can be investigated in a geometrical context using regression techniques. A simple approach is to carry out a linear regression of a shape variable (e.g. Bookstein shape co-ordinates or principal component scores) on a chosen size variable (e.g. the centroid size). The objects remain invariant with respect to location and rotation, but not scale. Simple exploratory plots of the data are useful in investigating the relationship between size and shape.

Two such examples are given in sections 5.5.2 and 5.5.3 where the size variable is defined to be the centroid size of each configuration of landmarks (defined previously to be the square root of the sum of the squared Euclidean distances from each landmark point to the centroid). In the first example, Bookstein co-ordinates define the shape variables of the object (described previously), which are plotted against the centroid size in order to try and capture the relationship between the size and shape of the mandibles of a given group, at a given age. The second example utilises principal components (resulting from Procrustes superimposition) to capture shape and centroid size, to examine correlations between them and therefore investigate any obvious relationships that may exist between size and shape.

5.4.2 Shape analysis using Procrustes and/or Bookstein co-ordinates

Many plots can be drawn in order to try to capture the shape of an object or group of objects, as well as perhaps, differences in shape between 2 objects, or differences in shape between the 'average' shapes of a sample of two groups of objects. These plots may include analysis of Bookstein shape variables, or examination of the resulting principal components from GPA methods as outlined in sections 5.3 and 5.2.3 respectively. Again, applications specific to mandibular description are given in section 5.5.

In addition to these illustrative plots, there are formal hypothesis tests which can be utilised in order to investigate 'shape', as well as additional methodology which allows the process of 'shape change' to be investigated.

5.4.2.1 Formal tests of differences in shape between objects

Formally, an inference procedure for shape analysis based on tangent space methods is considered i.e. using the Procrustes tangent space co-ordinates. Each object / configuration after Procrustes matching is represented as a point in what is known as Kendall's shape space. The Procrustes distance coefficient between any two forms is non-Euclidean and can be thought of as the closest great circle distance between them. For practical purposes however, statistical analyses (like principal components analysis) of Procrustes-fitted data are generally carried out in the tangent plane to shape space (which, as long as variations are small, adequately approximate the curving of Kendall's shape space). The distances between the forms can then be treated as if they are Euclidean, and normal statistical assumptions can be made. This method is valid only in data sets with small variability in shape between objects then. If the data are concentrated i.e. small shape variability, then the standard multivariate analysis in the linear space using the Procrustes tangent shape co-ordinates can be performed by way of standard Hotelling's T^2 tests. A one sample Hotelling's T^2 test would test whether or not the mean shape of a sample of objects followed a particular 'reference' or perhaps 'template' shape. In the context of our data, this could be a reference norm of a 'typical' 9 year old female mandible if it were available. Of more use perhaps, is the two sample Hotelling's T^2 test. This test might for example consider whether or not the mean shape of a group of female mandibles (at a particular age) is the same as the mean shape of a group of males (of the same age). Or indeed, whether or not the mean shape of a group of 9-year-old female mandibles is the same as the mean shape of say, 11-year-old female mandibles etc. This test is used in the analyses of the mandibular data only when the sample sizes are sufficiently large. To

test differences between males and females at each age it turns out that this test cannot in fact be carried out. This is because we have 19 landmark points to characterise the mandibular outlines, which results in 34 Procrustes shape variables (2k-4). This has to be subtracted from the respective sample sizes for the males and females (for each age), in the test statistic, but our largest combined sample size is that for age 15 where we still only have 14 males and 7 females. The test can be used on the pooled data to examine whether or not there is a difference in shape, on average, between ages 9 and 15 and between ages 11 and 15 (with respective pooled sample sizes of 18 and 21 and 13 and 21). Again however, even the combined sample sizes are too small to test between ages 9 & 11, 9 & 13 or 11 & 13.

There are other tests that can be considered under different circumstances e.g. Goodall's F test (Goodall 1991), but they are not considered here, nor applied to the mandibular data.

5.4.2.2 Methods for describing shape change between objects

One method that is considered a particularly useful tool for describing the shape change between objects is that attributed to Bookstein 1989. Much in the spirit of D'Arcy Thompson, grids are drawn on the original configurations, and 'deformed' in the matching process to describe shape change. This method, thin plate splines, is applied to the mandibular data to illustrate the shape change between the average female shape and the average male shape, at each age.

5.5 Application : Analysis of the Mandibular Data

This section examines the many useful plots that can be obtained using Procrustes analysis (and Bookstein co-ordinates), applied to the sample of mandibular data described in Chapter 3. These methods are utilised in an attempt to summarise the size and shape of the mandibular outlines (configurations) in each age group for both males and females. The notion of 'mean' shape of a sample of configurations is investigated, for each sex at a given age and whether or not there is a difference in this mean shape between the males and females of that particular age is explored. Further, an attempt is made to summarise the main shape changes that might be taking place in both male and female samples, at each age in terms of Bookstein co-ordinates or principal components from Procrustes analysis. Also, where appropriate, formal tests are used to investigate whether or not there is a difference in mean shape between males and females, over the range of ages. Subjective assessment is made when formal testing is not appropriate due to inadequate sample sizes. If there is no evidence of a difference, the males and females can be combined and a test of whether or not there is a difference between the mean shape of all configurations at a certain age with those of another age carried out. Once again formal testing is considered only where sample sizes are of adequate size. For example, the mean shape of all males and females aged 9 with the mean shape of all males and females aged 15. The relationship between size and shape is also investigated, again using Bookstein co-ordinates and principal components analysis from Procrustes analysis.

5.5.1 Preliminary Plots

Investigation of the mandibular data begins by plotting the raw data available, uncorrected for size, characterised here by the full 78 landmark point representations. Figure 5.1 depicts the mandibular outline for the first two females in the data sample, aged 9. It would seem that these two females are slightly different in terms of size and shape.

Further, it can be seen from Figure 5.2 that each of the mandibular outlines for females aged 9 (there are 6 females aged 9 in our sample, each depicted by a different symbol) could all indeed be slightly different in terms of overall size and shape.

Similar observations can be made for males, aged 9 from Figures 5.3 and 5.4 where there are 12 males aged 9 in the sample. However, although there is some evidence of within-sex variability of the mandibular outline for both males and females, it can be seen that most of the variability is in fact confined to particular areas of the bone. For the females, there appears to be more variation in the anterior border of the mandible and around the condyle, mandibular notch and coronoid process areas of the bone. There tends to be a similar pattern of variability in the male sample, aged 9 in that there is indeed evidence of variability within the 12 males in the anterior border of the mandible and around the condyle, mandibular notch and coronoid process areas of the bone. The patterns here become harder to discern however since there are more males plotted on the same graph. A pattern of variability also emerges along the lower border of the mandible and the posterior border of the ramus, as well as the alveolous.

Such an overall pattern of intra-sex variability will almost certainly be related to the fact that some people simply 'grow' more quickly than others.

Any differences (if they exist) between the sexes can perhaps be gleaned from Figure 5.5 where females and males are depicted side by side. There does not appear to be any obvious differences between males and females aged 9 in this sample where it can be seen that the outlines are basically equivalent in terms of overall height, width and length. This is however very difficult to appreciate and will be investigated further later by plotting and superimposing average outlines for males and females.

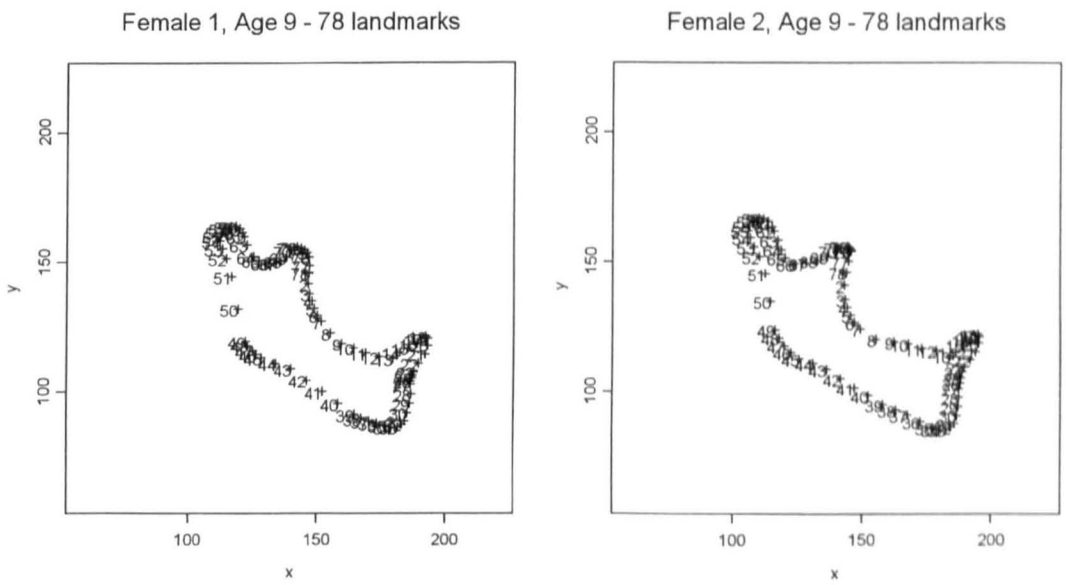

Figure 5.1 Mandibular Outline of 78 Predicted Points. First 2 females. Age 9.

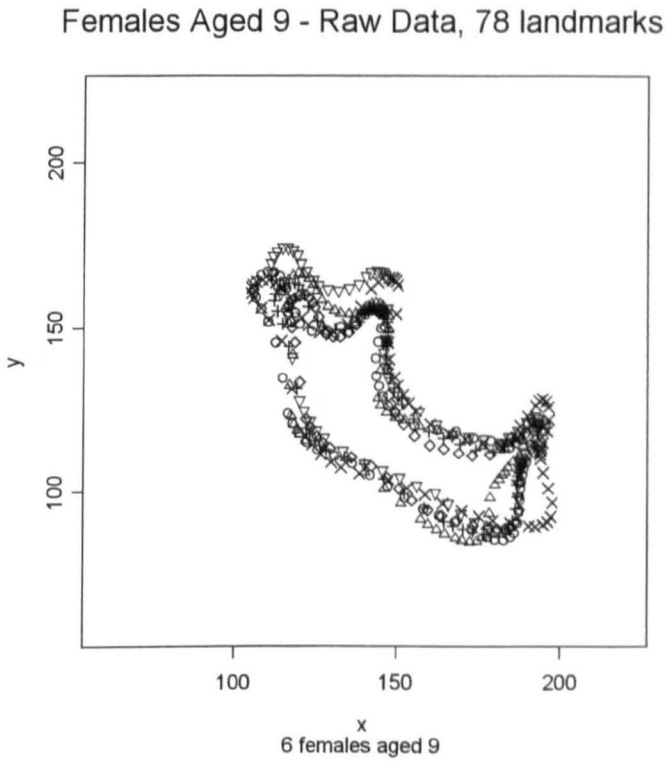

Figure 5.2 **Mandibular outlines. All 6 females. Age 9.**

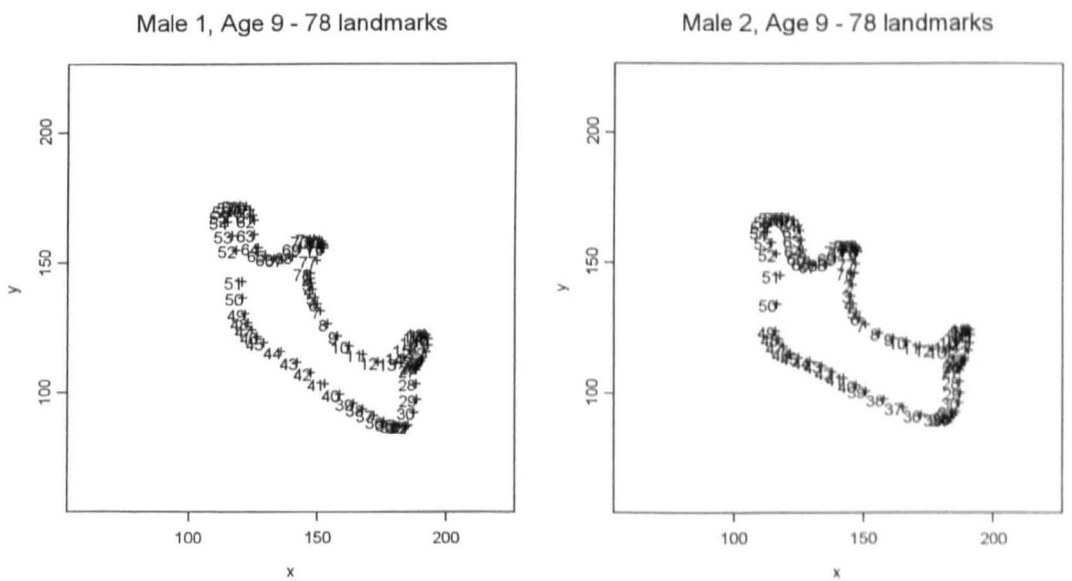

Figure 5.3 **Mandibular Outline of 78 Predicted Points. First 2 males. Age 9.**

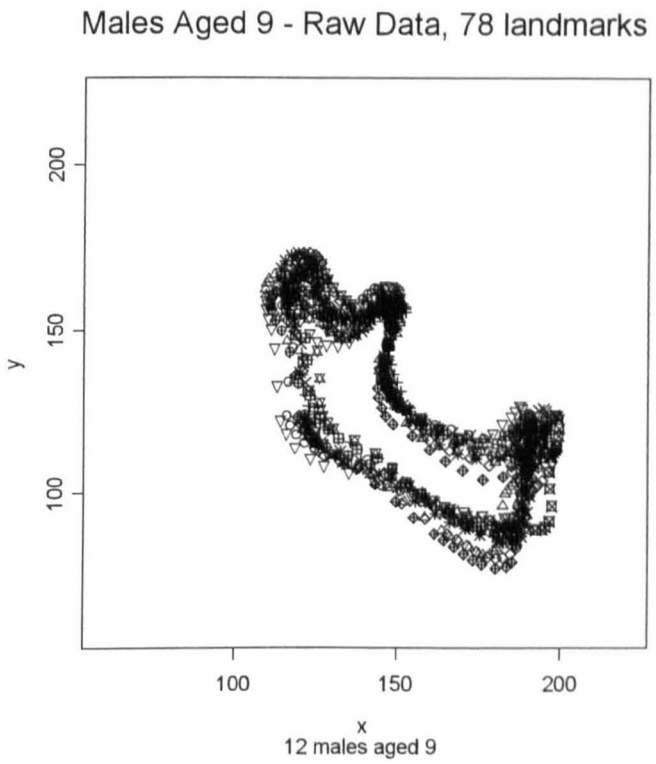

Figure 5.4 **Mandibular outlines. All 12 males. Age 9.**

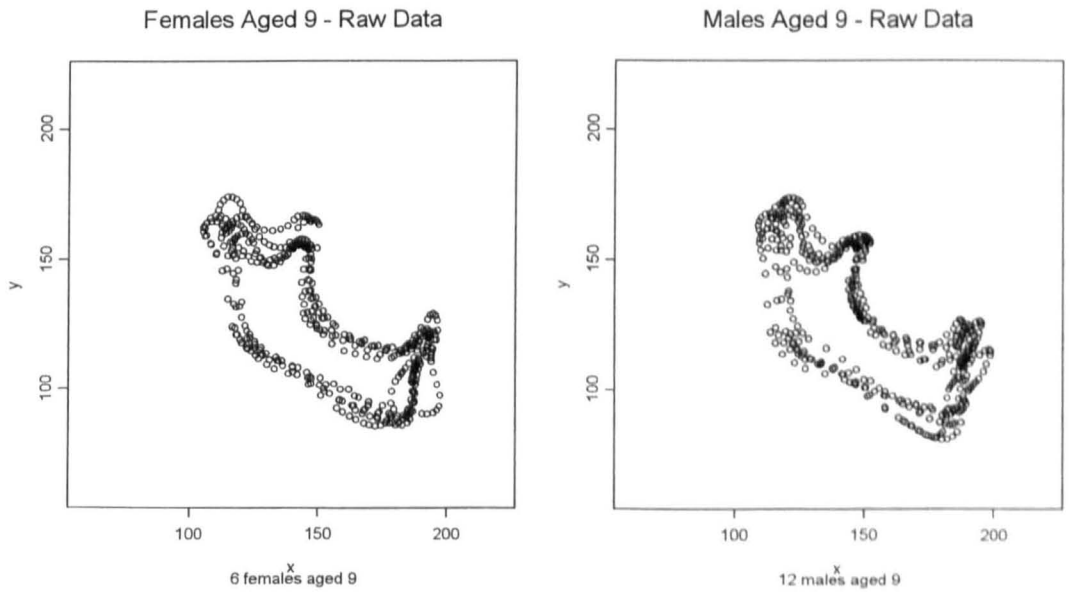

Figure 5.5 **Mandibular outlines. All 6 females and 12 males. Age 9.**

Similar plots were produced for both the males and females in the data sample for all the other ages 11, 13 and 15, with 78 points used to characterise each mandibular outline. There are 9 males and 4 females aged 11, 10 males and 7 females aged 15 and 14 males and 7 females aged 15. These plots are not illustrated here. However, similar to that observed for age 9, there seemed to be slight differences within as well as between the sexes in terms of the overall size and shape of the mandibular outlines, at all ages.

Although most of the differences seemed to be very small (both within samples and between males and females, at each age) and may not be statistically significant, they still warrant further investigation, where possible. Further, the size of each 'form' should be minimised to enable shape alone to be examined, using in this chapter, Procrustes analysis and / or Bookstein co-ordinates and formal tests used where possible to investigate differences in shape. In addition to plots of the raw data then, which take into account both size and shape of each configuration in the sample, configurations can be translated, rotated and re-scaled to investigate whether or not there is any difference in shape only (using Procrustes methods and / or Bookstein co-ordinates). The mean shape for males and females can also be calculated and plotted (again using Procrustes methods and / or Bookstein co-ordinates). Further, a formal Hotelling's T^2 test can be used to investigate if the full Procrustes estimate of mean shapes are in fact different (see later).

Subsequent analyses of the mandibular data concentrate on the 19 anatomical landmark points only. The original landmark points 51 and 18 i.e. the most anterior point on the posterior aspect of the ascending ramus with respect to the condylar plane

and the tip of the lower central incisor respectively, are taken to be new baseline points 1 and 2 in these analyses. This is due to the fact that baseline points have to be a sensible distance apart for meaningful analysis as explained earlier. The original landmark points 1 and 2 would have been too close together for this purpose, where original landmark 2 is not an anatomical landmark point anyway.

Only a small number of the many plots produced during the analyses are included here for illustrative purposes. All analyses were carried out at all ages however. A brief summary is made where appropriate to cover the age groups and plots not shown.

5.5.2 Bookstein Co-ordinates

As mentioned previously, the mandibular outlines for this part of the analysis are characterised by the 19 anatomical landmark points as defined in Chapter 3, where landmarks 51 and 18 are now taken to be the new baseline points 1 and 2 respectively. This new designation of the 19 anatomical landmark points is outlined in Table 5.1 and illustrated in Figure 5.6.

Figure 5.7 shows a scatter plot of the raw data for Female 1, aged 9, characterised by this new designation of points.

Original Point Number	New Designation	Anatomical Landmark Definition
1 (and 78)	3	PNS the point of intersection of the ANS-PNS plane with the outline of the anterior ascending ramus
3	4	the most posterior aspect of the anterior ascending ramus with respect to the condylar plane
13	5	the point of intersection of the border of the alveolar bone and the posterior lower central incisal margin
18	2	the tip of the lower central incisor
23	6	the point of intersection between the anterior lower central incisal margin and the alveolar bone
27	7	Point B the most posterior point on the anterior aspect of the body of the mandible with respect to the mandibular plane
31	8	Pogonion the most anterior point on the anterior mandibular body with respect to a perpendicular drawn from the mandibular plane
35	9	(Menton / Cephalometric Gnathion The most inferior point on the symphysis of the mandible
39	10	the most inferior point on the anterior mandibular body with respect to the mandibular plane
43	11	the most superior point of the lower border of the mandible with respect to the mandibular plane
45	12	Gonion the most inferior point of the posterior mandibular body with respect to the mandibular plane
49	13	the most posterior point on the lower aspect of the posterior ascending ramus with respect to the condylar plane
51	1	the most anterior point on the posterior aspect of the ascending ramus with respect to the condylar plane
54	14	+ point 49 = condylar plane the most posterior point on the mandibular condyle with respect to the condylar plane
58	15	the most superior point of the condyle with respect to the condylar neck
62	16	the point of intersection on the anterior surface of the condyle drawn by a perpendicular from point 54 (tangent point that marks the change in curvature between the condyle head and the mandibular notch)
67	17	the most inferior point of the mandibular notch with respect to a perpendicular drawn from the condylar plane
72	18	the tip of the coronoid process
76	19	the most anterior point of the coronoid process with respect to a parallel from the condylar plane

Table 5.1 New designation of anatomical landmark points.

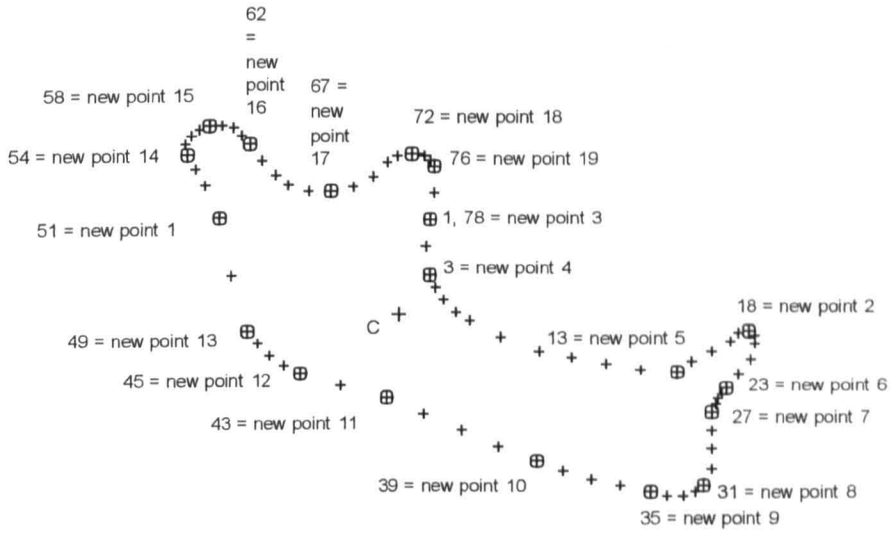

Figure 5.6 **Illustration of the new designation of anatomical landmark points.**

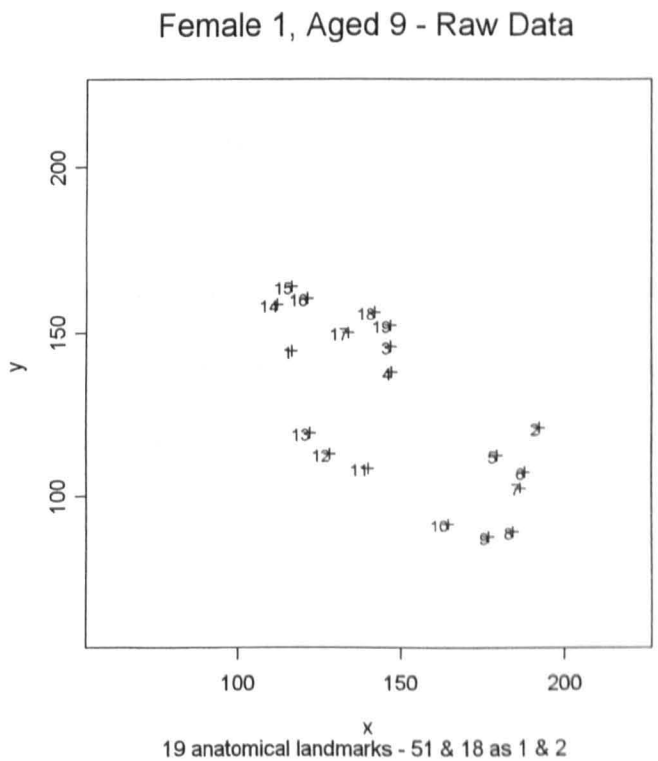

Figure 5.7 **Scatter plot of raw data. Female 1. Age 9.**

Scatter plots for each of the mandibular outlines, again characterised by these 19 anatomical landmarks for the 6 females and 12 males aged 9 in the sample are depicted in Figure 5.8. Each outline is depicted using a different symbol.

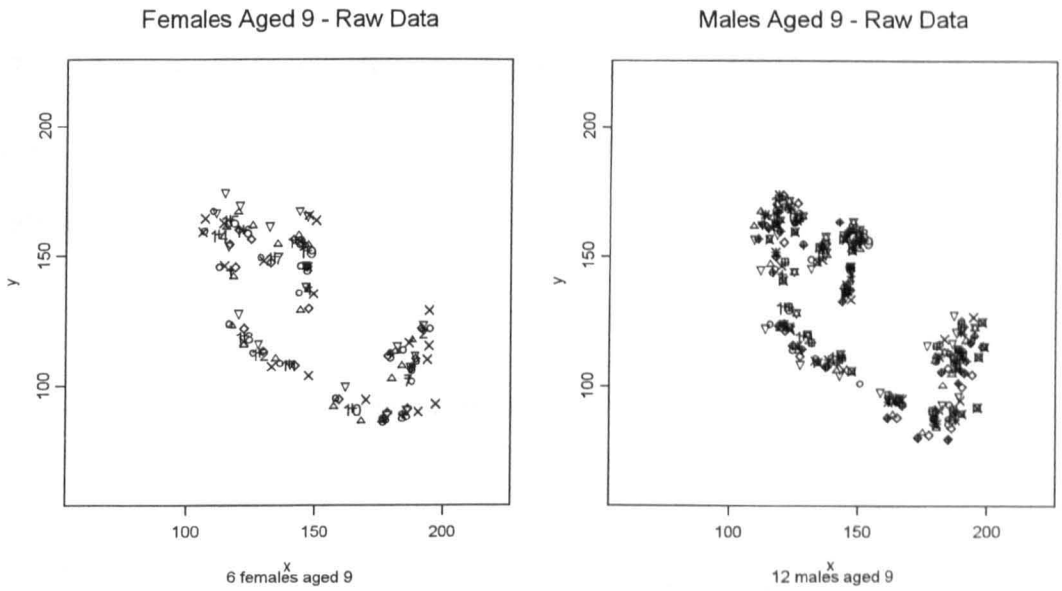

Figure 5.8 Scatter plots of raw data. 6 Females and 12 Males. Age 9.

It could be said that although the outlines are fairly close together overall, there does appear to be a slight difference within each group in terms of the overall size and shape of the bone, in that there is some variation in landmark points at each of the 19 landmarks.

Any shape differences in the mandibular outlines within the sample of 6 females and 12 males, aged 9 are however, difficult to ascertain whilst the effect of size remains in the outlines. This size effect can be eliminated, leaving only shape differences, by transforming the original 19 anatomical landmark points to give Bookstein co-

ordinates, removing similarity transformations by translating, rotating and re-scaling such that landmarks 1 and 2 are sent to (-0.5, 0) and (0.5, 0) respectively as explained previously. Figure 5.9 depicts the Bookstein shape variables for both females and males, aged 9. Each configuration (mandibular outline) is registered on the baseline landmarks 1 and 2, giving scatter plots of the Bookstein co-ordinates of the remaining k-2 = 17 landmark points after translation, rotation and re-scaling. Producing such scatter plots of the Bookstein co-ordinates is often the first stage in any simple shape analysis.

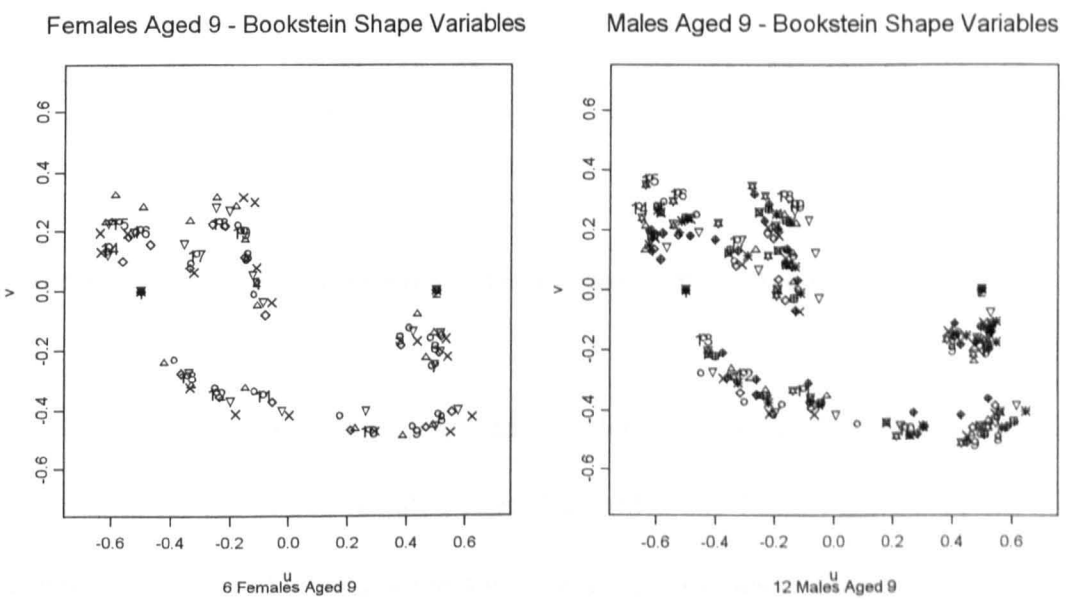

Figure 5.9 Scatter plots of the Bookstein shape variables. 6 Females and 12 Males. Age 9.

It can be seen that there is some evidence of variability between the outlines for the 6 females and 12 males, of differing degrees, at each landmark point.

A 'mean' estimate of shape can be calculated from these Bookstein shape variables for both groups and plotted, as illustrated in Figure 5.10.

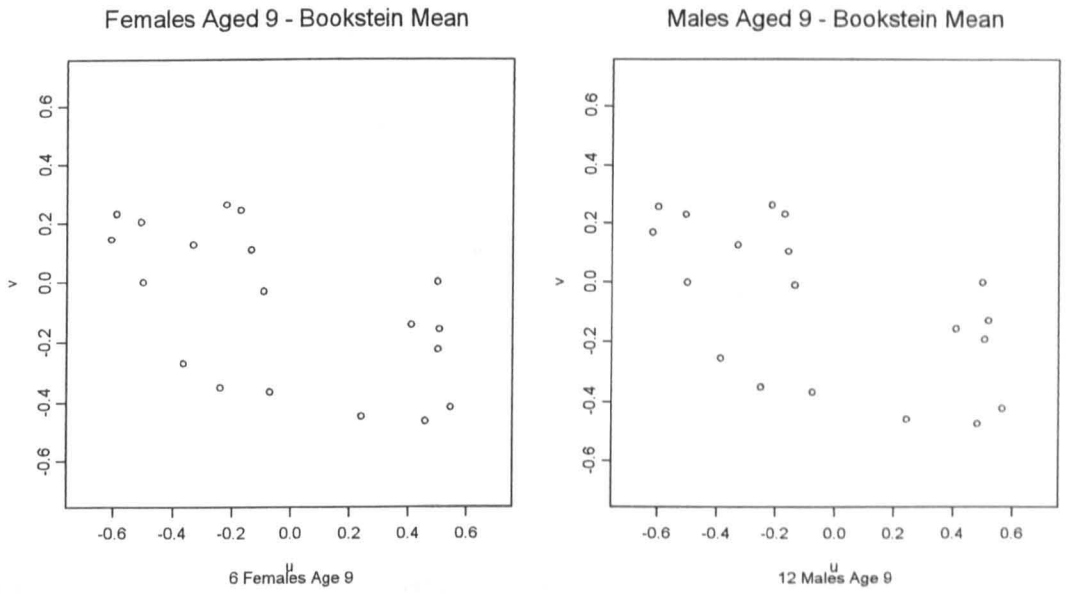

Figure 5.10 Bookstein 'mean' shape. 6 Females and 12 Males. Age 9

These mean shapes can be superimposed in order to get a feel for whether or not the mean shapes for males and females, aged 9 are different. From Figure 5.11 we might say that the 9-year-old male and female mandibular outlines in this sample are in fact on average, very close in terms of the shape of the bone. It is clear that each of the k-2 landmark points after translation, rotation and re-scaling using new landmark points 1 and 2 as a baseline, are in very close 'agreement' between the sexes in this sample of material. Whether or not the population mean shape are different is not tested formally here.

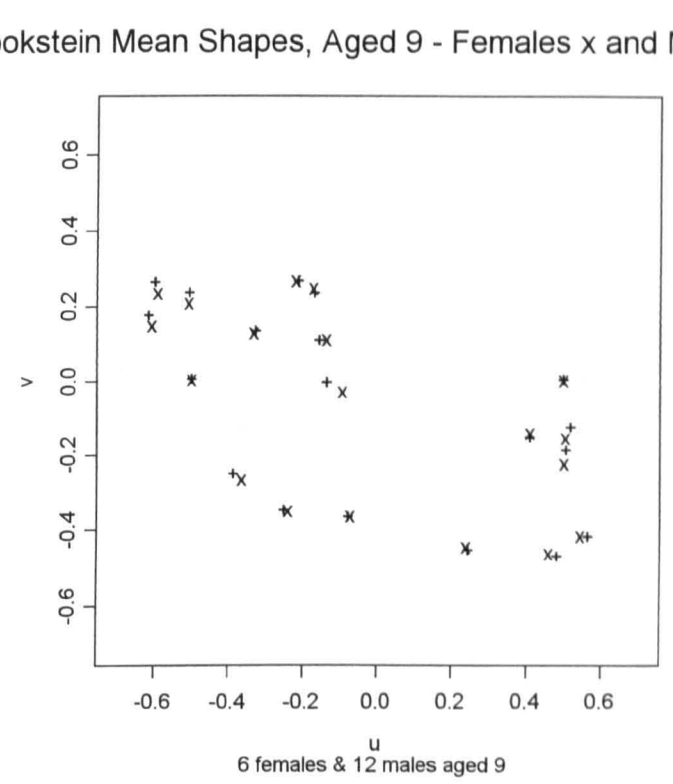

Figure 5.11 **Bookstein 'mean' shape. 6 Females superimposed on 12 Males. Age 9.**

Equivalent plots were produced for both males and females for ages 11, 13 and 15. These are depicted in Figures 5.12 – 5.15 for the 9 males and 4 females aged 11; in Figures 5.16 – 5.19 for the 10 males and 7 females aged 13 and Figures 5.20 – 5.23 for the 14 males and 7 females aged 15.

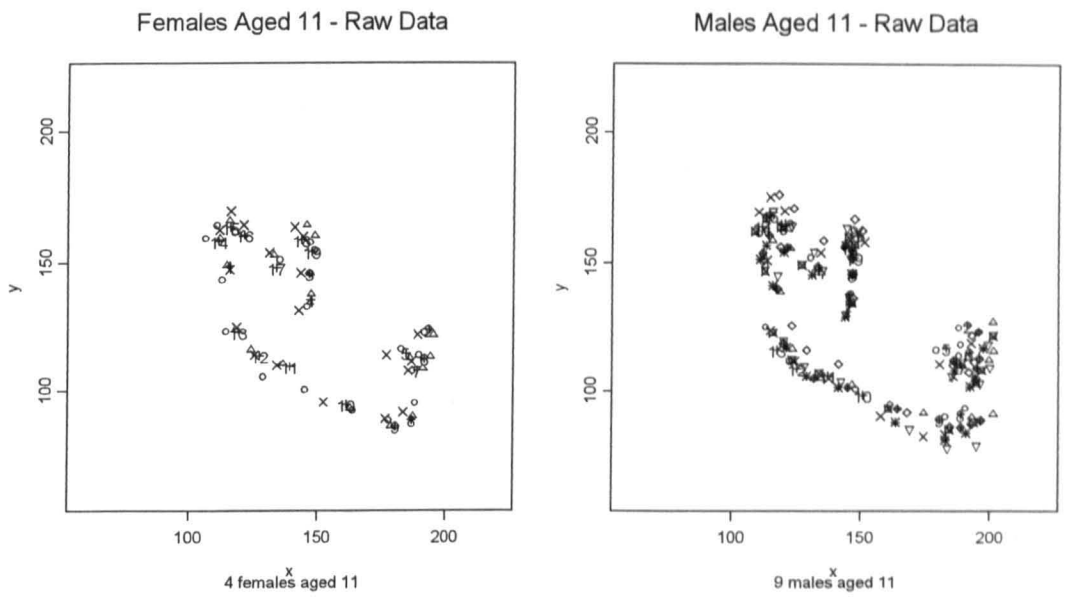

Figure 5.12 **Scatter plots of raw data. 4 Females and 9 Males. Age 11.**

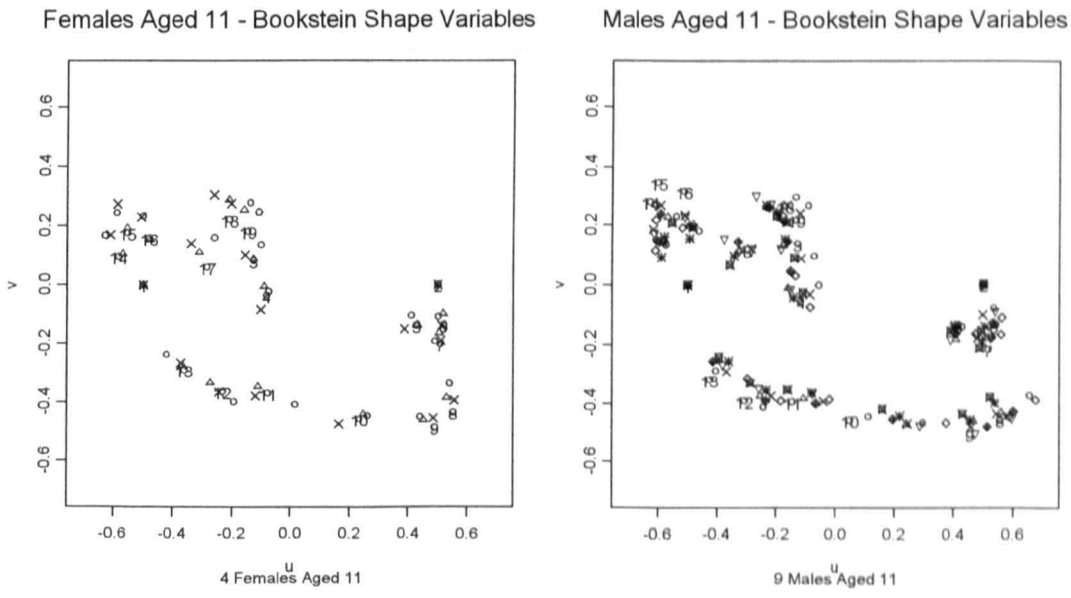

Figure 5.13 **Scatter plots of the Bookstein shape variables. 4 Females and 9 Males. Age 11.**

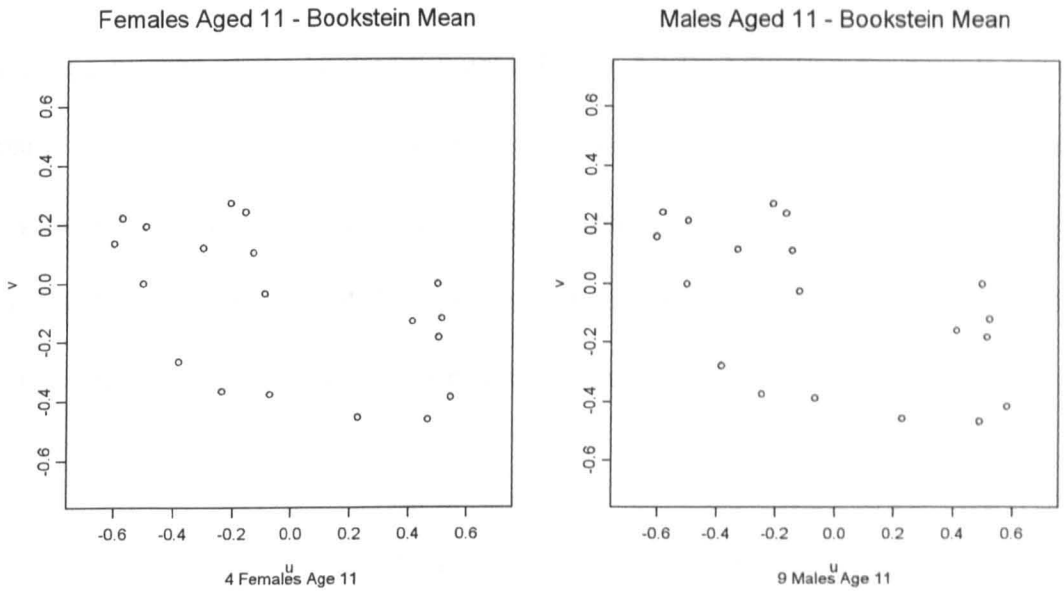

Figure 5.14 **Bookstein 'mean' shape. 4 Females and 9 Males. Age 11.**

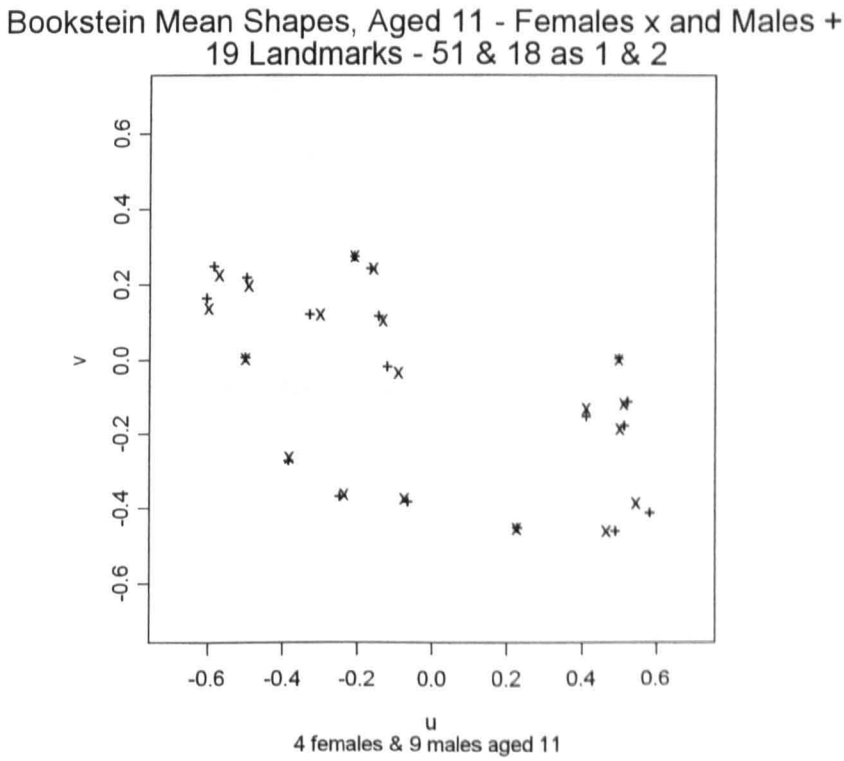

Figure 5.15 **Bookstein 'mean' shape. 4 Females superimposed on 9 Males. Age 11.**

For Age 11 it can be seen that there does seem, as for age 9, to be a slight difference in overall size and shape within the 4 females and 9 males in that there exists some variation in each of the landmark points (Figure 5.12). Adjusting for size, it is again observed that slight variations in shape only exist in the Bookstein shape variables (Figure 5.13). Calculation of an estimate of mean shape for males and females (Figure 5.14) and superimposition of these outlines (Figure 5.15) leads us to observe that there is probably no difference in mean shape between males and females.

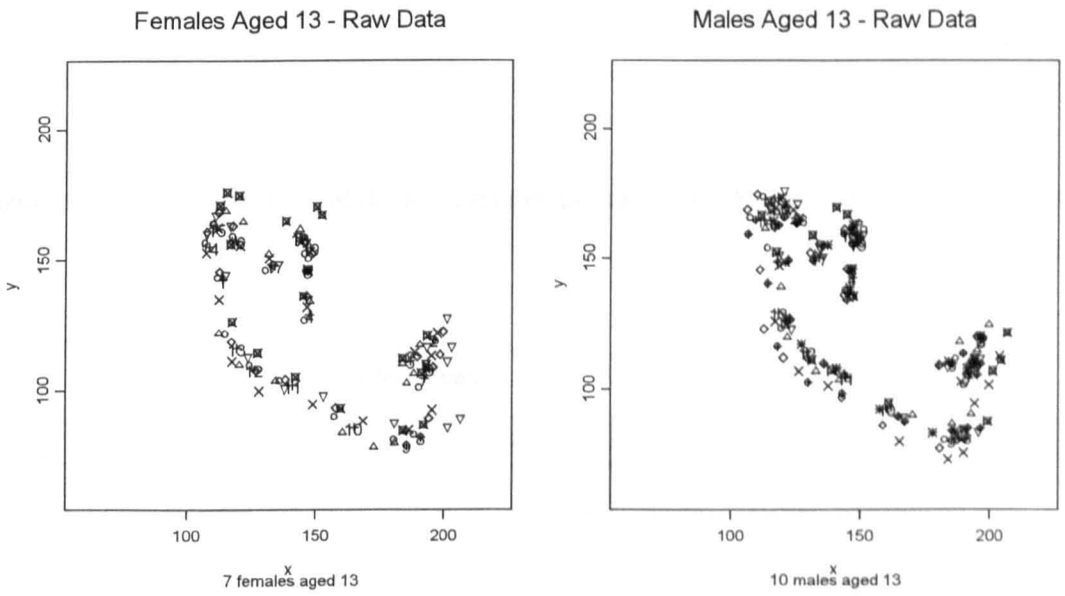

Figure 5.16 **Scatter plots of raw data. 7 Females and 10 Males. Age 13.**

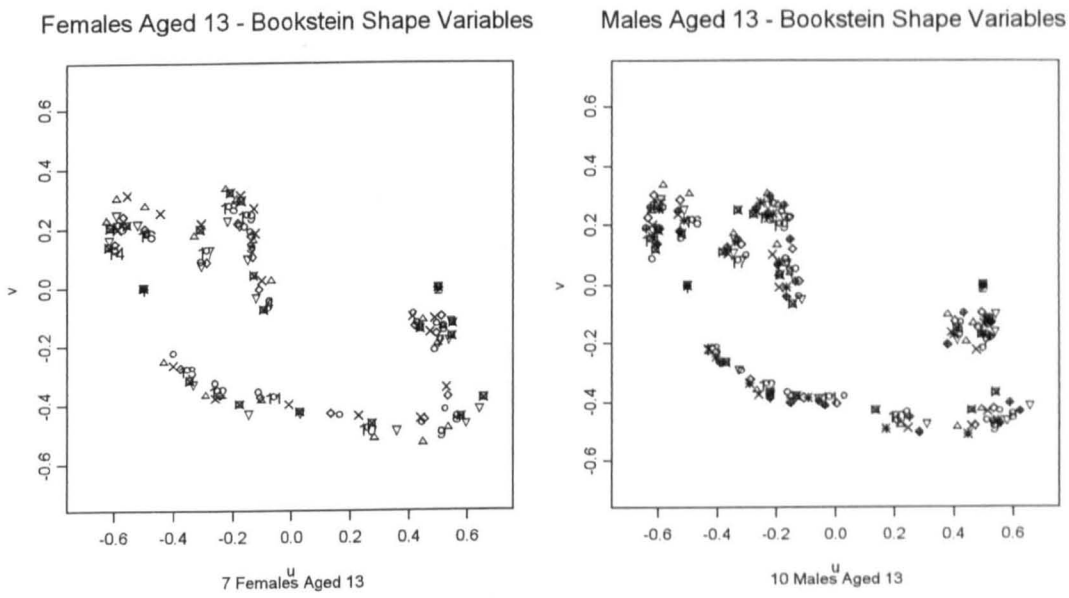

Figure 5.17 **Scatter plots of the Bookstein shape variables. 7 Females and 10 Males. Age 13.**

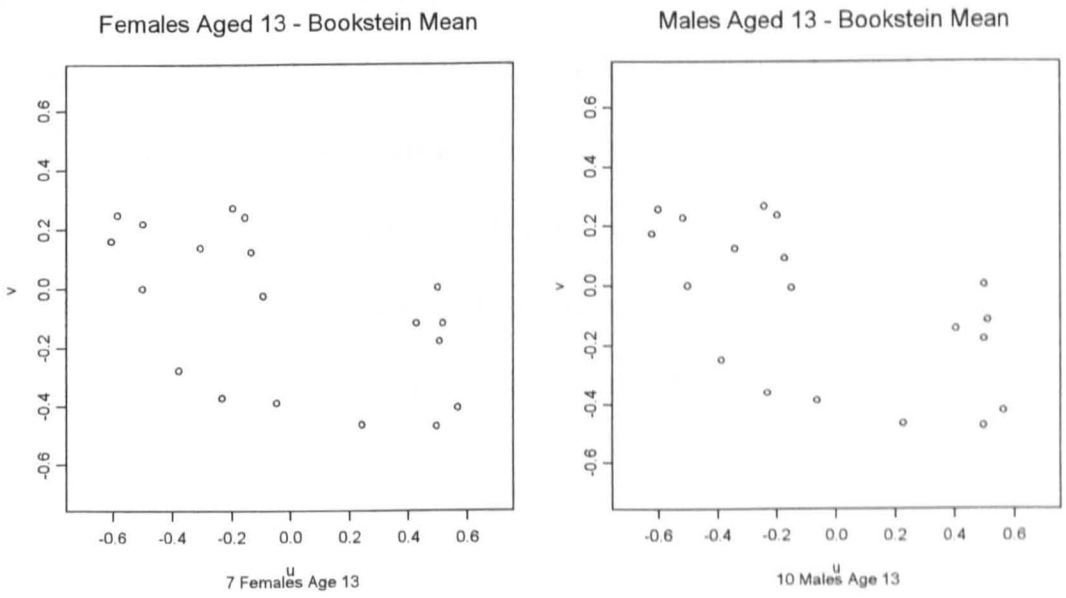

Figure 5.18 **Bookstein 'mean' shape. 7 Females and 10 Males. Age 13.**

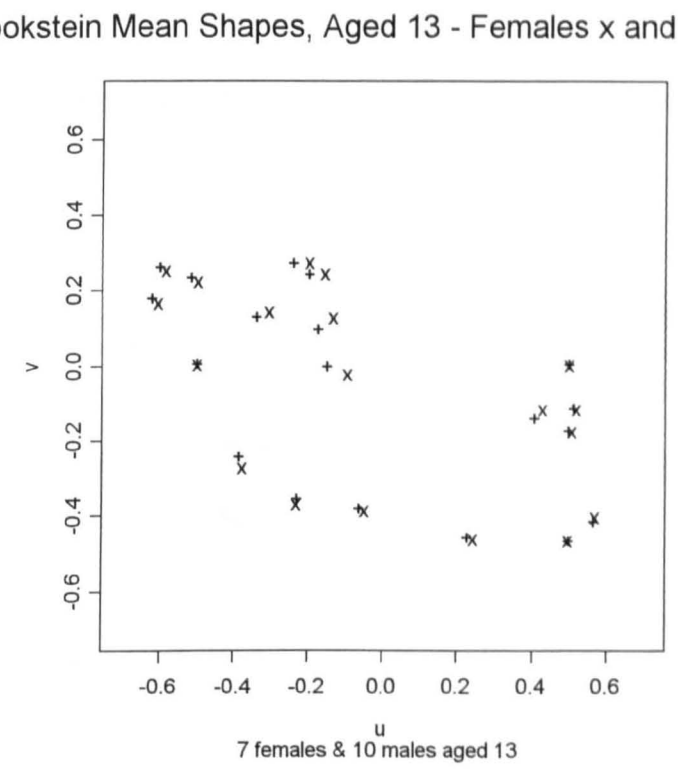

Figure 5.19 **Bookstein 'mean' shape. 7 Females superimposed on 10 Males. Age 13.**

There again appears to be slight variations in size and shape (Figure 5.16) and shape only (Figure 5.17) for the 7 females and 10 males in our sample, aged 13. The mean shape differences between males and females (Figure 5.19) at this age seem to be more exaggerated in the condyle, mandibular notch and coronoid process areas of the bone, and also in the anterior border of the ramus and perhaps the alveolous, compared to ages 9 and 11. These differences do still appear to be very small however.

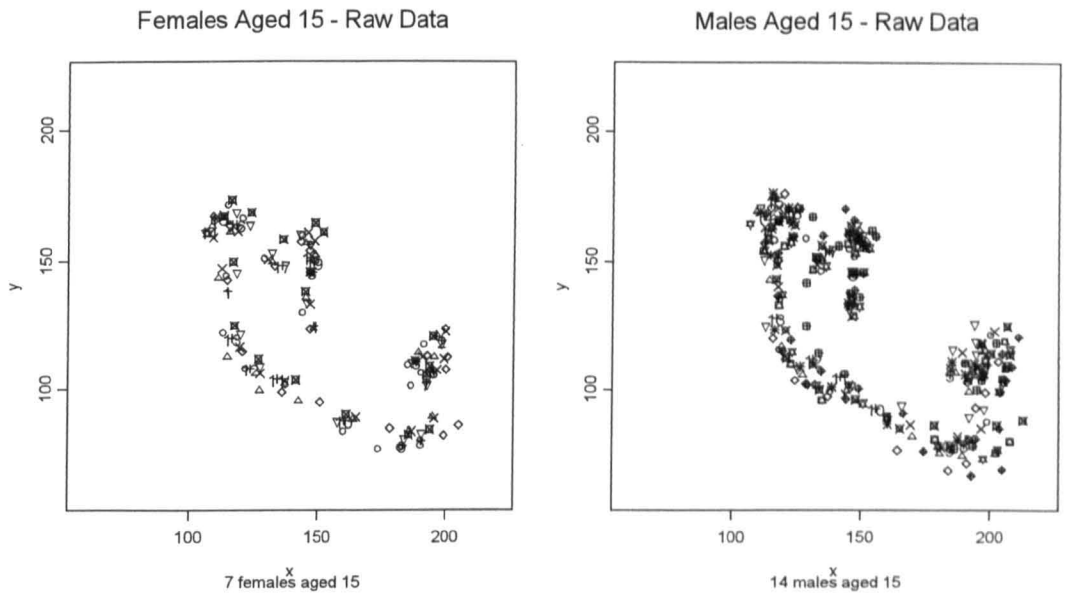

Figure 5.20 **Scatter plots of raw data. 7 Females and 14 Males. Age 15.**

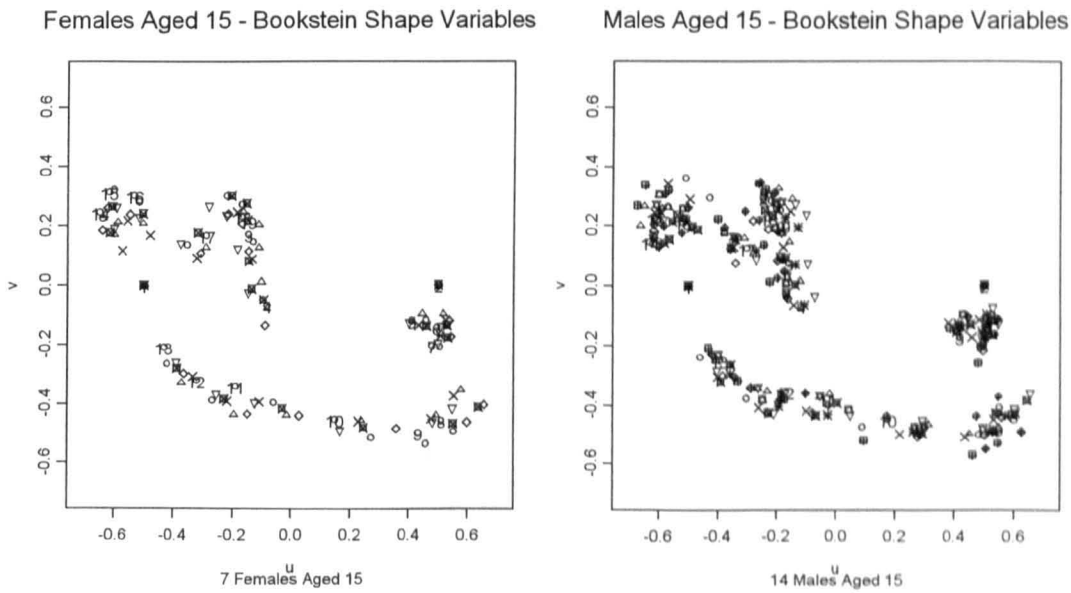

Figure 5.21 **Scatter plots of the Bookstein shape variables. 7 Females and 14 Males. Age 15.**

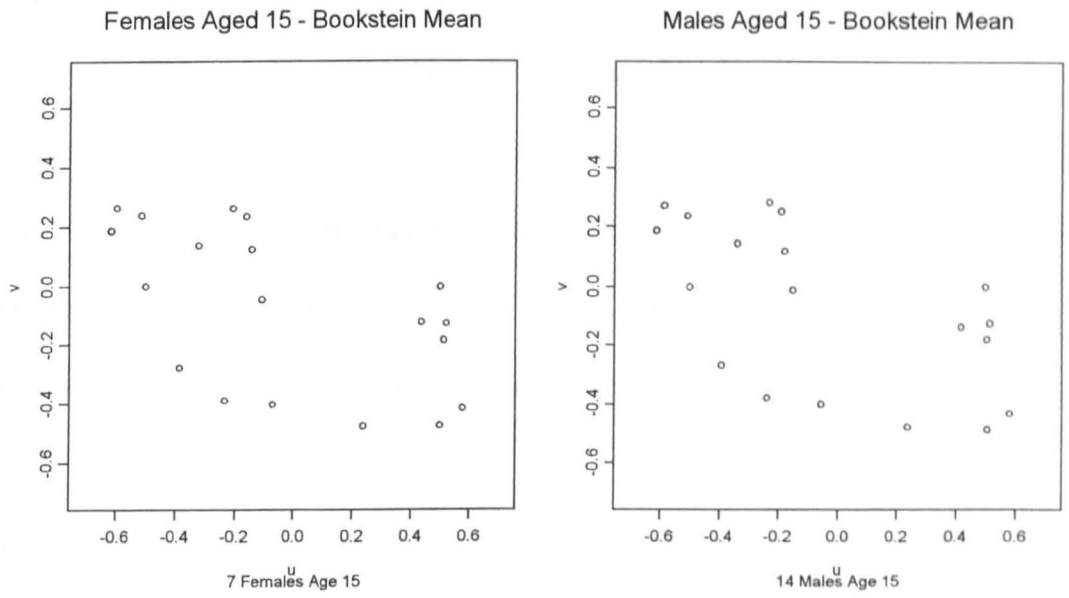

Figure 5.22 **Bookstein 'mean' shape. 7 Females and 14 Males. Age 15.**

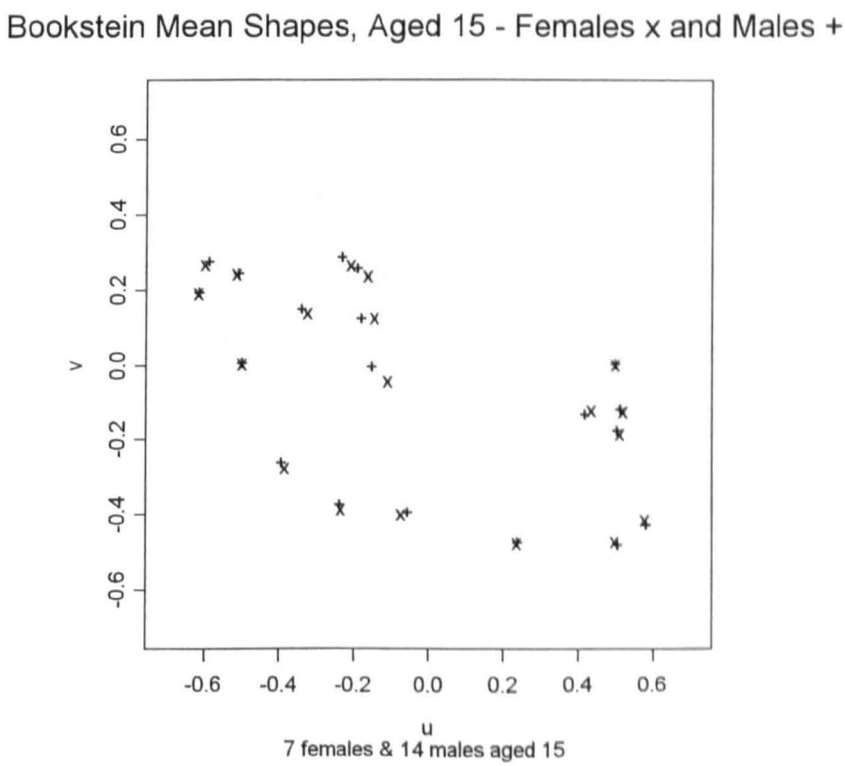

Figure 5.23 **Bookstein mean shape. 7 Females superimposed on 14 Males. Age 15.**

The 7 females and 14 males, aged 15 depict once again, a similar picture - some, but a very small amount of variation exists in overall size and shape (Figure 5.20) and in shape only (Figure 5.21), within both the male and female samples. Further, as for age 13, the mean shapes for males and females tend on average to be very close. Again there is some evidence of slightly larger differences in the mandibular notch and coronoid process areas of the bone, and also in the anterior border of the ramus and perhaps the alveolous compared to ages 9 and 11 (Figure 5.23).

The relationship between size and shape, which is captured to some extent in plots of the raw data, can be further investigated by way of Bookstein shape variables.

A series of pictures for each mandibular outline, for each of the sexes, for each age are shown in Figures 5.24 – 5.27 (a) and (b). Each series begins with the Bookstein mean shape for a particular group of configurations (mandibular outlines), either males or females, for a particular age. The raw data for each of the configurations that contributed to that particular Bookstein mean shape (either males or females, for a particular age) are then plotted. The respective shape distances from the Bookstein mean shape and The centroid size for each of these configurations are quoted (before transforming the original (x,y) co-ordinates into Bookstein co-ordinates (shape variables) by registering (new) landmarks 1 and 2 of each configuration at a chosen (-0.5,0), (0,0.5) baseline). The shape distances (after registration) of each configuration from the Bookstein mean shape are also given. All shape distances and centroid sizes are given for each of the configurations in the top right hand corner and bottom right hand corner respectively.

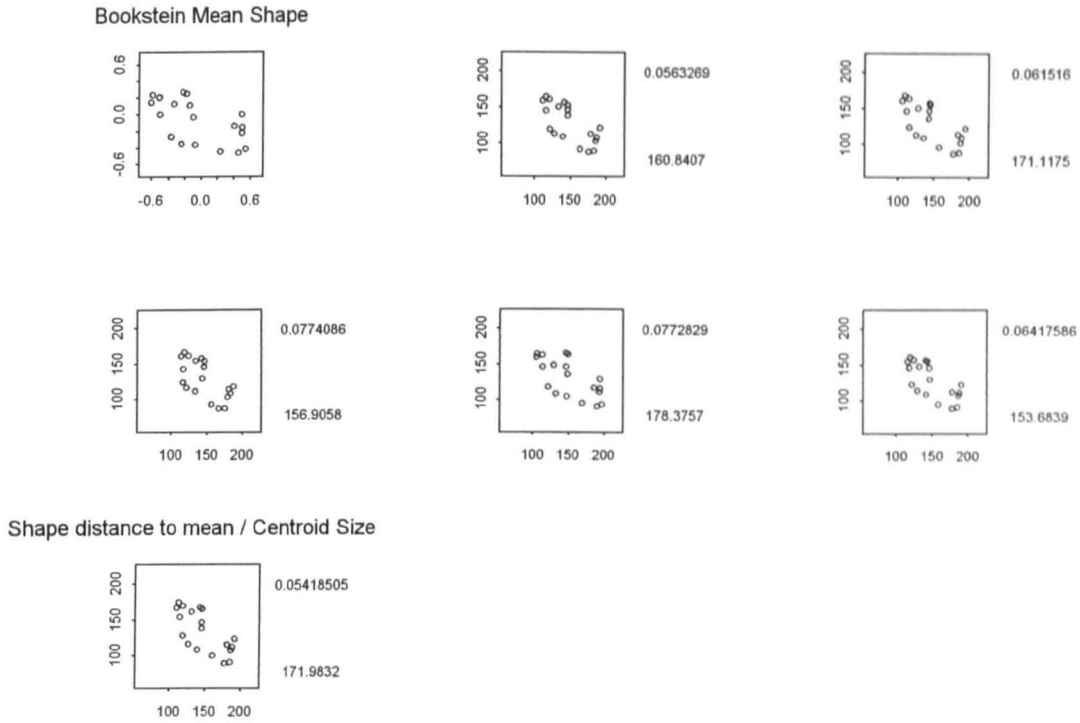

Figure 5.24a **Shape distance to Bookstein mean and Centroid Size. 6 Females. Age 9.**

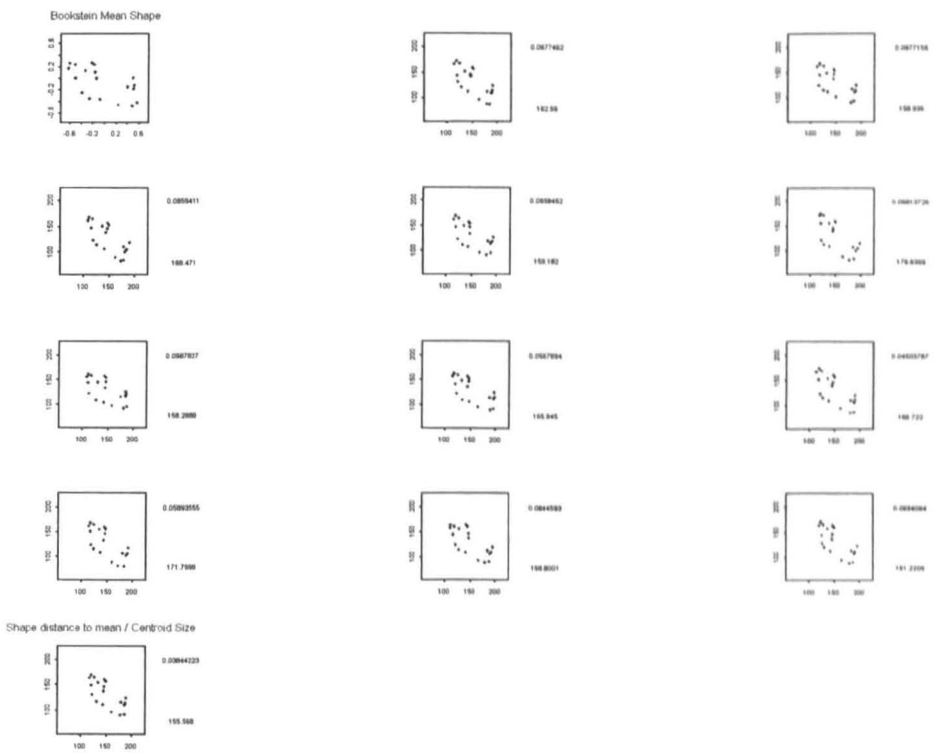

Figure 5.24b **Shape distance to Bookstein mean and Centroid Size. 12 Males. Age 9.**

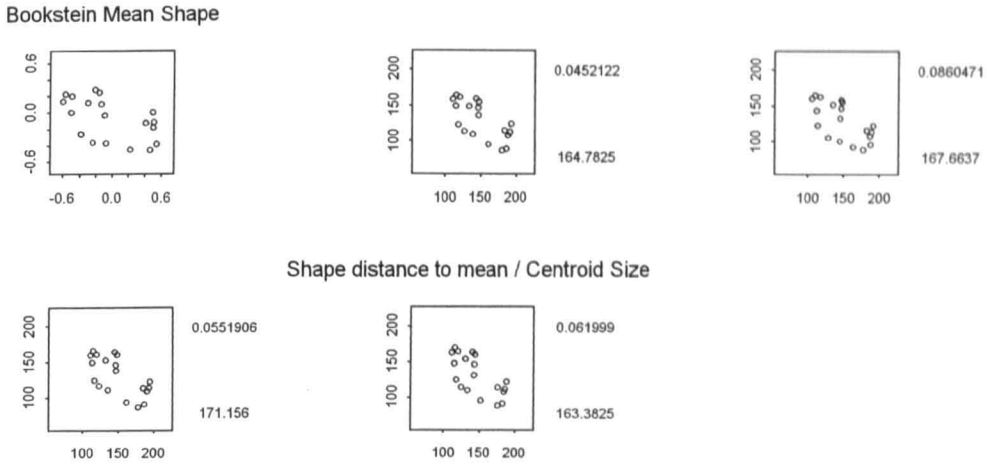

Figure 5.25a Shape distance to Bookstein mean and Centroid Size. 4 Females. Age 11.

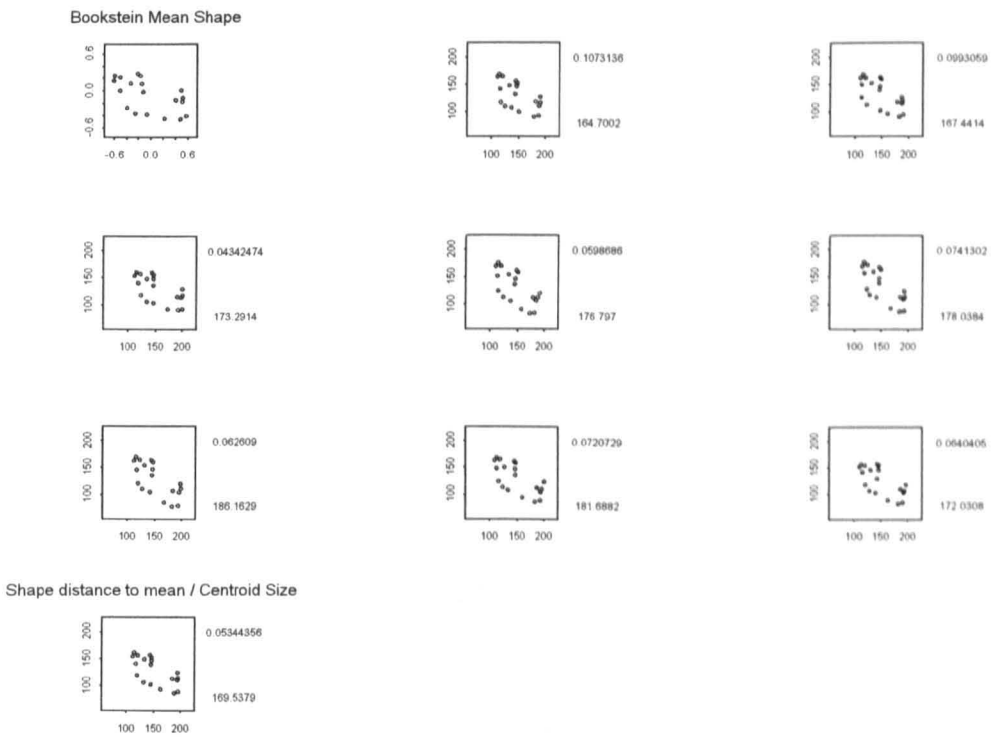

Figure 5.25b Shape distance to Bookstein mean and Centroid Size. 9 Males. Age 11.

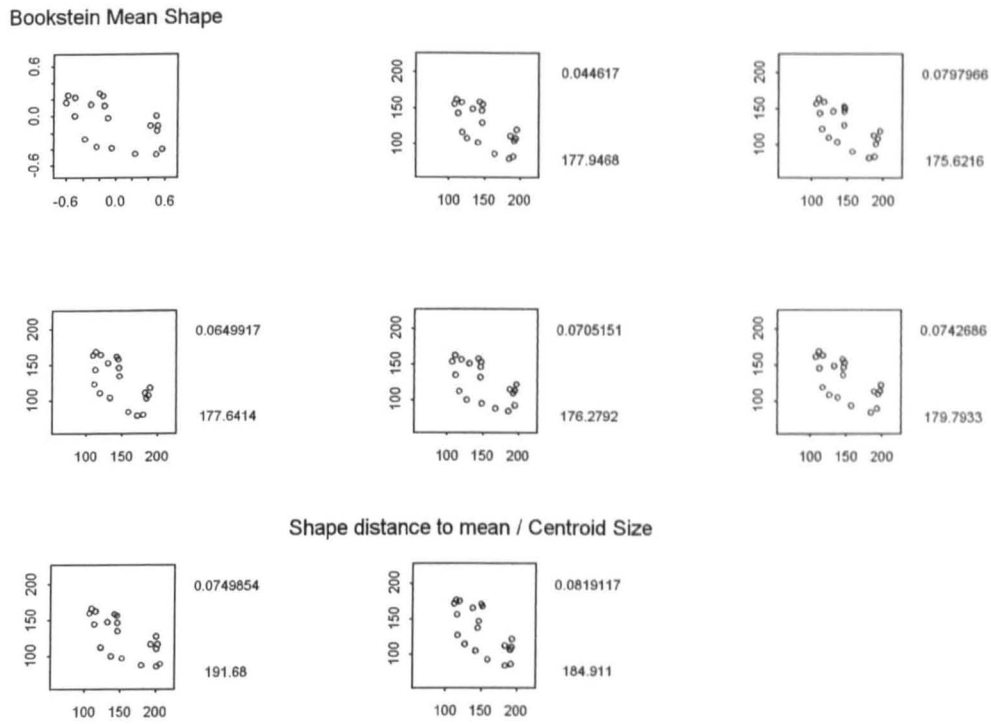

Figure 5.26a Shape distance to Bookstein mean and Centroid Size. 7 Females. Age 13.

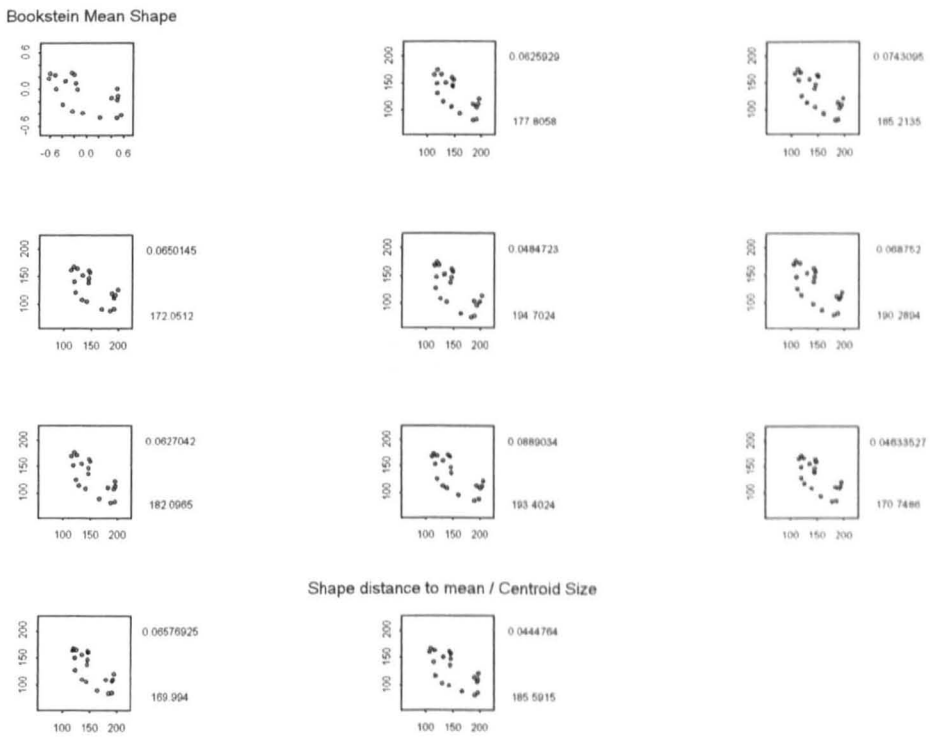

Figure 5.26b Shape distance to Bookstein mean and Centroid Size. 10 Males. Age 13.

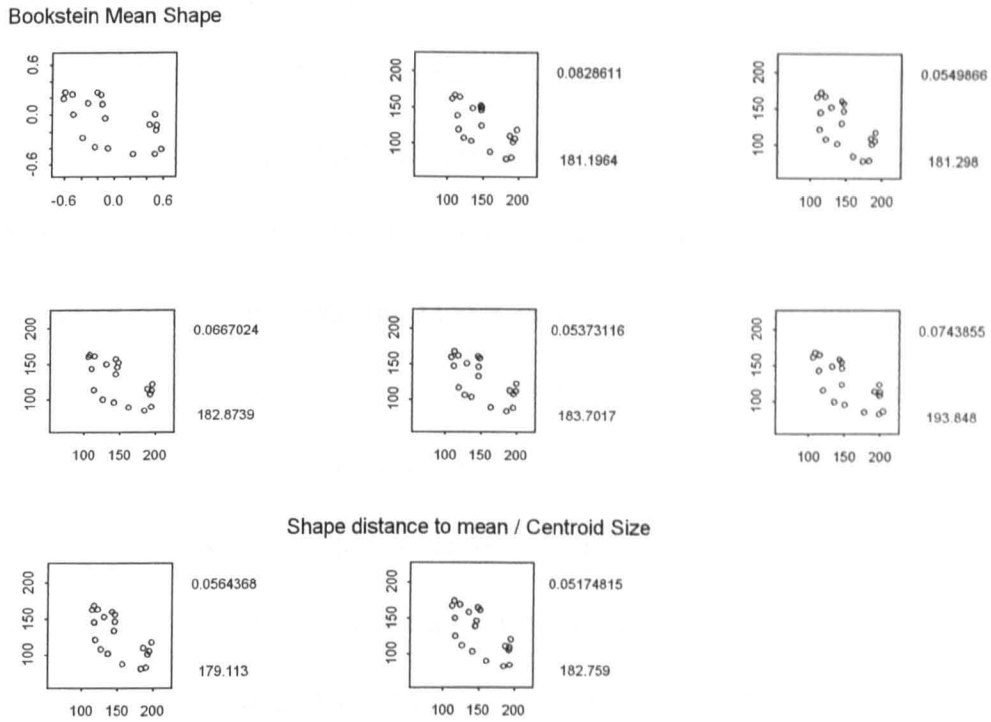

Figure 5.27a Shape distance to Bookstein mean and Centroid Size. 7 Females. Age 15.

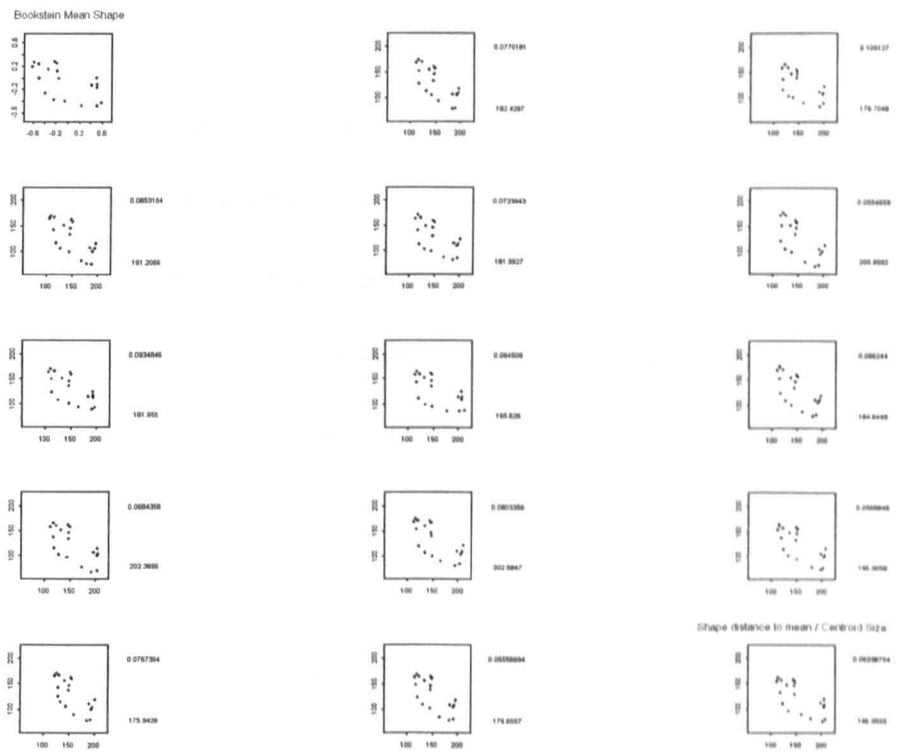

Figure 5.27b Shape distance to Bookstein mean and Centroid Size. 14 Males. Age 15.

It is interesting to note that centroid sizes range from 154 to 178, 163 to 171, 176 to 192 and 179 to 194 for ages 9, 11, 13 and 15 for females and males respectively. It can be said then, that size is indeed increasing over the range of ages for both males and females (the ranges of centroid size are increasing with increasing age). There is however a lot of overlap between the ranges of different ages, for both males and females. The shape distances of each configuration from the Bookstein mean shape within the male and female samples, for the different ages give some indication of the within-sample and between-sample variation in shape. Both between males and females at particular ages, and between ages for the male and female groups. These values are 0.054-0.078 and 0.036-0.098; 0.045-0.086 and 0.043-0.101; 0.045-0.080 and 0.044-0.089; 0.052-0.083 and 0.055-0.105 for females and males aged 9, 11, 13 and 15 respectively. It can be seen then, that these values tend to be fairly similar within-samples and between females and males for each age group (there tends to be a great deal of overlap in the ranges between sexes of the same age). Further, there also tends to be great deal of overlap in the ranges between females at different ages and males at different ages. These observations would suggest that there does not appear to be a great deal of difference as regards the shape of the mandible, within male and female samples and between male and female samples, and also over the range of ages for both males and females. Similar observations have already been made with the Bookstein co-ordinates.

These shape distance measures from the Bookstein mean shape and centroid size values for each mandibular outline in the appropriate samples can also be plotted against one another in order to examine the relationship between size and shape. Such

plots are shown in Figures 5.28 – 5.31 (a) and (b) both females and males respectively, at each age.

It can be seen from these figures that, for both males and females, at all ages, there is no clear pattern of a relationship between size and shape. Where a particular configuration in a sample has the largest centroid size for example, it does not necessarily have the largest shape distance from the Bookstein mean shape for that group, or vice versa. There does appear however to be some 'loose' patterns in some of these plots which may suggest some relationship between size and shape, but not a convincing one.

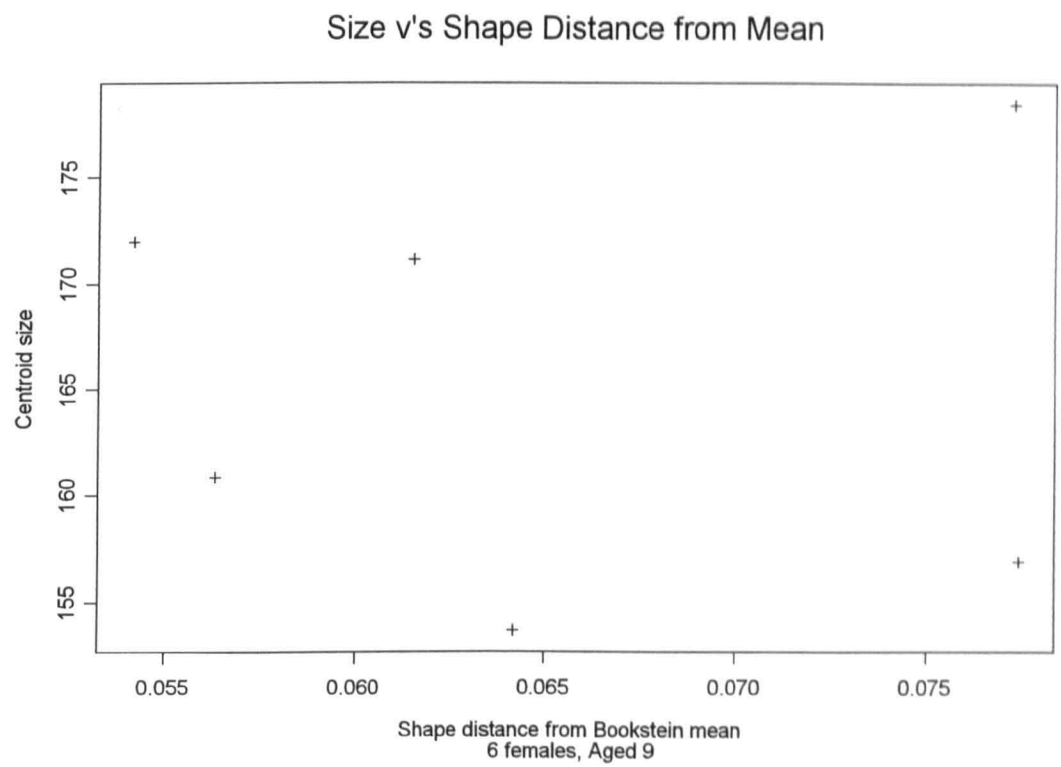

Figure 5.28a **Shape distance to Bookstein mean versus Centroid Size. Females. Age 9.**

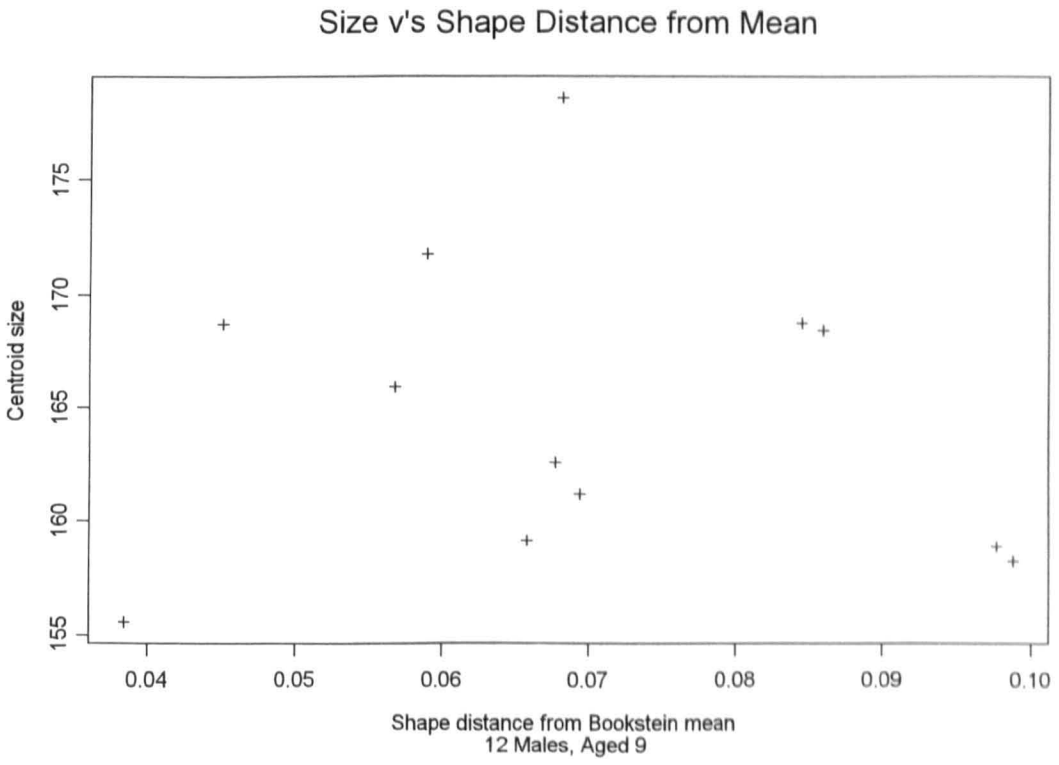

Figure 5.28b **Shape distance to Bookstein mean versus Centroid Size. Males. Age 9.**

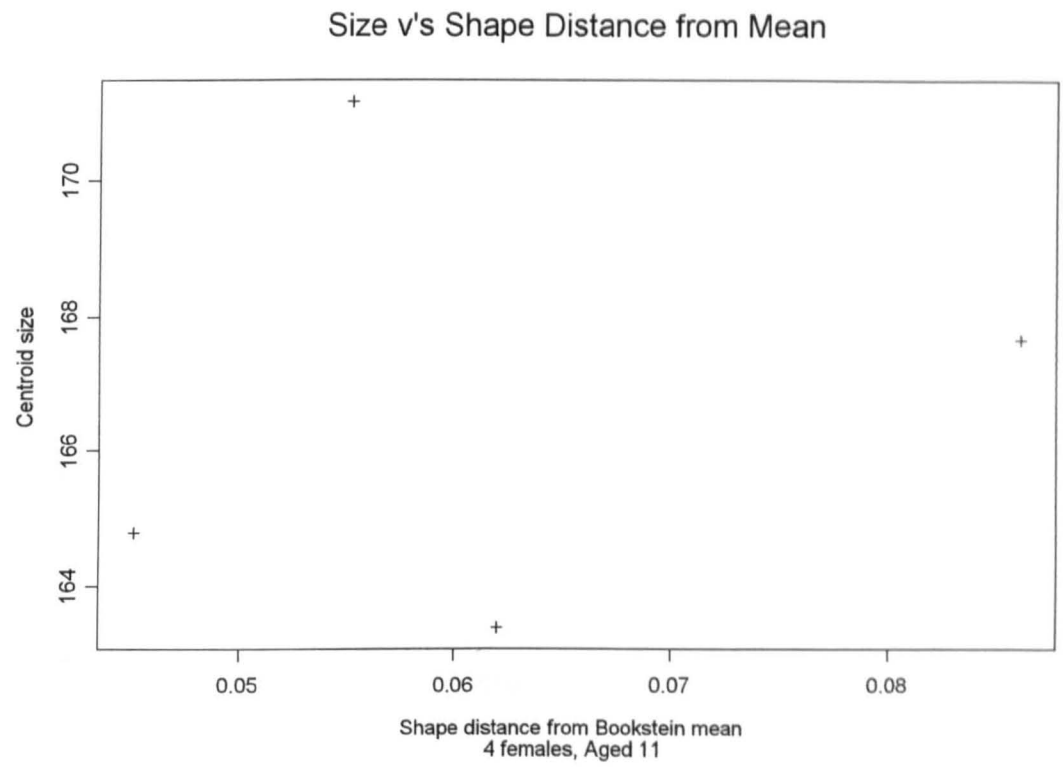

Figure 5.29a **Shape distance to Bookstein mean versus Centroid Size. Females. Age 11.**

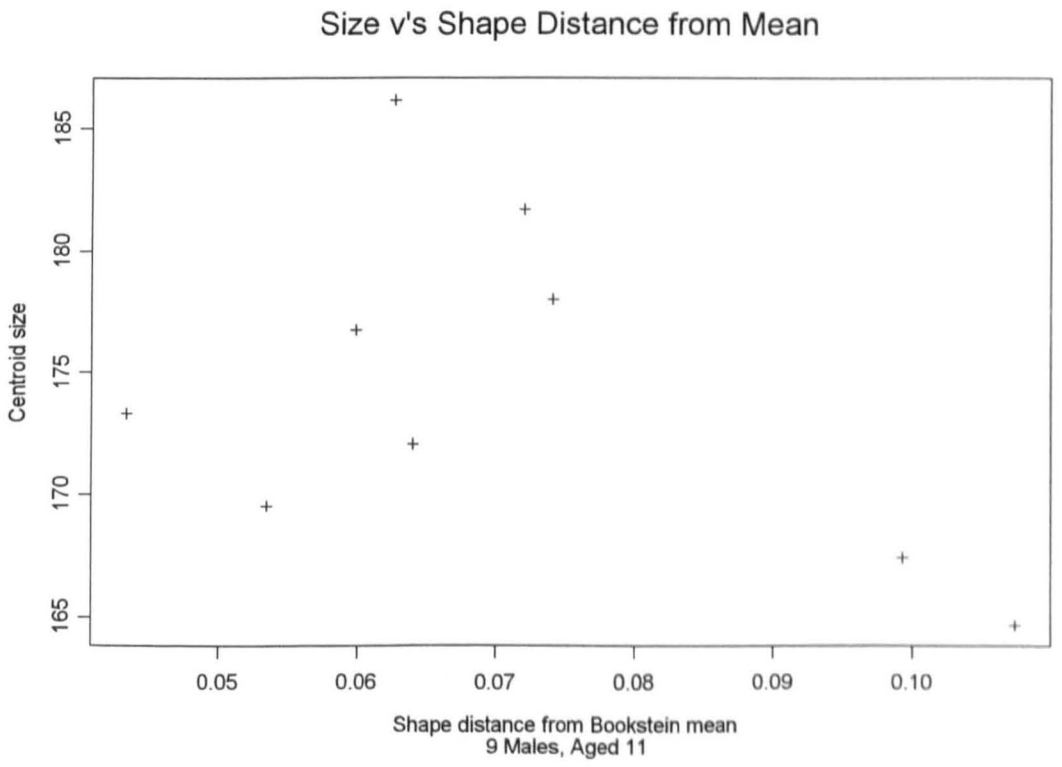

Figure 5.29b **Shape distance to Bookstein mean versus Centroid Size. Males. Age 11.**

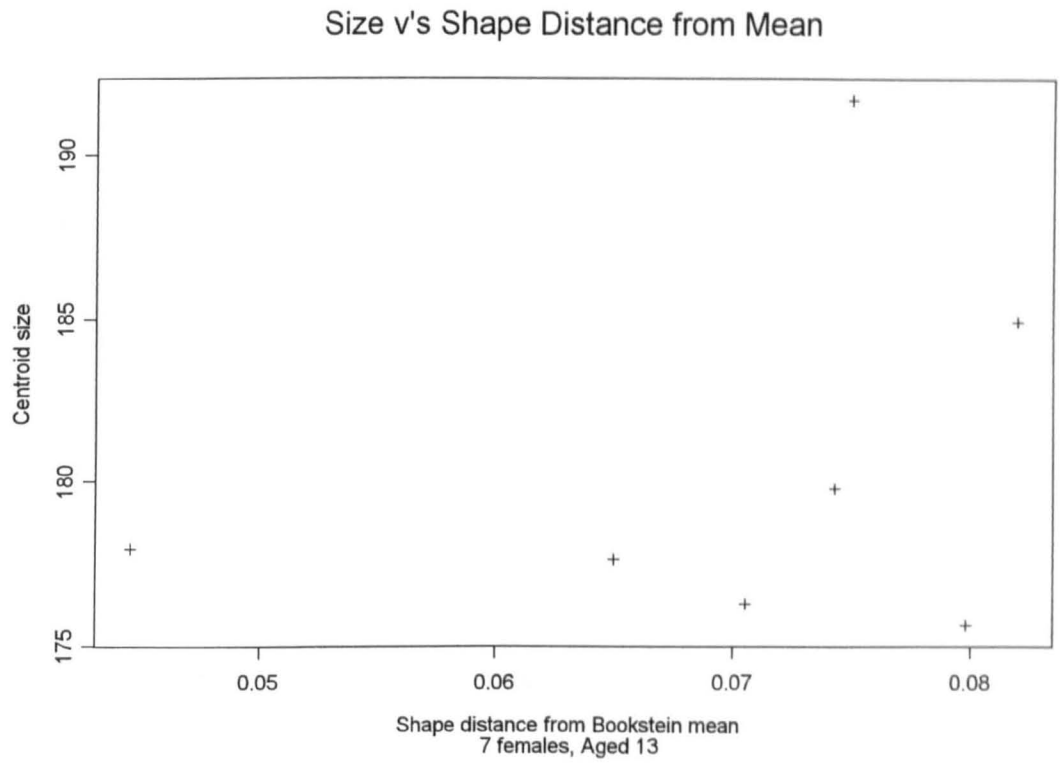

Figure 5.30a **Shape distance to Bookstein mean versus Centroid Size. Females. Age 13.**

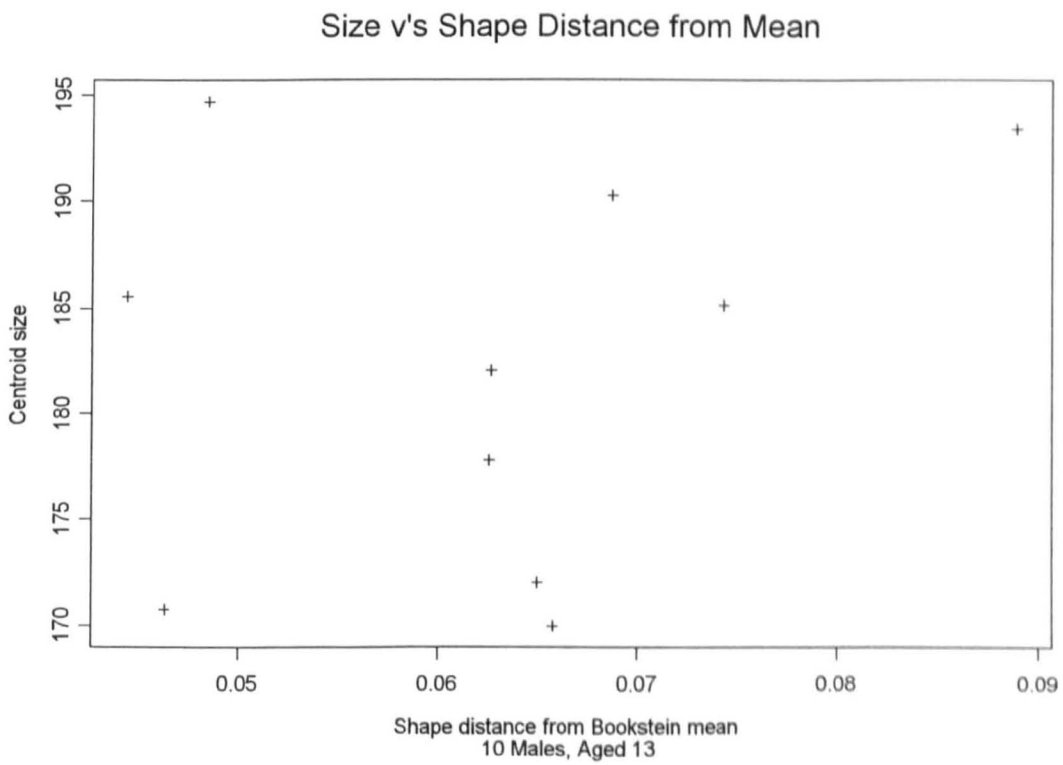

Figure 5.30b **Shape distance to Bookstein mean versus Centroid Size. Males. Age 13.**

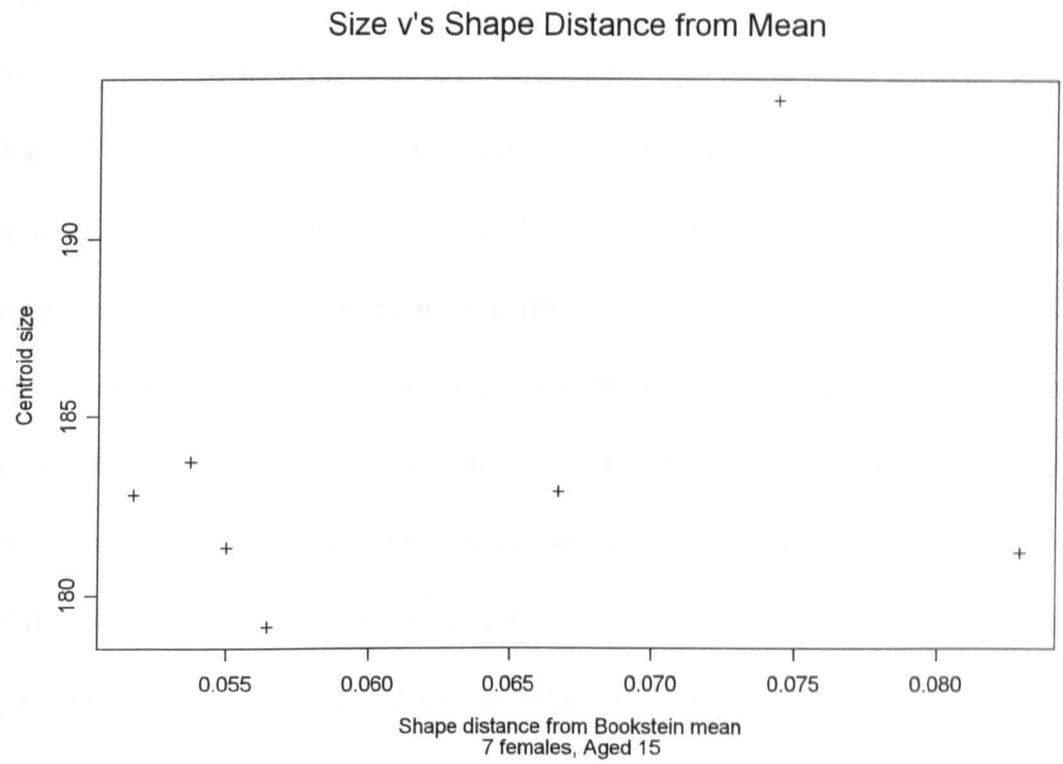

Figure 5.31a **Shape distance to Bookstein mean versus Centroid Size. Females. Age 15.**

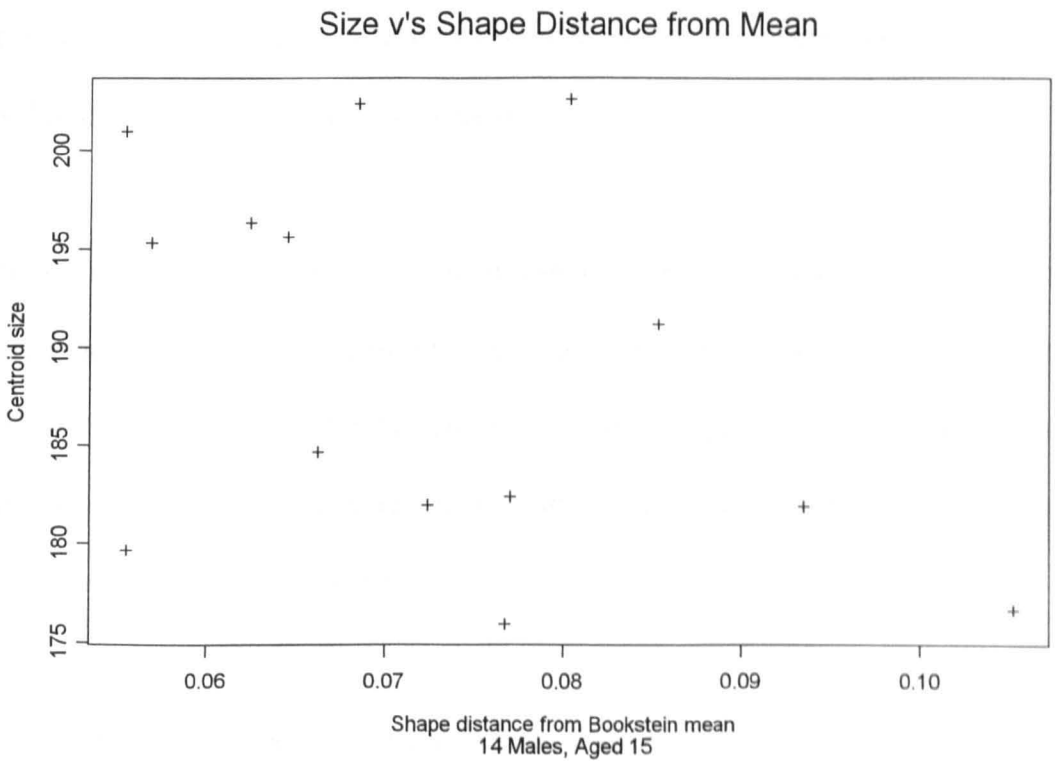

Figure 5.31b **Shape distance to Bookstein mean versus Centroid Size. Males. Age 15.**

Pair wise scatter plots of the centroid size S versus each of the shape co-ordinates can also be produced to investigate any correlations that might exist between size and shape. There are too many of these plots to include here. To illustrate and give an idea of what we might expect and / or be looking out for in this part of the analysis, examples of these plots are given for males aged 15 in Figures 5.32 (a) to (d). There are 14 males of that age in the sample and therefore anything interesting might be more likely to be observed than it would be for example, if females aged 11 were looked at since there are only 4 subjects of that age and sex. The centroid size for each of the 14 males in the sample (resulting in 14 points in each of the plots) are plotted against each of the Bookstein shape variables, i.e. each of the u_i's and each of the v_i's, (of which there are k-2=17 and i = 3,.....19 for this set of mandibular data). Pair wise plots of each of the shape variables can also be examined at this time to illustrate another important point as discussed earlier where it was noted that an artefact of this co-ordinate system in that correlations are induced into the shape variables, even when the landmarks themselves are uncorrelated.

From Figures 5.32 (a) to (d) then, it can be seen then that there are no strong correlations between the centroid size S and any of the shape variables. Similar observations were made for the group of females, aged 15. This corroborates the random scatter of points depicted in the scatter plots of shape distance from Bookstein mean versus centroid size earlier.

Further, it is easy to see that there are strong positive correlations between some of the shape variables themselves, namely u_3 & u_4, u_5, u_6; u_4 & u_5, u6; u_5 & u_6; u_9 & u_{10}; v_4 & v_5; v_9 & v_{10} and so on. These correlations can be difficult to interpret however, due to

the fact that this is an artefact of this co-ordinate system in that correlations are induced into the shape variables, even when the landmarks themselves are uncorrelated.

Pair wise scatter plots for males and females, for all other age groups (11, 13 and 15) showed similar results. There did appear to be some weak correlations between the centroid size and some of the shape variables however. The strongest correlations between size and some of the shape variables seemed to be in the female group, for ages 9 and 13, and the male group, aged 13. This is reflected in the scatter plots of shape distance from Bookstein mean versus centroid size, some of which depict vague increasing / decreasing relationships between size and shape. Patterns are by no means clear-cut however. There may be some relationship between the size and shape of the mandibular outlines, particularly for these ages, but not a strong linear relationship or anything. It is worth noting that relationships between size and shape are very difficult to interpret and pick out from this data since the sample sizes are so small.

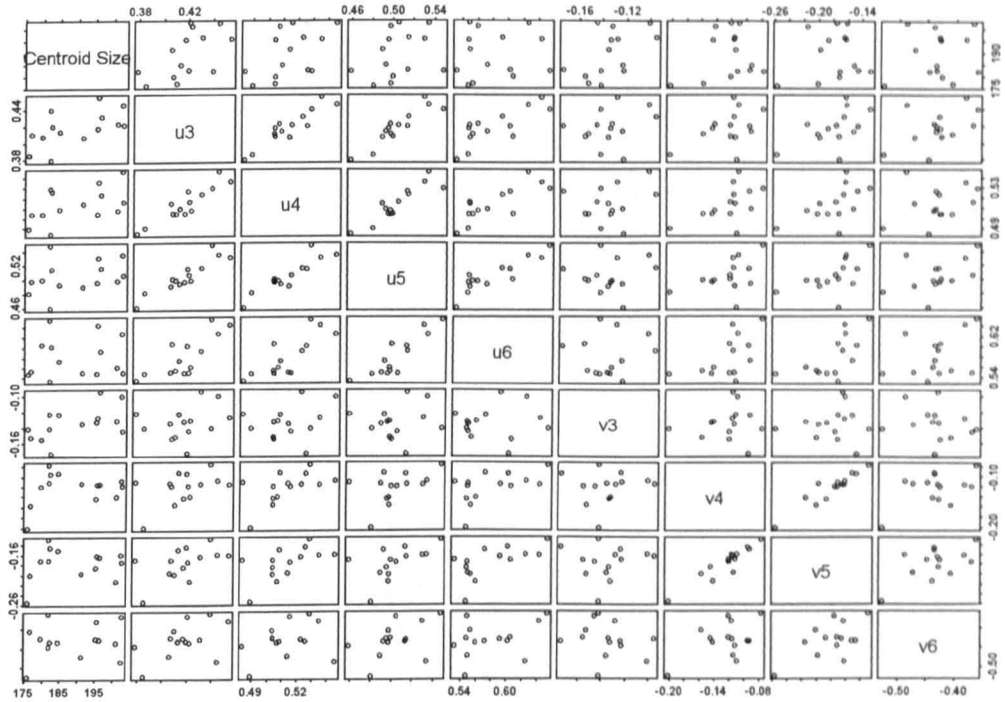

Figure 5.32a **Pair wise scatter plots of centroid size S and Bookstein co-ordinates u_3, u_4, u_5, u_6 and v_3, v_4, v_5, v_6. 14 Males. Age 15.**

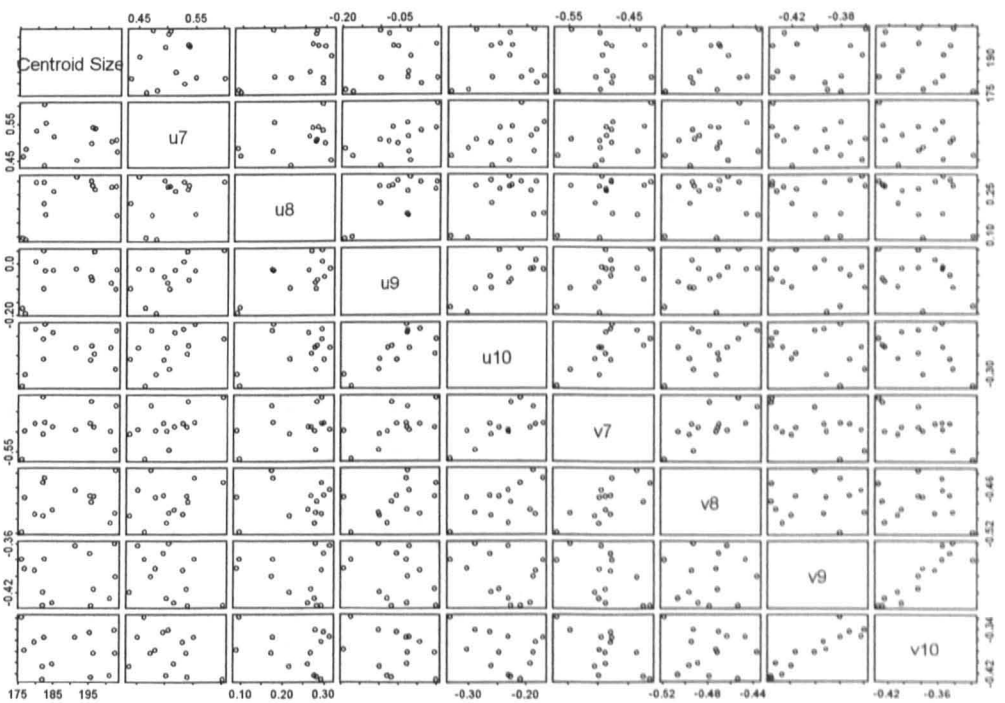

Figure 5.32b **Pair wise scatter plots. Centroid size S and Bookstein co-ordinates u_7, u_8, u_9, u_{10} and v_7, v_8, v_9, v_{10}. 14 Males. Age 15.**

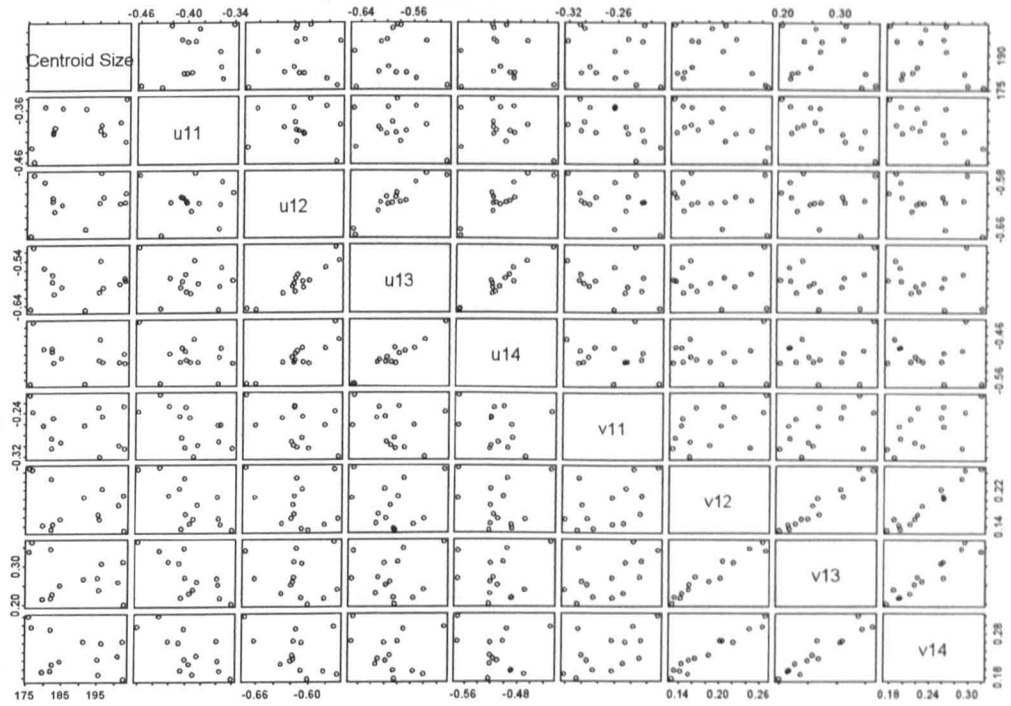

Figure 5.32c **Pair wise scatter plots of centroid size S and Bookstein co-ordinates u_{11}, u_{12}, u_{13}, u_{14} and v_{11}, v_{12}, v_{13}, v_{14}. 14 Males. Age 15.**

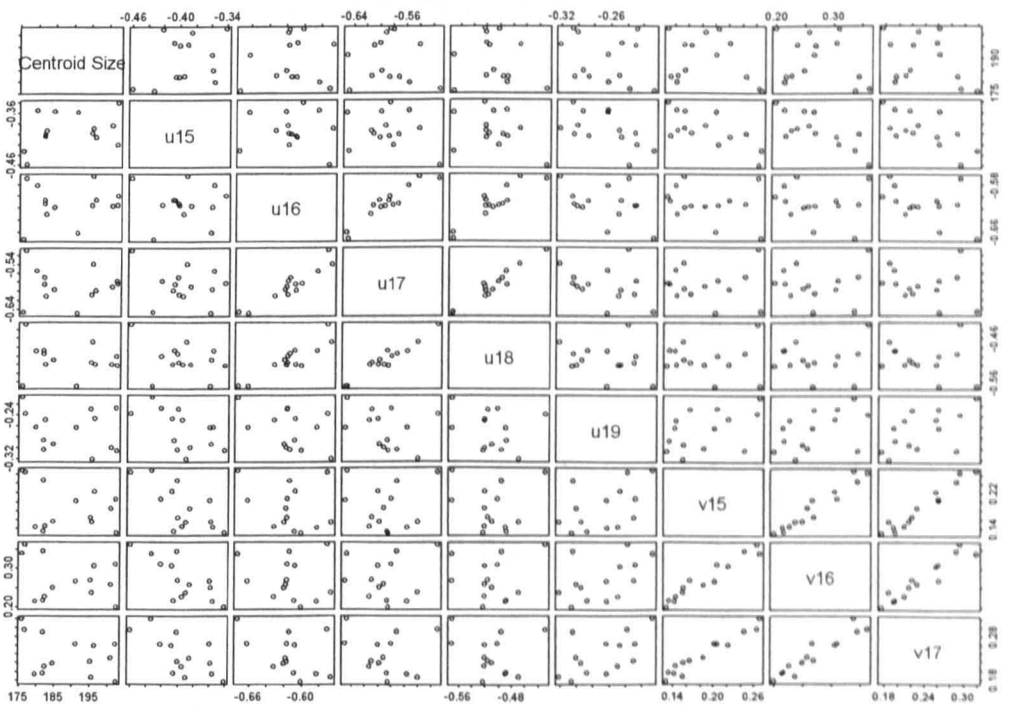

Figure 5.32d **Pair wise scatter plots of centroid size S and Bookstein co-ordinates u_{15}, u_{16}, u_{17}, u_{18}, u_{19} and v_{15}, v_{16}, v_{17}, v_{18}, v_{19}. 14 Males. Age 15.**

The variability of the shape variables is less straight forward to interpret using Bookstein co-ordinates, as discussed previously. This method is therefore not used to investigate the structure of shape variability in the mandibular data. This is addressed in the next section using Procrustes analysis.

5.5.3 Procrustes Analysis

Procrustes analysis of the mandibular data involves several steps (and lots of informative plots!).

As with the analysis using Bookstein co-ordinates, the two dimensional outlines for each mandible are characterised by 19 anatomical landmark points as defined in Chapter 3, with original landmarks 51 & 18 now new landmarks 1 & 2. This new designation is the same as that used for the Bookstein co-ordinate analysis outlined in Table 5.1.

As before, the first step in this analysis is to examine plots of the raw data.

The Procrustes rotated data for both the females and males (at each age) are then calculated and displayed, as is the full Procrustes estimate of mean shape for the sample of females and males (at each age). However, unlike testing for the mean difference between males and females at each age using the predicted points from the elliptical Fourier function, a two sample Hotelling's T^2 test cannot be used to formally

test for average shape differences between the sexes here. This is due to the fact that there are not enough subjects in the individual female and male samples.

Various representations of the Principal Components are then given to investigate shape variability within the males and females at each age.

The mean shapes are then superimposed and compared, followed by examination of a pooled data set for each age since the mean shapes for males and females are found not to be too different, and therefore can be combined.

The full Procrustes mean shapes at each age for the pooled data samples are superimposed and examined to investigate whether or not there are differences in shape over the whole range of ages, from age 9 through to age 15. Formal Hotelling's T^2 tests are carried out where appropriate i.e. when combined sample sizes are of adequate size.

Pair wise scatter plots of centroid size, full Procrustes distance to the pooled mean and the first few principal component scores are also displayed for the pooled data in order to investigate the separation of males and females further.

The relationship between size and shape is also investigated using Procrustes analysis, similar to that using Bookstein co-ordinates, by plotting pair wise scatter plots of centroid size and the shape variables, defined here to be the (x,y) co-ordinates of the full Procrustes co-ordinates for males and females at each age.

Finally, an alternative look at shape change between males and females is addressed by displaying deformation grids of the female average shape to the male average shape (for all ages) using the method of thin plate spines.

Figures 5.33 (a) and (b) depict the raw digitised mandibular outline data for each individual outline for the 6 females and 12 males aged 9. In addition, Figures 5.34 (a) and (b) depict each outline, for the same 6 females and 12 males superimposed, using a different symbol to depict each outline. It can be said from these plots that, although the overall outlines (overall size and shape) tend to be very close, there exists some variability within females and males at most of the landmark points. Similar patterns of variability were observed for the female and male samples at all other ages.

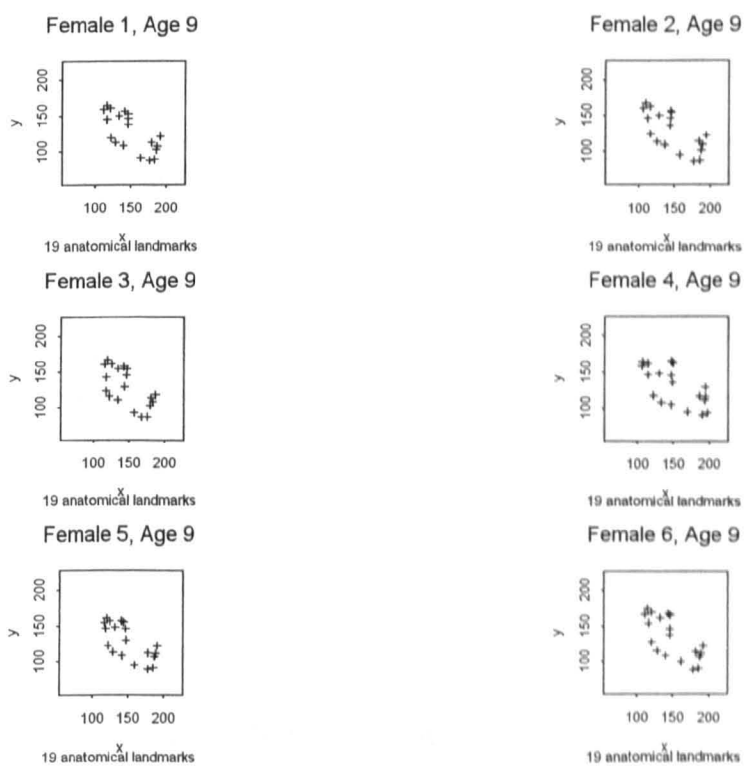

Figure 5.33a Mandibular outline. Raw Data. 6 Females. Age 9.

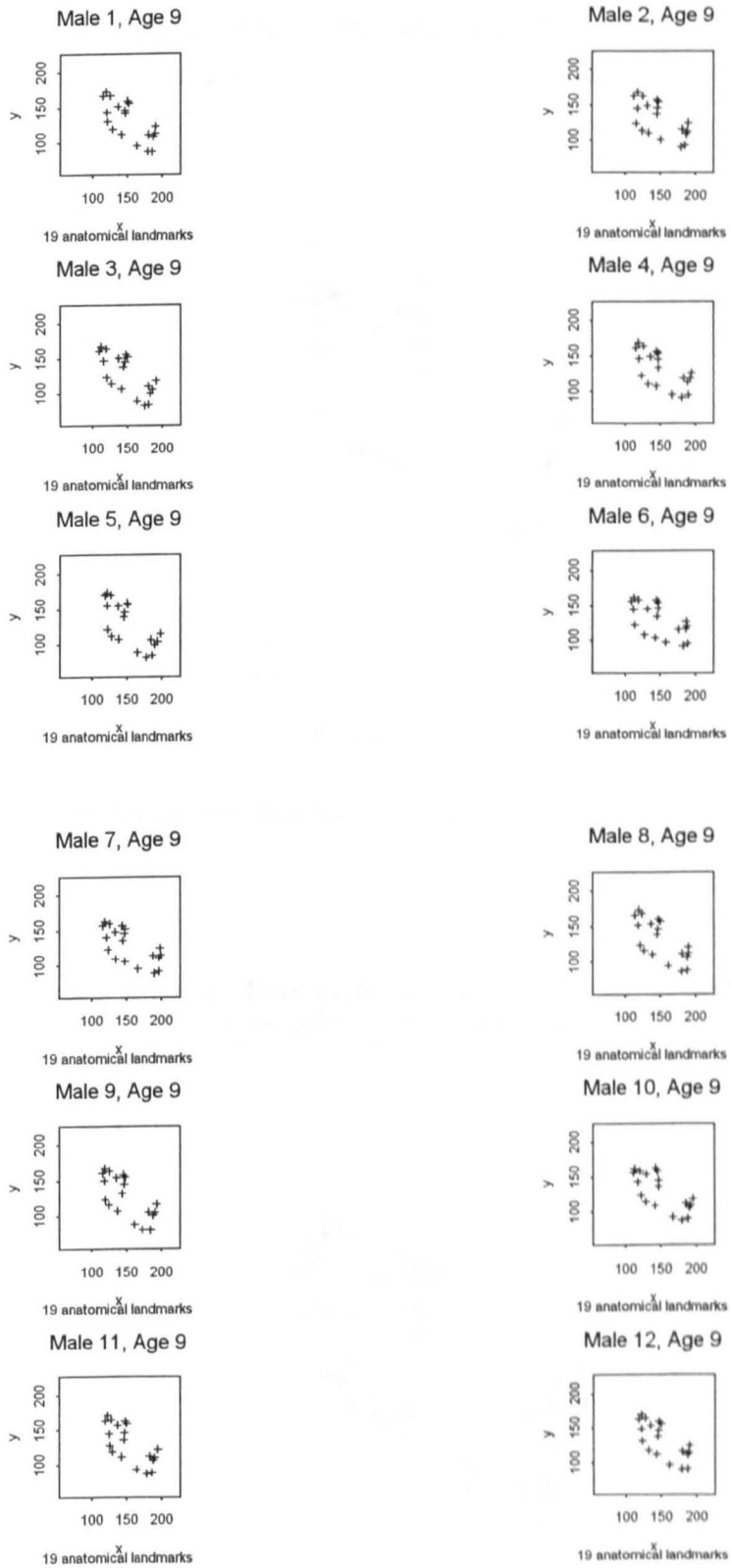

Figure 5.33b Mandibular outline. Raw Data. 12 Males. Age 9.

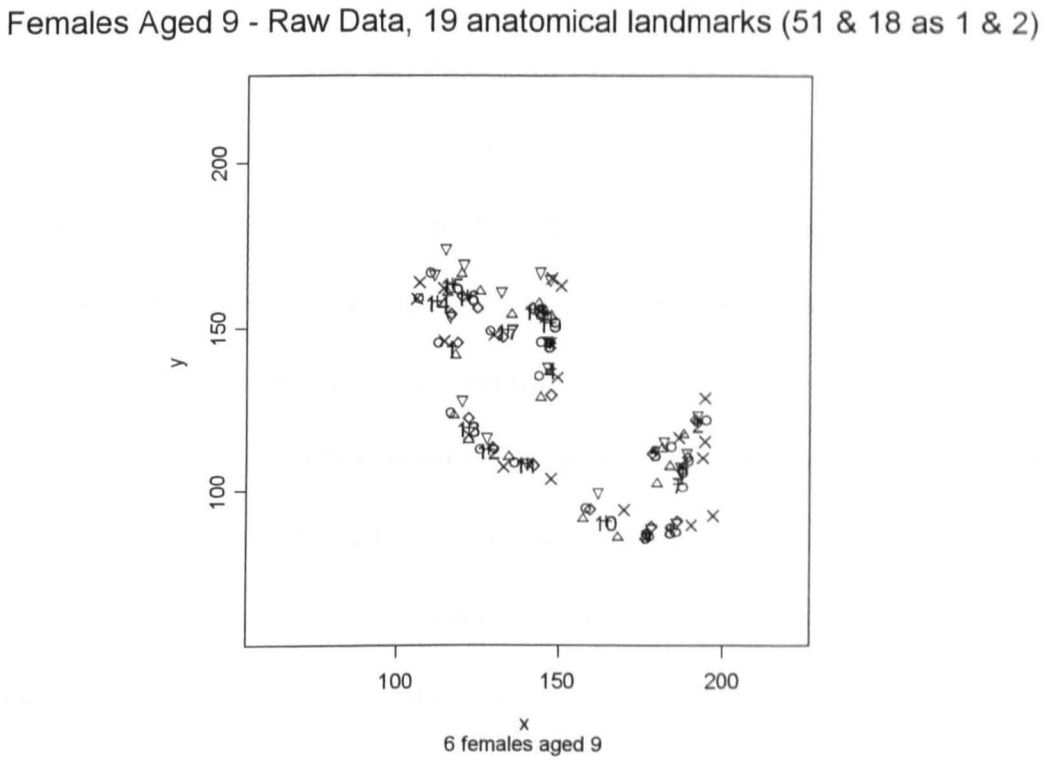

Figure 5.34a **Mandibular outlines. Raw Data. 6 Females. Age 9.**

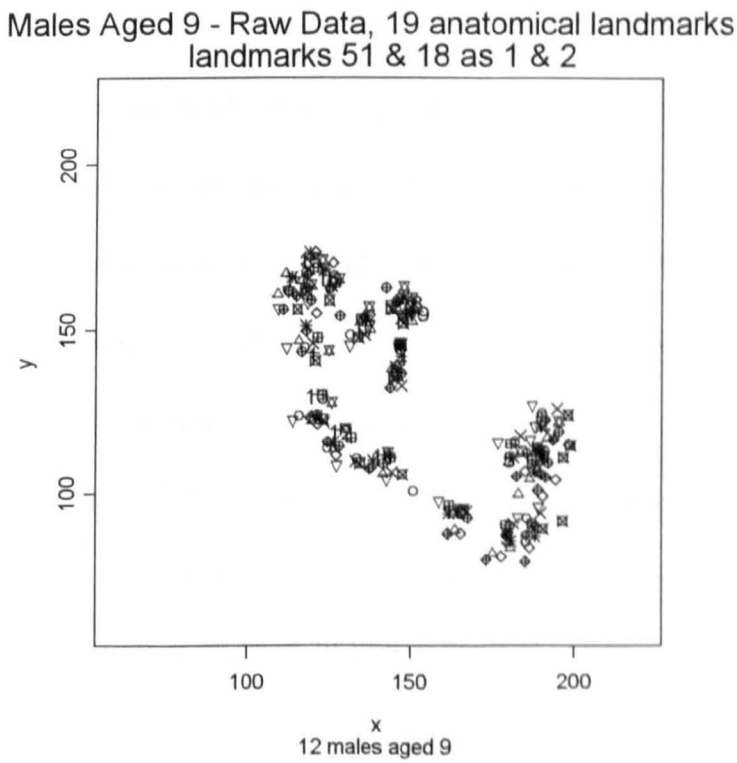

Figure 5.34b **Mandibular outlines. Raw Data. 12 Males Aged 9.**

Considering shape only, Figures 5.35 (a) and (b) we see the superimposed female and male mandibular outlines using full Procrustes superimposition (GPA) where the full Procrustes fits for the 6 females and 12 males, aged 9 have been calculated separately and plotted. Each of the configurations in the sample under consideration (the 6 females and 12 males, aged 9 as illustrated here) has been pre-scaled to unit centroid size, centred and superimposed on the centroid at (0,0), and rotated so that the line joining landmarks 1 and 2 is horizontal (but these points are not forced to (-0.5,0) and (0.5,0) now). Therefore, the 'clumps' of circles at each point on the mandibular outline represent the Procrustes rotated data for each configuration in the sample under consideration i.e. 6 circles at each point for the female sample (Figure 5.35a) and 12 for the male sample (Figure 5.35b) for age 9. As a reminder, the new designation of points is equivalent to those used in the Bookstein co-ordinate analysis and is illustrated in the plot for females, age 9.

For each sex, again the landmarks match up quite closely which implies that shape variability within the samples, at age 9, is evident but small (indicated by the closeness of each clump of points at each of the landmark points). In fact, to obtain an overall measure of shape variability the within sample root mean square of the full Procrustes distance from each configuration to the full Procrustes mean can be considered. The root mean square of the full Procrustes distance to the estimated mean shape within each group is 0.066 for the females and 0.072 for the males aged 9. The smaller these values, the less variability there exists within the samples.

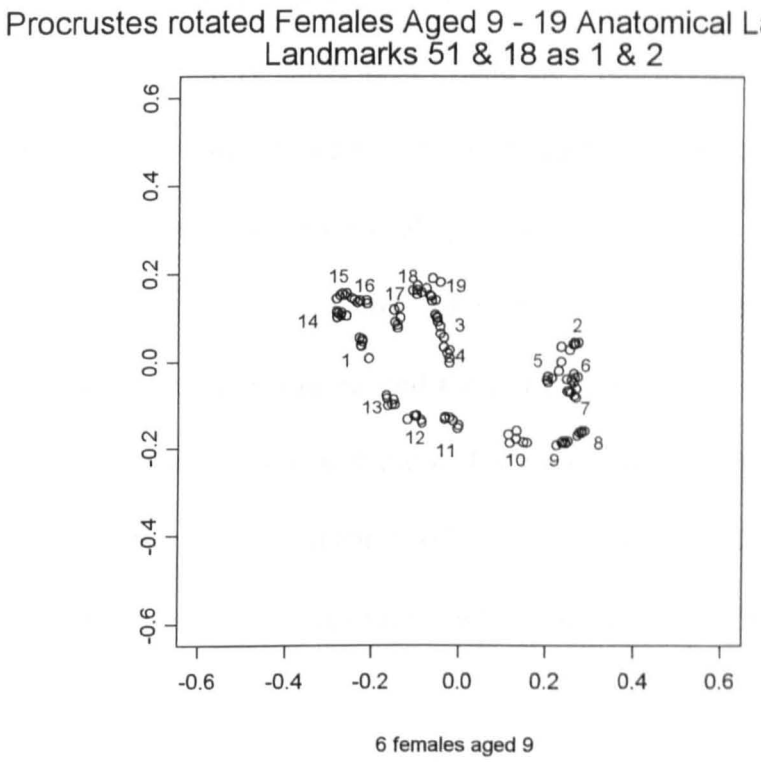

Figure 5.35a **Procrustes rotated outlines. 6 Females. Age 9.**

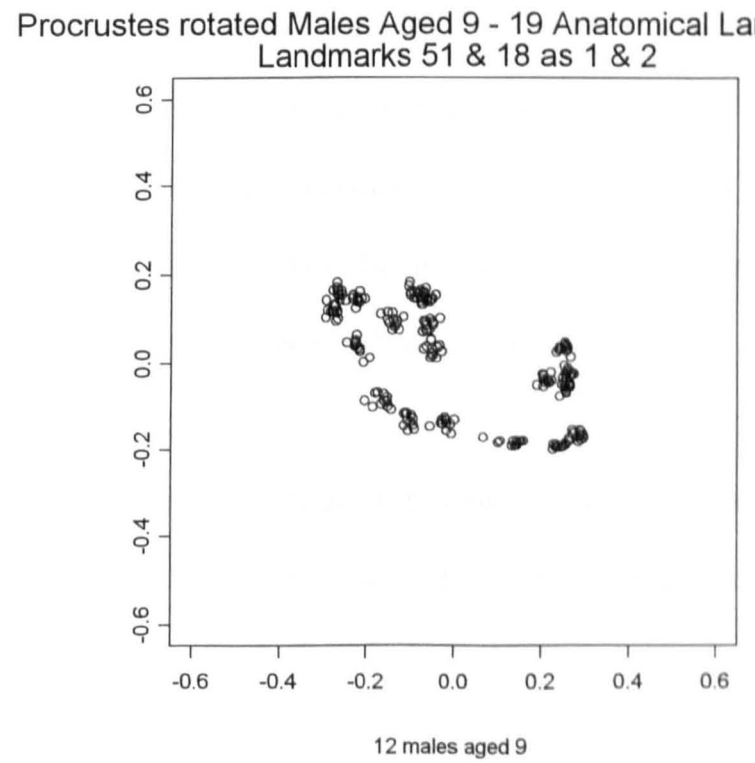

Figure 5.35b **Procrustes rotated outlines. 12 Males. Age 9.**

The full Procrustes superimposition was also carried out for the 4 females and 9 males aged 11; the 7 females and 10 males aged 13 and the 7 females and 14 males aged 15. Again, the variability in the landmark points within female and male samples at these ages was small. Further, the corresponding measures of shape variability in these samples were 0.064, 0.073; 0.071, 0.064 and 0.064, 0.074 for females and males aged 11, 13 and 15 respectively. It can be said then, that shape variability within females and males is small, for all ages, and the males tend to be slightly more variable in shape than the females with the exception of age 11. It is worthwhile to note that there are of course more males (in all age groups) which may have an effect on the measure of shape variability.

The full Procrustes estimate of mean shape for each sex (at each age) was then calculated and plotted. This is found from the dominant eigenvector of the complex sum of squares and products matrix for each sex (at each age). The Procrustes mean shape is centred (on the centroid, at (0,0)), with unit size (unit centroid size), and rotated so that the line joining landmarks 1 and 2 is horizontal (but these points are not forced to (-0.5,0) and (0.5,0) now). These estimates of mean shape for females and males separately aged 9 can be seen in Figures 5.36 (a) and (b).

These full Procrustes estimated mean shapes for the females and males illustrated here are superimposed (by OPA or GPA) and displayed later, for all ages (Figures 40 (a) to (d)).

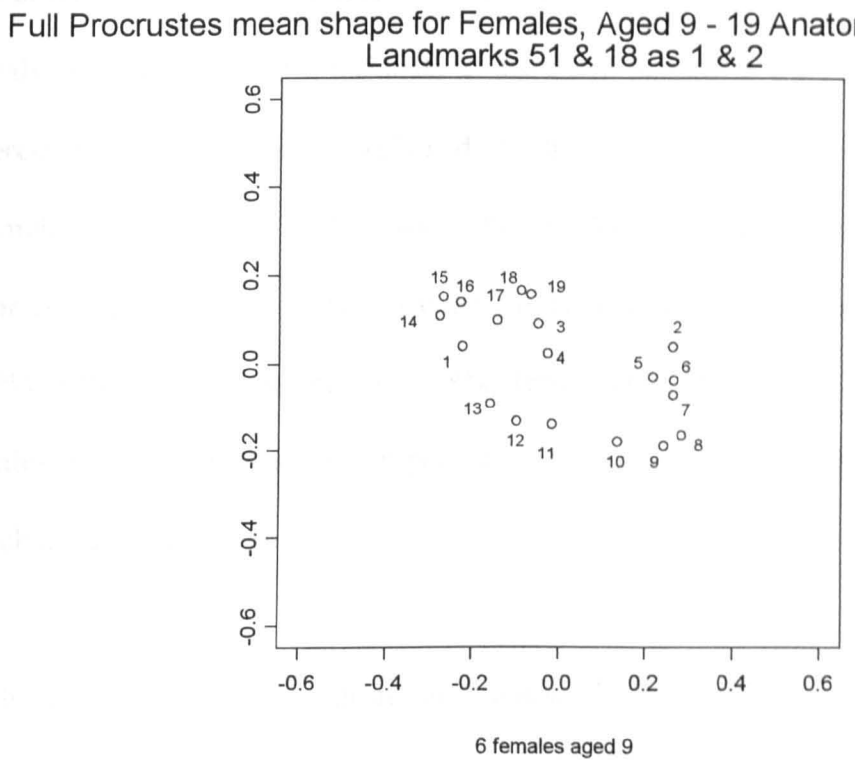

Figure 5.36a **Full Procrustes estimate of Mean Shape. 6 Females. Age 9.**

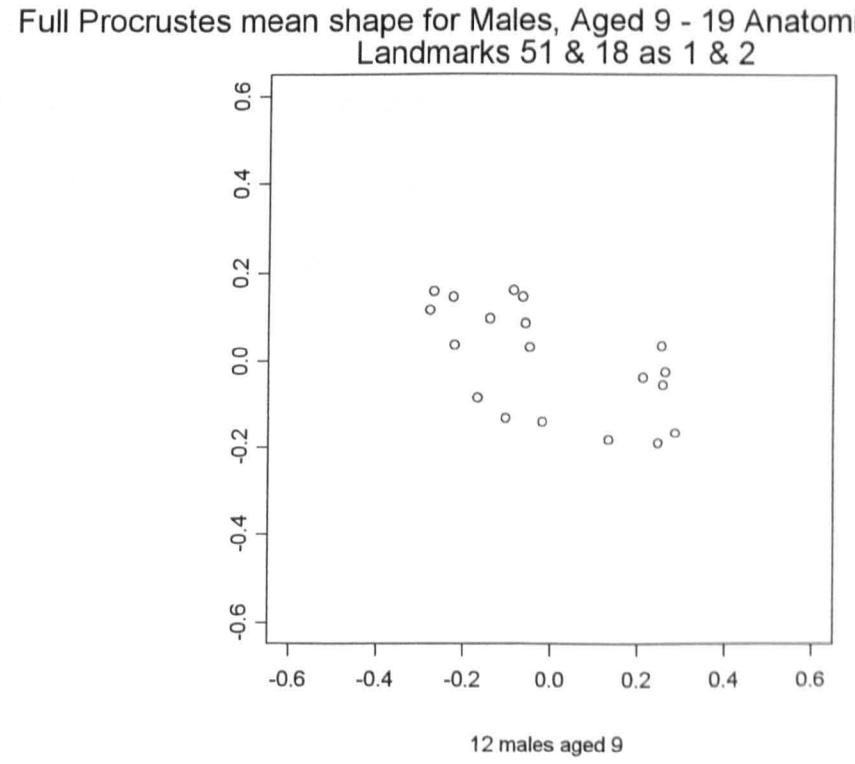

Figure 5.36b **Full Procrustes estimate of Mean Shape. 12 Males. Age 9.**

In order to examine the structure of variability within a sample, principal components analysis of the Procrustes residuals as discussed in section 5.2.1 are considered. The percentages of variability explained by the first three principal components for females, aged 9 are 38%, 21% and 20%, and 33%, 17% and 15% for males aged 9. For ages 11, 13 and 15, these values are 47%, 27%, 10%; 40%, 21%, 16%; 31%, 27%, 18% for females, and 34%, 28%, 16%; 29%, 20%, 15%; 27%, 21%, 15% for males. So, the first principal component is moderately high, but not extremely high, in each group, at each age.

One representation of the principal components from such an analysis is, for each principal component, shapes at +3 standard deviations away from the mean are calculated and plotted. Such a plot for the first two principal components for each sex, aged 9 is given in Figures 5.37 (a) and (b). The mean shape is drawn with vectors to an icon (outline) +3 standard deviations along the first two principal components away from the mean shape. The circles represent the landmark points of the full Procrustes mean, and the lines represent the direction of shift of these points +3 standard deviations away from the mean.

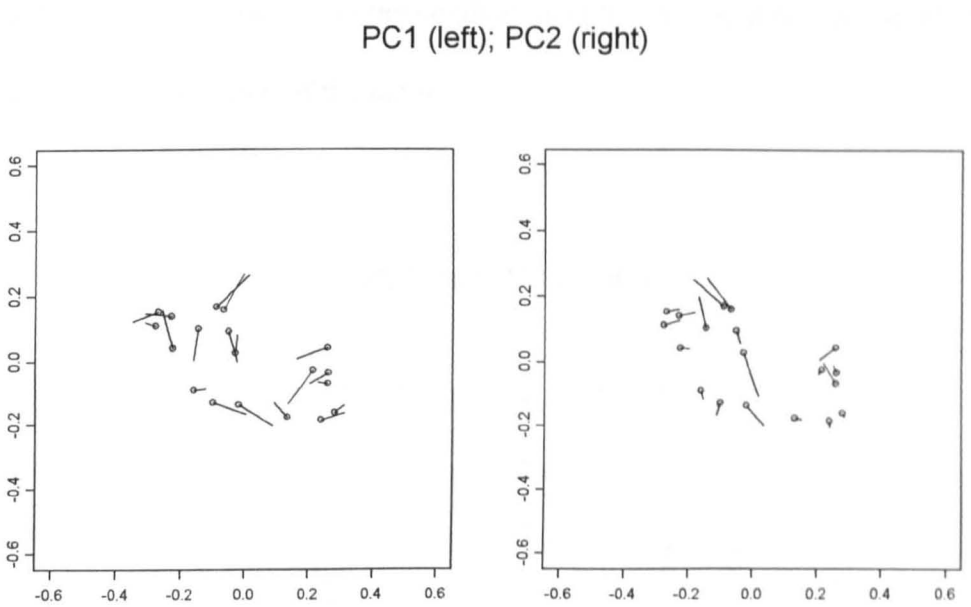

Figure 5.37a Procrustes mean shape and vectors to +3 s.d's along the 1st and 2nd PCs. Females. Age 9.

For the females, the first principal component involves movement, to a certain extent, in all the areas of the bone (in all anatomical landmarks). It appears to include the 'outward' movement of landmarks 4, 8, 9, 11, 12, 14, 15, 16, 18, 19, and the 'inward' movement of landmarks 3, 2, 6, 7, 10, 13, 17. Further, in this first principal component, landmark 1 (old anatomical landmark 51) tends to move 'up'. This overall pattern tends to capture an increase in the overall height and width of the bone. Localised sculpturing in shape with a 'deepening' of the mandibular notch, an anti-clockwise rotation of the lower and anterior borders of the mandible and lower incisor (with a concurrent increase in length of the bone) is also captured. There is less overall movement in the second principal component where landmarks on the lower and anterior borders hardly move at all. There does tend to be a rotational movement in the lower incisor however and this principal component also tends to be capturing an

increased amount of variability in the condyle, mandibular notch and coronoid process and also the anterior border of the ramus.

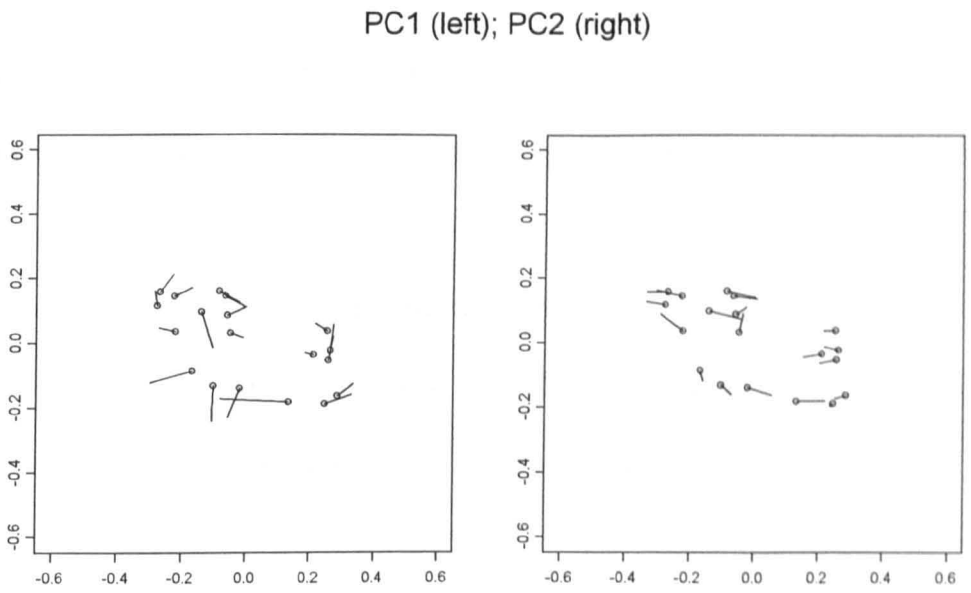

Figure 5.37b Procrustes mean shape and vectors to +3 s.d's along the 1st and 2nd PCs. Males. Age 9.

In the males, the pattern of variability seems to be slightly different in particular landmarks, but tends, to a certain extent, to produce the same overall increase in length, width and height of the bone. The first principal component here involves 'outward' movement of landmarks 3, 4, 8, 9, 11, 12, 13, 1, 14, 15, 16, 18 and 19. Again there appears to be a contribution to the 'deepening' of the mandibular notch in landmark 17, and a lengthening of the bone with an anti-clockwise rotation of the anterior border of the mandible, and this time, a concurrent clockwise rotation of the lower border of the mandible. The lower incisor also appears to be rotating in an anti-clockwise direction due to the movement in landmarks 5, 2, 6 and 7. Once again, there

tends to be less movement in the landmarks in the second principal component (although more than observed for the female sample), where this principal component tends to capture variability in the condyle, mandibular notch and coronoid process.

Alternative representations of the principal components for the full data set of 6 females and 12 males aged 9 are displayed in Figures 5.38 and 5.39 (a) & (b).

In Figures 5.38 (a) and (b), each plot shows the shapes at –3, -2, -1 standard deviations (---.---.---) ; the mean shape (+----+----); as well as the shapes at +1, +2, +3 standard deviations (+.....+....+)along each of the first two principal components.

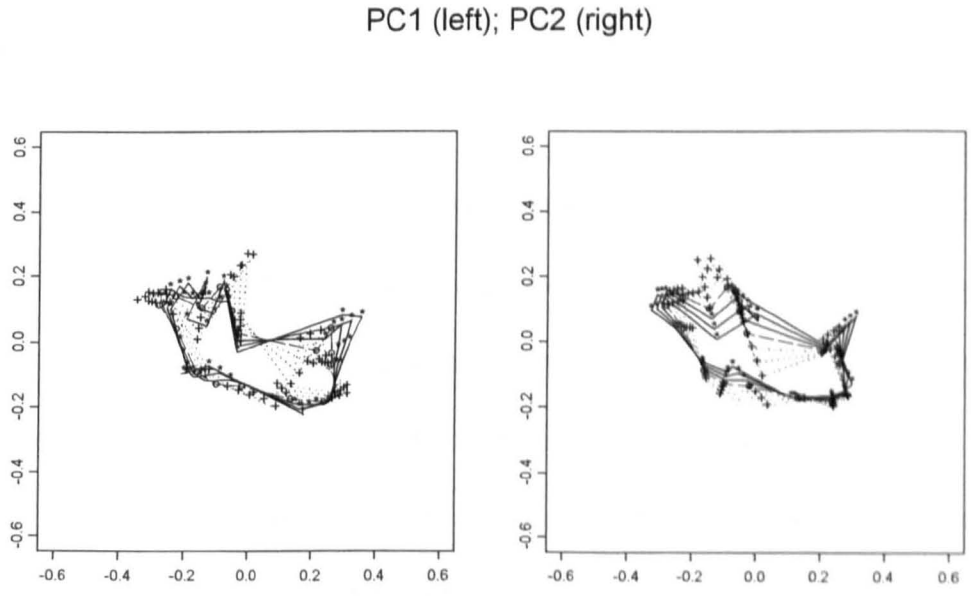

Figure 5.38a Mean shape and shapes at +1, +2, +3 s.d's and –1, -2, -3 s.d's along the 1st and 2nd PCs. Females. Age 9.

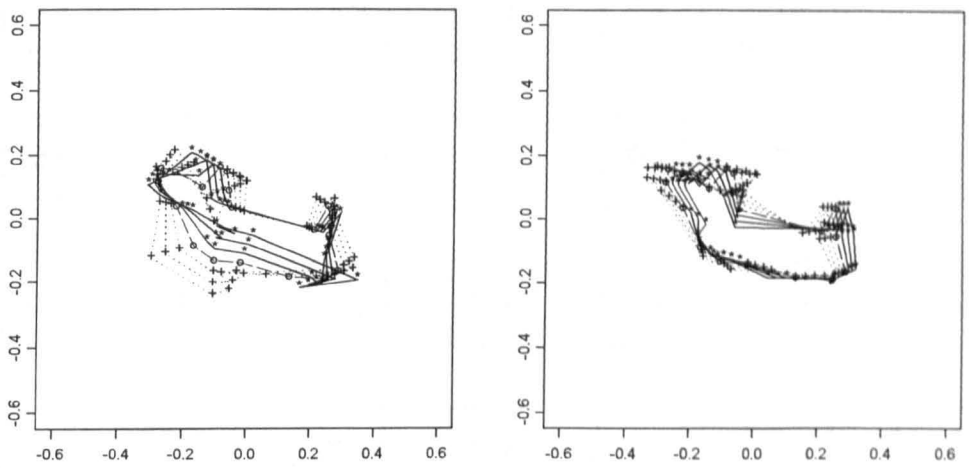

Figure 5.38b Mean shape and shapes at +1, +2, +3 s.d's and –1, -2, -3 s.d's along the 1st and 2nd PCs. Males. Age 9.

The final representation of principal components analysis of the females and males, aged 9 data in Figures 5.39 (a) and (b) depict a series of shapes evaluated along the first five principal components. Each row represents a principal component (the ith row represents the ith principal component) with configurations evaluated at –3, -2, -1, 0, 1, 2, 3 standard deviations along each principal component from the Procrustes mean. The central figure in each row is the full Procrustes mean shape. The shapes on either side of this mean show shapes at -3, -2, -1, and +1, +2, +3 standard deviations along that particular principal component.

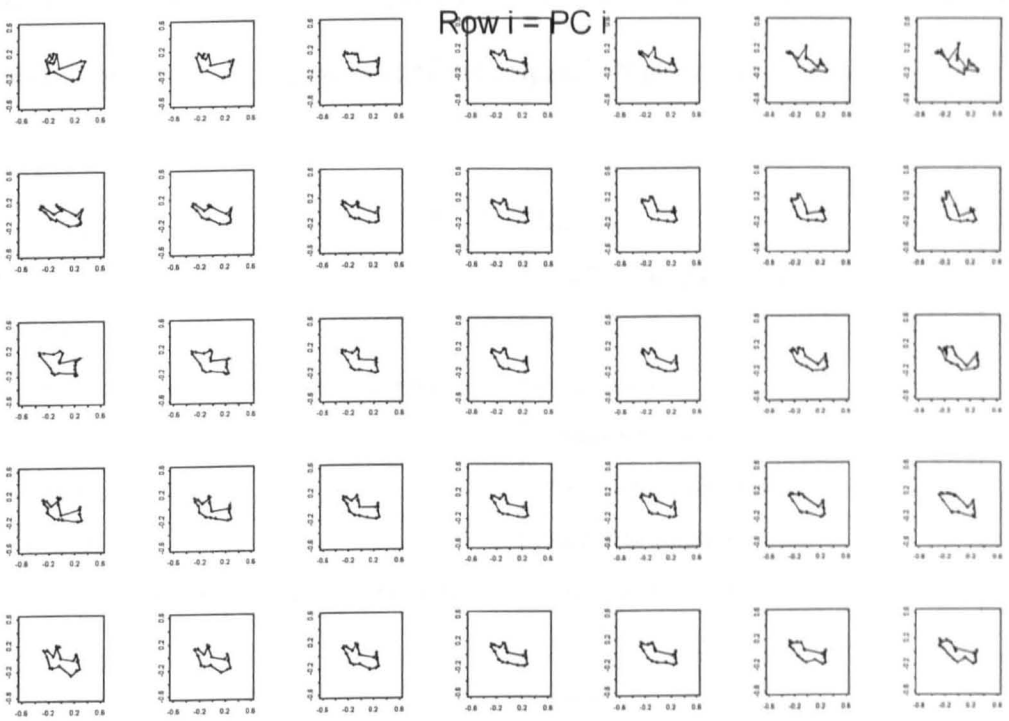

Figure 5.39a **Series of shapes evaluated along the first 5 PCs. Females. Age 9.**

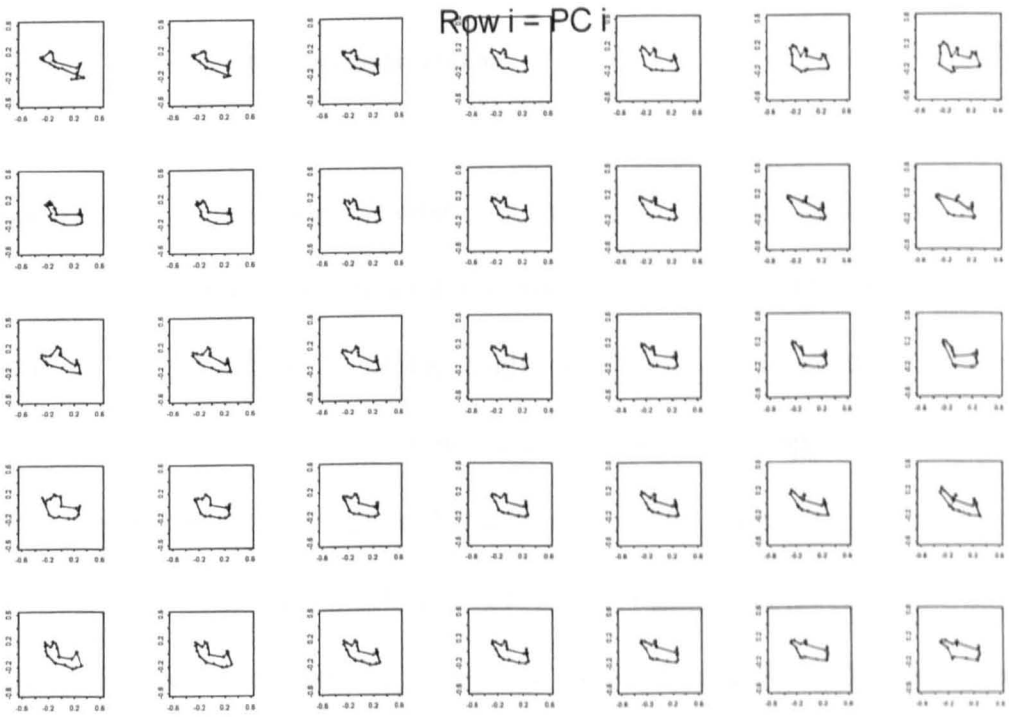

Figure 5.39b **Series of shapes evaluated along the first 5 PCs. Males. Age 9.**

To aid interpretation, Table 5.2 provides a reminder of the different areas of the mandible (considered in the context of the original 78 point system).

Points	Description
1-7	Anterior border of the ramus
7-13	Alveolus
13-23 (now includes new point 2 = old point 18)	Lower incisor
23-31	Anterior border of the mandible
35-45	Lower border of the mandible
45-49	Angle of the mandible
49-54 (now includes new point 1 = old point 51)	Posterior border of the ramus
54-62	Condyle
62-67	Mandibular notch
72-78	Coronoid process

Table 5.2 Areas of the mandibular outline.

From these plots similar overall patterns in males and females, aged 9 can be seen. The first principal component includes information about the relative size, or width of the body of the mandible, where the angle of the mandible increases / decreases depending on which direction you move from the mean shape. There is also a simultaneous movement in the overall length of the bone, capturing the variability in the anterior border of the mandible. The first principal component can also be interpreted as partly capturing the 'depth' of the condyle and mandibular notch, as well as capturing the amount that the lower incisor moves backwards / forwards. There appears to be less overall movement in the landmarks for the second principal component, where the second principal component tends to measure the angle of the anterior ramus and the overall 'sculpturing' of the condyle and mandibular notch.

These observations can be seen in all three representations. The third representation (Figures 5.39 (a) and (b)) includes principal components 3, 4 and 5 also. It can be seen here that the third principal component tends to measure the length of the posterior border of the ramus and the angle of the mandible (and hence, like principal component 1, captures the width of the body of the mandible). The fourth captures similar effects to principal component 2. Finally, the fifth principal component includes information about the movement and position of the alveolus, in a contrasting way to how the second principal component captures the variability in the anterior border of the ramus.

Fairly similar overall patterns of shape variability in each principal component were seen for the male and female groups at other ages.

Having investigated within sample variation attention is now returned to the comparison between male and female samples at each age. The full Procrustes superimposition of the female average shape and the male average shape (by GPA), for each age, is shown in Figures 5.40 (a) to (d). The female mean is depicted by x, and the male mean by +.

A two sample Hotelling's T^2 test could be used to formally test for average shape differences between the sexes. However as outlined previously, this test cannot be used here since there are not enough subjects in the female and male samples.

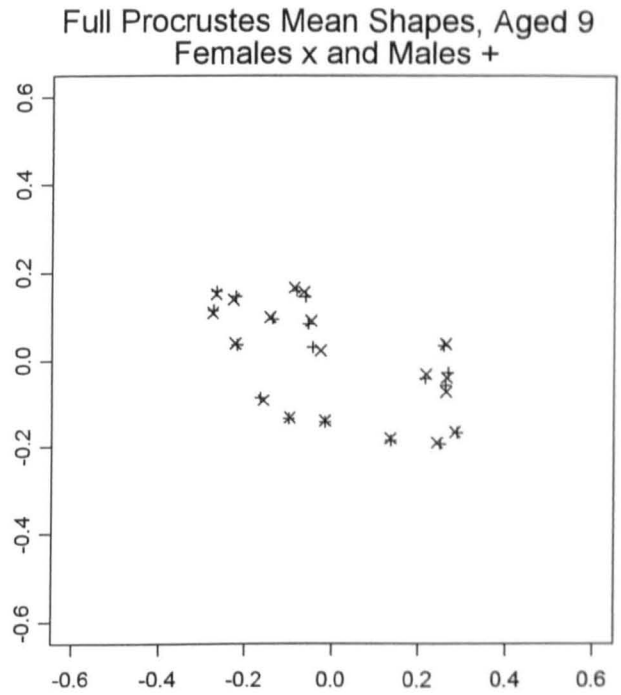

Figure 5.40a **Full Procrustes estimate of mean shape. Females x and Males +. Age 9.**

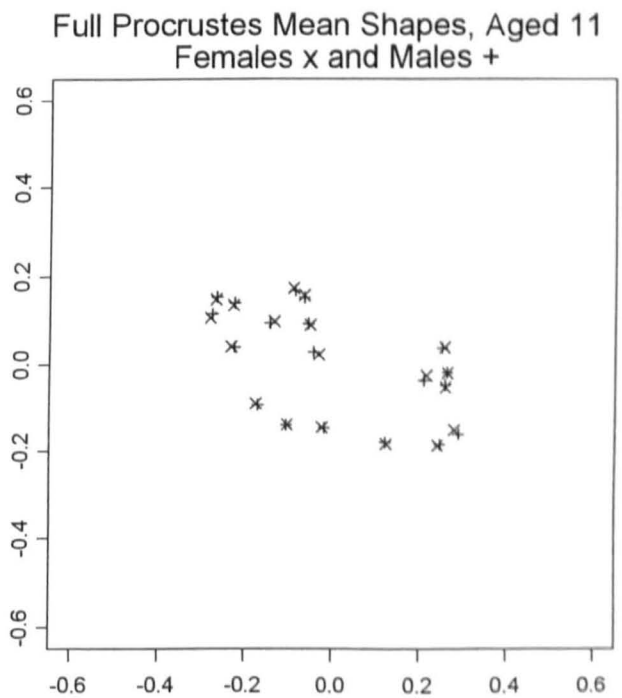

Figure 5.40b **Full Procrustes estimate of mean shape. Females x and Males +. Age 11.**

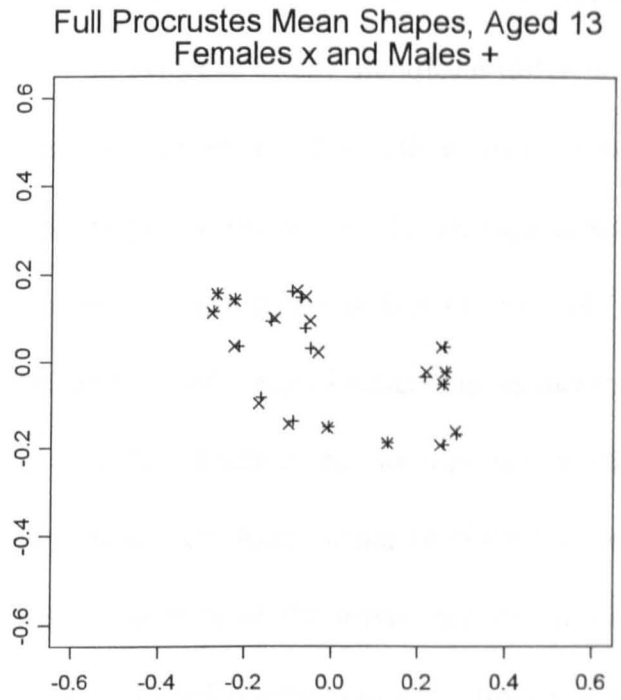

Figure 5.40c **Full Procrustes estimate of mean shape. Females x and Males +. Age 13.**

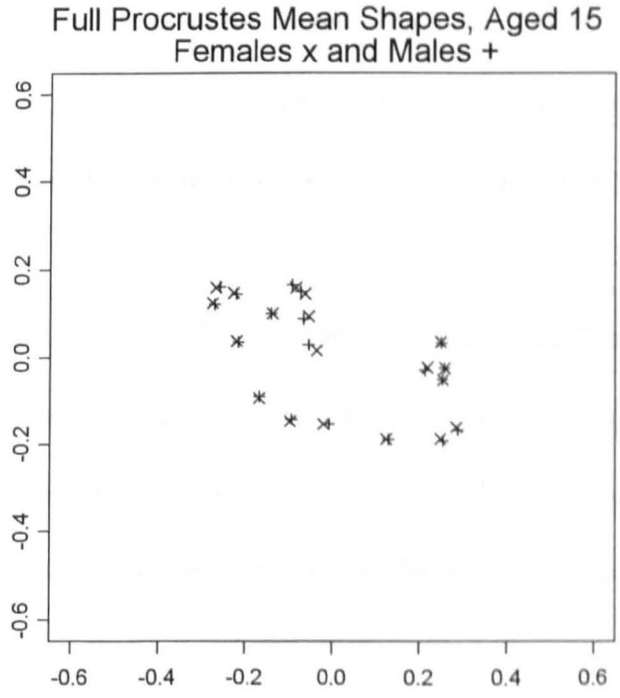

Figure 5.40d **Full Procrustes estimate of mean shape. Females x and Males +. Age 15.**

Subjectively however, from the plots of the full Procrustes estimate of mean shape it can be said that there is no evidence of any significant difference in shape between males and females, on average, at any age. The outlines are extremely close, at each of the 19 anatomical landmark points, for each of the four age groups. Further, the full Procrustes distance between the mean shapes is found to be 0.041 for age 9; 0.034 for age 11; 0.045 for age 13 and 0.039 for age 15 which implies that the mean outlines for females and males are very close together, for all ages. It is worthwhile to point out that very similar observations were found using Bookstein co-ordinates. Further, it was observed from subjective plots of the mean predicted mandibular outlines for males and females using predicted points from the elliptical Fourier function (and formal Hotelling's T^2 tests at each age) that there was unlikely to be a difference between the sexes, on average.

The male and female data can then, be pooled. This results in 18 subjects for age 9 (6 females and 12 males); 13 for age 11 (4 females and 9 males); 17 for age 13 (7 females and 10 males) and 13 subjects for age 115 (7 females and 14 males).

As for the separate male and females samples at each age, the Procrustes rotated data for the pooled samples at each age are calculated and displayed, as is the full Procrustes estimate of mean shape for the pooled samples, and the various representations of the principal components. Resulting plots are given in Figures 5.41 (a) to (e).

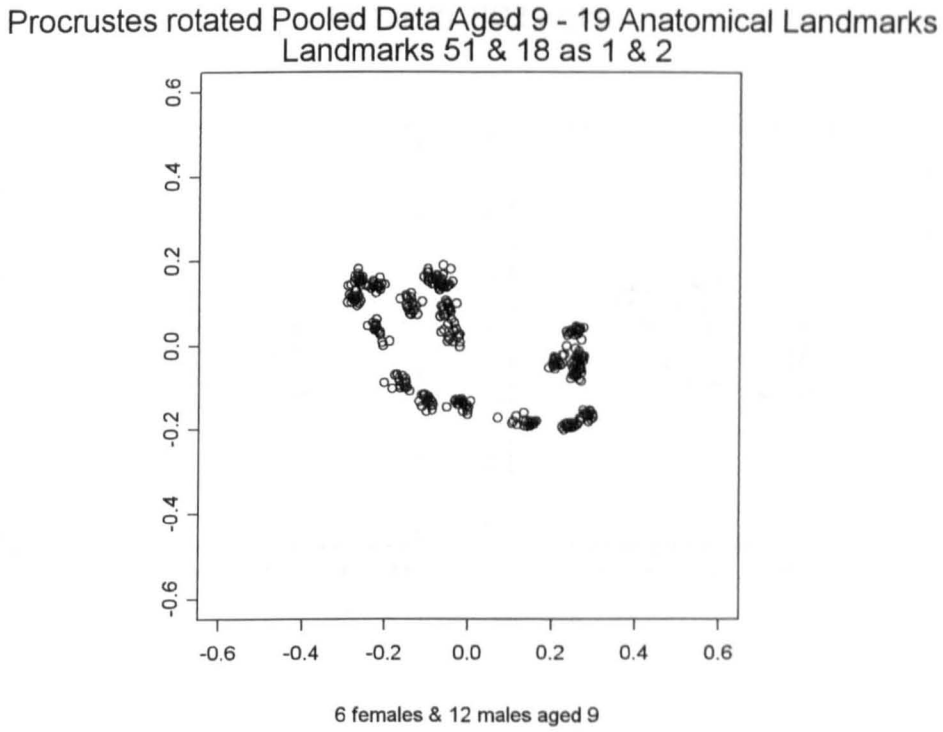

Figure 5.41a **Procrustes rotated outlines. Pooled sample. 6 Females and 12 Males. Age 9.**

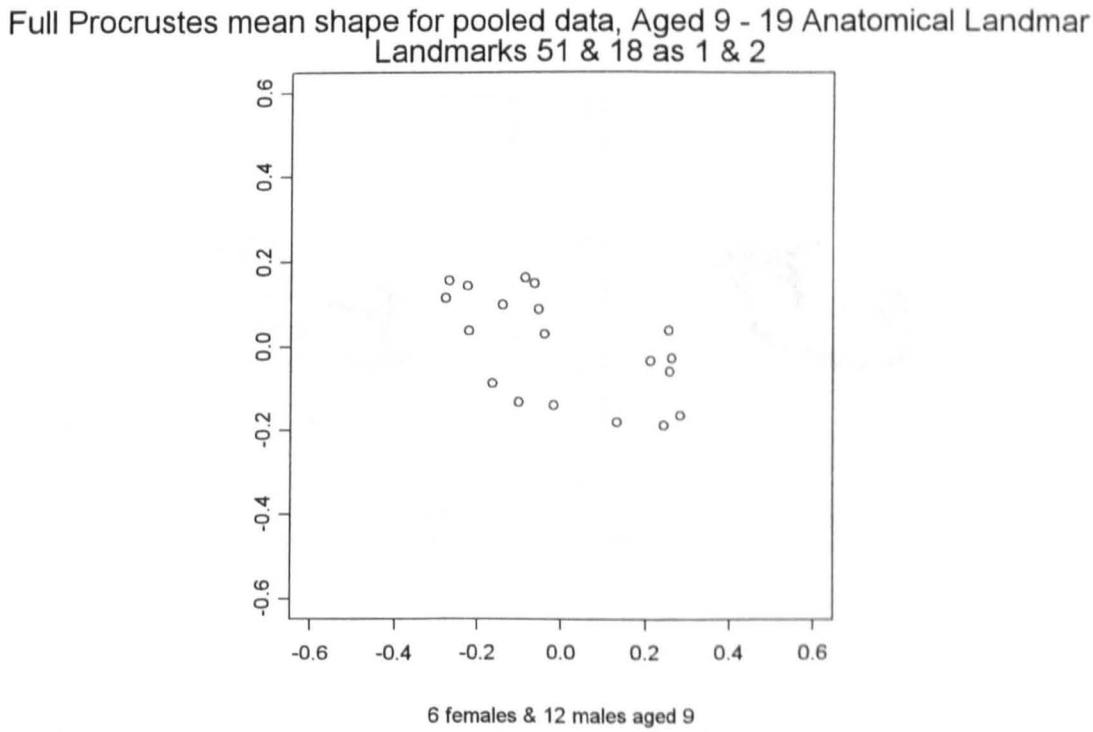

Figure 5.41b **Full Procrustes estimate of Mean Shape. Pooled sample. 6 Females and 12 Males. Age 9.**

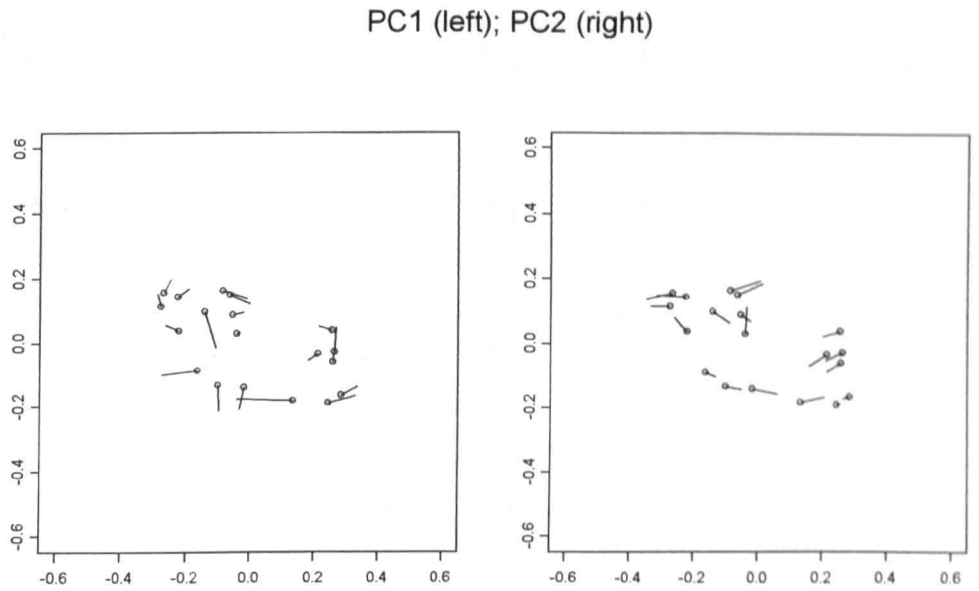

Figure 5.41c **Procrustes mean shape and vectors to +3 s.d's along the 1st and 2nd PCs. Pooled sample. 6 Females and 12 Males. Age 9.**

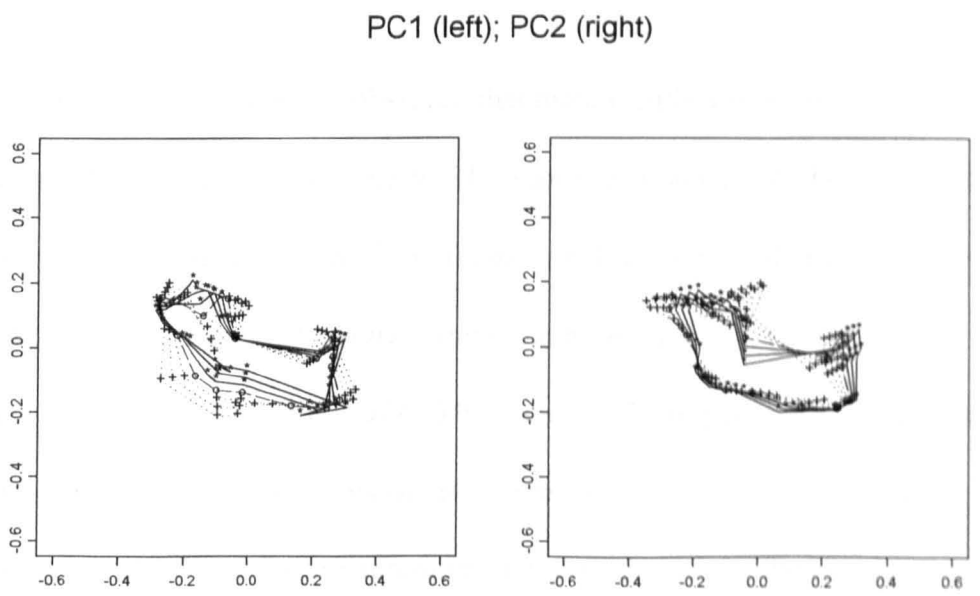

Figure 5.41d **Mean shape and shapes at +1, +2, +3 s.d's and –1, -2, -3 s.d's along the 1st and 2nd PCs. Pooled sample. 6 Females and 12 Males. Age 9.**

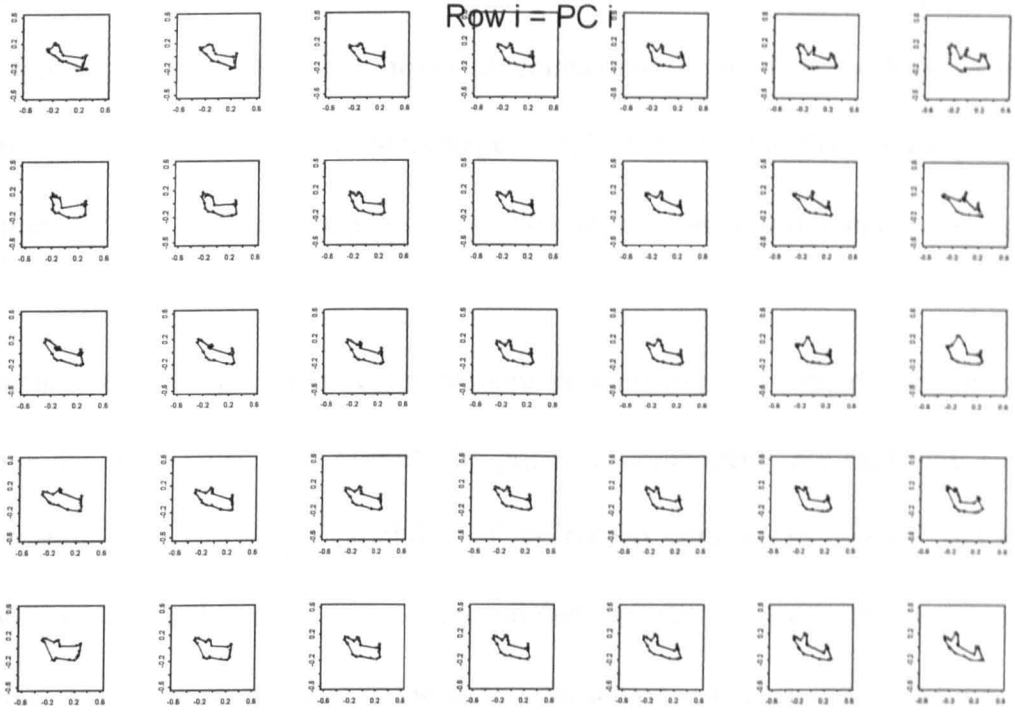

Figure 5.41e Series of shapes evaluated along the first 5 PCs. Pooled sample. 6 Females and 12 Males. Age 9.

From Figure 5.41 (a), it is again observed that there is little variability in shape within all the mandibular outlines for age 9. The root mean square of the full Procrustes distance to the estimated mean shape (shown in Figure 5.41 (b)) is 0.073 for this particular pooled sample that suggests small variation in shape. Corresponding values for ages 11, 13 and 15 were 0.072, 0.071 and 0.073 respectively, which likewise indicate that there is little variation in shape (as do plots for these ages). It is interesting to note that these are approximately the same as for the separate male and female samples in this data sample that is comforting when the data has been pooled. Principal components analysis of the Procrustes residuals is again considered to examine the structure of shape variability within the pooled samples. For age 9, the percentage of variability explained by the first three principal components are 25%, 18%, and 12%. Corresponding values are 30%, 24% and 12%; 23%, 20% and 14%

and 23%, 19% and 14% for ages 11, 13 and 15 respectively. As for the separate male and female samples, the first principal component is moderately high, but not extremely high. Overall, the percentages explained by the first three principal components are a bit lower than observed in the separate male and female samples.

From the different illustrative representations of some of the principal components, it is once again observed that, overall, the principal components are capturing similar information about the shape variability of the pooled samples. In essence, the shape variability within the male, female and pooled samples seems to be very similar, although not necessarily capturing the same information at in each individual principal component. Further, it would seem that more principal components are required to explain the totality of the variability in the pooled samples for each age. It is observed however, that again the first principal component includes information about the relative size, or width of the body of the mandible with a simultaneous movement in the overall length of the bone and a measure of the 'depth' of the condyle and mandibular notch. To a certain extent, it also appears to capture some information on the backwards / forwards position of the lower incisor. The second principal component again tends to measure the angle of the anterior ramus and the overall sculpturing of the condyle and mandibular notch. However, from Figure 5.41 (e), we can see that the third principal component for the pooled sample tends to be capturing information, similar to the second principal component. Information about the length of the anterior border of the ramus, and therefore it includes the effect of the localised sculpting of the coronoid process. The fourth principal component includes the measurement of the length of the posterior border of the ramus and in turn measures how convex the angle of the mandible is (and hence, like principal component 1,

captures the width of the body of the mandible). Finally, for the pooled data sample, aged 9, the fifth principal components captures information about the movement and position of the alveolus, and hence the relative movement and position of the lower incisor, much like the same principal component for the separate male and female samples.

Again, fairly similar overall observations were made for the pooled samples for the other ages 11, 13 and 15.

Plots of the full Procrustes mean shapes for the pooled data can also be produced for all ages on the same graph to determine whether or not there might be a difference in shape over the range of ages. Age 9 is depicted by a circle, age 11 by an *, age 13 by + and age 15 by x.

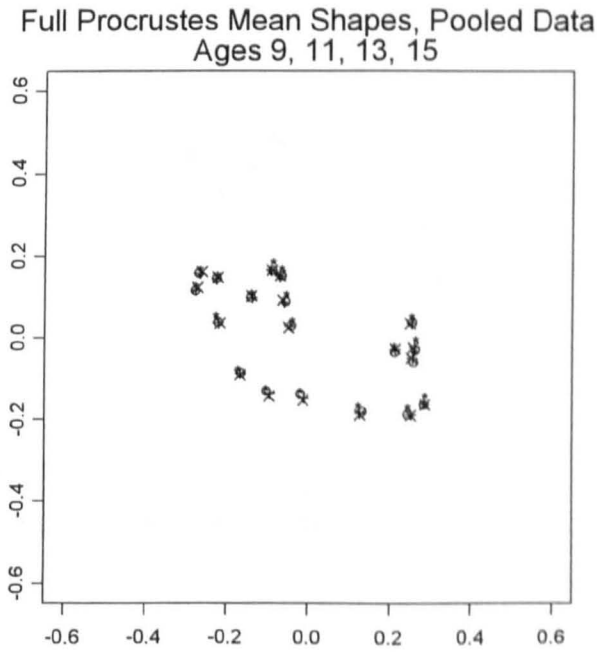

Figure 5.42 Full Procrustes estimate of mean shape. Changes in shape from ages 9, 11, 13 and 15.

From Figure 5.42 it would seem that there are small differences through ages 9 to 15. Changes in shape are evident e.g. along the lower border of mandible age 15 is lowest. These changes are small however.

Formal Hotelling's T^2 test for those age groups that can be tested, ages 9 and 15 and 13 and 15 provide no evidence of a significant difference in mean shape between ages 9 and 15 ($p=0.29$) or between ages 13 and 15 ($p=0.61$). Plots for these age groups are shown in Figures 5.43 (a) and (b) from which it can be seen that each of the anatomical landmarks for the two ages being compared are extremely close, around all areas of the mandibular outline.

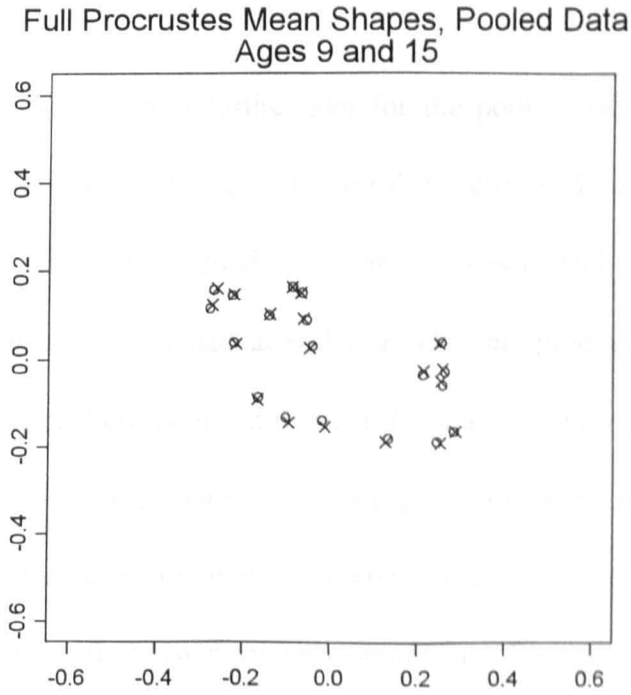

Figure 5.43a **Full Procrustes estimate of mean shape. Changes in shape from age 9 to 15.**

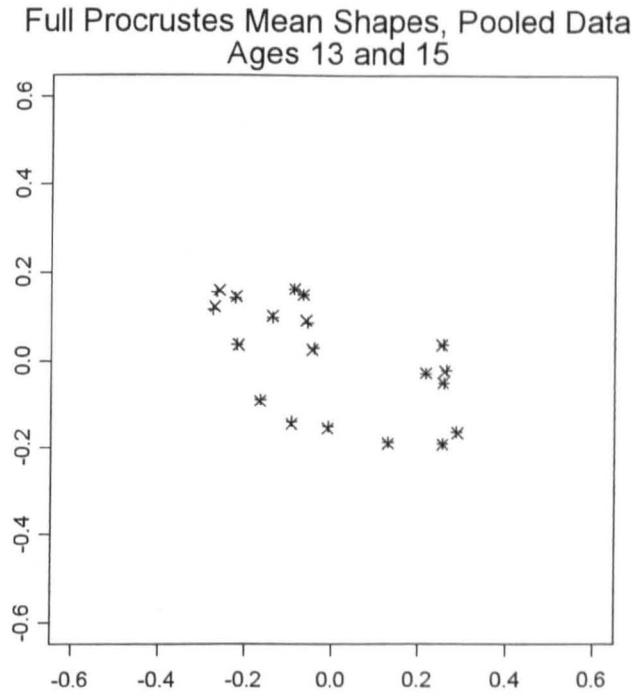

Figure 5.43b Full Procrustes estimate of mean shape. Changes in shape from age 13 to 15.

Figures 5.44 (a) to (d) display a further plot for the pooled data. These pair wise scatter plots display the centroid sizes (S), the full Procrustes distances to the pooled mean (rho) and the first five principal component scores (which attempt to capture shape) for the mandibular outline data at each age. They are produced in an attempt to examine whether or not there is any difference between the two groups, males and females, in terms of size and shape. The principal component scores here simply represent the scores for each principal component, in the direction of any observed groups difference. Of the first few principal components, for each age, none of them have high scores.

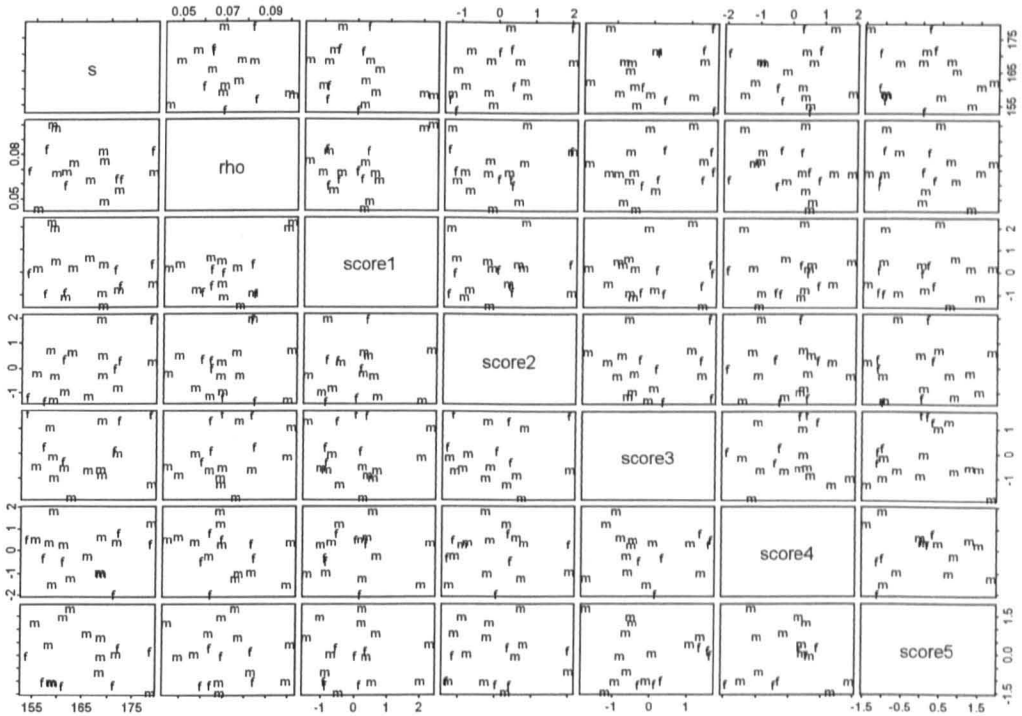

Figure 5.44a Pair wise plots of the centroid sizes, Riemannian distances to the mean and pooled PC scores. Pooled sample. 6 Females and 12 Males. Age 9.

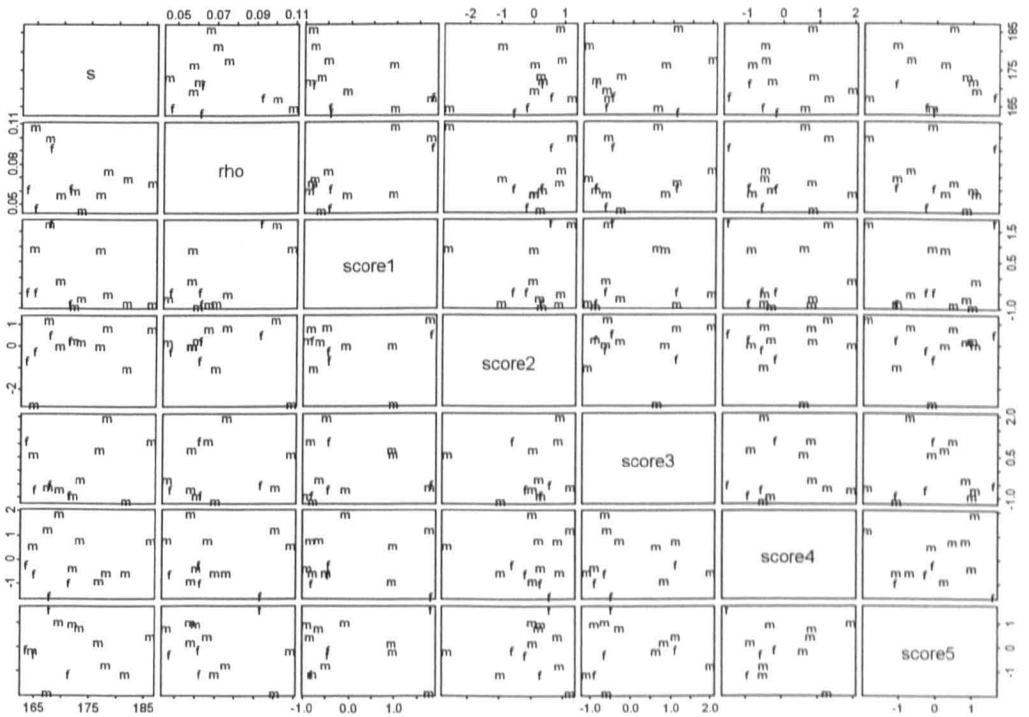

Figure 5.44b Pair wise plots of the centroid sizes, Riemannian distances to the mean and pooled PC scores. Pooled sample. 4 Females and 9 Males. Age 11.

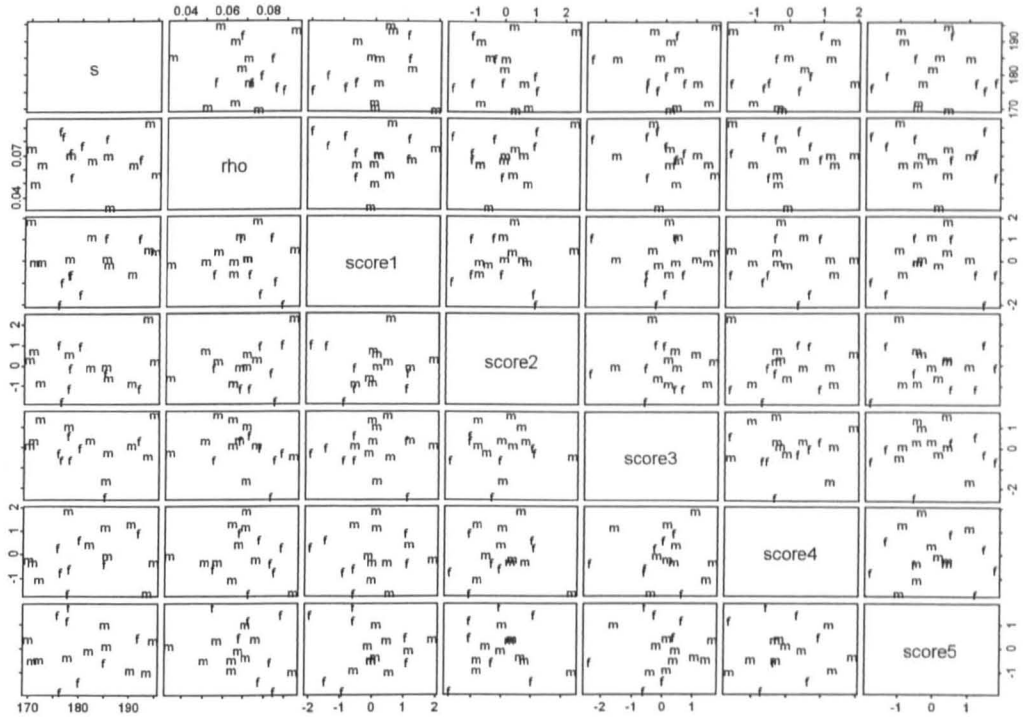

Figure 5.44c Pair wise plots of the centroid sizes, Riemannian distances to the mean and pooled PC scores. Pooled sample. 7 Females and 10 Males. Age 13.

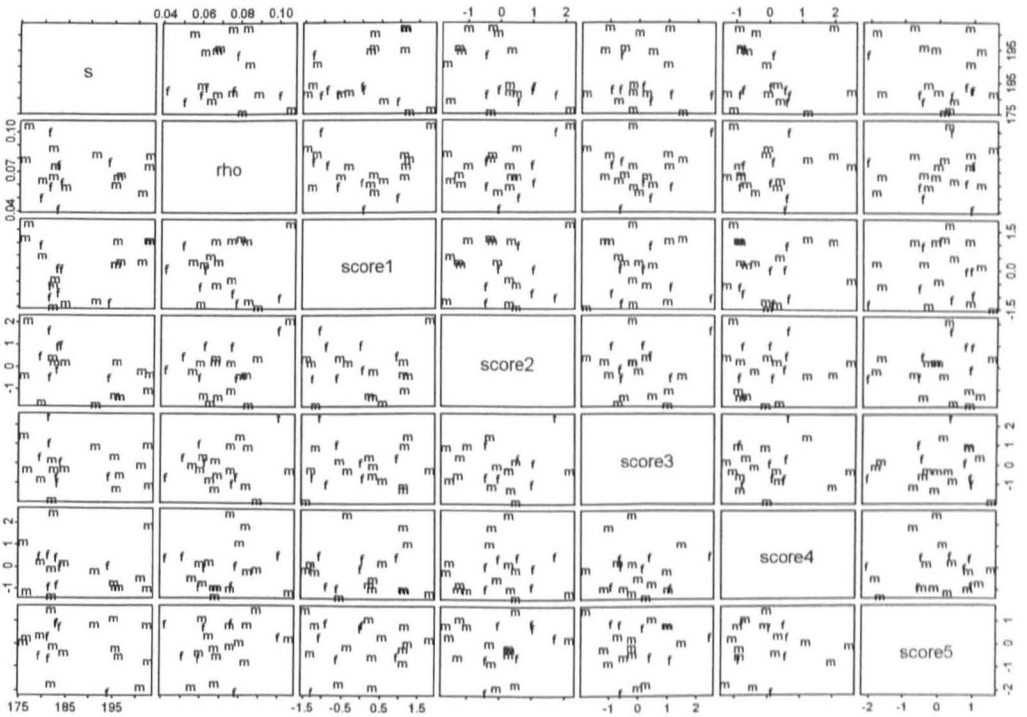

Figure 5.44d Pair wise plots of the centroid sizes, Riemannian distances to the mean and pooled PC scores. Pooled sample. 7 Females and 14 Males. Age 15.

From Figures 5.44 (a) to (d), none of the principal component scores separate males and females well. In addition, it can be seen that the groups do not differ in size, defined by centroid size, since again there is no clear separation of centroid size for males and females. Also, there is also no clear separation in the distances from the male and female configurations to the pooled mean shape.

Further, there does not seem to be any correlation between the principal component scores and centroid size and / or distance to the pooled mean shape. If for example the first principal component measured a certain (shape) attribute and it was correlated to size, this may have a biologically reasonable explanation. For instance, it might be possible for the shape attribute that the principal component was capturing to be directly related to the overall size of the mandible. The overall length of the lower border of the mandible might be captured by the first principal component that might be directly related to the overall size of the mandible perhaps.

Pair wise plots for the pooled data for the other ages, 9, 11 and 13 were similar in that there was no clear separation between males and females in terms of centroid size, distance to the pooled mean estimate of shape, or in the first few principal component scores. Also, there did not appear to be any correlation between the principal component scores and centroid size and / or distance to the pooled mean shape.

These plots corroborate the previous subjective impression in that there is no clear evidence of a difference between males and females, at each age. And also that there is no clear relationship between size and shape for the pooled samples of data, at each age.

The relationship between size and shape can also be examined using Procrustes analysis. Similar to Bookstein co-ordinates analysis, pair wise scatter plots can be displayed for appropriate size and shape variables. The centroid size (S) is once again the size variable for this analysis and the (x,y) co-ordinates of outlines for the full Procrustes tangent co-ordinates (referred to as icon co-ordinates) represent the shape variables. We illustrate in Figure 5.45 the icons for full Procrustes tangent co-ordinates (shape variables) for the 14 males, aged 15.

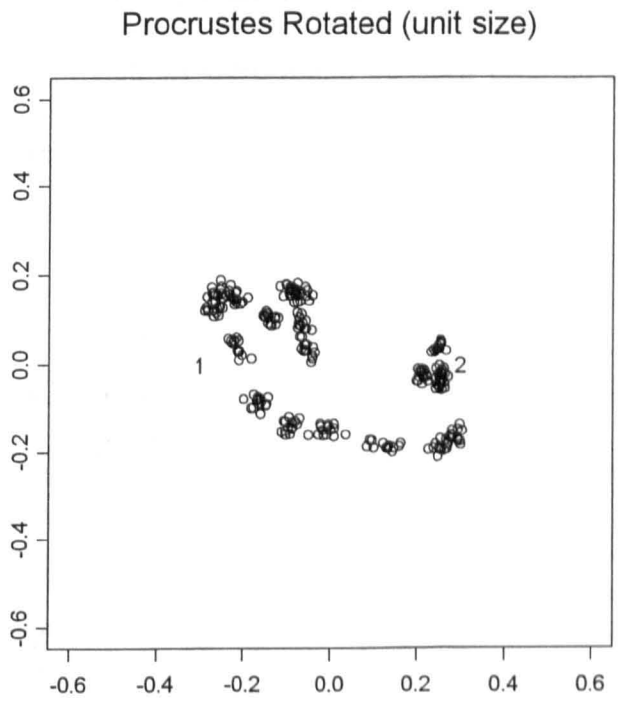

Figure 5.45 Icons for full Procrustes tangent co-ordinates. 14 Males, Age 15.

Each of the 14 mandibular outlines in the sample (configurations) is centred (on the centroid, at (0,0)), is of unit centroid size and is rotated to be as close as possible to the full Procrustes estimate of mean shape. There is clearly some variability in the landmark points. This variability tends to be circular or elliptical in nature.

Pair wise plots of the icon co-ordinates and centroid size are given in Figure 5.46 (a) to (e).

These plots show some fairly strong correlations, mainly between some of the icon co-ordinates, e.g. x_3 and x_4, y_3 and y_4, x_5 and x_6, x_7, y_6 and y_7 etc. Centroid size does not seem to be strongly correlated with any of the shape co-ordinates. This was the case for females, aged 15, as well as both males and females at all other ages, and also for the pooled data samples. Similar to that found in the Bookstein analysis, there were some weak correlations that might suggest size and shape are related in some small way. No very strong correlations were found between centroid size and any of the shape variables however.

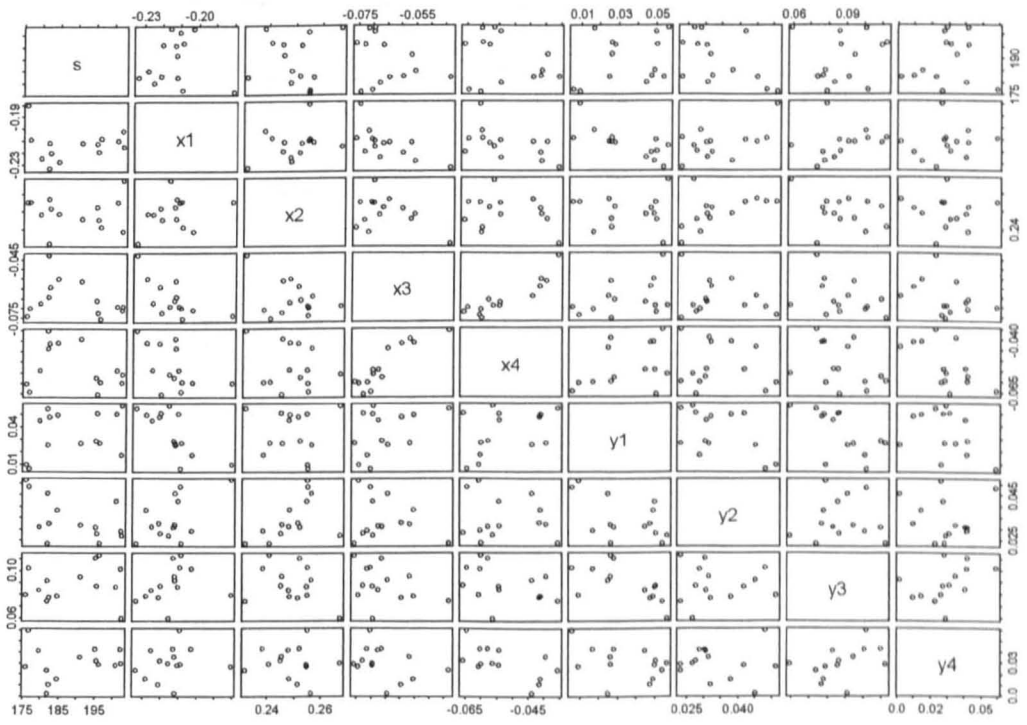

Figure 5.46a Pair wise scatter plots for centroid size (S) and the (x_1,x_2,x_3,x_4, y_1,y_2,y_3,y_4) co-ordinates of outlines for the full Procrustes tangent co-ordinates. 14 Males. Age 15.

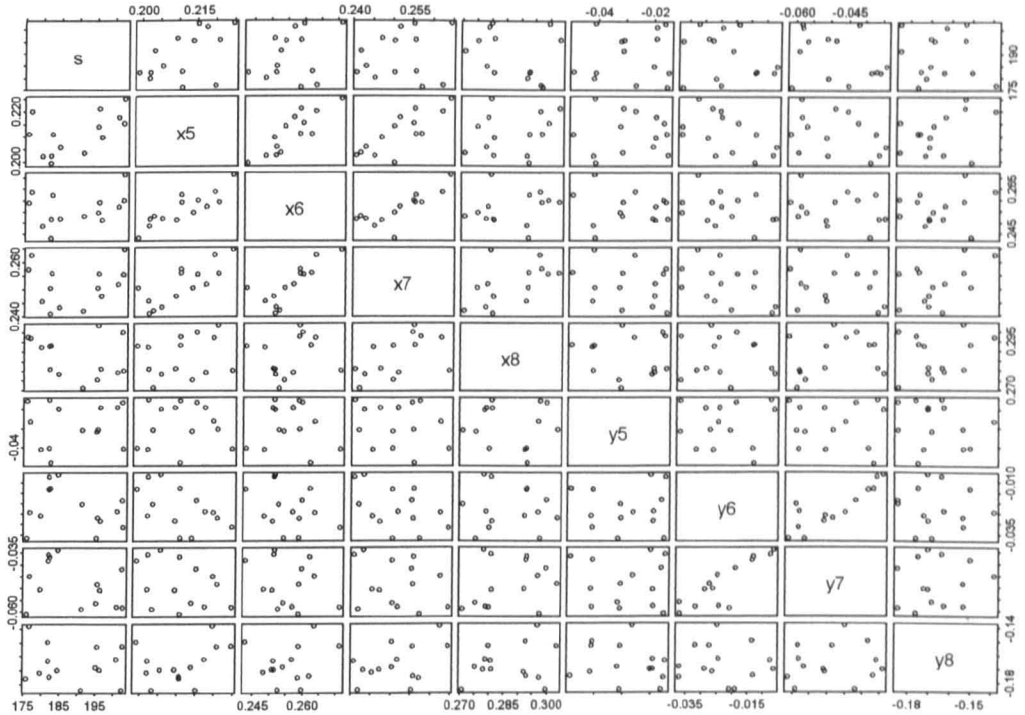

Figure 5.46b Pair wise scatter plots for centroid size (S) and the (x_5,x_6,x_7,x_8, y_5,y_6,y_7,y_8) co-ordinates of outlines for the full Procrustes tangent co-ordinates. 14 Males. Age 15.

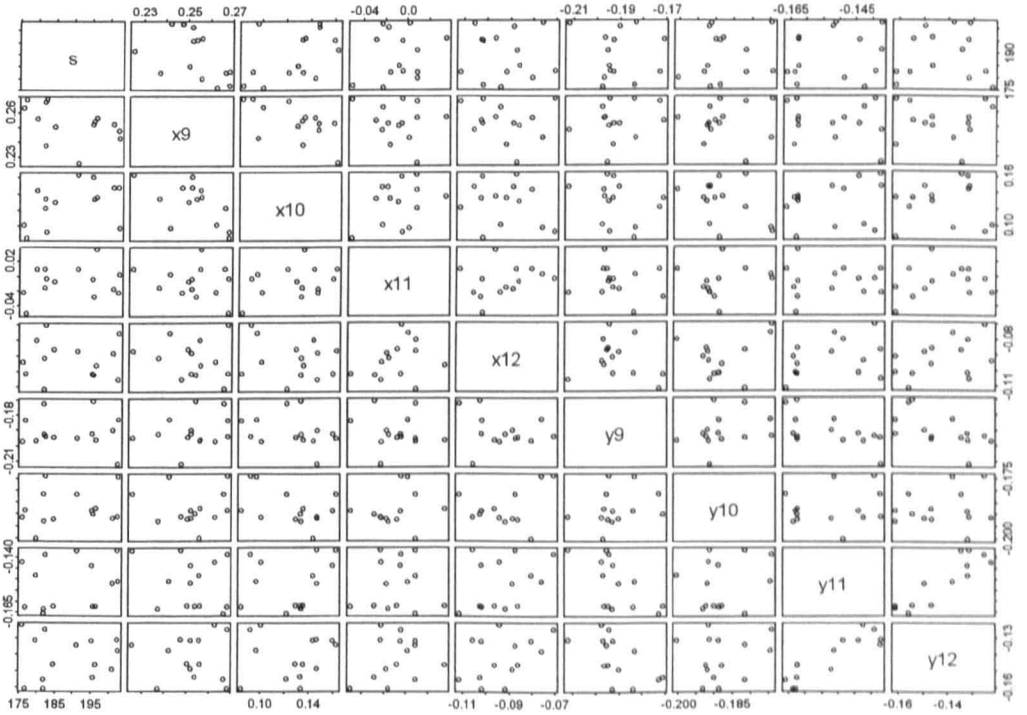

Figure 5.46c Pair wise scatter plots for centroid size (S) and the (x_9,x_{10},x_{11},x_{12}, y_9,y_{10},y_{11},y_{12}) co-ordinates of outlines for the full Procrustes tangent co-ordinates. 14 Males. Age 15.

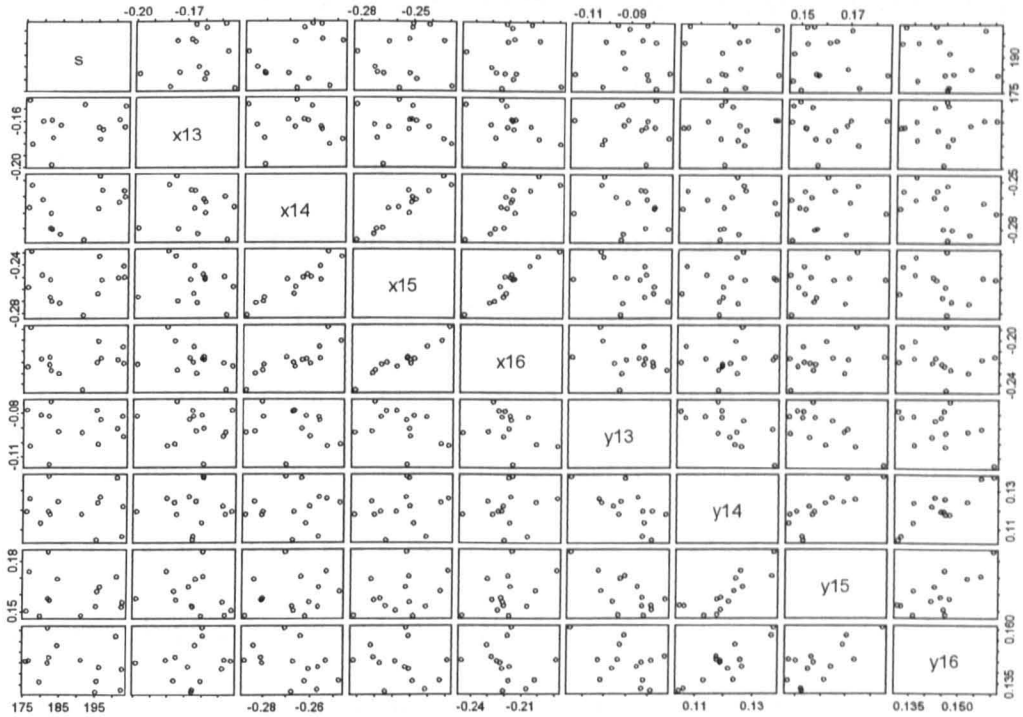

Figure 5.46d **Pair wise scatter plots for centroid size (S) and the (x_{13},x_{14},x_{15},x_{16}, y_{13},y_{14},y_{15},y_{16}) co-ordinates of outlines for the full Procrustes tangent co-ordinates. 14 Males. Age 15.**

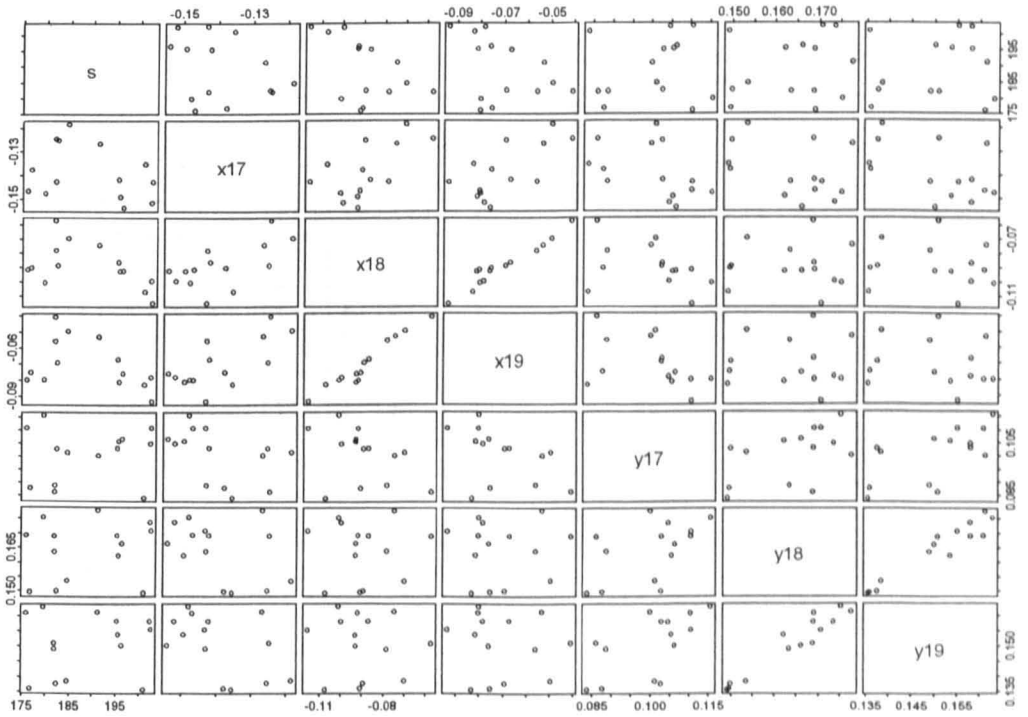

Figure 5.46e **Pair wise scatter plots for centroid size (S) and the (x_{17},x_{18},x_{18}, y_{17},y_{18},y_{19}) co-ordinates of outlines for the full Procrustes tangent co-ordinates. 14 Males. Age 15.**

Finally, the method of thin plate splines (TPS) introduced briefly in Chapter 1 is used here to illustrate shape change from one group to another. Basically, a regular square grid is drawn over the first configuration (in this case the full Procrustes mean shape for the females) and at each point where two lines on the grid meet, the corresponding position in the second figure is calculated using a pair of thin-plate splines transformation. The junction points are joined with lines in the same order as in the first figure, to give a deformed grid over the second figure. For the mandibular data, in Figures 5.47 (a) to (d) we see a thin-plate spline transformation grid between the female mean shape estimate and the male mean shape estimate, for each age. The square grid is placed on the estimated female mean shape and the curved grid is pictured on the estimated male mean shape.

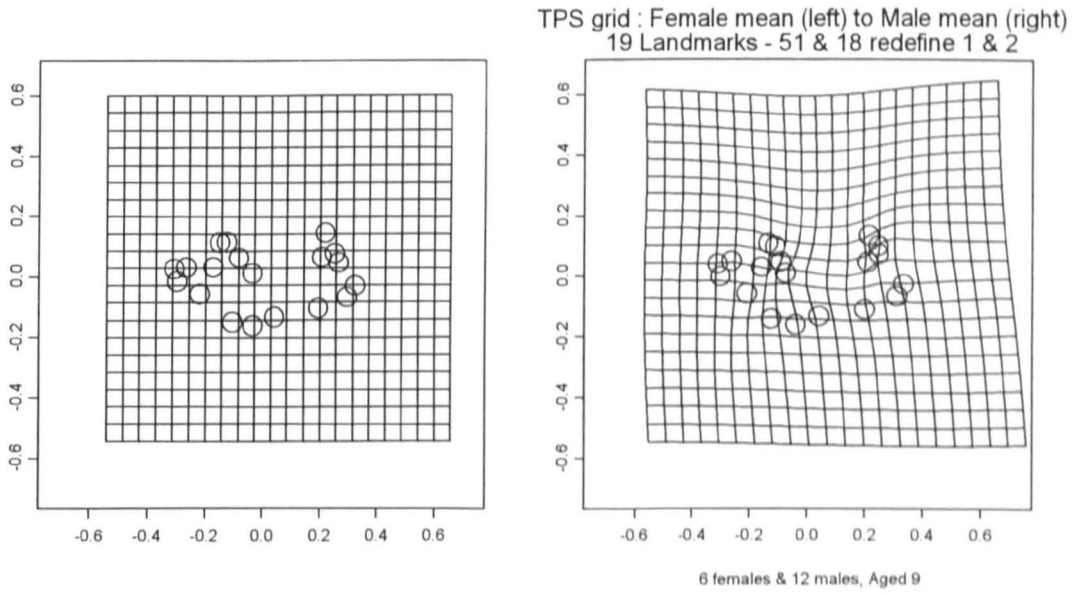

Figure 5.47a TPS Grid. Female mean to Male mean. Age 9.

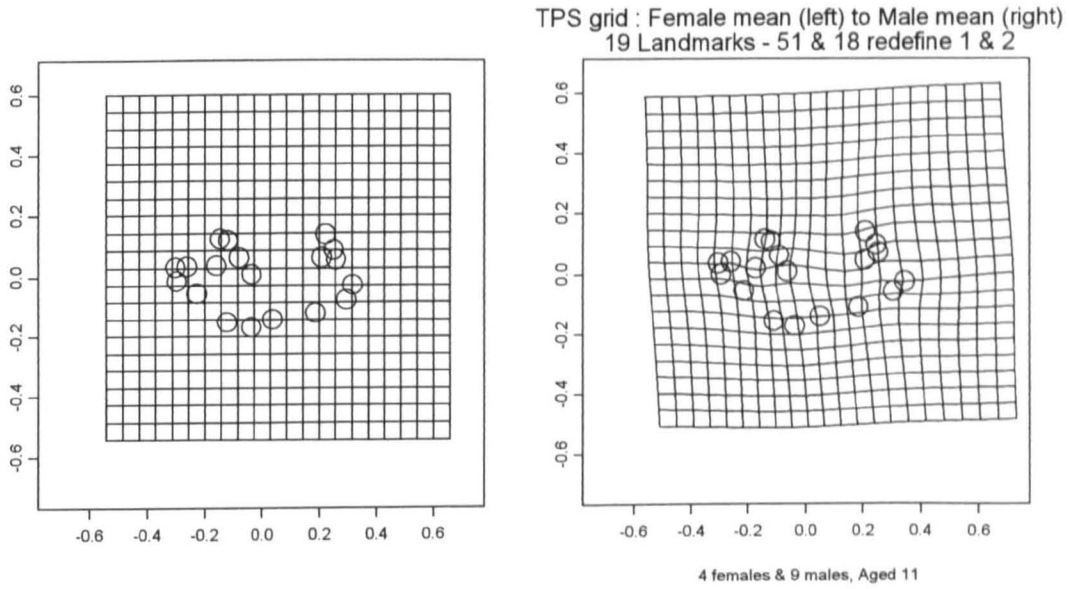

Figure 5.47b TPS Grid. Female mean to Male mean. Age11.

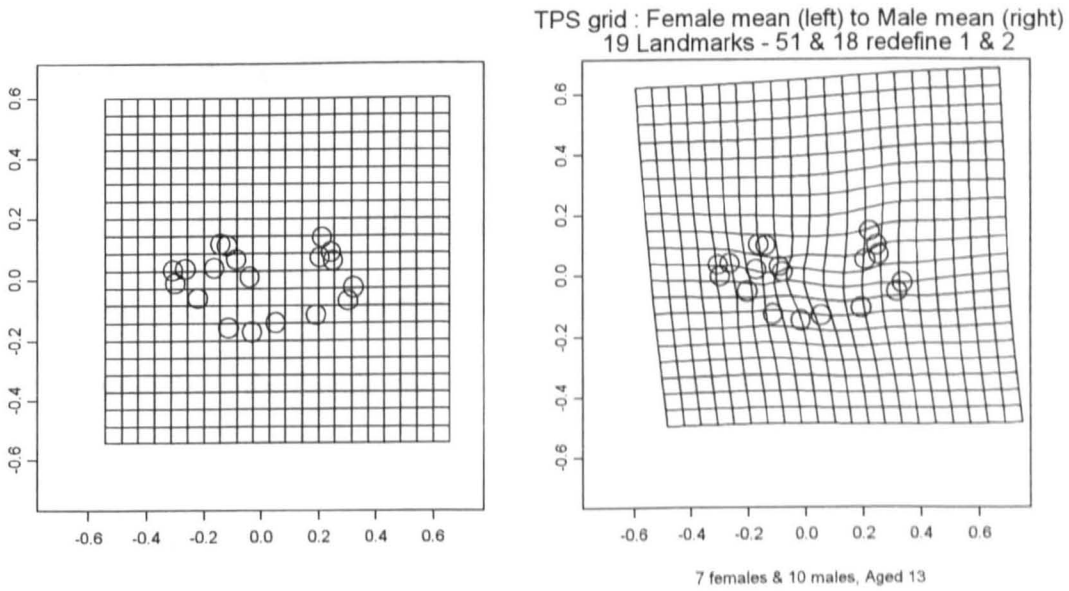

Figure 5.47c TPS Grid. Female mean to Male mean. Age13.

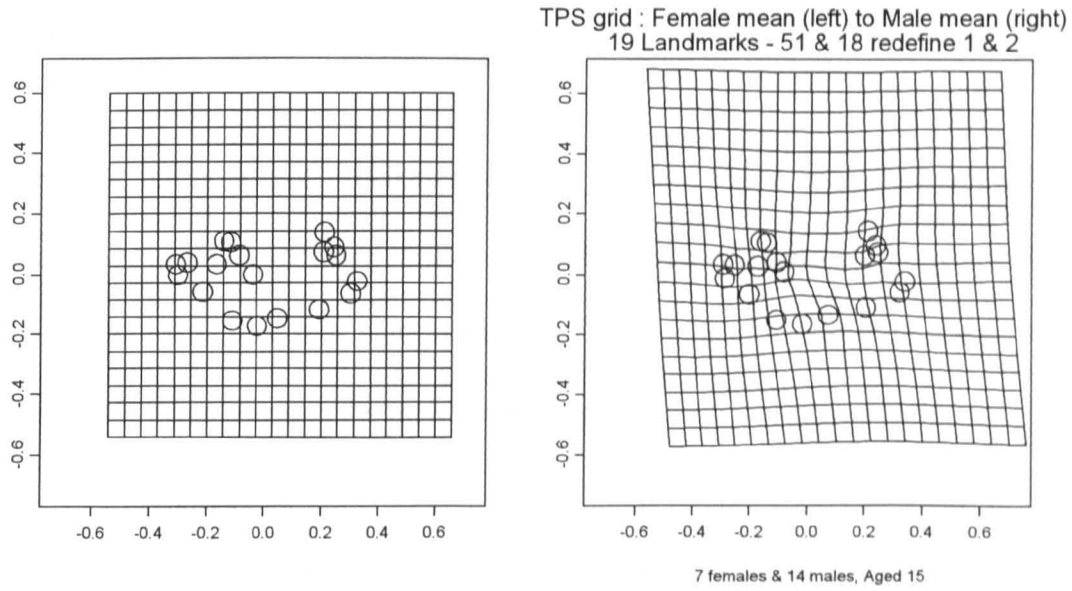

Figure 5.47d TPS Grid. Female mean to Male mean. Age15.

It is fairly clear that there is evidence of a small shape change between females and males – evident in the condylar, mandibular notch, coronoid process areas of the bone, and the alveolous and the tip of the mandible, fairly similar for each age. This could be interpreted as disagreeing with previous observations and a decision to pool the data but again, these changes are seen to be extremely small with slight deformations of the TPS grids from the female outline to the male outline, for each age.

A pair of thin-plate splines could also be used to deform a square grid from age stages 9 to 11, grid from age stages 9 to 13 and from age stages 9 to 15. A series of deformed grids like this would be useful in examining the changes over time. This was not done here however.

5.6 Conclusion

In this chapter the notion of Procrustes analysis within a shape analysis framework, as well as the very useful descriptive method of Bookstein co-ordinates has been introduced. In addition, the method of thin plate splines has been utilised to illustrate shape change from the female mean shape to the male mean shape.

It has been demonstrated that these methods provide a useful insight into the description of size and shape of a sample of objects. In particular these methods have been used to describe the size and shape, and shape variability of the mandibular data for males and females between the ages of 9 to 15.

Similar observations were made using both Procrustes and analysis Bookstein co-ordinates. From the raw data, it seems likely that there are some slight differences in overall size and shape within samples, for both males and females, for all ages. In terms of shape differences, again it seems likely that there are some extremely small differences within samples, for both males and females, for all ages. Differences in shape were not evident between males and females, at any age. It would seem that there are small differences in shape between ages 9 to 15. These changes are very small and for the ages that could be tested, were not statistically significant.

There did not appear to be any association between the size and shape of the mandibular outlines in either the male or female samples, for all ages, or when the samples were combined at each age.

Further, investigating shape variability using Procrustes methods by way of principal components analysis, it was found that the first principal component tended to explain a moderate amount of the totality of shape variability in male and female samples, as well as a combined sample, for all ages (where values were found to be lower overall in the combined samples). There is obviously a lot going on and some of the principal components appear to be capturing the same components of variability. In general, the first principal component tends to include information about the relative size of the bone, in terms of height, width and overall length. The first principal component can also be interpreted as partly capturing the depth of the condyle and mandibular notch, as well as capturing the amount that the lower incisor moves backwards / forwards. There appears to be less overall movement in the landmarks for the second principal component, where this tends to measure the angle of the anterior ramus and the overall sculpturing of the condyle, mandibular notch and coronoid process. The third principal component tends to measure the length of the posterior border of the ramus and the angle of the mandible (and hence, like principal component 1, captures the width of the body of the mandible) whilst the fourth captures similar effects to principal component 2. Finally, the fifth principal component includes information about the movement and position of the

alveolus, in a contrasting way to how the second principal component captures the variability in the anterior border of the ramus. Broadly similar results are found for males and females, as well as combined samples, and different age groups.

Chapter 6

Discussion

There is a general need for mathematical and statistical descriptions of complex irregular forms. In this thesis, this requirement has been addressed in the context of one particular problem in dentistry. The methods currently available to researchers to meet this need have been reviewed and two appropriate methods have been utilised in an attempt to describe size and shape changes in the human mandible from 9 to 15 years for a particular sample of data.

The elliptical Fourier function (EFF), a boundary outline, or landmark-independent method, has been contrasted with Procrustes analysis, a homologous point, or landmark-dependent method. Both have desirable aspects, but both also have, to some extent, associated theoretical and practical problems. The similarities and differences, advantages and disadvantages of these two methods will now be discussed.

The same amount of work was involved in preparing the sample of data for analysis by either method. The implementation of each of the methods was straightforward using the suite of programs designed for the EFF method and a series of Splus functions for the Procrustes analysis (compiled by Ian L Dryden, University of Leeds).

Both methods have been seen to be very useful in a visually descriptive sense.

Further, it has been established that both methods allow 'form' to be partitioned into independent size and shape components, following which it is possible to make uncorrelated assessments of the components of size and shape.

In the particular context discussed in this thesis, the following conclusions were reached about mandibular growth using the EFF.

Overall, it was observed that the mandible was indeed 'growing' i.e. changing in size and shape, between 9 and 15 years old. Males and females in the sample tended, on average, to display similar patterns of overall growth. On average, the bones tended to be increasing in overall length, height and width over the range of ages. It was also observed that the female growth spurt was more noticeable than the male growth spurt in this sample of data.

Concentrating on shape change only, it was observed that small changes were apparent in a few areas around the mandibular outline. Shape changes were observed in particular in the anterior border of the ramus, the alveolus and the lower incisor. There also appeared to be slight shape changes in the area of the coronoid process. A slight increase in concavity in the anterior border of the ramus and a slight decrease in concavity in the alveolus was also observed over the range of ages. In addition, the lower incisor seemed to move posteriorly and become more upright over time. Further, the mandibular notch appeared to shallow and the coronoid process moved in a posterior direction. The observed shape changes were all very small however and

probably not statistically significant, although this was not tested formally due to the small sample sizes. Broadly similar patterns were again found in males and females in respect of shape change only.

Comparison between average predicted outlines for males and females found no significant difference between the sexes as regards overall size and shape and shape only changes between ages 9 to 15.

In addition, from the error study analyses carried out using centroid-to-predicted outline distances calculated by the EFF, it was found that the repeatability of tracings done by the same observer was satisfactory. Tracings carried out by different observers were not in close enough 'agreement' however, to allow the two studies to be combined together.

It is important to realise that in theoretical terms EFF is fundamentally a mathematical approach, in contrast to Procrustes analysis that is fundamentally a statistical technique. They have different objectives in that EFF aims to obtain a mathematical description of an individual object (or form), whereas Procrustes analysis aims to obtain a statistical model for the natural variation across a group of forms. So, in EFF, harmonics are added sequentially in order to improve the fit of the mathematical description of the particular object currently under consideration. In Procrustes' contrasting approach principal components are added sequentially in order to explain more and more of the variation among objects.

EFF provides a very effective mathematical description of an individual form. In fact, an excellent fit may be achieved using only the first 15 to 20 of the 39 possible harmonics. The raw material for statistical analysis is provided as a secondary consequence of the fitting process of EFF. However, EFF is not the most obvious or efficient approach to this task. Naively, one might expect to be able to use the mathematical descriptors (harmonic information) obtained from each of a group of objects for statistical purposes, but this is not the case. A simple example of the difficulties faced is the fact that the Fourier coefficients determined by EFF are not invariant to rotation of the form. This means that comparisons of individual harmonics among shapes will not necessarily provide readily interpretable comparisons. Aside from this, the fact that the Fourier coefficients are highly non-linear functions of the form indicates that making inferences back from sample summaries of these coefficients to population parameters in terms of the original geometry is very difficult.

This means that, starting with EFF, statistical analysis must be conducted on the predicted points. Since the mathematical description available from EFF is almost an exact representation of the object, use of the fitted points is effectively equivalent to using the observed points, once the forms have all been registered at their centroid and each dimension scaled to a value consistent with an overall unit area for each form. There are simpler methods available for registering and area-standardising forms, so from a statistical point of view it is hard to see a use for EFF.

In summary then, EFF is a useful method for describing individual forms, but it is not obviously successful as a basis for statistical analysis.

By contrast, Procrustes analysis is inherently a statistical model-building technique. It models the data inherent in a complex biological form in a straightforward linear manner. With Procrustes, we can register each form using the similarity transformations of location, rotation and scaling and work on the fitted form by means of a linear model. Estimates of mean shapes can be calculated and standard multivariate procedures (as long as we have sufficiently large sample sizes) can be used to formally test whether or not differences exist between age groups or sexes. With Procrustes analysis, shape variability within groups can also be investigated by way of principal component analysis.

Similar observations were made about mandibular growth, in the sample investigated in this thesis, using both Procrustes analysis and the useful technique based on Bookstein co-ordinates. From the raw data, it seemed likely that there might be some slight differences in overall size and shape within samples, for both males and females, for all ages. In terms of shape differences, again it seemed likely that there were some extremely small differences within samples, for both males and females, for all ages.

As with EFF analysis, there appeared to be some very small differences in shape between ages 9 to 15, on average. The observed shape changes were all very small however and were not statistically significant for the ages tested. Again, differences in shape were not evident between males and females on average, at any age.

Further using both Procrustes analysis and Bookstein co-ordinates, there did not appear to be any association between the size and shape of the mandibular outlines in either the male or female samples, for all ages.

In addition, shape variability within male and female samples was investigated using Procrustes methods by way of principal components analysis where broadly similar results were found for males and females, as well as combined samples, and different age groups. It was found that the first principal component tended to explain a moderate amount of the totality of shape variability in male and female samples, as well as a combined sample, for all ages. Some of the principal components appeared to be capturing the same components of variability. In general, the first principal component tended to include information about the relative size of the bone, in terms of height, width and overall length. It could also be interpreted as partly capturing the 'depth' of the condyle and mandibular notch, as well as capturing the amount that the lower incisor moved backwards / forwards. There appeared to be less overall movement in the landmarks for the second principal component, which tended to measure the angle of the anterior ramus and the overall 'sculpturing' of the condyle, mandibular notch and coronoid process. Further, the third principal component tended to measure the length of the posterior border of the ramus and the angle of the mandible (and hence, like principal component 1, captured the width of the body of the mandible) and the fourth seemed to capture similar effects to principal component 2. Finally, the fifth principal component included information about the movement and position of the alveolus, in a contrasting way to how the second principal component captures the variability in the anterior border of the ramus.

It is worth stressing that co-ordinate data analysis (like Procrustes and Bookstein methods) allows for a description of complex objects in which landmarks can be readily related to one another. As such the description of form can be thought of as complete, in the sense that all landmark locations are fully defined. However, practical considerations in identifying equivalent landmarks, in choosing the correct number of useful landmark points to characterise the object(s) under investigation and in omitting the information between such landmarks might be thought of as disadvantages of such a method. It is important that the landmarks are in some way equivalent between objects (homologous). Homology has been described as a 1:1 correspondence between objects (forms) in some biologically meaningful way. Although this is not a problem in the context of this thesis, it is sometimes difficult to identify such 'equivalent' landmarks in some studies. A further issue arises in the context of different types of landmarks, since by their nature, some can be readily located, whereas others can only be approximately identified. Practical considerations, therefore, play a role in limiting the number of landmarks that can be usefully included in any study. This applies to a certain extent in the mandibular study where it is not so much of an issue of inclusion, but more that the landmark points could sometimes be difficult to locate. Training and supervision was given to help in the correct identification of points however. In addition, when using homologous landmark points to determine the geometry of the shape of an object, the boundary information connecting these points is of secondary concern. This approach might be considered as flawed if the underlying biology appears to be driven by the characteristics of the boundary. Problems are presented in cases where no landmarks can be identified in a particular region of an object because of a lack of surface features, on particularly smooth areas of bone for

example. In this case it is possible to interpolate landmarks according to the locations of the homologous landmarks. It is doubtful that such landmarks (usually termed pseudo-landmarks) can be considered as homologous between forms however, since their location relates to mathematical as well as biological constraints. This consideration is important in studies that may use several constructed landmarks and this constraint should be considered in the analysis of the mandibular data since many intermediate points have been defined. Most of the analyses concentrated only on the 19 anatomical landmarks however.

In summary then, we can say that the methods of elliptical Fourier function and Procrustes / Bookstein co-ordinates both provide a very useful framework in which to describe the size and shape of complex irregular forms like the mandible. The initial collection of data is identical no matter which method is used, and the application of each method to a set of data, like the mandibular data examined in this thesis, is fairly straightforward using such methods. A series of very informative plots are produced in all cases and equivalent subjective impressions may be obtained, as they were in this study. Each method in its own way provided useful information in describing the size and shape of a complex object, like the mandible. Procrustes methods' (including the very useful method using Bookstein co-ordinates) is preferred for statistical purposes since it provides not only good visual tools but also a parametric framework in which to draw formal statistical inferences.

Overall, it can be said that there are advantages and limitations to all shape analysis procedures (whether landmark-dependent like Procrustes or landmark-free systems like Fourier analysis). It is apparent that no single method successfully builds both the homologous point information (the landmarks) and the boundary curve information (the outline) into a single numerical model. Most methods however are very good descriptors of shape, and many can partition the size and shape of a form. The usefulness of any particular method in any particular context really depends on the aims of the study.

There is perhaps a case to be made for the use of more than one method in the description of size and shape of complex irregular forms. An investigator could then confirm or modify the conclusions drawn by using one technique e.g. EFF, in the light of studies using another e.g. Procrustes. It could be argued that such confirmatory analyses should form an important part of any morphometric study since all techniques suffer to a certain extent from their own peculiar constraints and limitations.

Appendix

A.1 CMA collection form

The form used in the Glasgow Dental Hospital and School to collect information in respect to the cranio-facial complex is included.

A.2 A Lateral skull radiograph

An example of a lateral skull radiograph is included.

DEPARTMENT OF ORTHODONTICS

GLASGOW DENTAL HOSPITAL AND SCHOOL

Box No.

ORTHODONTIC DEPT.

Surname	Christian Names Sex	Unit Number
Referred By	Consultant (Diagnostician)	Operator
Cephalograms Dates taken	Photographs Dates taken	X-Rays Dates taken
Patient's Main Complaint		Attitude to Treatment

Relevant
Med/Dent. History

	Patient		Norms for age
	Height cms		
	Weight Kg		

Parents Occupation

Sibs (Note Twins) Number

Number treated at G.D.H

Ethnic origin: Gt. Britain, Ireland | Other Caucasian (white), India/Pakistan | Negroid, Mongoloid | Mixed, Unknown

External Facial Exam

a) Skeletal Class

b) FMP Angle — High | Average | Low

Cephalogram Analysis

		Date					Date			
81 ± 3	SNA				27 ± 3	MMPA				
78 ± 3	SNB				109 ± 6	$\underline{1}$ – MAX. P				
3 ± 2	ANB				92 ± 6	$\overline{1}$ – MP				
	Class				132 ± 5	$\underline{1} - \overline{1}$				

Soft Tissues

Lips — Draw Lip Line

Competent | Incompetent

Habitual Posture: Together | Apart

Circumoral Muscles

Tone: Firm | Average | Lax

Activity:

	0	+	++
Swallow			
Expressive Behaviour			

Tongue

Resting Posture: High | Low | L. Lip

Thrust:

	Speech	Swallowing
Forward		
Lateral		

CENTRE LINE SHIFT

Mandibular Deviation None ☐ Forward ☐ Distal ☐ R ☐ L ☐

Speech

Habits

Oral Hygiene

Periodontal State

Caries State

Carious teeth requiring attention

Teeth of doubtful prognosis

Prone ☐

Average ☐

Resistant ☐

Teeth unerupted

Teeth erupted

Teeth erupted

Teeth unerupted

PERMANENT TEETH ABSENT

Tooth alignment and inclination

Incisors

Canines

Premolars

Molars

ROTATED TEETH

Crowding

8 - 3	2 - 2	3 - 8
8 - 3	2 - 2	3 - 8

Arch Shape U ☐ L ☐

*Bolton Analysis

Overall ☐ Anterior ☐

		2/	1/	/1	/2	5/	4/	3/	/3	/4	/5
Maxilla											
Crown size	mm					7	7	8	8	7	7
Space required						22			22		
Space available											
Space – + Shortage/Surplus											

Measure teeth if erupted

		2/	1/	/1	/2	5/	4/	3/	/3	/4	/5
Mandible											
Crown size	mm					7	7	7	7	7	7
Space required						21			21		
Space available											
Space – + Shortage/Surplus											

*OVERALL $\frac{\text{Sum Md } 6-6}{\text{Sum Mx } 6-6} \times 100$ Mean 91 ± 2

ANTERIOR $\frac{\text{Sum Md } 3-3}{\text{Sum Mx } 3-3} \times 100$ Mean 77 ± 2

Overjet ☐ mm

Overbite ☐ mm

Complete ☐

Incomplete ☐

Crossbite

Teeth affected

Incisor Relationship I II 1. II 2 II indef. III

Buccal Relationship Right I II III Left I II III

Other factors

Classification and Diagnosis

Aim of Treatment

Treatment Plan

Sig

Date

Parent advised

Date

Stage 1

Appliances

2

3

4

Retention

Prognosis

Date	TREATMENT NOTES	N.V.	Student Sig.	Staff Sig.

X-RAY


GLASGOW DENTAL HOSPITAL
NAME
NO

RIGHT HAND SIDE OF X-RAY COULD NOT BE SCANNED DUE TO THE BINDING

A.3 CMA landmarks, planes, angles and distances

In this section, the definitions of the landmarks, linear distances and angles typically calculated in CMA are adapted from 'A Textbook of Orthodontics' Chapter 6.

Cephalometric Landmarks

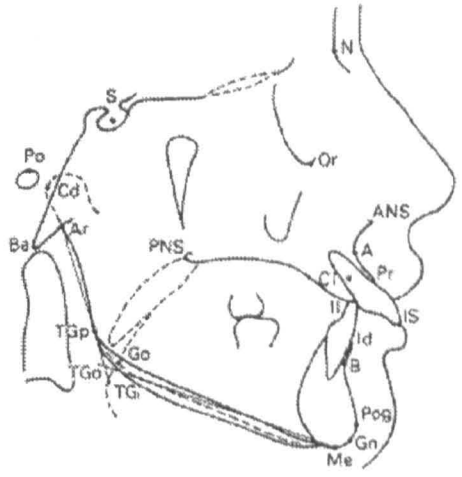

The definitions of the cephalometric landmarks assume that the radiograph is oriented with the Frankfort plane horizontal. Many landmarks are bilateral but when the two sides are superimposed perfectly, only a single point is identifiable. Where the two sides are distinct, both should be traced and the midpoint taken as the landmark.

Anterior Nasal Spine (ANS) – *The tip of the anterior nasal spine.* Must not be confused with the alar cartilages.

Articulare (Ar) – *The intersection of the posterior border of the neck of the mandibular condyle and the lower margin of the posterior cranial base.* A constructed point used to indicate the position of the mandibular joint relative to the cranial base.

Basion (Ba) – *The most posterior inferior point on the clivus (basiocciput).* Represents the posterior limit of the midline cranial base. May be difficult to locate due to shadow by the occipital condyles.

Centroid of the upper incisor root (C) – *The midpoint on the root axis of the most prominent upper incisor.*

Condylion (Cd) – *The most superior posterior point on the head of the mandibular condyle.* Cannot be located reliably on a standard cephalogram due to shadow of petrous temporal obscuring condylar head. Articulare is often used as an alternative point.

Gnathion (Gn) – *The most inferior point on the mandibular symphysis in the midline.* Can be located by inspection, or constructed as the intersection of the margin of the symphysis with the bisector of the angle between the facial line (N-Pog) and the mandibular line (TG_i-Me).

Gonion (Go) – *The most inferior point on the angle of the mandible.* It may be located by inspection or constructed using the bisector of the angle between the ramal line (Ar-TG_p) and the mandibular line (TG_i-Me). Alternatively, can use the constructed point TG_o.

Incision inferius (II) – *The tip of the crown of the most prominent lower incisor.*

Incision superious (IS) - *The tip of the crown of the most prominent upper incisor.*

Infradentale (Id) – *The intersection of the alveolar crest and the outline of the most prominent mandibular incisor.*

Menton (Me) – *The lowermost point of the mandibular symphysis in the midline.* Where the chin is grooved, the most inferior points are bilateral but the midline contour can be seen slightly above them.

Nasion (N) – *The most anterior point on the frontonasal suture.* Care should be taken to locate.

Orbitale (Or) – *The most inferior anterior point on the margin of the orbit.* Can be unreliable.

Pogonion (Pog) – *The most anterior point on the bony chin.*

Point A (A) – *The most posterior point on the profile of the maxilla between the anterior nasal spine and the alveolar crest.* Also known as *subspinale*. Represents the anterior limit of the maxillary apical base. Difficult to locate reliably because the soft tissues of the cheeks may be superimposed on it.

Point B (B) – *The most posterior point on the profile of the mandible between the chin point and the alveolar crest.* Also known as *supramentale*. Represents the anterior limit of the mandibular apical base.

Porion (Po) – *The uppermost, outermost point on the bony external auditory meatus.* Can be difficult to locate.

Posterior Nasal Spine (PNS) – *The tip of the posterior nasl spine.* Can be constructed if obscured by unerupted molars.

Prosthion (Pr) – *The intersection of the alveolar crest and the outline of the most prominent maxillary incisor.*

Sella (S) – *The midpoint of the sella turcica.*

TG_i - *The inferior tangent point at the angle of the mandible.* Identified as the point of contact of the tangent to the angle of the mandible that passes through menton.

TG_p – *The posterior tangent point at the angle of the mandible.* Identified as the point of contact of the tangent to the angle of the mandible that passes through articulare.

TG_o – *The intersection of the lines Me-TG_i and Ar-TG_i.* Constructed point that can be used as an alternative to gonion.

Reference Lines

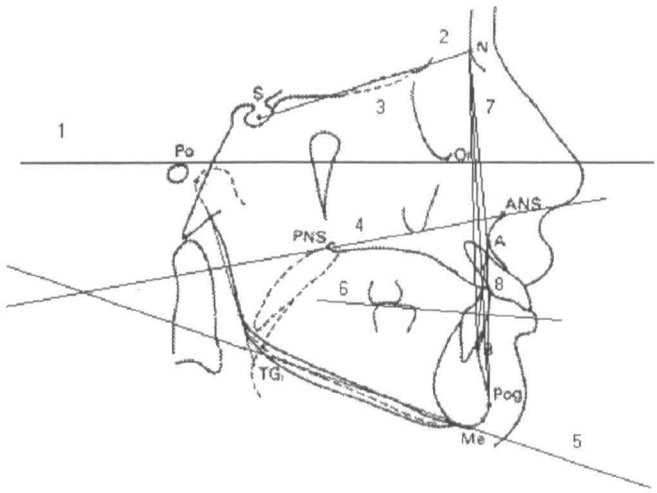

The true horizontal – If the patient can be posed with the head in the natural position when the radiograph is taken then the true horizontal may be identified. The problem lies in posing the patient reliably. Can be time consuming and is seldom done. Would be useful for the assessment of anteroposterior jaw relationships if could master positioning.

1. Frankfort plane – Passes through porion and orbitale. Defined at a conference of craniometrists held in Frankfort (1884) as approximating to the true horizontal when the head is held in the normal postural position. Designed to allow for

comparison of the skulls of different species, and race of man. Subsequently adopted for use in cephalometric analysis.

2. Sella –nasion line – This line is taken to represent the anterior cranial base, which undergoes little change from growth or remodelling after about 6 years of age when the sphenoethmoidal synchondrosis fuses. Valuable baseline in the measurement and comparison of jaw relationships between individuals and within the ine case at different ages. When jaw relationships are measured relative to the SN line it is important to recognise that variations in its orientation and in the position of nasion in particular, can give false impressions of the true relationships.
3. De Coster's line – This follows the floor of the anterior cranial base close to the midline from the anterior margin of the ethmoid bone to sella turcica. Useful for superimposition of serial radiographs taken after 7 years of age.
4. Maxillary plane – ANS to PNS - The inclination of the upper incisors is commonly measured to this line.
5. Mandibular plane – Defined in a number of different ways; the anterior landmark may be menton or gnathion and the posterior landmark may be TG_0 or gonion. The inclination of the lower incisors is measured to this line; and its angulation to the maxillary line gives a measure of lower anterior face height. TG_0 to menton is used here.
6. Occlusal plane – As with the mandibular line, the occlusal line can be defined in different ways. Can be defined as the line passing midway between the tips of the mesiobuccal cusps of the upper and lower first permanent molars, and the lower incisor edges. This may give an unreliable assessment of the general line of the occlusion when there is deep overbite. The functional occlusal plane (FOP) tends to be useful for most purposes where, it passes through the occlusion of the

premolars or deciduous molars and the first permanent molars. The cuspal outlines of these teeth may not be clear and it is sometimes difficult to locate the FOP accurately, particularly in mixed dentition. Important to recognise that whatever occlusal plane is used, its orientation may change with growth or treatment and it is therefore not an entirely satisfactory reference.

7. The Facial plane (N-Pog) – This line has been used to help assess the facial profile. The angle of the facial line to the Frankfort horizontal (the facial angle) indicates whether ones profile is prognathic, retrognathic, or orthognathic i.e. protrusive, retrusive or upright. Basically, sticks out, in or normal.
8. The Line from Point A to Pogonion (A-Pog) - This line has been used to measure the anteroposterior position of the crowns of the incisor teeth.

Skeletal Measurements – Angles, ratios and linear distances

Obviously, if a measurement is to be intelligible, its average value and range of variation must be known. Most linear and some angular measurements vary according to age, sex, race and so for these, many different 'norm' values are required. The cephalometric 'norms' as defined in 'A textbook of Orthodontics' are given in brackets, (in degrees for angles, % for ratios or mm for linear distances). These values are Caucasian and are derived from a number of groups of individuals with normal occlusions.

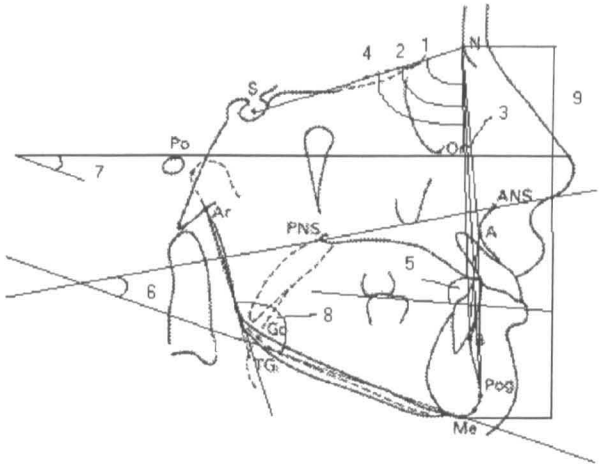

1. Angle S-N-A (82 ± 3 degrees) - *Prognathism of the maxillary apical base.*
2. Angle S-N-B (79 ± 3 degrees) - *Prognathism of the mandibular dental base.*
3. Angle A-N-B (3 ± 1 degrees) – *The anteroposterior apical base relationship (skeletal pattern).*
4. Angle S-N-Pog (80 ± 3 degrees) - *Mandibular prognathism.*
5. Angle A-B/FOP (90 ± 5 degrees) – *Measures the apical base by reference to the FOP.*
6. Mx-Mn or MM angle (27 ± 5 degrees) - *Maxillary-mandibular planes angle.* Provides a measure of the divergence of the intermaxillary space anteriorly.
7. FM angle (27 ± 5 degrees) - *Frankfort-mandibular plane angle.* Highly correlated with the MM angle. Little point in measuring both. Can be measured clinically, but is less reliable than the MM angle.
8. Ar-TG_p/TG_i-Me (126 ± 5 degrees) – *Gonial angle*. Essentially measures the slope of the mandibular plane since the slope of the posterior border of the mandibular ramus varies little. Therefore, it is highly correlated with the MM angle and there is little point in measuring both.

9. Me-Mx/N-Me (50-55%) – *Face height ratio.* Used to estimate the anterior intermaxillary height.

Dentoskeletal Measurements – Angles, ratios and linear distances

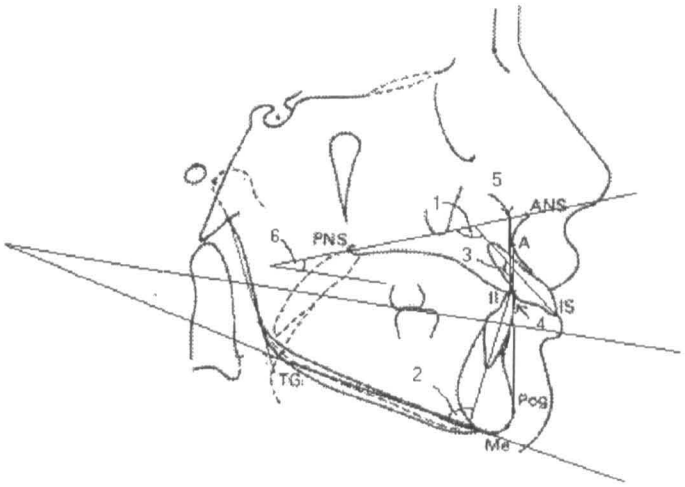

1. UI/Mx (108 ± 5 degrees) – *Upper incisor to maxillary plane angle*. Measurement of this inclination determines the types of tooth movement required to correct any anomalies in the incisor relationships.
2. LI/Mn (92 ± 5 degrees) – *Lower incisor to mandibular plane angle*. The lower incisor angulation should not be interpreted without reference to other variables which have an effect on the angle. For example, the balance between the lips and the tongue influences the labiolingual position of the crowns of the lower incisors and therefore their inclination. The average and range of variation here is appropriate only where the maxillary mandibular planes angle and skeletal pattern are within normal limits.
3. UI/LI (133 ± 10 degrees) – *Interincisor angle*. Associated with the depth of the overbite when there is incisor contact.

4. E ↓ A-Pog (0 – 2 mm) - *Lower incisor edge to A-Pog distance.* In well balanced faces with good occlusions, the lower incisor edge lies on or close to the A-Pog line.

5. E ↓ C ↑ (0 – 2 mm) - *Lower incisor edge to upper incisor centroid distance.* Closely associated with overbite depth – the further behind the centroid the lower edge lies, the deeper the overbite is liable to be (except if the overbite is incomplete).

6. FOP/Mx (10 ± 4 degrees) – *Functional occlusal plane to maxillary plane angle.* Correlated with the divergence of the intermaxillary space (MM angle).

A.4 An original tracing ready for digitisation

An original tracing which has been prepared according the protocol outlined in Chapter 3 is included.

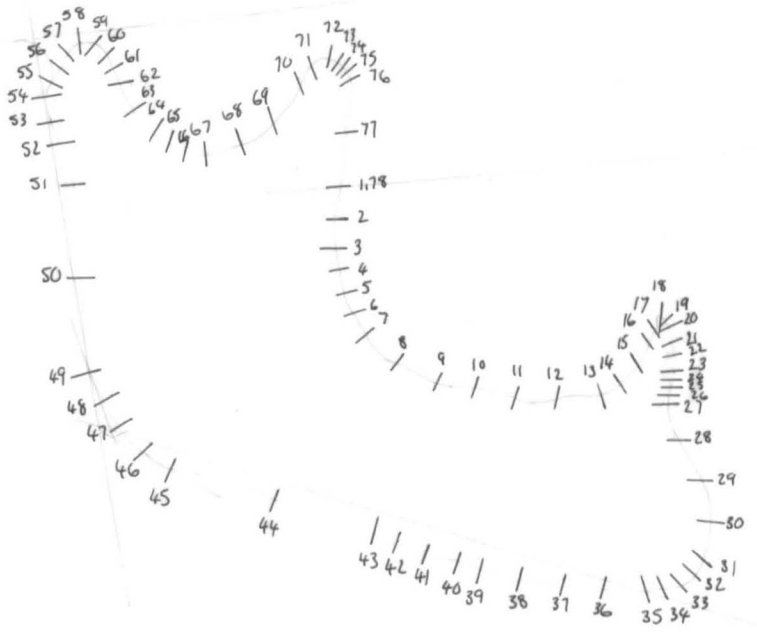

Bibliography

Albrecht GH. (1978). Some comments on the use of ratios. *Syst Zool.* 27, 67-71.

Anstey RL and Delmet DA. (1973). Fourier analysis of zooecial shapes in fossil Bryozoans. *Geol. Soc. Am. Bull.* 84, 1753-64.

Atchley WR, Gaskins CT and Anderson D. (1976). Statistical properties of ratios. I Empirical results. *Syst. Zool.* 25, 137-48.

Atchley WR, Gaskins CT and Anderson D. (1978). Ratios, regression intercepts, and the scaling of data. *Syst. Zool.* 27, 78-83.

Bathe KJ and Wilson EL. (1976). *Numerical Methods in Finite Element Analysis.* Englewood Cliffs. New Jersey. Prentice-Hall.

Benson RH, Chapman RE and Siegel AF. (1982). On the measurement of morphology and its shape. *Paleobiology.* 8, 328-39.

Bevis RR, Hayles AB, Isaacso RJ and Sather AH. (1977). Facial growth response to human growth hormone in hypopituitary dwarfs. *Angle Orthod.* 47(3), 193-205.

Bibby RE. (1979). A cephalometric study of sexual dimorphism. *Am. J. Orthod.* 76, 256-9.

Bjork A. (1955). Facial growth in man studied with the aid of metallic implants. *Acta Odontol. Scand.* 13, 9-34.

Bjork A and Skieller V. (1972). Facial development and tooth eruption. An implant study at the age of puberty. *Am. J. Orthod.* 62, 339-83.

Bjork A and Skieller V. (1983). Normal and abnormal growth of the mandible: a synthesis of longitudinal cephalometric implant studies over a period of 25 years. *Eur. J. Orthod.* 5, 1-46.

Blackith RE and Reyment RA. (1971). *Multivariate Morphometrics.* New York. Academic Press.

Blum H. (1973). Biological shape and visual science. *J. Theor. Biol.* 38, 205-87.

Bookstein FL. (1977). The study of shape transformations after D'Arcy Thompson. *Mathematical Biosciences.* 34, 177-219.

Bookstein FL. (1977). Orthogenesis of the Hominids: An exploration using biorthogonal grids. *Science.* 197, 901-4.

Bookstein FL. (1978). *The Measurement of Biological Shape and Shape Change.* Lecture notes in biomathematics. Vol. 24. New York. Springer-Verlag.

Bookstein FL. (1980). When one form is between two others: An application of Biorthogonal Analysis. *Am. Zool.* 20, 627-41.

Bookstein FL. (1982). On the cephalometrics of skeletal change. *Am. J. Orthod.* 82, 177-82.

Bookstein FL. (1983). The geometry of craniofacial growth invariants. *Am. J. Orthod.* 83, 221-34.

Bookstein FL. (1984). A statistical method for biological shape comparisons. *J. Theoretical Biol.* 107, 475-520.

Bookstein FL. (1986). Size and shape spaces for landmark data in two dimensions. *Statistical Science.* 1, 181-242.

Bookstein FL. (1989). Principal warps: thin plate splines and the decomposition of deformations. *IEEE Transactions on Pattern Analysis and Machine Intelligence.* 11, 567-85.

Bookstein FL. (1991). *Morphometric Tools for Landmark Data.* Cambridge. Cambridge University Press.

Bookstein FL, Strauss RE, Humphries JM. (1982). A comment on the use of Fourier methods in systematics. *Syst Zool.* 31, 85-92.

Bozzini C, Barcelo AC, Alippi RM, Leal TL and Bozzini CE. (1989). The concentration of dietary casein required for normal mandibular growth in the rat. *J. Dent. Res.* 68(5), 840-2.

Broadbent BH. (1937). The face of the normal child. *Angle Orthodontist.* 7, 183-208.

Burstone CJ. (1963). Process of maturation and growth prediction. *Am. J. Orthod.* 49, 907-19.

Chen SYY, Lestrel PE, Kerr WJS, McColl JH. (2000). Describing shape changes in the human mandible using elliptical Fourier functions *Europ. J. Orthod.* 22, 205-16.

Cheverud JM, Lewis Jl, Bachrach W and Lew WD. (1983). The measurement of form and variation in form: An application of 3D quantatative morphology by finite element methods. *Am. J. Phys. Anthrop.* 62, 151-63.

Cheverud JM and Richtsmeier JT. (1986). Finite element scaling applied to sexual dimorphism in rhesus macaque (*Macca mulatta*) facial growth. *Syst. Zool.* 35, 381-99.

Combined Dictionary and Thesaurus. (1995). Martin Manser and Megan Thomson (Eds). Chambers.

Corruccini RS. (1973). Size and shape in similarity coefficients based on metric characters. *Am. J. Phys. Anthrop.* 38, 743-54.

Corruccini RS. (1977). Correlation properties of morphometric ratios. *Syst. Zool.* 26, 211-14.

Diaz G, Quacci C and Dell'Orbo C. (1990). Recognition of cell surface modulation by elliptic Fourier analysis. *Comp. Meth. Prog. Biomed.* 31, 57-62.

Diaz G, Zuccarelli A, Pelligra I and Ghiani A. (1989). Elliptic Fourier analysis of cell and nuclear shapes. *Comp Biomed Res.* 22, 405-14.

Dodson P. (1978). On the use of ratios on growth studies. *Syst Zool.* 27, 62-7.

Dryden IL and Mardia KV. (1998). *Statistical Shape Analysis.* Chichester. Wiley.

Dryden IL and Mardia KV. (1992). Size and shape analysis of landmark data. *Biometrika.* 79, 57-68.

Dudas M and Sassouni V. (1973). The hereditary components of mandibular growth. A longitudinal twin study. *Angle Orthod.* 43(3), 314-22.

Ehrlich R and Weinberg B. (1970). An exact method for the characterisation of grain shape. *J. Sed. Petrol.* 40, 205-12.

Ehrlich R, Baxter-Pharr R, Healy-Williams N. (1983). Comments on the validity of Fourier descriptors in systematics: a reply to Bookstein et al. *Syst Zool.* 32, 202-6.

Enlow DH. (1975). *Handbook of Facial Growth.* Philadelphia: WB Saunders.

Enlow DH and Harris DB. (1964). A study of the postnatal growth of the human mandible. *Am. J. Orthod.* 50, 25-50.

Farkas LG, Posnick JC and Hreczko TM. (1992). Growth patterns of the face: a morphometric study. *Cleft Palate Craniofac. J.* 29(4), 308-15.

Ferrario VF, Sforza C, Serrao G et al. (1994). Shape of the human corpus-callosum. Elliptic Fourier analysis on midsagital magnetic-resonance scans. *Investigative Radiology.* 29, 677-81.

Ferson S, Rohlf FJ and Koehn RK. (1985). Measuring shape variation of two-dimensional outlines. *Syst. Zool.* 43, 59-68.

Full WE and Ehrlich R. (1982). Some approaches for location of centroids of quartz grain outlines to increase homology between Fourier amplitude spectra. *Mathematical Geology.* 14, 43-55.

Full WE and Ehrlich R. (1986). Fundamental problems associated with "eigenshape analysis" and similar "factor" analysis procedures. *Mathematical Geology.* 18,451-63.

Gero J and Mazzullo J. (1984). Analysis of artefact shape using Fourier series in closed form. *J. Field Archeol.* 11, 315-22.

Glasby CA, Horgan GW, Gibson GJ and Hitchcock D. (1995). Fish shape analysis using landmarks. *Biometrical Journal.* 37, 481-95.

Goldstein H. (1979). Allometry and the study of shape. In *The Design and Analysis of Longitudinal Studies: Their Role in the Measurement of Change.* Academic Press. London.

Goodall CR and Bose A. (1987). Procrustes techniques for the analysis of shape and shape change. *Am. J. Phys. Anthrop.* 72, 204.

Goodall CR. (1991). Procrustes methods in the statistical analysis of shape. *J. Roy. Stat. Soc. Series B.* 53, 285-339.

Gower JC. (1971). Statistical methods of comparing different multivariate analyses of the same data. In *Mathematics in the Archeological and Historical Sciences.* pp138-49. Hodson FR, Kendall DG and Tautu P (eds). Edinburgh. University Press.

Gower JC. (1975). Generalised Procrustes analysis. *Psychometrika.* 40, 33-50.

Harris JE. (1962). A cephalometric analysis of mandibular growth rate. *Am. J. Orthod.*. 48, 161-74.

Healy JR and Tanner JM. (1981). Size and shape in relation to growth and form. *Symp. Zool. Soc. (Lond.).* 46, 19-35.

Hills M. (1978). On Ratios - A response to Atchley, Gaskins and Anderson. *Syst Zool.* 27, 61-2

Houston WJB, Stephens CD and Tulley WJ. (1992). *A Textbook of Orthodontics.* 2nd Edition. Wright Publication.

Huxley JS. (1924). Constant differential growth ratios and their significance. *Nature.* 114, 895-6.

Huxley JS. (1932). *Problems of relative growth.* Methuen. London.

Johnson DR, O'Higgins P, McAndrew TJ, Adams LM and Flinn RM. (1985). Measurement of biological shape: A general method applied to mouse vertebrae. *J. Embryol. Exp. Morph.* 90, 363-7.

Kaesler RL and Waters J. (1972). A Fourier analysis of the Ostracode margin. *Geol. Soc. Am. Bull.* 83, 1169-78.

Kerr WJS. (1979). A longitudinal cephalometric study of dentofacial growth from 5 to 15 years. *Br. J. Orthod.* 6, 115-21.

Kuhl FP and Giardina CR. (1982). Elliptic Fourier features of a closed contour. *Comp Graph Imag Proc.* 18, 236-58.

Kiliaridis S. (1995). Masticatory muscle influence on craniofacial growth. *Acta Odontol. Scand.* 53(3), 196-202.

Kincaid DT and Schneider RB. (1983). Quantification of leaf shape with a microcomputer and Fourier transform. *Can. J. Bot.* 61, 2333-42.

Krieborg S et al. (1981). Abnormalities of the cranial base in deidocranial dysostosis. *Am. J. Orthod.* 79, 549-57.

Lavelle CLB. (1985). A preliminary study of mandibular shape. *J. Cran. Genet. Dev. Biol.* 5, 159-65.

Lele S. (1991). Some comments on coordinate-free and scale-invariant methods in morphometrics. *Am. J. Phys. Anthrop.* 85, 407-17.

Lele S and Richtsmeier JT. (1991). Euclidean distance matrix analysis: A coordinate-free approach for comparing biological shapes using landmark data. *Am. J. Phys. Anthrop.* 86, 415-27.

Lele S and Richtsmeier JT. (1992). On comparing biological shapes: Detection of influential landmarks. *Am. J. Phys. Anthrop.* 87, 49-65.

Lestrel PE. (1974). Some problems in the assessment of morphological size and shape differences. *Yearbk PhysAnthropol.* 18, 140-62.

Lestrel PE. (1980). A quantatative approach to skeletal morphology: Fourier analysis. *Soc. Phot. Inst. Engrs. (SPIE).* 166, 80-93.

Lestrel PE. (1987). A new quantatative method for fitting growth data: Eliptical Fourier functions. *Am. J. Phys. Anthrop.* 72, 224.

Lestrel PE. (1989a). Method for analysing complex two-dimensional forms: Elliptical Fourier functions. *Am. J. Hum. Biol.* 1, 149-64.

Lestrel PE. (1989b). Some approaches toward the mathematical modelling of the craniofacial complex. *J. Craniofac. Genet. Dev. Biol.* 9, 77-91.

Lestrel PE. (1997a). Morphometrics of craniofacial form: A Fourier analytic procedure to describe complex morphological shapes. In *Fundamentals of craniofacial Growth.* pp155-87. Dixon AD, Hoyte DAN and Ronning O (eds). New York. CRC Press.

Lestrel PE. (1997b). In *Fourier Descriptors and their Applications in Biology.* pp3-44. Lestrel PE (ed). Cambridge. Cambridge University Press.

Lestrel PE and Brown HD. (1976). Fourier analysis of adolescent growth of the cranial vault: a longitudinal study. *Human Biology.* 48, 517-28.

Lestrel PE and Kerr WJS. (1992). Shape changes due to functional appliances. *Calif. Dent. J.* 20, 30-6.

Lestrel PE and Kerr WJS. (1993). Quantification of function regulator therapy using elliptical Fourier functions. *Europ. J. Orthod.* 15, 481-91.

Lestrel PE and Huggare JA. (1997). Cranial base changes in shunt-treated hydrocephalics. In *Fourier Descriptors and their Applications in Biology.* Pp322-39. Lestrel PE (ed). Cambridge. Cambridge University Press.

Lestrel PE and Roche AF. (1976). Fourier analysis of the cranium in Trisomy 21. *Growth.* 40, 385-98.

Lewis AB and Roche AF. (1972). Elongation of the cranial base in girls during pubescence *Angle Orthod.* 42,358-67.

Lewis AB and Roche AF. (1974). Cranial base elongation in boys during pubescence. *Angle Orthod.* 44,83-93.

Lewis AB, Roche AF and Wagner B. (1982). Growth of the mandible during pubescence. *Angle Orthod.* 52, 325-42.

Lohmann GP. (1983). Eigenshape analysis of microfossils: A general morphometric procedure for describing changes in shape. *Mathematical Geology.* 15, 659-72.

Lohmann GP and Schweitzer PN. (1990). On eigenshape analysis. *In Proceedings of the Michigan Morphometric Workshop*. No.2 pp147-66. Rohlf FJ and Bookstein FL (eds). University of Michigan. Museum of Zoology Special Publication.

Lowe B, Philips C, Lestrel PE and Fields HW. (1994). Skeletal jaw relationships: A quantatative assessment using elliptical Fourier functions. *Angle Orthod.* 64,299-309.

Lu KJ. (1965). Harmonic analysis of the human face. *Biometrics.* 21, 491-505.

Mardia KV and Dryden IL. (1989b). The statistical analysis of shape data. *Biometrika.* 76, 71-282.

McNamara JA. (1985). The role of functional appliances in contemporary orthodontics. In *New Vistas in Orthodontics.* LE Johnston. Philadelphia: Lee & Febiger.

McNamara JA, Bookstein FL and Shaughnessy TG. (1985). Skeletal and dental changes following functional regulator therapy on class II patients. *Am. J. Orthod.* 88, 91-110.

Medewar PB. (1950). Transformation of shape. *Proc. Roy. Soc. (Lond.) B.* 137, 474-79.

Meikle MC. (1973). The role of the condyle in the postnatal growth of the mandible. *Am. J. Orthod.* 64(1), 50-62.

Mills JRE. (1970). The application and importance of cephalometry in orthodontic treatment. *The Orthodontist.* 2(2), 32-47.

Mills JRE. (1983). A clinician looks at facial growth. *Br. J. Orthod.* 10, 58-72.

Morant GMA. (1923). First study of the Tibetan skull. *Biometrika.* 14, 253-60.

Morant GM. (1930). A biometric study of the human mandible. *Biometrika.* 37, 84-122.

Mosier CI. (1939). Determining a simple structure when loadings for certain tests are known. *Psychometrika.* 4, 149-62.

Mosimann JE. (1975a). Statistical problems of size and shape. I. Biological applications and basic theorems. In *Statistical Distributions in Scientific Work.* Vol 2, pp187-217. Dordrecht-Holland. D Reidel.

Mosimann JE. (1975b). Statistical problems of size and shape. II. Characterisations of the lognormal, gamma and Dirichlet distributions. In *Statistical Distributions in Scientific Work.* Vol 2, pp219-39. Dordrecht-Holland. D Reidel.

Mosimann JE. (1988). Size and shape analysis. In *Encyclopedia of Statistical Sciences.* Vol 8, pp 497-507. Kotz S and Johnson NL (eds). New York. Wiley.

Nafe R, Kalousti V, Choritz H and Georgii A. (1992). Elliptic Fourier analysis of megakaryocyte nuclei in chronic myeloproliferative disorders. *Anal. Quant. Cytol. Histol.* 14,391-97.

Needham AE. (1950). The form-transformation of the abdomen of the female peacrab, *Pinnotheres pisum. Proc. Roc.Soc. (Lond.) B.* 137, 115-36.

O'Higgins P and Williams NW. (1987). An investigation into the use of Fourier coefficients in charcterising cranial shape primates. J. *Zool. Lond.* 211, 409-30.

O'Reilly MT and Yanniello GJ. (1988). Mandibular growth changes and maturation of cervical vertebrae – a longitudinal cephalometric study. *Angle Orthodontist.* 58(2), 179-84.

Parnell JN and Lestrel PE. (1977). A computer program for fitting irregular two-dimensional forms. *Computer Programs in Biomedicine.* 7,145-61.

Penrose LS. (1954). Distance, size and shape. *Ann. Eugen.* 18, 337-43.

Ranly DMA. (1988). *A Synopsis of Craniofacial Growth.* 2nd Edition. USA. Prentice-Hall.

Rao CR. (1948). The utilisation of multiple measurements in problems of biological classification. *J. Roy. Stat. Soc. (Ser B.).* 10, 159-203.

Read DW and Lestrel PE. (1986). A comment upon the uses of homologous-point measures in systematics: A reply to Bookstein et al. *Syst. Zool.* 33, 241-53.

Reeve ECR and Huxley JS. (1945). Some problems in the study of allometric growth. In *Essays on Growth and Form presented to D'arcy Wentworth Thompson.* pp121-156. Le Gros Clark WE and Medawar PB (eds). Oxford. Clarendon Press.

Reyment RA, Blackith RE and Campbell NA. (1984). *Multivariate Morphometrics.* 2nd Edition. New York. Academic Press.

Reyment RA. (1991). *Multidimensional Paleobiology.* Oxford. Pergamon Press.

Richards OW and Kavanagh AJ. (1945). The analysis of the growing form. In *Essays on Growth and Form presented to D'arcy Wentworth Thompson.* pp188-230. Le Gros Clark WE and Medawar PB (eds). Oxford. Clarendon Press.

Richtsmeier JT and Lele S. (1990). Analysis of craniofacial growth in Crouzon syndrome using landmark data. *J. Cranio. Gen. Dev. Biol.*. 10, 39-62.

Roberts DM et al. (1983). Morphometric analysis of outline shape applied to the peritrich genus vorticella. *Syst. Zool.* 32(4), 377-88.

Rohlf FJ. (1986). Relationships among eigenshape analysis, Fourier analysis and analysis of coordinates. *Mathematical Geology*. 18, 845-54.

Rohlf FJ and Archie JW. (1984). A comparison of Fourier methods for the description of wing shapes in mosquitos (*Diptera culicidae*). *Syst Zool.* 33, 302-17.

Rohlf FJ and Slice D. (1990). Methods for comparison of sets of landmarks. *Syst. Zool.* 39, 40-59.

Schweitzer PN, Kaesler RL and Lohmann GP. (1986). Ontogeny and heterochrony in the ostracode Cavellina coreyell from the lower Permian rocks in Kansas. *Paleobiology*. 12, 290-301.

Shepstone L, Rogers J, Kirwan J, et al. (1999). The shape of the distal femur: a palaeopathological comparison of eburnated and non-eburnated femora. *Ann. Rheumatic Diseases*. 58, 72-8.

Siegel AF and Benson RH. (1982). A robust comparison of biological shapes. *Biometrics*. 38, 341-50.

Singh GD, McNamara JA, Lozanoff S. (1997). Localisation of deformations of the midfacial complex in subjects with class III malocclusions employing thin plate spline analysis. *J. Anat.* 191, 595-602.

Singh GD, McNamara JA, Lozanoff S. (1998). Procrustes, Euclidean and cephalometric analyses of the morphology of the mandible in human class III malocclusions. *Arch. Oral. Biol.* 43, 535-43.

Singh GD, McNamara JA, Lozanoff S. (1998). Components of soft tissue deformations in subjects with untreated angle's class III malocclusions: thin plate spline analysis. *J. Cranio. Gen. Devel. Biol.* 18, 219-27.

Singh GD, McNamara JA and Lozanoff S. (1999). Finite-element morphometry of soft tissue morphology in subjects with untreated class III malocclusions. *Angle Orthod.* 69, 215-24.

Sneath PHA and Sokal RR. (1973). *Numerical Taxonomy.* p573. San Francisco. Freeman.

Sprent P. (1972). The mathematics of size and shape. *Biometrics.* 28, 23-37.

Strauss RE and Bookstein FL. (1982). The truss: body reconstruction in morphometrics. *Syst. Zool.* 31, 113-35.

Tanner JM. (1962). *Growth at adolescence.* Oxford. Blackwell Scientific Publications.

Thilander B. (1995). Basic mechanisms in craniofacial growth. *Acta Odontol Scand* 53,144-51.

Thompson DW. (1917). *On Growth and Form*. Cambridge University Press. Cambridge. UK.

Thompson DW. (1942). *On Growth and Form*. 2nd Edition. Cambridge University Press. Cambridge. UK.

Tuomenin M, Kantomaa T and Pirttiniemi P. (1993). Effect of food consistency on the shape of the articular eminence and the mandible. An experimental study on the rabbit. *Acta Odontol. Scand.* 51(2), 65-72.

Vogl C, Atchley WR, Cowley DE, Crenshaw P, Murray JD and Pomp D. (1993). The epigenetic influence of growth hormone on skeletal development. *Growth Dev. Ageing.* 57(3), 163-82.

Webber RL and Blum H. (1979). Angular invariants in developing human mandibles. *Science*. 206, 689-91.

White RJ and Prentice HC. (1988). Comparison of shape description methods for biological outlines. In *Classification and Related Methods in Data Analysis*. Bock. HH (ed). Amsterdam. Elsevier Science Pub BV.

Wolfe CA. (1997). Software for elliptical Fourier analysis. In *Fourier descriptors and their applications in biology.* pp415-34. Lestrel PE (ed). Cambridge. Cambridge University Press.

Zahn CT and Roskies RZ. (1972). Fourier descriptors for plane closed curves. *IEEE Transactions of Computing*. C-21, 269-81.

Ziezold H. (1994). Mean figures and mean shapes applied to biological figure and shape distributions in the plane. *Biometrical Journal*. 36, 491-510.

Zuckerman S. (1950). The pattern of change in size and shape. *Proc. Roy. Soc. (Lond.) B.* 137, 433-42.